Quantifying the Biotic Enhancement of Mineral Weathering by Moss

Michael John Collingwood Crouch

Thesis presented in part-fulfilment of the degree of
Master of Science by Research in accordance with the regulations of
The University of East Anglia

School of Environmental Sciences
University of East Anglia
University Plain
Norwich
NR4 7TJ
UK

March 2010

"Life improves the capacity of the environment to sustain life… Life makes needed nutrients more readily available…through the tremendous chemical interplay from organism to organism."

Extract from Frank Herbert's 'Dune', 1965.

Abstract

Addressing the paucity of reliable, robust studies into the weathering effect exerted by biota onto rocks and minerals: mineral weathering by the moss *Physcomitrella patens* was measured in a novel *in vitro* microcosm study.

A sterile technique was maintained in order to ensure that *P. patens* was the only organism exerting weathering affects within the microcosms, control microcosms were devoid of biota entirely. After the weathering period ($\bar{x}$ = 112 days) the moss and aqueous solutions resulting from microcosms were analysed for Al, Ca, Fe, K, Mg, Na and Si using Inductively Coupled Plasma - Atomic Emission Spectroscopy (ICP-AES) and for PO_4^{3-} and SiO_4^{4-} using a Nutrient Auto-Analyser.

Results show strong biotic enhancements for all ICP analytes and PO_4^{3-} (except Na). Biotic enhancements were strongest for Fe on most substrates, reaching levels of <625x abiotic weathering in andesite microcosms ($\bar{\mu}$ = 330.7x) and <493.6x on granite (all significant at $P<0.01$). Aqueous phase biotic enhancements for PO_4^{3-} were 5.3x on vermiculite and 4.2x on granite.

Experimental substrates were analysed using X-Ray Fluorescence Spectroscopy (XRF) in order to ascertain their petrologies and to enable comparison with weathering results to determine whether ions were being preferentially weathered over their baseline levels. Weathering of plant macronutrients is enhanced over the baseline stoichiometries, but biotic influence on this effect appears negligible.

This study has a bearing upon hypotheses linking the effects of increased land-surface weathering to the Ordovician glaciation due to the proliferation of bryophyte organisms across the land surface. Furthermore this study finds that *P. patens* is an excellent model bryophyte for studies of weathering as well as its more common use as the model bryophyte in genetic studies.

Keywords: Biogeochemistry, Enhancement, Microcosm, Mineral, Moss, Weathering.

Table of Contents

I: Figures, Tables and Equations

Figures

Figures (Continued)

Figures (Continued)

Tables

Tables (Continued)

Tables (Continued)

Equations

Equations (Continued)

II: Acknowledgements

First and foremost: I sincerely thank Martin Johnson for his coaching and mentoring (and for the large amount of time that he spent on these two tasks). It is no under-statement to say that the rigour of a number of the methodologies used in this study (particularly the blank taking procedure) and the quality of this thesis would be much the poorer were it not for Martin's helpful input. Similarly: I also sincerely thank Nuno Pires: Nuno conducted a lot of the early pilot work into the moss/mineral microcosms and trained me in a number of the requisite lab skills (sterile technique, tissue culturing etc.) I kindly thank Liam Dolan and Tim Lenton for their supervision, for having confidence in my abilities and for persuading me (at times) to get on with the things that mattered! I also thank Liam for sacrificing two of his holiday souvenirs for use as experimental substrates. Furthermore I thank my examiners: Alayne Street-Perrott and Brian Reid for their comments that helped to improve the final draft of this thesis.

For their warm welcome to The John Innes Centre (JIC), for showing me the ropes and generally creating a good atmosphere I thank the 'Rooties'. I also thank Tom Moore, Emma Greer and Heather Kingdom: Tom got me on the bar rota and Heather created the monster that is 'DJ Crouchie McGroovin'! Great times.

Brian Reid was particularly helpful in recommending a safe method for oxidising plant tissue which set me off of the right track with the moss biomass oxidation method development. Julian Andrews provided some very useful advice on petrology and appropriate methods of analysis as did Tom Bell on how to treat non-detects in a dataset. I thank Colin Goldblatt for bringing me some rocks back from the Lake District and Paul Disdle for showing me how to cut them up. I also thank Rich Boyle for many stimulating discussions on weathering!

For their expertise on matters analytical I thank Graham Chilvers (ICP Spectroscopy Technician), Keith Weston, Kim Wright and Jim Hunter (Nutrient Auto-Analyser). I also thank Bertrand Lézé (Technician i/c XRF). People at JIC who deserve special thanks include Roy Dunford for general advice and helping me find things and Andrew Davis who took superb photos of the microcosms. I also thank Mary-Anne Sangarde and her team in media preparation and Gary Creissen who conducted the light measurements. I kindly thank ELSA (Earth & Life System Alliance) for funding bench fees, instrumental and some consumable

costs and for allowing me to be a part of such an exciting collaboration. I am sure that the future of the Alliance will be an extremely bright one indeed.

At a personal level I thank my friends for their support: particularly Matt Tucker, Alys Earl, Beth Bradshaw, Sophie Fleming, Antoine Peraldi, Matt Watkins, Karina Hudek, The Paxtons and anybody else who supported and encouraged me. I also thank my brother for his periodic, stupid text messages (and for answering mine) and Nan and Malc for their support. Finally; I thank my Mum and Dad for funding and for putting up with all my seemingly recondite enthusiasms over the years!

1: Introduction

1.1 Motivation and Impetus for this Study

The motivation for this study was a need to determine whether or not moss weathers (breaks down as a result of its growth) various rocks and minerals and, if the moss does weather the rock, to determine the factor of increase of this weathering. This factor of increase is known as the 'Biotic Enhancement of Weathering' (e.g. Aghamiri & Schwartzman (2002) and Lenton & Watson (2004)).

The impetus for conducting this study was the need to test a novel hypothesis of Prof. Tim Lenton[1] and Prof. Liam Dolan[2] that a glaciation in the late Ordovician period of Earth's history was caused by the effects of increased land-surface weathering by bryophyte-like organisms (bryophytes are a division of the kingdom *Plantae* which includes mosses). A number of pre-existing hypotheses link the late Ordovician with increased weathering but these hypotheses vary in nature (see Section 1.4, hereafter the '§' symbol is used to denote a section).

There is a paucity of studies into the effects of biota upon mineral weathering (as noted by Schwartzman (2000) and Berner (2004)). From the formation of Geology as a discipline in its own right (circa the mid-18th Century) up until as recently as the late 1960s; the potential of biota as an important force for denuding and altering minerals and providing useful chemicals for other, evolving biota was largely unrecognised (Street-Perrott & Barker (2008); Hazen (2009)). Credit must be given to Vladimir Vernadsky, G. Evelyn Hutchison, Thomas Lovering and James Lovelock for trying to initiate a less reductionist approach to geology over this period. This dogma occurred largely as a product of a prevailing reductionist method that caused geologists to centre on more physical processes (such as vulcanism) to the detriment of studies into biota. Such a situation need not have occurred had geologists heeded more closely the words of a man often described as 'The Father of Geology', James Hutton. Hutton once wrote that he considered "the Earth to be a super-organism and that its proper study should be by physiology" (cit. in Lovelock (1979); UNU (1992)). In other words Hutton advised that a

[1] School of Environmental Sciences, University of East Anglia, NR4 7TJ, UK.
[2] Now at: Department of Plant Sciences, University of Oxford, OX1 3RB, UK.

non-reductionist, systems-based approach should be adopted when studying the Earth. This study will attempt to emulate such an approach.

1.2 The Ordovician

1.2.1 Introduction

The Ordovician is a system period in geological time that lasted between 488.3Ma (±1.7) (Million years ago) and 443.7Ma (±1.5) (NB all ages used in this thesis shall be those of Gradstein *et al.* (2004), as approved by the International Commission on Stratigraphy (ICS)). During the Upper Ordovician (460.9Ma ±1.6 to 443.7Ma ±1.5) the southern continents collected into a single supercontinent known as Gondwana (Crowley & Baum, 1991) (See Figure 1.1).

1.2.2 Glaciation

The precise onset of the Ordovician glaciation, the causes and the length of its duration are subject to debate (e.g. Brenchley *et al.* (1994); Pope & Steffen (2003), arguing for a short and long glaciation respectively). One point of consensus is that the Ordovician glaciation is unique in Earth's history in that its onset occurred during a period when the partial pressure of atmospheric carbon dioxide (pCO_2) was high (Pope & Steffen, 2003). Estimates vary, but pCO_2 in the Ordovician is estimated at 10-18 times greater than the Present Atmospheric Level (PAL) (*Op. cit.*, Yapp & Poths (1992)).

System Period	Series Epoch	Stage	Age at start (Ma)	Error (±Ma)
Silurian				
Ordovician	Upper	Hirnantian	445.6	1.5
		Katian	455.8	1.6
		Sandbian	460.9	1.6
	Middle	Darriwilian	468.1	1.6
		Dapingian	471.8	1.6
	Lower	Floian	478.6	1.7
		Tremadocian	488.3	1.7
Cambrian				

Table 1.1 – Geologic Time in the Ordovician (After Gradstein *et al.* (2004)).

It was previously thought that the Ordovician glaciation was a short-lived (<1Ma) event in the Hirnantian (see Table 1.1) (e.g. Brenchley *et al.* (1994)), there is however an increasing body of evidence that the glaciation began in the Middle Ordovician and ended in the late Hirnantian (e.g. Pope & Steffen (2003); Saltzman & Young (2005)). Such hypotheses are based on isotopic ratios contained within sediments formed in the Ordovician through a science known as Chemostratigraphy (see §1.4). Figure 1.1 (below) shows the position of Earth's continents in the late Ordovician

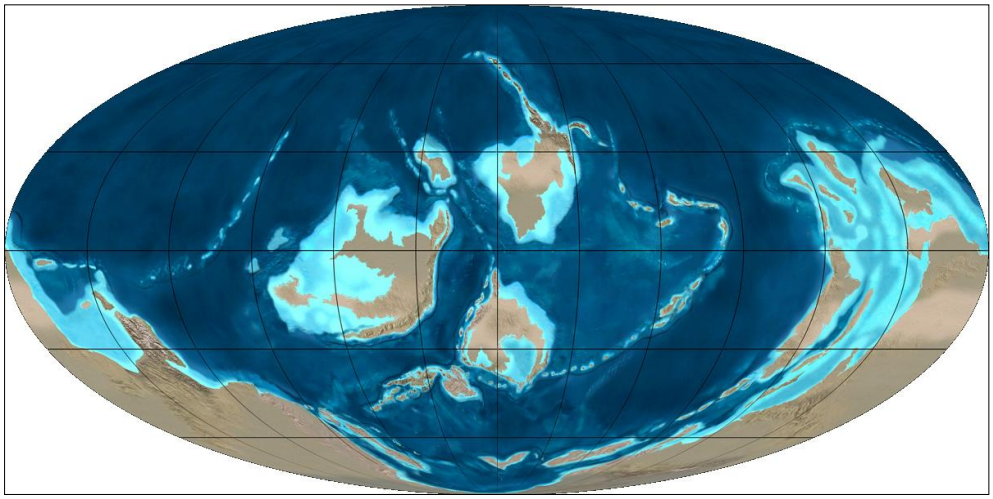

Figure 1.1 – Earth's continents during the Upper (late) Ordovician (≈450 million years ago) represented as a Mercator's projection. During the Upper Ordovician the southern continents gathered to form a single supercontinent: Gondwana. Graphic reproduced from Blakey (2009).[3]

[3] Reproduced under a Creative Commons Attribution ShareAlike 3.0 license.

1.3 The Geochemistry of Weathering and the Long-Term Carbon Cycle

As a plant grows its rootlets secrete organic acids and chelates which break down nutrient cations (Moulton & Berner, 1998). Upon the death of the plant (or parts of it) the decay of organic matter produces further organic acids and carbonic acid (H_2CO_3) (*Op. cit.*) These effects can be termed 'Biotic Weathering'. Weathering can also occur due to abiotic effects, for example: atmospheric carbon dioxide dissolving in water also forms carbonic acid (the affect of this reaction is likely to have been more important in the Ordovician period when the pCO_2 was higher than PAL).

Biotic weathering occurs as a result of physical and chemical effects; physical effects include the hydraulic pressure of plant roots breaking a substrate apart whereas chemical weathering refers to the hydrolysis of minerals by acids (Graham *et al.*, 2010). The focus of this thesis will be upon chemical weathering (the hydrolysis of minerals by acids, in this case resulting from mosses) though it is important to note that the two processes do not operate independently of each other.

Mineral weathering of calcium and magnesium-silicate compounds leads to the liberation of calcium and magnesium cations (Ca^{2+} and Mg^{2+}) which in a three-stage reaction with atmospheric CO_2 forms two bicarbonate ions ($2HCO_3^-$). These reactions are known as the Urey reactions (after Harold Urey 1893-1981). If $CO_{2\,(g)}$ is taken to react with a generalised Calcium-Silicate mineral ($CaSiO_3$), the reactions that take place can be represented as shown in Equation 1.1 (below).

$$1:\ 2CO_2 + 3H_2O + CaSiO_3 \rightarrow Ca^{2+} + 2HCO_3^- + H_4SiO_4$$

$$2:\ Ca^{2+} + 2HCO_3^- \rightarrow CaCO_3 + CO_2 + H_2O$$

$$3:\ H_4SiO_4 \rightarrow SiO_2 + 2H_2O$$

$$\mathbf{CO_2 + CaSiO_3 \rightarrow CaCO_3 + SiO_2}$$

Equations 1.1 – The Urey reactions (Berner, 2004), the sum of all three reactions given in bold. Note that for every two moles of $CO_{2\,(g)}$ only one mole is sequestered in these reactions.

If this reaction is applied to a calcium bearing plagioclase the following reaction occurs:-

$$3H_2O + 2CO_2 + CaAl_2Si_2O_8 \rightarrow Al_2Si_2O_5(OH)_4 + Ca^{2+} + 2HCO_3^-$$

Equation 1.2 – An example of the Urey reactions: a plagioclase feldspar is weathered to kaolinite clay, liberating a Ca^{2+} cation and two bicarbonate anions into solution (Moulton & Berner, 1998).

The formation of the HCO_3^- ion in the Urey reactions, and its subsequent burial in the oceans (leading to the formation of calcium carbonate ($CaCO_3$)) is the key mechanism regulating atmospheric Carbon over time-scales greater than 10 million years (>10Ma) (Berner, 2004). The carbon cycle on time scales >10Ma is regarded as the 'Long-Term' or 'Geological' carbon cycle (Gibbs *et al.* (1997) and Berner (1998)). Figure 1.2 (below) shows a schematic diagram of the long-term carbon cycle:-

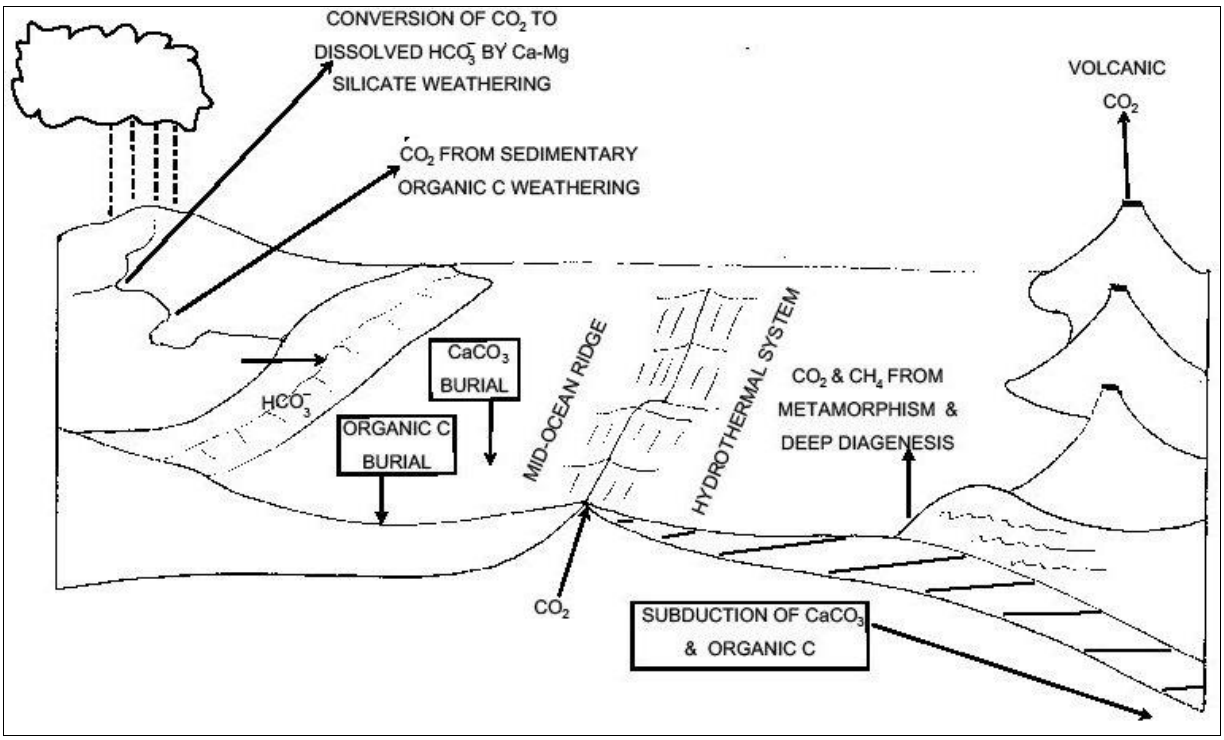

Figure 1.2 – The Long-Term carbon cycle (After Berner (2004)).

If the removal of $CO_{2(g)}$ from the atmosphere and the sequestration of the carbon fraction in the oceans as calcium carbonate ($CaCO_3$) or organic carbon reduces the atmospheric partial pressure of CO_2: air temperatures would be expected to decline as CO_2 is a greenhouse gas. A greenhouse gas is a gas present in the atmosphere which absorbs long-wave infra red radiation (heat) emitted from Earth's surface (Barry & Chorley, 2003). A decline in air temperatures could ultimately lead to changes in atmospheric currents which could initiate a glaciation (*Op. cit.*) Once a glaciation is initiated positive feedback processes occur, e.g. the ice-albedo (reflectivity) feedback, that cause more heat to be lost from Earth's surface further promoting the glacial state (*Op cit.*).

1.4 Chemostratigraphy

1.4.1 Carbon

The formation of the bicarbonate ion and its burial in the oceans can essentially be regarded as the following simplified process (the arrow representing weathering):-

$$CO_{2(g)} \rightarrow HCO_3^-{}_{(s)}$$

Over geological timescales the volume of carbon removed as organic carbon relative to the volume removed as carbonates is conserved at ~20‰ organic carbon (Lenton (2001); Fairchild & Kennedy (2007) etc.). Around 5% of the carbon in the system is re-emitted back to the atmosphere when oceanic crust is destroyed at destructive plate margins over timescales of ≥10Ma (Fairchild & Kennedy, 2007), and the carbon is released back to the atmosphere as $CO_{2(g)}$ via volcanoes (this is known as "degassing from the mantle") (*Op. cit.*).

Analysis of rocks formed from sedimentary deposits for the stable isotope Carbon-13 ($\delta^{13}C$) can reveal what fraction (f) of carbon was buried as carbonates (f_{carb}) relative to organic carbon (f_{org}) (*Op. cit.*). Isotopic mass balance requires that:

$f_{carb} + f_{org} = 1$

Equation 1.3 – Mass balance of $\delta^{13}C$ (After Fairchild & Kennedy (2007)).

Therefore any decrease or increase in carbon buried as organic carbon or carbonates results in a negative or positive excursion respectively from the isotopic standard (which in the case of carbonates is the Vienna Pee Dee Belemnite or 'VPDB' (Kump & Arthur, 1999)). These excursions are expressed as a per thousand (or 'per mille') deviation from standard (represented '‰') and calculated thus:-

$$\delta^{13}C = [(R_{sample}/R_{standard}) -1] \times 10^3$$

Equation 1.4 – Formula for calculating isotopic fractionation (Street-Perrott & Barker, 2008) where $R=\delta^{13}C/\delta^{12}C$.

Thus the magnitude of CO_2 released by mantle degassing on timescales >10Ma is -5‰. When several sedimentary rocks are analysed from different parts of (what was) Gondwana, data on carbon cycle fluxes in that particular period can be built up in a technique known as temporal isotopic fractionation.

1.4.2 The Ordovician

The chemostratigraphic evidence for the Ordovician glaciation lies in a positive $\delta^{18}O$ excursion in the Hirnantian from ~-9‰ in the Katian to ~-3‰ in the Hirnantian (Kump *et al.*, 1999). Positive $\delta^{18}O$ excursions indicate an increase in the build-up of land ice as $\delta^{18}O$ (being heavier than the $\delta^{16}O$ stable isotope) gets locked up in land ice (*Op. cit.*).

The main causes of the Ordovician glaciation are a matter of debate. A general matter of consensus appears to be that there was a large positive $\delta^{13}C$ excursion in marine carbonate of as much as +7‰ in the Hirnantian (443.7Ma) (Kump *et al.* (1999); Pope & Steffen (2003); Saltzman & Young (2005)). Saltzman & Young (2005) argue that there was an earlier, smaller $\delta^{13}C$ excursion of ~+3‰ at ~462Ma which roughly corresponds to the Darriwilian on the ICS timescale (henceforth known as the Darriwilian Excursion, see Figure 1.3, overleaf). Positive excursions in the $\delta^{13}C$ record indicate that an increasing proportion of carbon is being buried in the oceans in the form of HCO_3^- (see Equation 1.3) (Saltzman & Young, 2005) and is indicative of an increase in continental weathering (as an increase in continental weathering increases the flux of HCO_3^- via the Urey reactions) (Kump *et al.* (1999); Sheehan (2001); Saltzman & Young (2005)). If Saltzman & Young are correct and the Darriwilian Excursion represents the onset of the Ordovician glaciation; this would indicate that the glaciation lasted ~18Ma, with Pope & Steffen's estimate of 10-14Ma seeming reasonable. This is substantially longer than the 1Ma glaciation suggested by Kump *et al.* (1999) and others.

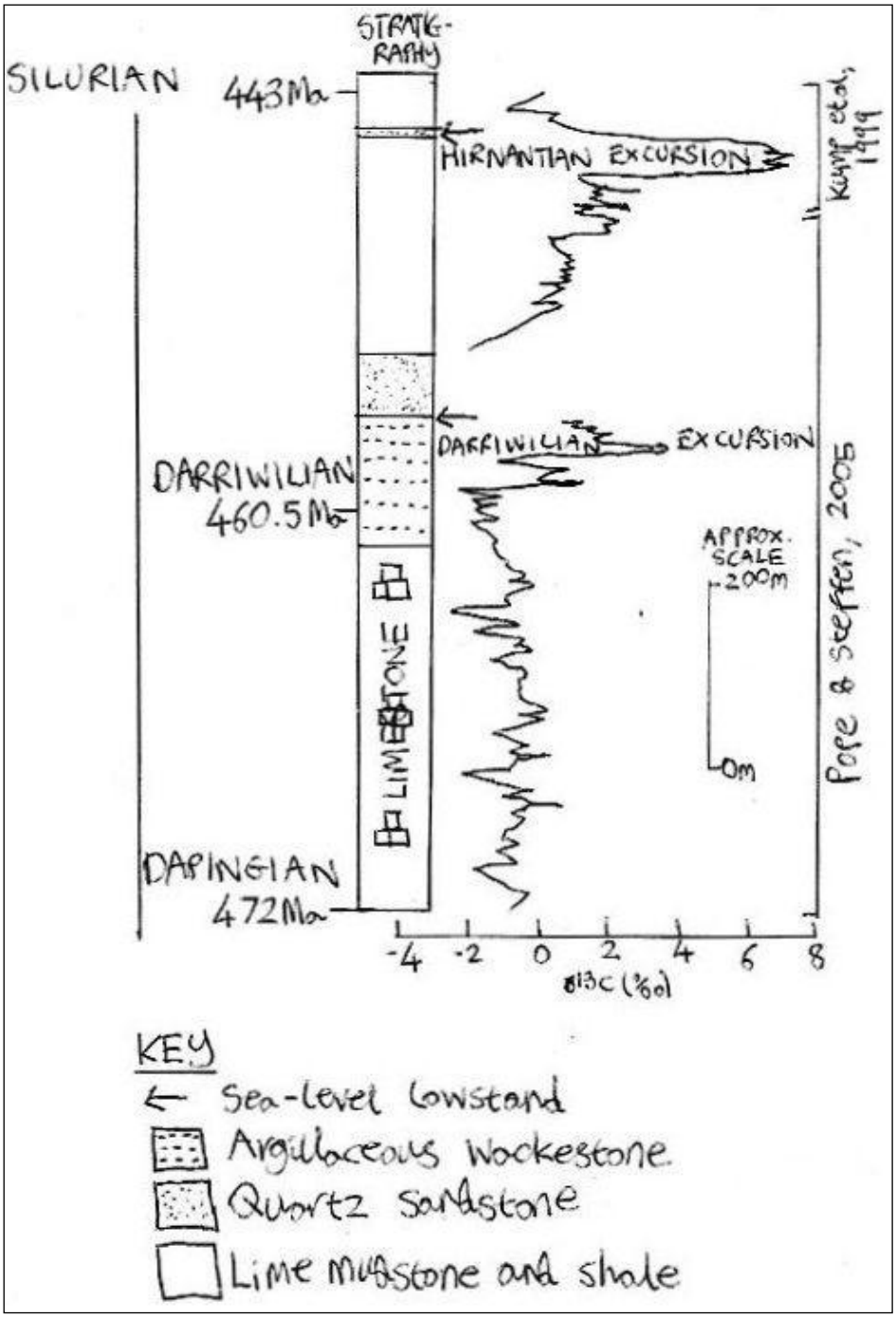

Figure 1.3 (Left) - $\delta^{13}C$ excursions and stratigraphy in the Ordovician (after Pope & Steffen (2003).

Another factor is that increasing continental weathering increases the net flux of phosphate (PO_4^{3-}) from the land surface to the oceans (Lenton, 2001). This phosphate then exerts a fertilising effect upon marine autotrophs which proliferate, fixing carbon from atmospheric CO_2 and burying it on the ocean floor as organic carbon upon their death (*Op. cit.*; Libes (1992)). This causes a decrease in atmospheric pCO_2 as a result of organic carbon burial (Lenton, 2001), an effect known as the 'biological pump' (Libes, 1992). This effect, along with increased organic and inorganic (HCO_3^-) carbon burial, may partially explain how

atmospheric pCO_2 was able to decline from levels 10-18x PAL to a threshold sufficient to trigger a glaciation Kump *et al.* (1999) suggest a threshold of ~10x PAL as sufficient).

In addition to the two $\delta^{13}C$ excursions; cores from the Copenhagen Formation in Nevada, USA (used to infer the Darriwilian Excursion) demonstrate a shift around the Lower/Middle Ordovician boundary (see Table 1.1) from a limestone stratigraphy to (in order of their appearance in the rock record) argillaceous clays, quartz sandstone and finally (around the beginning of the Katian stage age) mudstones and shales (*Op. cit.*). Whilst this was largely due to the Taconic Orogeny (mountain building period) (Gibbs *et al.* (1997); USGS (2003)); the shift from limestone (indicating that marine fauna is the major depositional material) to clays and sandstones (weathering products of terrestrial rocks) to mudstones (see Figure 1.3) could be indicative of increased terrestrial weathering and finally (once mudstones begin to form) an indication of substantial terrestrial colonisation by plants and substantial deposition of organic matter resulting from this. The phosphate burst and appearance of rock denudation products in the rock record are consistent with hypotheses linking increased weathering to the Ordovician glaciation (e.g. Kump *et al.* (1999) and others) and is supported by the spore evidence of Wellman *et al.* (2003) and Steemans *et al.* (2009). Indisputably; other factors such as an increase in the albedo of the south-pole (e.g. Kump *et al.* (1999)) as Gondwana glaciated are of key importance. Gibbs *et al.* (1997) suggest that of the aforementioned glaciation inducing factors; atmospheric pCO_2 is the most important factor in initiating short (<1Ma) glaciations whereas changes in continental positioning (affecting radiative balance and deep ocean currents) are important in triggering longer (>1Ma) glaciations.

1.5 Mosses

1.5.1 Moss Life Cycle

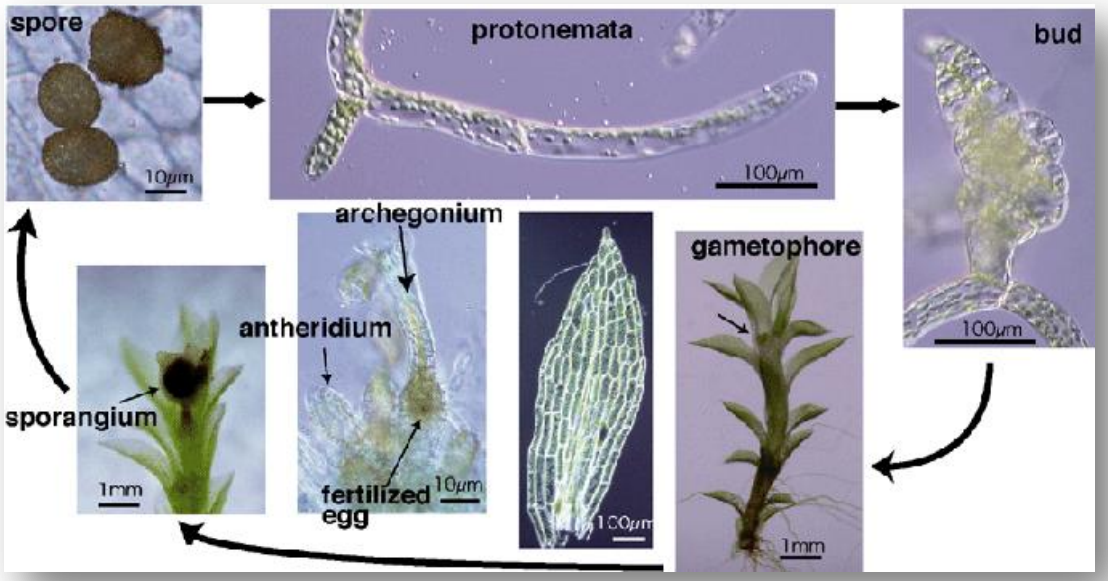

Figure 1.4 – Diagram of the moss life cycle (Source: Hasebe (2009). Figure reproduced with kind permission). Spores form the first stage of the moss life-cycle, followed by specialised cells known as chloronema or caulonema (collectively known as protonema). A bud then forms from the protonemata which eventually forms a haploid gametophyte. In the next stage of the life cycle the sex organs are formed, the moss is then capable of producing diploid sporangia completing the life-cycle.

Most stages of the moss life-cycle (from spore to gametophore) are asexual (haploid) (See Figure 1.4), only the final stage of the moss life cycle (sporangium, when spores are formed) is diploid (Reski & Cove, 2004). In the protonema stage: moss forms chloronema or caulonema cells (Schaefer, 2002). Chloronema cells are densely packed with chloroplasts (and so appear green) and grow upwards, caulonema cells contain far fewer chloroplasts (are less green) and are longer (*Op. cit.*). A moss will only reach the sporangium stage of development if environmental conditions (e.g. light, water and nutrients) are favourable (Taiz & Zeiger, 2002). The dominant stage in the moss life-cycle is the haploid gametophore stage whereas in the seed plants of today the dominant stage is the diploid sporophytes (Reski & Cove, 2004).

Mosses are land plants (embryophytes). The mosses of today have evolved with few changes from the first embryophytes (*Op. cit.*). Like all other embryophytes mosses derive their organic carbon from photosynthesis.

1.5.2 Paleobotany

It is believed that the earliest land plants (embryophytes) were bryophyte-like in structure and physiology (Steemans *et al.*, 2009). The period when bryophytes evolved is the subject of some controversy and the search for evidence to ever more precisely define the date of their evolution is the subject of much active, ongoing research. The main problem is that bryophyte tissues do not contain lignin and are instead composed of easily degradable tissues (Baars *et al.*, 2008), therefore bryophyte tissues do not fossilise easily, if at all (Wellman *et al.*, 2003). In order to pin-point the date of evolution of bryophytes one has to look for the presence of their primitive spores (cryptospores) within sediment cores (*Op. cit.*) a science known as Palynology.

The oldest "uncontroversial" record of cryptospores dates to the Darriwilian Stage Age of the Middle Ordovician (Steemans *et al.*, 2009) (the age of the Darriwilian $\delta^{13}C$ excursion) . Another (unpublished) study dates bryophyte radiation to >475Ma (UBC, 2010). In Steemans *et al's* study the most abundant spores recovered from Upper Ordovician sediments from a corehole taken in Saudi Arabia (in what was the northwest margin of Gondwana (Wellman *et al.*, 2003)) were cryptospores (Steemans *et al.*, 2009). This provides strong evidence that bryophyte-like organisms were well established in the late Ordovician, substantially earlier than previous estimates that dated this radiation to the Silurian (443.7Ma ±1.5 to 416.0Ma ±2.8) or even the Lower Devonian (416.0Ma±2.8 to 397.5±2.7). Furthermore cryptospores have been identified from cores across the globe and show "surprisingly little temporal and spatial vegetation… (Suggesting) a worldwide cosmopolitan flora" (Wellman *et al.*, 2003). Coupled with the fact that like the spores of extant (currently living) plants, the cryptospores are found in non-marine sediments and when they do occur in marine sediments their "abundance declines offshore" (*Op. cit.*), there is a strong body of evidence for widespread land colonisation of bryophyte-like organisms in the Ordovician. Stated simply: whilst current evidence suggests that mosses had not evolved by the Upper Ordovician, organisms with a

similar anatomy to mosses had evolved and had colonised a substantial portion of Earth's surface (Steemans *et al.*, 2009; Wellman *et al.*, 2003).

1.5.3 Moss Nutrient Requirements

Mosses require 19 essential elements for growth (Taiz & Zeiger, 2002). Carbon, hydrogen and oxygen are essential nutrients and are provided by ambient carbon dioxide and liquid water respectively (*Op. cit.*). The other 16 elements are referred to as 'Mineral Nutrients' and are provided by soil or nutrient media (*Op. cit.*). Eight of these essential mineral nutrients are of particular relevance to this thesis (see Table 1.2, overleaf).

Nutrient	Chemical Symbol	Key Functions
Calcium	Ca	Used to form the calcium pectate middle lamella of cell walls. Essential co-factor for some enzymes that hydrolyse ATP and phospholipids (the key cell-membrane component). Also involved in cell signalling for metabolic regulation.
Iron†	Fe	Component of iron proteins involved in photosynthesis and respiration.
Potassium	K	The key cation involved in osmoregulation by ensuring enough water is uptaken by a cell to maintain turgidity and cell electroneutrality. Essential co-factor for >40 enzymes.
Magnesium	Mg	Key constituent of chlorophyll molecule. Required by many phosphate transfer enzymes.
Sodium†	Na	Substitutes for K as an osmoregulator.
Silicon	Si	As amorphous silica: is a key cell-wall component facilitating rigidity and elasticity.
Phosphorus	P	Constituent of: ribose-phosphate component of nucleotide bases which form DNA, nucleic acids, phospholipids. Has a key role in reactions involving ATP (the biological energy currency).
Aluminium‡	Al	Plants typically contain 0.1-500ppm Al in their tissues (i.e. micronutrient quantities) and low levels of Al have been demonstrated to stimulate plant growth (Marschner, 1995 cit. in Taiz & Zeiger (2002)). However, Al is not generally considered to be a micronutrient.

Table 1.2 – Eight nutrient elements essential for moss growth and their key functions (After Taiz & Zeiger (2002)). All nutrients are macronutrients except for Fe and Na (†) which are considered micronutrients because they are required in lower concentrations relative to the macronutrients and Al (‡) which is not generally considered to be a nutrient, but possesses micronutrient qualities (*Op. cit.*).

Table 1.3 (below) shows the typical concentrations of the elements featured in Table 1.2, and their broad classification as either plant macronutrients or plant micronutrients:-

Macronutrients	Micronutrients
K (1.0%)	Fe (100ppm)
Ca (0.5%)	Na (10ppm)
Mg (0.2%)	Al? (0.1-500ppm)
P (0.2%)	
Si (0.1%)	

Table 1.3 – The mineral nutrients arranged highest-lowest according to their typical concentration in dry plant tissue given as a percentage for macronutrients and in parts per million (ppm) for micronutrients (After Taiz & Zeiger (2002)).

The experimental organism that was used in this work was *Physcomitrella patens* (henceforth known as '*P. patens'* or 'moss'). *P. patens* is the model organism for genetic studies of bryophytes (Reski & Cove, 2004) and is not known to grow on bare rock surfaces in the wild. However: Goffinet (2005) describes *P. patens* as an "Early pioneer on wet mineral soil" providing some indication that conditions rich in minerals but low in organic matter tend to favour the moss. Other recorded *P. patens* habitats include river banks and fields and it is distributed across continental and northern Europe, United States, southern Canada and western Siberia (*Op. cit.*).

Pilot experiments were conducted in October 2007 to determine whether or not moss protonemal tissue would grow on clay and vermiculite minerals and silica sand. These pilot experiments were purely visual and qualitative in nature to see if the moss gained green tissue whilst growing on these substrates. Results of these experiments indicated that the moss grows reasonably well on clay and vermiculite, increasing in size until it reaches the gametophyte phase. The moss did not grow on sand and died within 2-3 weeks. This is almost certainly because silica sand is devoid of essential nutrients for moss growth and is also highly unweatherable (Andrews *et al.* (2004) and Baars *et al.* (2008)).

An experiment was also conducted in which spores of *P. patens* were inoculated onto clay to see if the moss could grow from the first stage of its life-cycle on the microcosms. Within eight months these spores grew in diameter from a size not visible to the naked eye to <1mm but did not grow any further. After 22 months the microcosms were highly desiccated and no further growth had occurred, indicating that moss could not be successfully grown from spores in microcosms on clay using the method established in this thesis. Once it was established that the moss could grow from protonemal inoculum on minerals, the moss was inoculated onto less-weatherable substrates (e.g. granite and andesite).

1.6 Petrology

1.6.1 Silicate Chemistry

Silicon is the second most abundant element in Earth's crust (after oxygen), its oxidised form Silica or Quartz (SiO_2) forms 65% by mass of Earth's crust (Andrews *et al.*, 2004). Consequently silicon is always the most abundant element in minerals, the fundamental building block of which is the SiO_4 tetrahedron. Depending on how the SiO_4 tetrahedra bond the resulting giant lattice takes the form of a number of different shapes (or 'polymorphs') (*Op. cit.*). Two such polymorphs are 'Sheet silicates' and 'Framework Silicates' (*Op. cit.*) (see Figure 1.5 overleaf).

Figure 1.5 (Right and Below) – Simplified, schematic diagrams of sheet (A) and framework (B) silicates (after (Andrews *et al.*, 2004)) demonstrating how the silicate tetrahedra bond into chain-like structures and how cations substitute into the space between the two silicate tetrahedral layers in framework silicates (B).

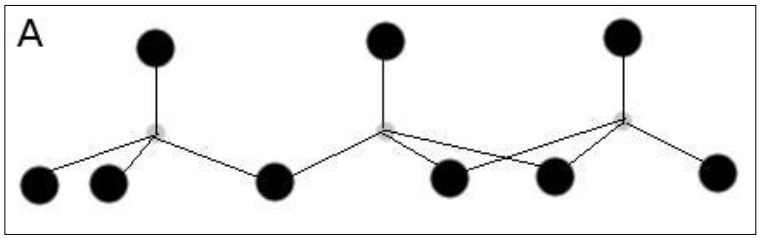

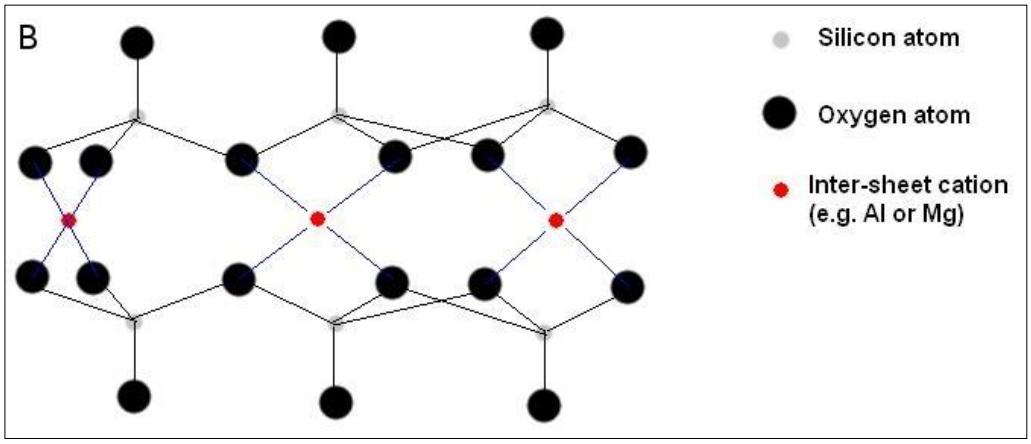

Figure 1.5B demonstrates how 'inter-sheet cations' (most usually Al but can be other cations such as Mg) substitute into the space between two silicate sheets. Examples of sheet silicates (A) include all the clay minerals and micas such as muscovite (Andrews *et al.*, 2004). The framework silicates (B) include feldspar minerals (*Op. cit.*).

1.6.2 Petrology of Experimental Substrates

Table 1.4 (overleaf) gives the key experimental substrates in this procedure and their key petrological characteristics:-

Substrate Name	Description
Andesite	Andesite is an igneous, volcanic rock containing a large proportion of feldspar (an aluminosilicate mineral) (Mackenzie & Adams, 1994).
Granite	Granite is an igneous rock containing ~70% Quartz (SiO_2) by mass of rock (Blatt *et al.*, 2006). Also contains feldspar (Mackenzie & Adams, 1994).
Vermiculite	Vermiculite is a framework, exfoliated aluminosilicate mineral that is chemically similar to smectite clay (Andrews *et al.* (2004); Deer et al. (1966)). It is formed by alteration of the mineral biotite or volcanic minerals (e.g. chlorites and hornblende) by either weathering or hydrothermal action (Deer *et al.*, 1966). Mg is the main inter-sheet cation (*Op. cit.*).
Clay	Clay minerals are sheet silicates formed by the weathering of other rocks (Andrews *et al.*, 2004). The chemical composition of clays varies depending on the extent of alteration (Deer *et al.*, 1966).
Basalt	Basalt is a fine-grained, plagioclase-rich, igneous rock (Mackenzie & Adams, 1994).
Chlorite	Chlorite has a layered structure similar to mica in which Mg, Al and Fe are susceptible to isomorphic substitution (Deer *et al.*, 1966).

Table 1.4 – The experimental substrates and their key petrological properties.

1.7 Measuring Weathering

Weathering cannot be directly measured, therefore other parameters have to be measured that are assumed to be proportional to weathering. Previous studies have used the thickness of secondary material formed as a result of weathering (the 'weathering crust') to calculate weathering rates (e.g. Jackson & Keller (1970)). Some studies (e.g. Jackson & Keller (1970); Ford Cochran & Berner (1996) etc.) have used *in situ* ion microprobe analysis to analyse rock surfaces colonised by biota and un-colonised rock to measure chemical differences indicative of weathering. Other studies (e.g. Moulton & Berner (1998); Aghamiri & Schwartzman (2002) etc.) exploit the fact that when ions are weathered they tend to enter the aqueous phase. This aqueous solution can be used as a matrix for chemical analysis, hence weathering can be

measured. Moulton & Berner (1998) describe "The flux of dissolved… cations, anions, and silica… (as a) sensitive indicator of the extent of silicate rock weathering".

All of the studies previously mentioned in this section are 'mesocosm experiments', that is to say: experiments that study real-world processes on a small-scale *in-situ*. This thesis reports the results from a 'microcosm study', meaning that experiments into real-word processes will be conducted on a very small scale *in-vitro* (in sterile conditions in the laboratory). There are two main benefits to microcosm experiments over mesocosm experiments:-

1. It is far simpler to control experimental variables (e.g. sterility, heating and lighting regimes) in a laboratory setting.
2. Microcosm experiments can be repeated many times at minimal cost compared with mesocosm studies (which tend to involve higher cost and the much greater logistical difficulties associated with work in the field).

Care must be taken with respect to point 1; over-controlling environmental variables can make experiments innately un-realistic and can have an adverse effect on experimental results (see White & Brantley (2003) for a discussion of this effect in a geochemical context).

1.8 Summary

Drawing on the commonality of a number of different studies into the potential causes of the Ordovician glaciation and the results of some very recent palynolological studies into bryophyte evolution and distribution, and the synergy between stratigraphic and palynological data e.g. the fact that the oldest record of bryophyte-like cryptospores (Steemans *et al.*, 2009) coincides with the first ('Darriwilian') $\delta^{13}C$ excursion, a very interesting hypothesis emerges. If this study proves that bryophytes significantly increase the biotic enhancement of mineral weathering it will lend weight to hypotheses regarding increased weathering as the 'smoking gun' of the Ordovician glaciation (Kump *et al.* (1999); Sheehan (2001); Saltzman & Young (2005)) and will establish a new hypothesis that early bryophyte-like organisms were responsible for this increased weathering.

A literature search using ISI Web of Knowledge, Web of Science[4] and Google Scholar[5] revealed no precedent for microcosm studies into the biotic enhancement of mineral weathering by moss. The literature search was conducted on 2/1/2010 using the search terms 'microcosm AND moss AND weathering', and the only similar study was Baars *et al.* (2008) which concentrated on the effects of carbon dioxide saturation on the soil zone.

The primary aim of this study will therefore be to measure the biotic enhancement of mineral weathering on different rocks and minerals in a microcosm study. The resulting data will be used to validate or falsify the null and alternative hypothesis outlined in the following section. Figure 1.6 (below) shows photographs of a microcosm.

Figure 1.6 - Side and plan views of a Basalt microcosm (after a weathering period of 138 days).

[4] http://apps.isiknowledge.com
[5] http://scholar.google.co.uk

1.9 Conceptual Framework

If $W_{abiotic}$ = abiotic weathering measurable by the method to be employed in this study, W_{biotic}= biotic weathering measurable by the method and W_{moss} = the amounts of analytes resulting from moss recovered from moss colonised ('mossed') microcosms, the following can be deduced:-

$$W_{total} = W_{abiotic} + W_{biotic} + W_{moss}$$

Equation 1.5 – Total weathering must equal the sum of abiotic weathering, biotic weathering and weathered ions uptaken by the moss.

For the purposes of this study the amounts of analytes contained within the aqueous solution removed from control microcosms after correction for the relevant blanks will be assumed to represent abiotic weathering (henceforth referred to as W_a). The amounts of analytes contained within the aqueous solution resulting from mossed microcosms will be taken to represent total aqueous weathering, after correction for the relevant blanks (i.e. both abiotic and biotic aqueous weathering) and will henceforth be referred to as W_b. After correction for the relevant blanks W_{moss} must represent the amount of analyte resulting from weathering that is taken up by the moss. Given that W_b actually represents both abiotic and biotic weathering Equation 1.5 can be reformed thus:-

$$W_{tot} = W_b + W_{moss}$$

Equation 1.6 – Actual equation for total weathering (W_{tot}) inferred from the amounts of analytes contained within biotic (mossed) microcosm components.

Net biotic weathering (W_{netbio}), i.e. the additional weathering occurring in a microcosm as a result of biota being present, can be regarded as being:-

$$W_{netbio} = (W_b + W_{moss}) - W_a$$

Equation 1.7 – Calculation for net biotic weathering (W_{netbio}).

The biotic enhancement of weathering (Ψ) can therefore be defined as a factor of net biotic weathering divided by abiotic weathering thus:-

$$\Psi = \frac{W_{netbio}}{W_a}$$

Equation 1.8 – The Biotic Enhancement of Weathering calculation.

Where $\Psi \leq 1$ there is no measurable biotic enhancement of weathering, where $\Psi > 1$ there is biotic enhancement of weathering, measurable using the methods to be employed in this study. Below are a null (H_0) and an alternative (H_1) hypothesis related to the biotic enhancement of weathering:-

H_0 = W_{tot} for analyte x on substrate y is not statistically greater than W_a for analyte x on substrate y at the $P<0.05$ level. Analyte x is not biotically enhanced on substrate y.

H_1 = W_{tot} for analyte x on substrate y is statistically greater than W_a for analyte x on substrate y at the $P<0.05$ level. Analyte x is biotically enhanced on substrate y.

2: Experimental Methods

2.1 Overall Approach

The work reported in this thesis used an approach similar to Moulton & Berner (1998); Aghamiri & Schwartzman (2002) and others in that it exploited the fact that the products of weathering are removed from a rock's surface by water (in the natural environment this water takes the form of precipitation or the flow of rivers), the polar nature of the water molecule attracting weathered ions.

The experimental procedure itself was a microcosm study: the microcosms consisted of plastic jars into which a small amount of rock or mineral substrate was placed. Moss cells suspended in a constant volume of water were added to half of these microcosms and the other half had the same volume of water added and served as controls. Excess concentration of an analyte in the moss-colonised microcosms above the concentration present in control microcosms (after corrections for blanks etc.) can be assumed to result directly as a consequence of the moss weathering the rock (provided the procedure is undertaken correctly).

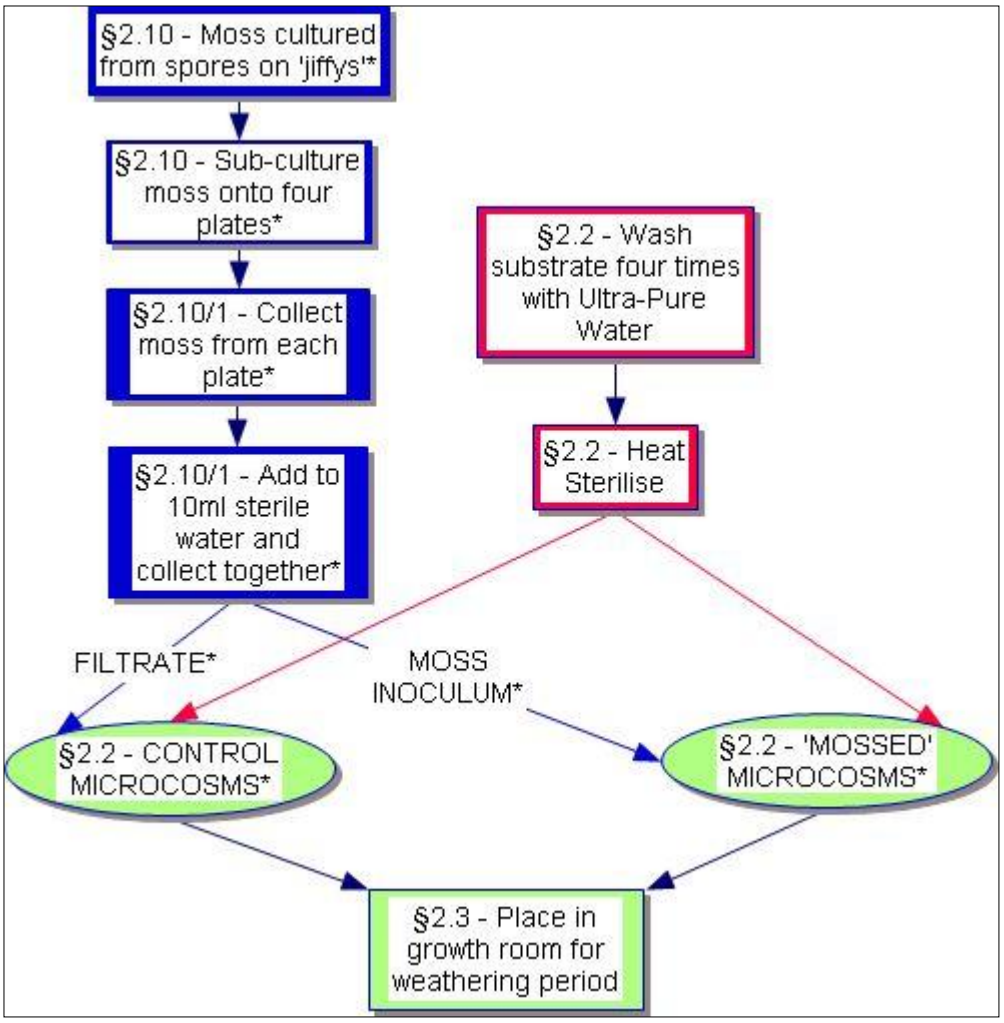

Figure 2.1 – Summary flow chart of key stages in the experimental procedure from the culturing of the moss on compost plugs ('jiffys') through to the weathering period of the microcosms with the section number where the process is discussed fully noted.

An asterisk (*) indicates that this part of the procedure was conducted using sterile technique (see §2.9).

As a number of new methods were developed during the experimental procedure a number of new terms were devised. Terms were also devised in order to adequately explain a concept as succinctly as possible. Devised terms are explained when they first appear.

2.2 Substrate and Microcosm Preparation

Table 2.1 (below) gives details of the experimental substrates, their sources and details of how substrate petrology was determined:-

Experimental Substrate	Source and Identification
Andesite	Supplied by: John Wainwright and Co. Ltd., Moons Hill Quarry, Radstock, UK. XRF analysed.
Granite	Bradstone Silver Granite supplied by: Aggregate Industries PLC, Hulland Ward, Ashbourne, Derbyshire, DE6 3ET, UK. Granite quarried in Penryn, Cornwall, UK. XRF analysed.
Vermiculite	Supplied by: Sinclair, Lincoln, UK. XRF analysed.
Clay	Of unknown origin. Supplied by a horticultural products company. No XRF analysis, examined using naked eye.
Basalt	A limited amount (one rock), collected in Indonesia. No XRF analysis, examined using naked eye.
Chlorite	Collected in the Dunmail Raise area of the Lake District National Park, England (OS Grid Ref. NY334073). XRF analysed.

Table 2.1 – The experimental substrates, their source and mode of identification. Andesite and granite formed the key experimental substrates.

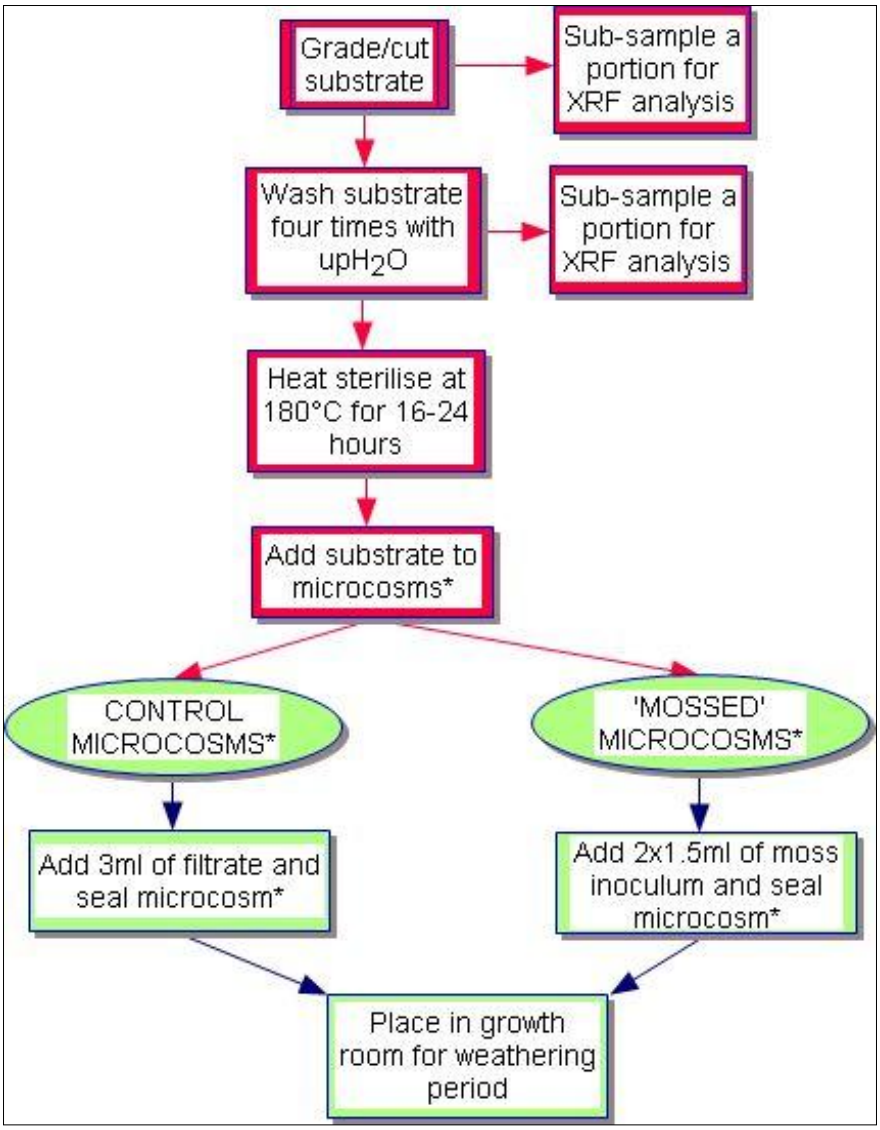

Figure 2.2 (Left) – Flow chart depicting the main stages in the substrate and microcosm preparation procedures. An asterisk (*) indicates that this part of the procedure was conducted using sterile technique (see §2.9).

Figure 2.2 (above) summarises the key stages in the substrate and microcosm preparation stages: basalt and chlorite rocks were cut into rectangular prisms ~20mm x ~10mm x ~5mm using a diamond tipped saw. Granite and vermiculite were simply graded using sieves decreasing in aperture size from 4mm at the top to 1mm at the bottom of the column. This column of sieves was placed into an Endecotts[8] test sieve shaker, and the substrate placed into the sieve with the largest aperture diameter at the top of the stack. The sieve shaker was then timed to shake for a period of 10 minutes. After 10 minutes the fraction yielding the most material was retained (>2.8mm for granite, >1.4mm for vermiculite), the remaining material

[8] Endecotts Ltd., 9 Lombard Road, London, SW19 3TZ, UK.

was discarded. After 10 minutes the clasts were well sorted. Only a limited number of experiments were conducted on clay, basalt and the chlorite rock due to a shortage of available material.

After grading/cutting the material was washed three times with ultra pure water (henceforth referred to as 'upH_2O') in order to remove any nutrients which may have been adsorbed to the surface of the substrate (the full washing protocol can be found in Appendix i.ii.i and an analysis of the washes can be found in Appendix ii.iii). Ideally, the only nutrients that should be present in the microcosm system are those within the substrate itself and those within the solutions added to microcosms in order to conduct the experiment. By sampling these fractions the budget can be closed, therefore any nutrients contained within the moss tissue (after correction for that contained within solutions added to the microcosms) must result as a consequence of weathering.

The substrate was then heat sterilised in order to kill any biota capable of weathering the substrate (e.g. fungi, bacteria). Substrates were sterilised in a 180°C oven for a period of not less than 16 hours and not more than 24 hours. Heat sterilising had the added effect of killing any biota that may have been present, whilst also driving off all water ensuring that dry substrate was used to prepare the microcosms. Substrates were frequently stored for prolonged periods (sometimes as long as 3 months) in between uses, material was stored in glass beakers covered with aluminium foil and was heat sterilised again prior to re-use as a precaution against contamination by biota.

In early pilot experiments (not analysed) the substrate was autoclaved instead of heat sterilised, resulting in the substrate becoming highly saturated with water. This was not ideal because there was no way of ensuring that the water was absorbed homogeneously throughout the substrate, and such varying dilution rates could adversely affect the data relating to ionic dissolution into the aqueous phase obtained at the end of the experiment. Samples of both washed and unwashed rock/mineral were taken for solid phase XRF analysis in order to determine the chemical composition of the substrate. For the substrates consisting of large clasts (granite, chlorite and basalt) approximately six clasts were added to a plastic screw-top jar[9] using sterilised forceps. The masses of granite added to the microcosms in the 30/4/08,

[9] Sterilin Ltd., Angel Lane, Bargoed, Caerphilly, CF81 9FW.

2/9/08 and 11/9/08 granite experiments were recorded, the mean mass of granite added in these three experiments being 23.66g (±4.70). Enough material was added to cover the bottom of the jar, as far as possible. For the finer-grained substrates (andesite, vermiculite and clay) an exemplar jar was set up with material added to a depth of ~6.5mm. This depth of material equated to a number of heaped spoonfuls and this number of spoonfuls was added to subsequent pots using a sterilised metal spoon.

Control microcosms were prepared by adding 3ml of filtrate using a 5ml air displacement pipette. The lids to the jars when then screwed down under a laminar flow hood (all pipette tips were autoclaved prior to use). Mossed microcosms were prepared by adding a total of 3ml of moss inoculum in 2x1.5ml increments in order to promote horizontal growth across the surface, rather than 'bunching up' the moss into one mass (for details on how moss inoculum and filtrate were prepared see §2.11). Tips were specially prepared for this purpose by cutting off the narrow ends using a razor blade (as the moss inoculum tended to get stuck). Care was taken to ensure that the same length was cut-off each tip as this could affect the volume pipetted. Moss rapidly settles at the bottom of a container, to avoid this; the inoculum was swirled gently by hand before the suspension was drawn into the pipette tip. The lids to the jars were then screwed down as previously described.

2.3 Microcosm Treatment

Jars were placed in a random fashion to avoid artefacts due to a lack of spatial heterogeneity within the growth room. Microcosms were grown for at least 90 days, except in cases where moss began to die sooner than this, in which case the microcosms were sampled as soon as possible after death occurred. Dead moss was observed to turn a shade of yellow/brown or a translucent, bleached colour. The mean weathering period across all experiments was 112 days. Within 24-72 hours of inoculation water condenses into droplets on the wall of the sterile jar. On sampling the microcosms a very small volume of water can also be found condensed on the lid. Table 2.2 (overleaf) summarises all of the microcosm experiments and their growth periods.

Substrate	Sample size (n)	Date microcosms were initiated	Date microcosms were sampled	Weathering period (days)
Clay	*Mossed = 6†, Control = 6†.*	*18/12/07*	*19/2/08*	*63*
Vermiculite	*Mossed = 6†, Control = 6†.*	*18/12/07*	*19/2/08*	*63*
Vermiculite	Mossed = 20, Control = 20.	14/2/08	24/7/08	161
Vermiculite	Mossed = 17, Control = 17.	17/2/09	22/7/09	155
Granite	Mossed = 9, Control = 10.	30/4/08	18/8/08	110
Granite	Mossed = 7, Control = 10	24/6/08‡	9/11/08	138
Granite	Mossed = 7†, Control = 10†.	15/8/08	15/12/08	121
Granite	Mossed = 15, Control = 14.	2/9/08	22/12/08	111
Granite	Mossed = 14, Control = 14.	19/12/08	29/4/09	100
Granite	Mossed = 14, Control = 14.	12/1/09	10/6/09	149
Granite	Mossed = 14, Control = 15.	30/7/09‡	18/9/09	50*
Chlorite	Mossed = 7, Control = 7.	24/6/08‡	4/9/08	72*
Chlorite	Mossed = 7, Control = 7.	15/8/08	15/12/08	121
Basalt	*Mossed = 7†, Control = 5.*	*24/6/08‡*	*9/11/08*	*138*
Andesite	Mossed = 7, Control = 7.	28/11/08	2/2/09	66*
Andesite	Mossed = 11, Control = 9.	2/12/08	22/6/09	202
Andesite	Mossed = 24, Control = 21.	25/1/09	2/7/09	158
No substrate, Inoculum only	Mossed = 14, Control = 0.	30/7/09‡	18/9/09	50*

Table 2.2 – The microcosm experiments arranged by substrate and then in chronological order. Proof of concept/method development experiments are italicised. n = n used to form data in §4 or Appendix iv (with microcosms used for photography, spilled samples etc. excluded) unless otherwise stated with '†' symbol. Shaded experiments were initiated by Nuno Pires and sampled by the author.

† n = total n of microcosms initiated.
‡ Same inoculum used across all substrates for that date.
* Microcosms sampled <90 days because moss was dying.

2.4 Sampling the Moss Biomass from Microcosms

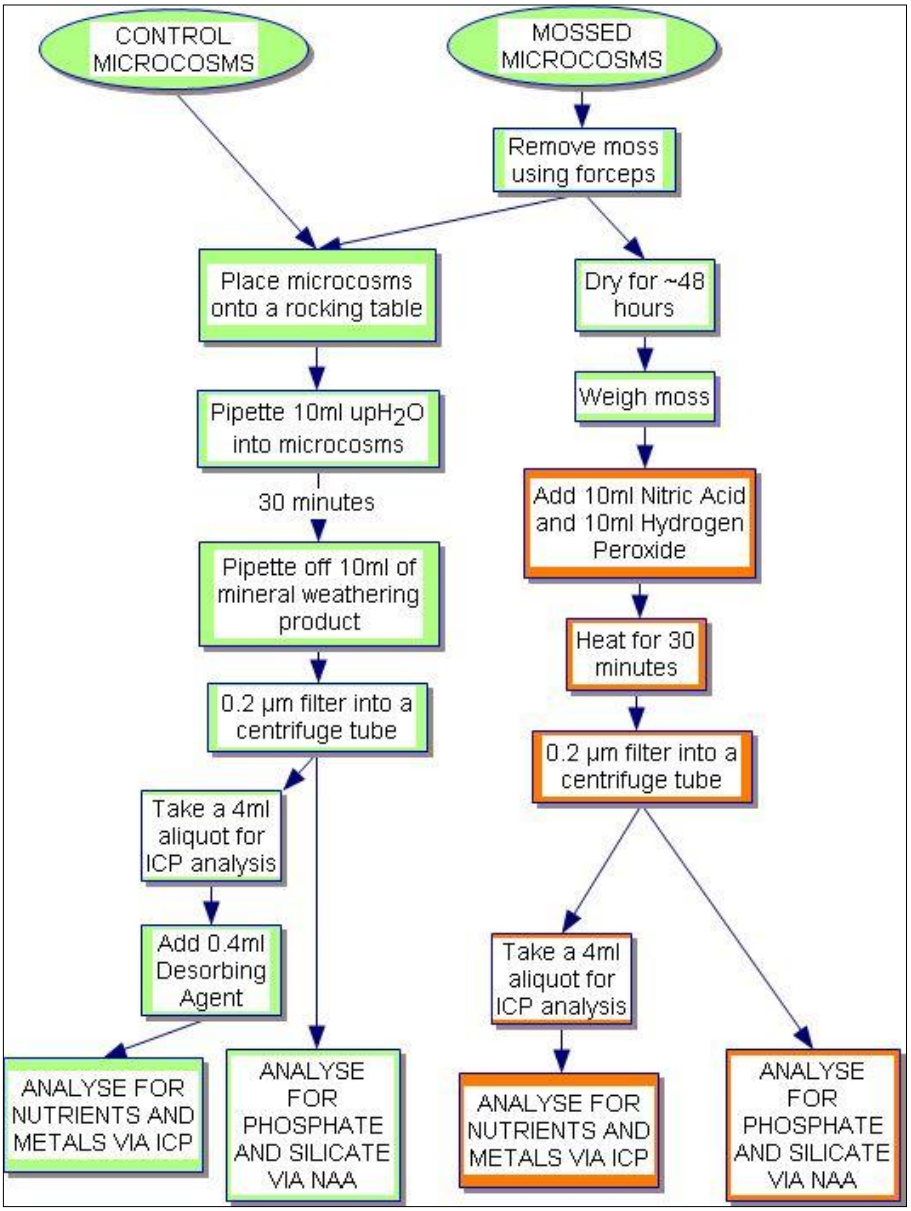

Figure 2.3 (Left) – Flow chart of the main stages in the microcosm sample preparation and sample analysis procedures
All stages in this flow chart were conducted using a clean but not sterile technique. For details on sample analysis see §3.

The microcosm sampling procedure was conducted on an open lab bench maintaining a clean but not sterile technique. In the case of mossed microcosms: the moss was removed from the microcosms using forceps and placed on filter paper. A 100ml plastic beaker was placed over the moss in order to minimise contamination. The moss was left to air dry for approximately 48 hours before being transferred to a new, pre-weighed 50ml centrifuge tube[10] (early pilot studies dried the moss in porcelain crucibles within a 55°C oven for 16 hours, but it was found

[10] Manufactured by: Corning Inc., One Riverfront Plaza, Corning, NY 14831, USA.

that a large mass of recovered moss was lost due to the moss adhering tightly to the crucible). The tube was then weighed again once the moss had been placed into the centrifuge tube (weighing was conducted using a balance with an accuracy of ±0.0001g) in order to give a mass of moss recovered from each mossed microcosm. The centrifuge tubes with moss were then stored at <4°C prior to wet oxidation.

It is important to note that in the large clast substrates (e.g. granite); some moss tissue remained in the microcosm after forcep removal (the mass of moss remaining in the microcosm being a small fraction of that which was recovered, one-tenth being a liberal estimate). For the fine grained substrates; it was very difficult to remove the moss biomass as the rhizines formed an extensive network between the small grains, causing moss and substrate to bind tightly together. This was especially the case for vermiculite microcosms due to the substrate's highly exfoliated morphology. Both the moss biomass from vermiculite (see Figure 2.4, below) and andesite microcosms were cleaned by placing the sample under a stereo microscope and cleaning with two forceps.

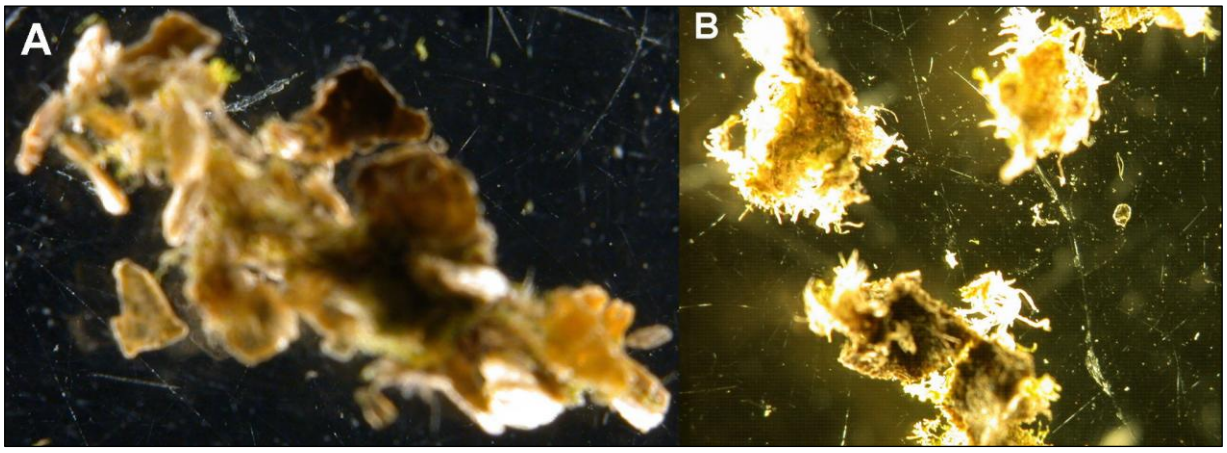

Figure 2.4 - Photomicrographs of moss and vermiculite removed from mossed microcosms. Micrograph A is an un-cleaned aggregation of vermiculite clasts bound by moss. Micrograph B shows vermiculite grains cleaned using forceps (at a higher magnification than Micrograph A). Protruding from the vermiculite clasts are *P. patens* gametophores attached to a soil-like vermiculite denudation product.

2.5 The Biomass Oxidation Method

2.5.1 Rationale

In order to determine the amounts of analyte within moss removed from microcosms and aliquots of the moss inoculum two key things were necessary:-

1: A method had to be found (or developed) to dissolve the nutrient and metal ions contained within the moss biomass as completely as possible.

2: The nutrient and metal ions within solutions then had to be measured using standard analytical methods available locally.

A literature search highlighted various methods employing concentrated acids and temperatures >100ºC (e.g. Sapkota *et al.* (2005) and Sucharova & Suchara (2006)). These methods were discounted because the risks were deemed to be unacceptable and because necessary equipment and facilities (e.g. a microwave autoclave and the facilities to handle strong acids) were not available locally and would have required highly specialised training. Therefore a new method had to be developed. Pilot oxidation experiments were conducted using tissue from the seed-plant *Arabidopsis thaliana* (for details of these experiments see Appendix i.i.i).

2.5.2 Methodology

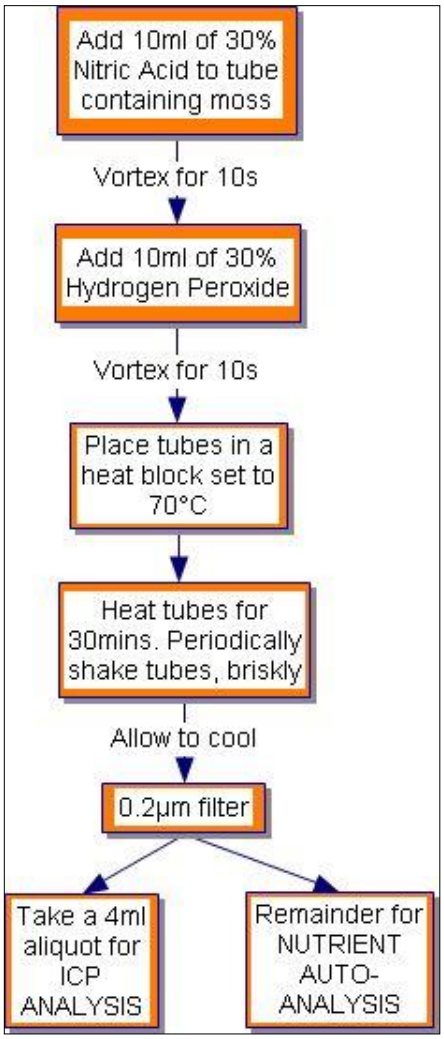

Figure 2.5 (Left) - Flow chart depicting the Biomass Oxidation Method. All stages in this flow chart were conducted using a clean but not sterile technique. Heating of acids was conducted in a fume cupboard and appropriate Personal Protective Equipment was worn at all times.

A heating block was set to 70°C and a centrifuge tube containing 20ml water and a thermometer was placed into it. Once the water reached 70°C (±5°C) the tubes containing moss and acid were heated for 30 minutes. Caps were kept loose for most of the procedure in order to allow oxygen gas formed as the Hydrogen Peroxide degrades to escape ($H_2O_{2(aq.)} \rightarrow O_{2(g)}$). Periodically the tubes were sealed and shaken briskly. The moss/acid mixtures were not allowed to exceed 75°C as at this temperature the solutions start to become unstable due to the more rapid evolution of oxygen gas.

After 30 minutes of heating the tubes were allowed to cool with the lids on top, outside of the heat block (but within the fume cupboard). Once the solutions had cooled to room temperature they were filtered using 0.2µm Sartorius Minisart® cellulose acetate syringe tip filters[11] (NB all filters used throughout the experimental procedure are of cellulose acetate type). The resulting samples were then stored at <4°C. The tubes should not be fully sealed but kept a ¼ turn loose as a precaution in case any more oxygen gas evolves

Early inoculum blanks (up to and including the 25/6/08 inoculum blanks) were frozen whilst the Biomass Oxidation Method was developed. All other inoculum samples were stored in a <4°C cold room for no more than two months. It is unlikely that the polypropylene plastic centrifuge tubes liberated contaminants into the oxidising solution at room temperature;

[11] Sartorius Stedim Biotech. GmbH, 37070 Goettingen, Germany.

however the author was concerned that the high temperatures encountered in the heating block may cause contaminants to be leached into solution from the centrifuge tube walls. Five tubes containing 20ml of upH_2O were therefore heated for 30 minutes with shaking in order to replicate the conditions encountered by moss samples during oxidations. This upH_2O was then analysed and the resulting data are given in Appendix ii.iv.

2.6 Sampling the Aqueous Solution from Microcosms

2.6.1 Introduction

Once the moss was removed from the mossed microcosms both mossed and control microcosms could be treated in the same manner and the resulting aqueous solution from all microcosms could be sampled.

Three different methods were used for microcosm water sampling during the method development phase before a suitable method was found. The method applied to each set of microcosm experiments is depicted in the table below:-

Microcosm water sampling method	Experiment/s method was applied to
1	October 2007 – Vermiculite and Clay
2	14/2/08 Vermiculite
3	30/4/08 Granite and all subsequent

Table 2.3 – The microcosm water sampling methods.

The changes in dilution factor brought about by these three different sampling methods have been corrected for during data analysis. Sampling Method 3 addressed the problem that the aqueous fraction from the microcosms was highly diluted by added upH_2O (by a factor of 23 and 18.6 for methods 1 and 2 respectively). The dilution factor for method 3 is 3.3.

2.6.2 Methodology

Fifteen microcosms at a time were placed onto a Luckham 4-RT rocking table[12] (see Figure 2.3, p42). The rocking table was switched on and 5ml of upH_2O was pipetted into the first microcosm, simultaneously a timer was started. Every minute 5ml of upH_2O was pipetted into the next microcosm in the sequence. After 15 mins had elapsed an extra 5ml of upH_2O was added to the first microcosm in the sequence and this process continued.

After 30 mins of elapsed time, 10ml of solution was drawn off of the first microcosm in two pipettings and placed into a new centrifuge tube. This process was continued every minute until 10ml of solution was drawn off of each microcosm. The 10ml resulting solution was then filtered using new 0.2µm filters into another centrifuge tube.

2.7 Photography

Plan and side photographs of the microcosms were taken in a studio, usually against a black background. Beads of condensation on the plastic jar sides frequently obscured the substrate and/or the moss, therefore swabs and a hair dryer had to be used to remove the condensation before photographing. Because of this treatment the aqueous solutions and moss from photographed microcosms were not sampled. Photographs can be seen in §4.3/4.4.

2.8 Cleaning Techniques

Two grades of ultra pure water were used in the procedure; some provided by an ELGA[13] Purelab® Mk.1 Option unit and some provided by the newer ELGA Purelab® Mk. 2 Genetic Ultra unit. Both of the 'ELGA' units intake reverse osmosis filtered, de-ionised water (henceforth known as dH_2O), pass it through a primary filter and then a secondary 'polishing' filter before treating the water with ultra-violet radiation to kill any biota. Water generated by the Mk. 1 unit had a resistivity of 15MΩ (pH 5.37), water generated by the Mk. 2 unit had a resistivity of 18MΩ (pH 5.13). Resistivity (MΩ) is inversely proportional to ionic

[12] Luckham Ltd., Burgess Hill, UK.
[13] ELGA Process Water, Marlow International, Park Way, Marlow, Bucks, SL7 1YL.

contamination (see Appendix ii.i.i). Unless otherwise stated 'upH_2O' refers to the 18MΩ water from the Mk. 2 unit. Ultra-Pure Water was stored in an aspirator which had been rinsed with a 5% solution of Decon 90®[15] (as per Spokes *et al.* (2000)) before rinsing with dH_2O until no foam was formed. A final rinse with upH_2O was then given.

Initially blanks of the ultra pure water were taken only when the aspirator was re-filled and sporadically between fillings. After 9/11/2008 blanks were taken on each day that a procedure was conducted using upH_2O. upH_2O blanks were taken from the beaker used to store the solution on the lab bench. Blanks were taken before experimental work commenced, by pouring upH_2O from the container directly into new centrifuge tubes which were then sealed prior to analysis by Inductively Coupled Plasma – Atomic Emission Spectrometry (ICP-AES, see §3.1/3.2).

2.9 Preparation of Cultures and Growth Conditions

Culturing and growth of the moss, preparation of the moss inoculum and preparation of the microcosms were all conducted using sterile technique (Taylor *et al.*, 1997). All of the processes were conducted under a laminar flow hood, the surfaces of which were pre-cleaned with a 70% ethanol solution. All metal instruments were treated with 70% ethanol solution and heated in a flame.

Where possible items of equipment (petri dishes, centrifuge tubes, serological pipette tips etc.) were purchased from suppliers who assured sterility by gamma irradiation sterilisation and hermetic sealing. Where items could not be purchased sterile (Gilson-type pipette tips, cellulose discs etc.) items were autoclaved using an Astell Scientific Swiftlock 2000/90[16] steam generator set to a programme of 121°C, for 20 minutes**.** Indicator tape was used to ensure that all autoclaved items had been exposed to steam. Sterile water was used extensively throughout the experimental procedure, which is upH_2O that is subsequently autoclaved in bijou jars (a small glass jar with a screw-top lid). Chemicals used in all parts of the procedure were of analytical reagent grade quality. Appendix ii.i.ii shows that there is less Al and Fe

[15] Decon Laboratories Ltd., Conway Street, Hove, East Sussex, BN3 3LY, UK.
[16] Astell Scientific Ltd, Sidcup, Kent, DA14 5DT, UK.

contamination in sterile water relative to 18MΩ (insignificant; 1σ error bars overlap), but significantly more Si contamination in the sterile water (possibly due to the fact that sterile water is autoclaved at high temperature and pressure in a silica glass bijou jar).

A clean technique was maintained by decontaminating lab-ware by Decon rinsing (as previously described) and then wrapping items with cling film, or sealing them at the top with cling film (e.g. beakers and measuring cylinders). Sterile technique had to take precedence over clean technique as it was imperative that the inoculum did not become infected with fungi as this could cause morbidity in the moss, and also introduce weathering artefacts due to acid exudates from the fungal hyphae (roots) (Hoffland *et al.*, 2004).

Moss cultures and microcosms were stored in a growth room. The growth room was maintained at 25ºC with a photoperiod of 16 hours light and 8 hours darkness, which is standard conditions for the culture of *P. patens* (Marienfeld *et al.*, 1989). The light was provided by two fluorescent tubes mounted above the shelves on which the cultures or microcosms were placed. Light flux and quality were measured using a Macam L300 Photometer[18]. Both fluorescent tubes radiated a total integrated light flux of 120µmol m^{-2} s^{1} (120µmol photons m^{-2} s^{1}) or 25.2W m^{-2}.

[18] Macam Radiometrics, 10 Kelvin Square, Livingston, Scotland.

2.10 Culturing of Moss Tissue

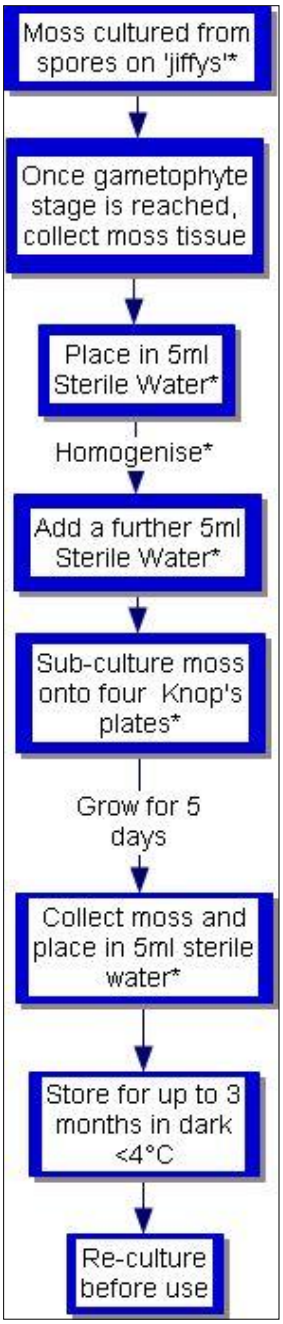

Figure 2.6 (Left) – Flow chart depicting the main processes in the moss tissue culturing procedure. An asterisk (*) indicates that this part of the procedure was conducted using sterile technique.

The moss was cultured from spores on autoclaved cylindrical plugs of peat enclosed in mesh (known as 'jiffys'). The jiffys were stored in a growth room until gametophores developed. The moss tissue was then collected and placed into a bijou jar containing 5ml of sterile water. The resulting moss-water suspension was homogenised for ten seconds using a Power Gen 500[19] homogeniser with polytron tips. A further 5ml of sterile water was added and the suspension was mixed by drawing into a 25ml serological pipette then egressing back into the bijou jar three times.

The suspension was then sub-cultured by dividing 2.5ml onto four plates containing solidified Knop's media (See Appendix i.ii.ii for full protocol). Knop's media is a low nutrient media containing KNO_3, $Ca(NO_3)_2$, KH_2PO_4, $MgSO_4$ and an iron salt (Taiz & Zeiger, 2002) and is the standard growth medium for *P. patens* (Marienfeld *et al.*, 1989). After five days in the growth room the moss was collected from each plate using a sterilised metal spatula, the moss from each plate was then placed into another 5ml bijou jar of sterile water, which could then be stored in the dark at <4°C for up to three months.

Prior to use the moss was re-cultured on Knop's plates in the same manner. Re-culturing is a standard procedure to ensure against fungal contamination. If fungal contamination did occur the fungus responsible tended to be red in colour, the red fungus strongly out-competing the moss with signs of fungal contamination being visible to the naked eye on some plates within four to six hours. All plates were checked for contamination prior to re-culturing using the naked eye and spot-checked using a stereo-microscope. Contaminated plates were isolated

[19] Thermo Fisher Scientific, Hudson, New Hampshire, USA.

from uncontaminated plates and 'killed' by autoclaving. Great care was taken not to use fungal contaminated plates for inoculum preparation; as a result only one microcosm across all experiments became contaminated with the red fungus (a microcosm in the 2/9/08 granite experiment which was excluded from the dataset).

After five days growth on Knop's plates the moss was removed, added to 5ml sterile water and homogenised. A further 5ml of sterile water was then added and the solution mixed in a pipette. The moss suspensions were then ready for use in inoculum preparation.

2.11 Moss Inoculum and Filtrate Preparation

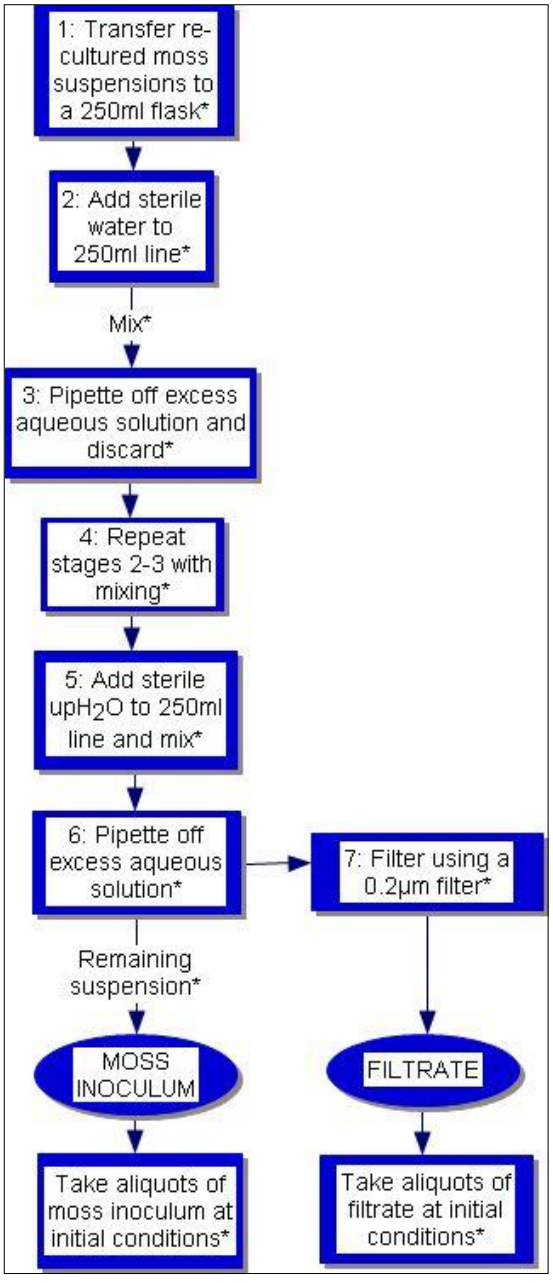

Figure 2.7 (Left) – Flow chart depicting the main stages in the moss inoculum and filtrate preparation procedures. An asterisk (*) indicates that this part of the procedure was conducted using sterile technique.

Using a 25ml pipette the moss suspensions were transferred to a sterile 250ml glass conical flask: sterile water was then added to the 250ml line and the solution was mixed using a pipette. Excess aqueous solution was then pipetted off until ~120ml of moss/water suspension remained (forming the first wash of the moss). The process was then repeated, giving a second wash of the moss with sterile water.

Sterile upH_2O was then added to the 250ml line (this was upH_2O that had been 0.2µm filtered into a separate sterile 250ml conical flask to exclude any biota that may be present). The suspension was then mixed and the excess aqueous solution was pipetted off and placed into a separate conical

flask until 80-120ml of concentrated moss suspension remained. The remaining concentrated moss suspension formed the moss inoculum and the excess aqueous solution (essentially the third wash of the moss inoculum) was filtered using a 0.2μm filter and is known as the 'filtrate'.

The volume of moss inoculum was measured before and after filtering the aqueous portion off. 12 inoculum pseudo-replicates were measured from five different inoculum preparations ($n \geq 2$ for each inoculum preparation). The mean volume of the inoculum before filtration was 19.0ml and the mean volume afterwards was 14.1ml indicating that 74.4% (±8.6%) of the moss inoculum was in the form of water. The washing procedure used to clean the moss and prepare it for inoculation and to prepare the filtrate is highly efficient at removing adsorbed contaminants and ensuring that the moss and filtrate are as clean as possible whilst maintaining the viability of moss as a living organism. Appendix ii.ii consists of graphs showing the levels of contamination present at the different preparation stages of the 29/7/09 inoculum.

3: Analytical Methods

3.1 Introduction

Three different analytical methods were used within the experimental procedure: an Inductively Coupled Plasma - Atomic Emission Spectrometer (henceforth known as the 'ICP-AES' or 'ICP') and a Nutrient Auto Analyser ('NAA') for aqueous phase analysis of the resulting solutions from microcosms and oxidised moss samples. An X-Ray Fluorescence Spectrometer ('XRF') was used for solid phase analysis of the rock and mineral substrates. ICP spectroscopy has been used in previous studies into the biotic enhancement of weathering such as Moulton & Berner (1998) and Aghamiri & Schwartzman (2002).

3.2 Sample Preparation

If not already done so samples were filtered using 0.2µm filters in order to prevent damage to the ICP's internal mechanisms (glassware such as the nebuliser is particularly susceptible to damage from fine solids) (Lajunen & Peramaki, 2004). The samples were then split into two aliquots: one for ICP analysis and another for Nutrient Auto-Analysis (NAA) and as a backup ICP sample in case of instrumental failure or other loss. A separate syringe and filter were used for each sample to prevent contamination (except pseudo-replicated samples and the substrate washes). In the case of the substrate washes (particularly for the initial washes of the fine-grained substrates) the filters clogged very quickly, and it was not uncommon to have to use three filters on one 50ml sample. Samples were then stored at <4°C. Samples were not routinely frozen (as suggested by Parsons *et al.* (1984) as previous experiments have shown that 15ml and 50ml centrifuge tubes manufactured by two different companies routinely crack at -20°C, resulting in sample loss (Crouch, 2007). Parsons *et al.* (1984) advise storing 50ml of sample in a 125ml screw-cap polyethylene bottle at -20°C if analysis cannot be conducted immediately, this reference was only discovered after conducting the experimental procedure, and in future this approach should be adopted where possible.

A 10% hydrochloric acid/upH_2O solution was added to ICP aliquots and blanks in a volume ratio of 1:10 hydrochloric acid:sample in order to desorb any metal ions which may have

adsorbed to the side of the centrifuge tubes (Lajunen & Peramaki, 2004). The 10% hydrochloric acid (henceforth known as the 'desorbing agent') was added and the samples lightly shaken immediately prior to an ICP run. Blanks of the desorbing agent were also taken at this point. This method assured (as far as possible) that contamination from the desorbing agent remained uniform across all samples in a run. Early desorbing agent (1/2/08 batch, used to desorb ICP runs 1-4 inclusive) was stored in a glass container and was subsequently found to be substantially contaminated with Al, Ca, K, Na and (particularly) Si. Contamination in this batch was 1-2 magnitude greater for these analytes than subsequent batches which were stored in polypropylene. Contamination of solutions stored in glassware by the glass itself is a known phenomenon (especially Si dissolution from glassware, even by relatively weak acids) (Liss & Spencer (1969) and Zhang *et al*. (1999)). The experimental implications for the contamination in this batch was that if the weathering signal was smaller than the contamination from glassware the weathering signal could be 'drowned out' by the contamination signal.

The only ICP samples which were not desorbed in the aforementioned manner were the moss oxidations as these samples already contain 2ml of their 4ml ICP volume as nitric acid, which is also a candidate desorbing agent (Lajunen & Peramaki, 2004). Furthermore: the reaction between hydrochloric acid and nitric acid could promote the evolution of toxic chlorine gas.

3.3 ICP-AES Analysis

3.3.1 Introduction

A Varian† Vista Pro Inductively Coupled Plasma, Optical Emission Spectrometer was used to determine the concentrations of the following analytes:-

ICP Analyte	Symbol	Emission Wavelength λ (nm)
Aluminium	Al	396.152
Calcium	Ca	422.673
Iron	Fe	259.940
Potassium	K	766.491
Magnesium	Mg	285.213
Sodium	Na	589.592
Silicon	Si	251.611

Table 3.1 – Table showing ICP-AES analytes and the emission wavelengths used to measure the concentration of those analytes (NB different emission wavelengths can be used to avoid spectral-overlap interference which could lead to erroneous concentrations being recorded for an analyte (Lajunen & Peramaki, 2004).

The ICP was fitted with a Varian SPS 5 sample preparation system for automated sampling. The concentration of samples was recorded automatically on a linked PC using Varian Vista Pro software. These data were then exported into Microsoft Excel.

3.3.2 Calibration

The ICP was calibrated using five standards. Two working standards were prepared using SpexCertiPrep[20]® ClaritasPPT® certified reference standards and ultra-pure (18MΩ) water supplied via a Milli-Q™ Advantage A10 system[21]. One working standard was a mixed elemental standard containing Al, Ca, Fe, K, Mg and Na and the other was a single elemental standard containing Si. This working standard was used to prepare five calibration standards, The concentrations of which are given in Table 3.2 (overleaf).

† Varian Inc., Palo Alto, California, USA.
[20] SpexCentriPrep Inc., 203 Norcross Avenue, Meutchen, NJ08840, USA.
[21] Millipore (UK) Ltd., 3-5 The Courtyards, Hatters Lane, Watford, Herts., WD18 8YH, UK.

	[Al]	[Ca]	[Fe]	[K]	[Mg]	[Na]	[Si]
Standard 1	0.7412	99.8004	0.3581	25.5766	41.1438	130.4928	7.1211
Standard 2	1.4825	199.6008	0.7162	51.1531	82.2876	260.9856	14.2422
Standard 3	2.2237	299.4012	1.0744	76.7297	123.4314	391.4785	21.3633
Standard 4	2.9650	399.2016	1.4325	102.3062	164.5752	521.9713	28.4844
Standard 5	3.7062	499.0020	1.7906	127.8828	205.7190	652.4641	35.6056

Table 3.2 – The ICP-AES standards (figures in μmol l^{-1}). Standards were prepared in mg l^{-1}, hence the non-round numbers.

Table 3.3 and Figure 3.1 (below and overleaf) give an example of the calibration data obtained by the ICP, in this case; the calibration for Al in Round 10:-

	Standard Concentration	ICP Calculated Concentration	Error
Blank	0.000000	0.000000	0.000
1	0.020000	0.019228	-0.001
2	0.040000	0.039002	-0.001
3	0.060000	0.059160	-0.001
4	0.080000	0.079412	-0.001
5	0.100000	0.101530	0.002

Table 3.3 – Standard concentrations [mg l^{-1}], their concentration as determined by the ICP [mg l^{-1}] and the difference between the ICP determined concentration and the standard (given as an error to 3 decimal places (d.p.)).

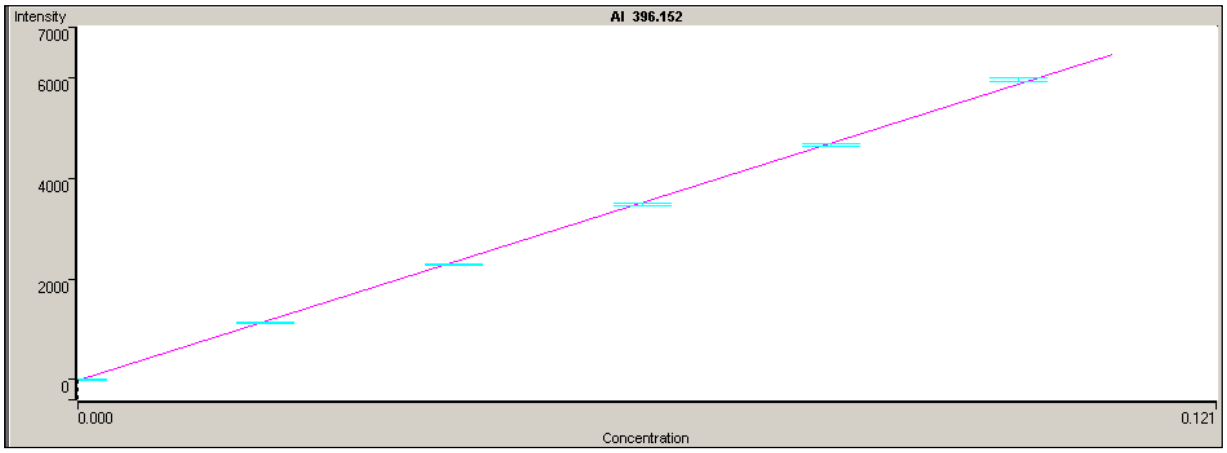

Figure 3.1 – Calibration plot for Al for ICP Round 10. X-axis is the measured concentration of the standards [mg l^{-1}], Y-axis is the intensity of the atomic emission (arbitrary units). Light blue bars represent the error. Correlation co-efficient (R_2) = 0.999755.

The analytical precision (or 'sensitivity') of an instrument varies between runs (on a day-to-day basis) and between analytes (Helsel, 2006). It is therefore inappropriate to refer to one value for the analytical precision of a given analyte, rather it is more appropriate to calculate analytical precision for each instrumental run. The analytical precision of the ICP for each analyte in each instrument run is summarised in the Table 3.4 (overleaf):-

	Al	Ca	Fe	K	Mg	Na	Si
Round 1	2.89E-05	N/A	1.87E-05	N/A	N/A	N/A	2.52E-03
Round 2	4.75E-04	3.59E-04	7.56E-04	2.17E-03	1.59E-04	2.32E-03	1.56E-03
Round 3	5.03E-04	3.87E-03	1.01E-04	9.73E-04	5.66E-04	1.44E-03	1.98E-03
Round 4	8.66E-06	1.95E-03	1.73E-06	5.07E-04	4.81E-04	7.75E-04	1.07E-03
Round 5	2.33E-04	6.01E-04	3.17E-04	1.21E-03	5.23E-05	3.90E-03	3.02E-03
Round 6	4.40E-04	8.22E-04	1.83E-04	2.64E-04	1.79E-04	2.13E-03	3.58E-03
Round 7	1.88E-04	4.69E-03	2.77E-04	1.15E-03	7.24E-04	6.26E-03	5.20E-04
Round 8	3.73E-04	5.45E-03†	4.70E-04	1.80E-03	5.09E-03	2.06E-03	1.33E-03
Round 9	2.56E-04	4.94E-04	4.27E-04	5.07E-04	2.90E-04	1.01E-03	1.58E-03
Round 10	5.44E-05	8.55E-04	4.98E-04	5.96E-04	3.89E-04	6.65E-04	1.88E-03
Mean	**2.56E-04**	**2.12E-03**	**3.05E-04**	**1.02E-03**	**8.81E-04**	**2.28E-03**	**1.90E-03**

Table 3.4 – Analytical precision of the ICP (mg/l) calculated using the formula $3\sigma_w$ where σ_w is the standard deviation of three ultra pure water blanks that are run through the ICP after the standards and before the first check standard.

† An ultra pure water blank was excluded from this calculation due to probable contamination.

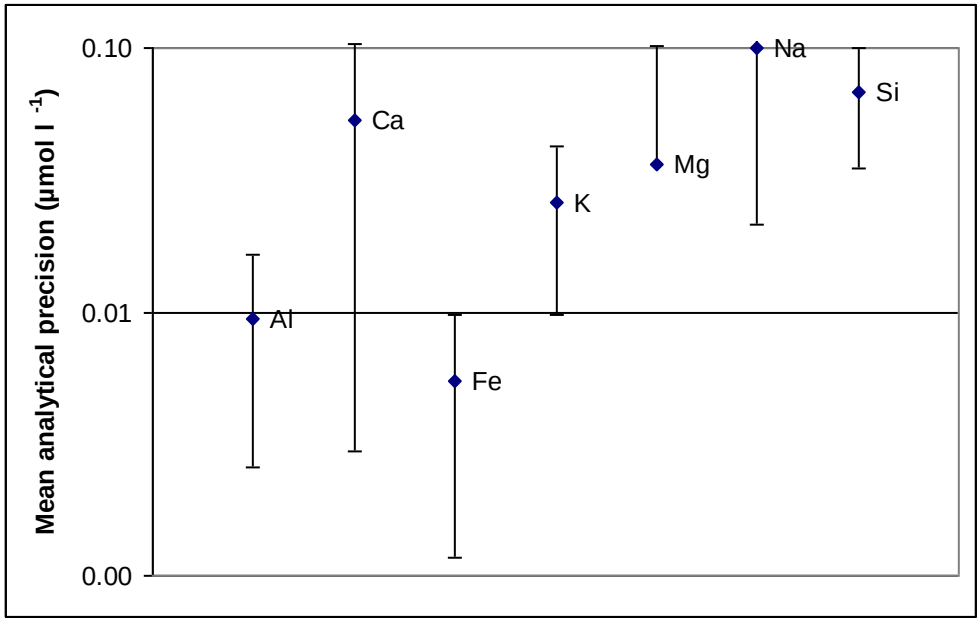

Figure 3.2 (Left) – Log plot of the mean analytical precision across all 10 ICP rounds with the σ of the dataset plotted as an error bar.

Every 20 samples a check standard was run through the ICP. The check standard was made from the same solutions as Standard 3 (the middle standard). The purpose of check standards is to check for instrumental drift, if this was found to occur a correction could have been applied. In this procedure if the check standards were found to drift by >10% the samples were simply run again (no correction for instrumental drift has been applied in this procedure).

The ICP outputs data in mg l^{-1}, these data were then converted to a whole amount in µmol before correction for the contamination in blanks etc (see Figure 3.3, overleaf).

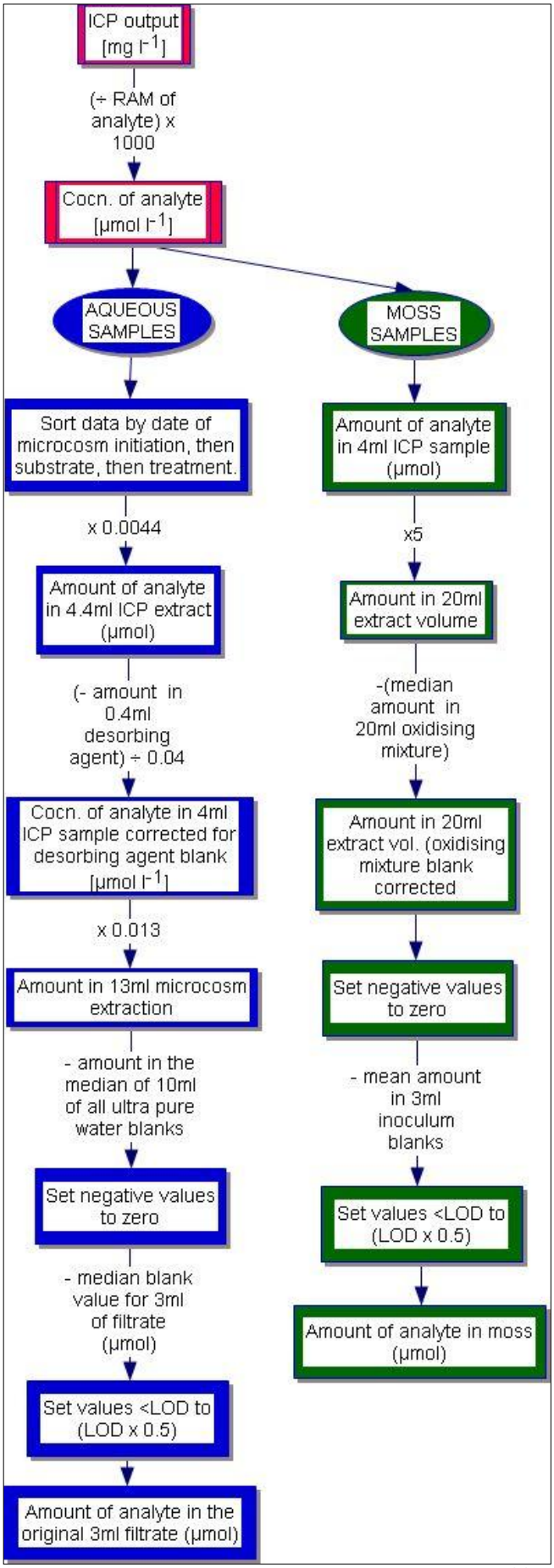

3.3.3 Data Manipulation

Figure 3.3 (Left) – Flow chart of the stages involved in working up the microcosmal data (making blank corrections, converting concentrations into whole amounts, correcting for non-detects (see next section) etc.)

The first stage in the ICP data workup procedure (red) was to convert the data outputted by the ICP (in mg l^{-1}) into molar units (µmol l^{-1}). The procedure then differs according to whether it is the moss from the microcosms (green) that is being analysed or the aqueous microcosm fraction (blue).

For aqueous samples: the amount of analyte in 4.4ml of sample is calculated (4ml sample + 0.4ml desorbing agent). The data are then corrected for the contamination in the desorbing agent and the amount of analyte in the 13ml microcosm extraction was calculated for (3ml filtrate + 10ml ultra pure water at the sampling stage). The amount of analyte in the 13ml microcosm extraction is then corrected for the contamination in 10ml upH_2O. Any values that become negative at this point were set to zero (these are non-detects, see next section). The data were then corrected for the contamination

in 3ml of filtrate and values less than the limit of detection (<LOD, also non-detects) were corrected for). The amount of analyte in the original 3ml filtrate (μmol) was then available and ready to use.

For moss samples no desorbing agent was used so the amount in a 4ml ICP sample was calculated. This was multiplied by 5 to give the amount of analyte in the 20ml nitric acid/hydrogen peroxide mixture which was then corrected for the amount of analyte in 10ml nitric acid and 10ml hydrogen peroxide. Any negative values were then set to zero and the data corrected for the amounts of analytes in 3ml of the inoculum blanks. Non-detects were then ready to be treated, and after this stage the data for the amount of analyte in the moss (μmol) was available and ready to use.

3.3.4 Non-Detects

In a dataset dealing with low amounts of analyte some values will fall below the analytical threshold (i.e. somewhere between 0 and the detection limit of the instrument). Non-detects in a dataset have to be treated (Helsel, 2006).

3.3.4.1 Blank Datasets

Non-detects in the desorbing agent, upH_2O, inoculum filtrate and the oxidising mixture blank datasets were treated in the following manner:-

1. All negative values were replaced with '0'.
2. Values >1 order of magnitude above the median of the dataset were censored (removed).
3. Values >median + 3σ were censored.

Due to a concern that stage 2 removed a large proportion of the moss inoculum dataset the following protocol was applied to that dataset:-

1. All negative values were replaced with '0'.
2. Values outside the range +/-2σ were censored.

A limit of detection (LOD) was then formed for the upH_2O and inoculum datasets using the formula:-

$$LOD = 2\sigma \text{ (of the censored dataset)}$$

These LOD values were then applied to the microcosm aqueous and the microcosm moss datasets respectively (the procedure is described in the next section).

3.3.4.2 Microcosmal Datasets

The upH_2O LOD was applied to the microcosmal aqueous fraction dataset and the inoculum LOD was applied to the microcosmal moss dataset as these components had the largest influence upon the two datasets. After correcting for the amounts of contaminants in the relevant blanks the following procedure was conducted:-

1. All negative values were replaced with '0'.
2. Values <LOD (non-detects) were substituted (replaced with) 0.5*LOD for that analyte.

0.5*LOD is the standard threshold for non-detects in aqueous chemistry (Helsel, 2006) (NB a separate LOD was established for inoculums analysed in ICP Round 5 and those analysed in Rounds 8-10 as the data differed markedly (e.g. $\bar{x}$ 0.15µmol Na for Round 5 inoculums, c.f. $\bar{x}$ 0.03 µmol Na for Rounds 8-10 inoculums).

3.3.5 Frequency Distribution Analyses

It was noted (after correcting the datasets for non-detects) that the mean amounts of most analytes in the all blank datasets were frequently substantially less than the standard deviation (an indicator that the data do not follow a pefect normal distribution). Frequency distribution analyses were therefore carried out on the upH_2O blank dataset and the inoculum at initial conditions dataset using SPSS Statistics[22] v17.0 software. It was found that the frequency distribution for most analytes in the upH_2O blank dataset (Ca, K, Mg, Na, Si) was a log-normal distribution (see Figure 3.4 below):-

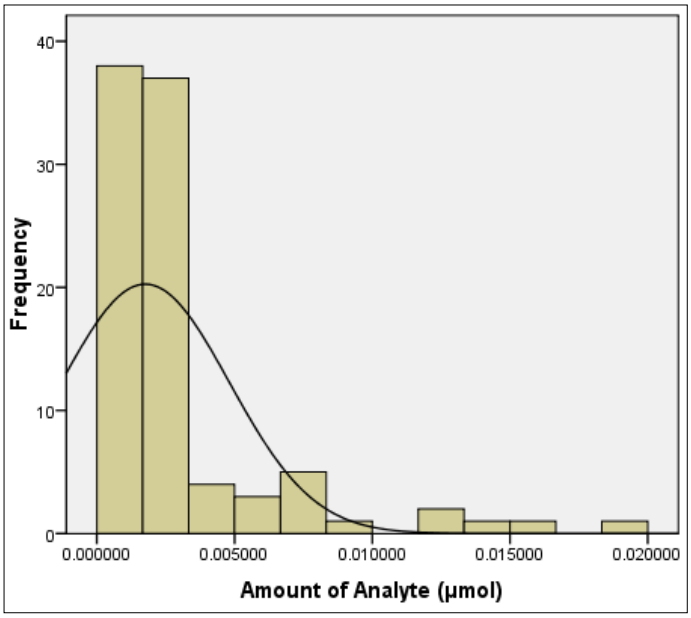

Figure 3.4 (Left) – An exemplar log-normal distribution: Ca in the upH_2O blanks dataset.
$\bar{x}$ = 0.00µmol, σ = 0.004, n=93.

Al and Fe gave positively skewed normal (Gaussian) distributions (see Figure 3.5, overleaf):-

[22] SPSS Inc., 233 South Wacker Drive, 11th Floor, Chicago, IL, 60606-6412, USA.

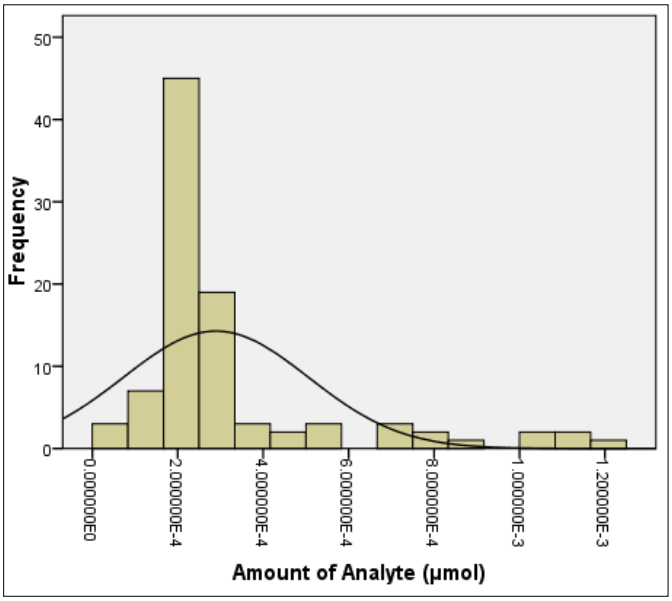

Figure 3.5 (Left) - An exemplar Gaussian (positively skewed) distribution: Al in the upH_2O blanks dataset.
$\bar{x}$ = 3.22x10^{-4} µmol,
σ = 2.486x10^{-4}, n=93.

Both Al and Fe exhibited this type of profile (the analytes that ICP measures with the highest limit of sensitivity, see Figure 3.2)).

The most common frequency distribution in the inoculum blank dataset was the log-normal distribution (Al, K, Na and Si) with Ca giving a positively skewed Gaussian distribution and Fe giving a negatively skewed Gaussian distribution. The frequency distribution for Mg is an almost perfect Gaussian distribution (see Figure 3.6, below):-

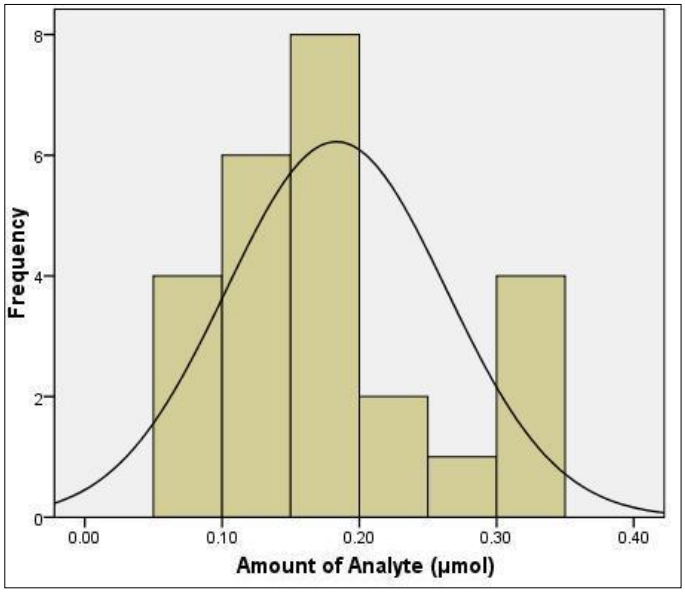

Figure 3.6 (Left) – A near-perfect (symmetrical) Gaussian distribution: Mg in the inoculum at initial conditions dataset. $\bar{x}$ = 0.18µmol, σ = 0.005, n=26.

3.4 Nutrient Auto Analysis

3.4.1 Introduction

A Skalar[23] Sanplus System Nutrient Auto Analyser (henceforth known as the 'NAA') was used to determine the amount of silicate and phosphate in each sample. The NAA works using an automated reagent-based method known as 'Automated air-segmented continuous flow analysis'. Sample entered the NAA using a Skalar 1000 auto sampler and was drawn in using a peristaltic pump. The sample was then split into four channels, one for each nutrient for which the NAA can analyse; the corresponding reagents were then drawn in from plastic bottles using another peristaltic pump. The sample and corresponding reagents were then mixed and reacted in a thin convoluted glass column and the resulting colour change was detected at the end of the channel by a filtered photometer (each analyte had its own dedicated photometer). See Appendix i.ii.iii for details of the feedstock chemicals used to produce the phosphate and silicate reagents.

The electronic signals from the photometers were then processed by a Skalar Sanplus System SA8616 before being exported to a PC with Skalar Analytical 5.1 software. Peaks in phosphate absorption were sometimes indistinguishable from the perpetually noisy baseline on the VDU screen. This problem was overcome by exporting data from the PC to a chart recorder. The heights from baselines to peaks were then measured manually using a ruler (see Figure 3.9). Silicate peaks were easily distinguishable from the baseline but PC compatibility problems meant that this data could not be saved; therefore the maximum absorption ('M Raw') value had to be manually recorded by the author.

Spurious data were sometimes obtained for aqueous samples, if remaining sample was available a repeat analysis was conducted. There were only ~60 sample containers for the NAA and these were rinsed in upH_2O and left to dry for a few minutes. Sample containers were not washed in Decon® solution and rinsed (as per Spokes *et al.* (2000)) as this process is time consuming and the processing of samples rapidly was considered a priority as instrument baselines are liable to drift or destabilise. Data for replicate samples analysed using the NAA were generally in greater agreement (and had a lower standard deviation) than samples

[23] Manufactured by: Skalar Analytical B.V., Breda, The Netherlands.

analysed via ICP, due to the lower sensitivity (analytical precision) of the NAA relative to the ICP. Therefore fewer blank replicate samples were analysed by NAA than ICP (2-3 replicates for NAA, compared with ~5 via ICP).

Nutrient auto analysers are commonly used to measure the concentration of nutrient species within aqueous solution (e.g. within seawater). A literature search by the author found no published examples of researchers using a nutrient auto analyser (NAA) to determine nutrient concentrations within plant tissue.

3.4.2 Calibration

The NAA was calibrated by running 4-5 standards through the instrument. The data were hand-plotted *in situ* and the calibration repeated until a calibration with a good best-fit trendline was obtained. The calibration data were then plotted using Microsoft Excel®; the baseline corrected Max M-Raw value (in the case of silicate) or peak height (in the case of phosphate) being plotted against the concentration of standard (μmol l^{-1}). Outlying calibrations were then removed and a trendline plotted and fixed through the (0, 0) co-ordinate. An exemplar calibration for silicate and phosphate can be seen in Figures 3.7 and 3.8 (below and overleaf):-

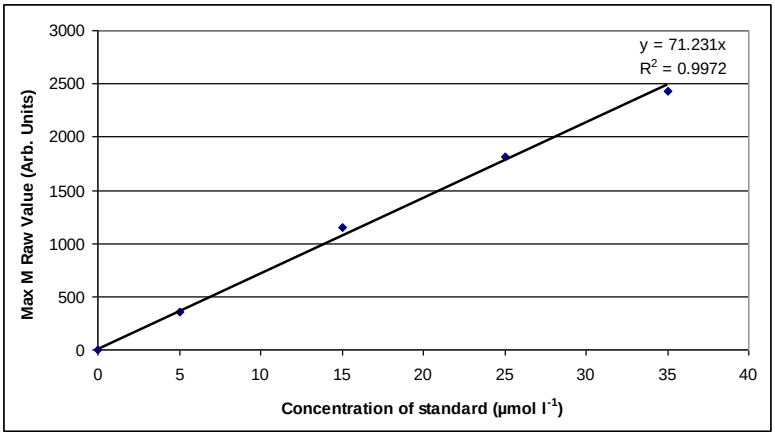

Figure 3.7 – An exemplar silicate calibration from 28/4/09.

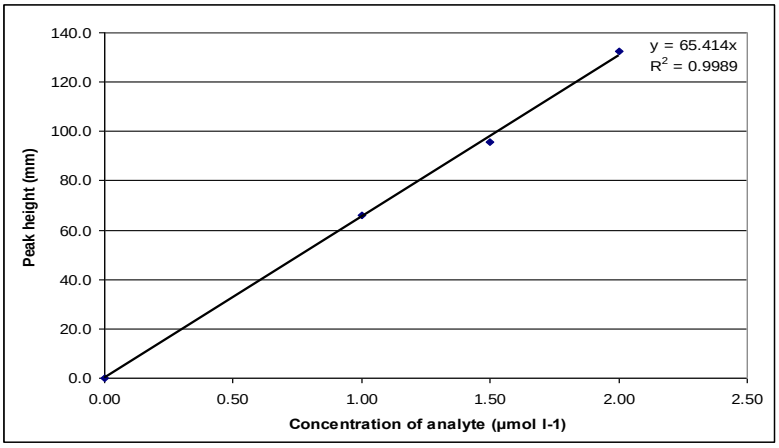

Figure 3.8 – An exemplar phosphate calibration from 31/3/09.

All calibration plots had an R_2 value of >0.92. Every 20-30 samples an instrumental drift check standard was run through the NAA (17.5µmol for silicate and 4µmol for phosphate, the same concentrations as the middle calibration standards). The NAA was re-calibrated if the check standard values exceeded the middle calibration standard values by >10%. Check standards were also run in the event of a witnessed baseline shift.

3.4.3 Interference Problems

On running oxidised samples through the NAA it was noted that a green colour formed in the phosphate column (upon reaction of the two phosphate reagents with the sample). In addition to this mal-formed peaks were formed on the phosphate chart recorder paper:-

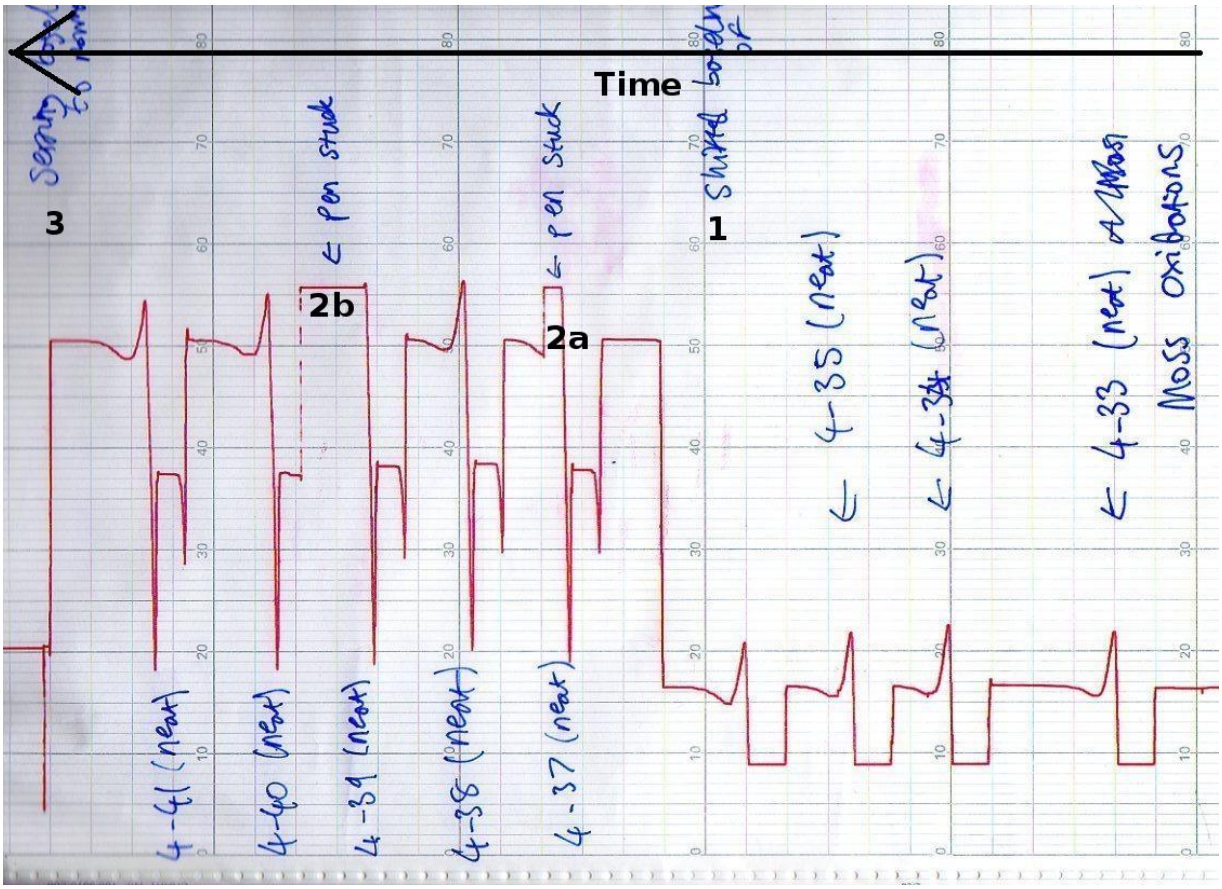

Figure 3.9 – Chart recorder paper showing the mal-formed peaks from the phosphate channel when moss oxidations are run through the NAA (time elapsed indicated by black arrow).

Four moss oxidations were run through the NAA before the baseline was shifted to the middle of the paper (‘1’). Five more moss oxidations were run through the NAA each showing extremely mal-formed double negative peaks (at ‘2a’ and ‘2b’ the chart recorder pen stuck). The baseline was reset to its normal position at ‘3’.

An experiment was designed to determine which chemical interaction was causing the interference: 1ml of 30% Hydrogen Peroxide solution or 1ml of 30% nitric acid solution was added to a new centrifuge tube. 1ml of each of the phosphate or silicate reagents was then added to the centrifuge tubes, the resulting mixture was then shaken by hand. Tubes containing the phosphate reagents were heated for five minutes in a water bath at 55°C (to replicate the conditions within the NAA). The colour changes that were observed immediately upon addition of the phosphate/silicate reagent containing ammonium molybdate tetrahydrate to hydrogen peroxide can be seen in Figure 3.10 (below):-

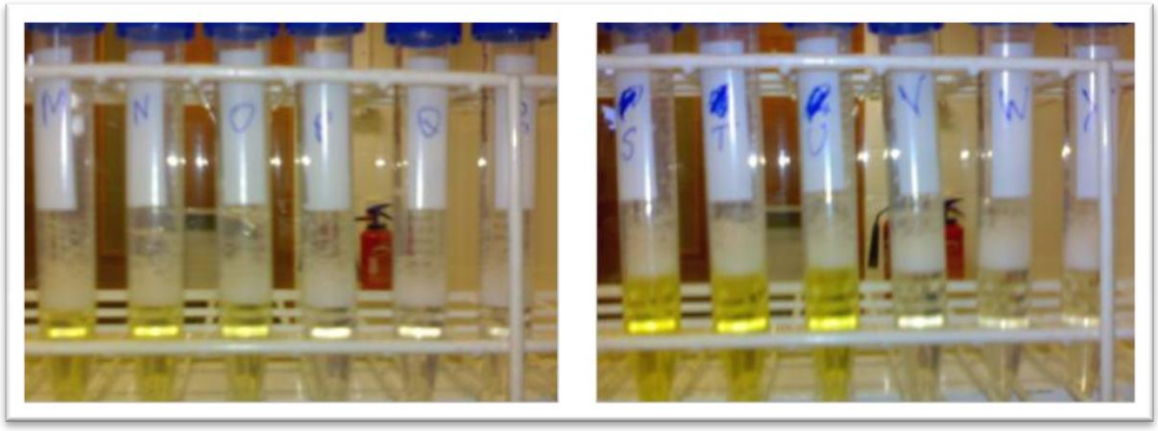

A: Phosphate Reagents B: Silicate Reagents

Figure 3.10 – The resulting colour change (extinction) when the phosphate or silicate ammonium molybdate reagent is mixed with 30% hydrogen peroxide (Tubes M-O and S-U, see Table 3.5) versus 30% nitric acid (P-R and V-X) confirms that an interaction between hydrogen peroxide and ammonium molybdate is the source of the extinction.

N.B. The tubes in Figure B contain more solution because 1ml of the three silicate reagents was added, as opposed to 1ml of the two phosphate reagents in Figure A. The foam on top of the resulting solutions are a product of the sodium dodecyl sulfate in the NAA reagent mixtures.

Sample Label	Oxidiser Added (1ml)	Reagents Added (1ml of each)
M, N, O	Hydrogen Peroxide	Phosphate
P, Q, R	Nitric Acid	Phosphate
S, T, U	Hydrogen Peroxide	Silicate
V, W, X	Nitric Acid	Silicate

Table 3.5 – Sample labelling regime for the interference determination experiment shown in Figure 3.10.

The experiment shown in Figure 3.10 confirms that a hydrogen peroxide/ammonium molybdate interaction is the cause of the extinction. Why this extinction appears green inside the columns of the NAA and yellow inside a centrifuge tube is unknown. A Perkin-Elmer Lambda 25[24] spectrophotometer in visual mode was then used to a run a spectrum scan from λ 390nm – λ 710nm on samples M through to X. The results are shown in Figures 3.11/12 (below and overleaf).

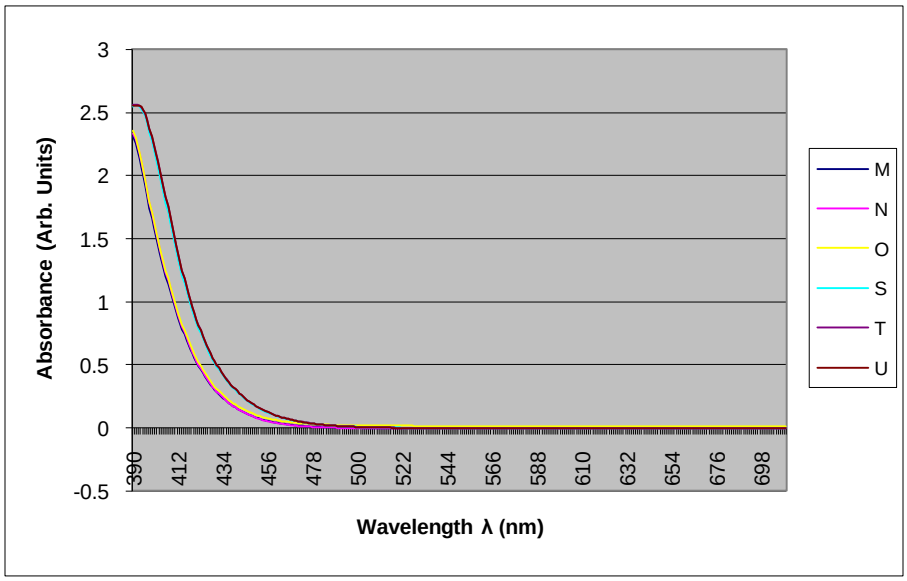

Figure 3.11 (Left) – The absorbencies across the visual spectrum for the samples containing hydrogen peroxide. Note that all samples show the beginnings of a peak forming at ~515nm reaching maximum amplitude at 391nm.

[24] Perkin-Elmer Inc., Shelton, CT 06484, USA.

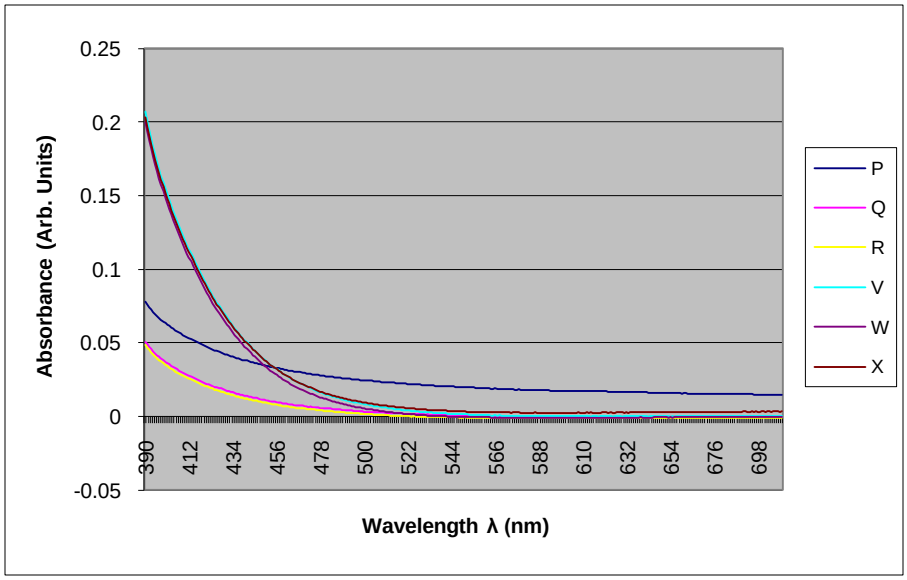

Figure 3.12 (Left) – Absorbencies for samples containing nitric acid. Note that the maximum absorbance is approx. an order of magnitude lower than the maximum absorbance in Figure 3.11.

NB Figures 3.11/12 show absorbencies whereas colour is an emission; therefore the peak will be expected to form in the area of the spectrum complementary to yellow which is violet (390-450nm) and it is this region that does indeed contain the highest absorbencies. Figures 3.11/12 are instrumental confirmation that the interference is caused by hydrogen peroxide and not nitric acid (or at least, to a far lesser extent by nitric acid).

In a second experiment; the phosphate and silicate reagents were added to 1ml of three oxidised moss samples and three inoculum oxidations. All of these samples turned yellow (because all of these samples contained hydrogen peroxide within the oxidising mixture), with the extinction being stronger in some samples than others.

3.4.4 NAA Data Calculations

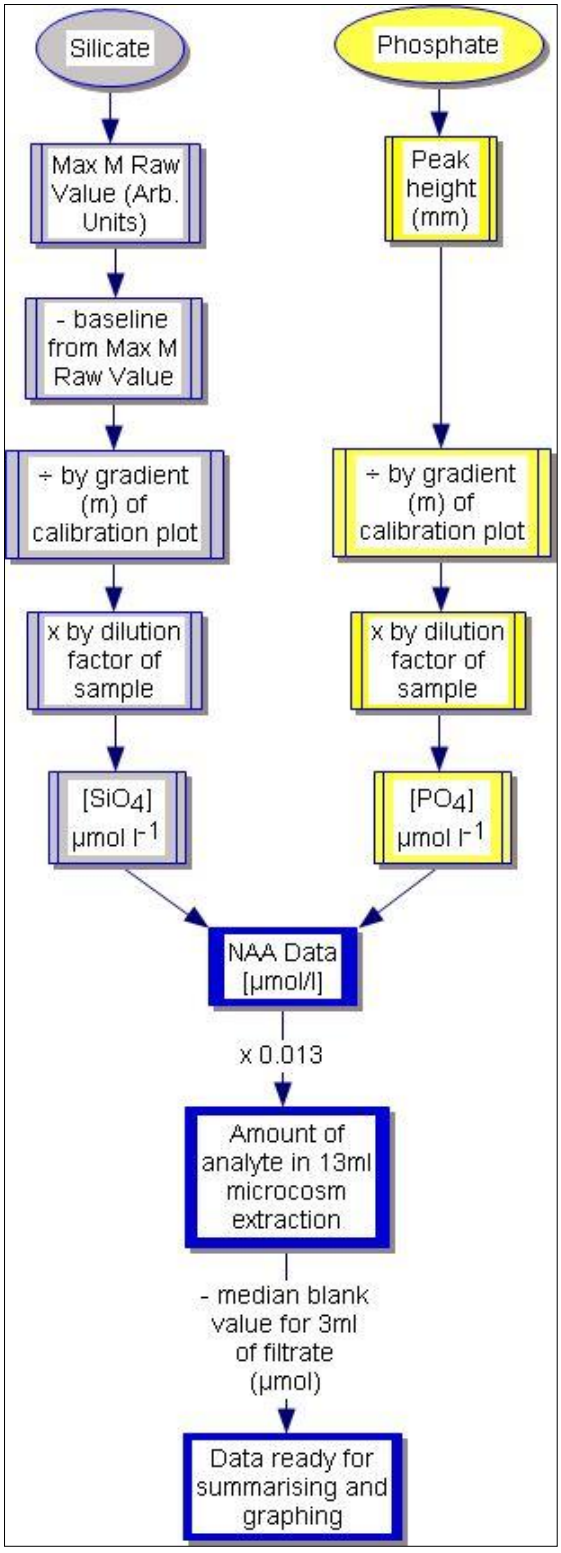

Figure 3.13 (Left) – Stages involved in working up NAA raw data to obtain results in µmol l^{-1} (grey for silicate, yellow for phosphate) and the blank correction procedure (in blue).

The procedures for working up the silicate NAA and the phosphate NAA data were different due to the two different methods of output: the Max M Raw Value (the photometer absorbance) in arbitrary units on a VDU for silicate and a height measured from baseline to peak on chart recorder paper for phosphate (in mm). Silicate requires an additional numerical correction for the baseline, then both sets of data were divided by the gradient of the relevant calibration plot.

Frequently samples had to be diluted in order to fit the obtained data within the calibration range of the NAA (this was particularly the case for silicate). Where samples were diluted the resulting data at this point were multiplied by the dilution factor yielding a concentration in µmol l^{-1}.

The blank correcting stages (in blue) are the same as for the ICP data, however no correction was required for the upH_2O blanks as no silicate or phosphate could be detected in any upH_2O blank via NAA.

3.5 X-Ray Fluorescence Spectroscopy (XRF)

3.5.1 Introduction

Figure 3.14 (below) summarises the key stages in XRF sample preparation:-

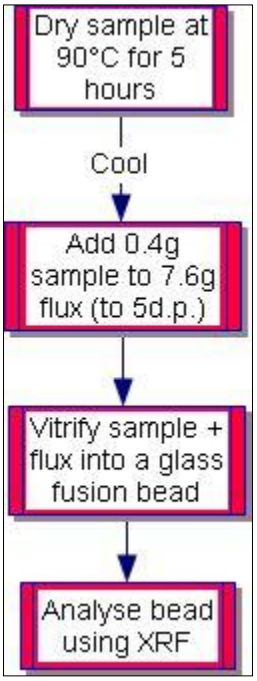

Figure 3.14 (Left) – Main stages involved in preparing a fusion bead for XRF analysis

Samples of mineral or rock were dried in an oven at 90°C for five hours and allowed to cool. The sample was then ground using a Retsch RS200[25] vibratory disc mill set to a programme of 700 r.p.m. for one minute. 7.6g of Socachim/XRF Scientific[26] X-Ray flux was placed into a platinum/gold crucible. The flux was a certified mixture of 66.0% lithium tetraborate and 34.0% lithium metaborate. 0.4g of rock sample was then added to the flux. Great care was taken to record masses accurately to five decimal places as the precise mass of rock is important for stoichiometric data analysis. The solution was then mixed using a metal spatula which had been pre-cleaned with propan-2-ol.

An XRF Scientific Phoenix machine was used to heat the crucibles using butane/oxygen flames melting the flux and sample and then casting the fusion beads which were subsequently analysed for the percentage abundance of the 'major elements' in a sample (that is the 10 most common elements comprising the Earth's crust, see Table 3.6) using a Bruker AXS S4 Pioneer[27] XRF spectrometer (NB A more detailed protocol for the entire XRF sample preparation procedure can be found in Appendix i.ii).

[25] Retsch GmbH, Rheinische Strasse 36, 42781 Haan, Germany.
[26] XRF Scientific Ltd., Perth, Australia.
[27] Bruker AXS Ltd., Banner Lane, Coventry, CV4 9GH, UK.

Analyte	Species
Magnesium	MgO
Aluminium	Al_2O_3
Silicon	SiO_2
Phosphorus	P_2O_5
Calcium	CaO
Titanium	TiO_2
Manganese	MnO
Potassium	K_2O
Iron	Fe_2O_3
Sodium	Na_2O

Table 3.6 – The XRF analytes. The resulting percentage by mass data is given in the form of oxidised species due to the fact that the high intensity x-ray beam causes inner electrons to be ejected from the species; forming an oxidised compound (Banwell, 1983).

3.5.2 XRF Data Calculations

Figure 3.15 (overleaf) shows how the original data output of the XRF (in % by mass for an oxidised compound) was converted into a whole amount in μmol g^{-1} enabling parity with the ICP and NAA data (which was worked into whole amounts of analyte in μmol). This was done by multiplying the XRF output by the total mass of sample (to 5d.p.) then dividing that value by the total percentage of sample comprising the major analytes (~91%, the other 9% comprising trace amounts of other elements). The figure obtained was then divided by the mass of the oxidised XRF analyte yielding a whole amount in mol g^{-1} which was then multiplied by 1000 to give an amount in μmol $g^{-1.}$

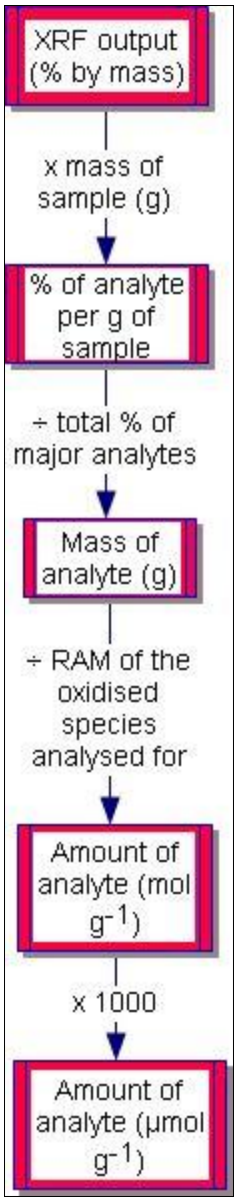

Figure 3.15 (Left) – Stages in manipulating the XRF data, originally in % by mass to µmol g^{-1}. This enables stoichiometries to be calculated that give parity to the ICP and NAA data (worked up to values in µmol).

4: Results and Discussion

4.1 Introduction

Experimental results generally show a strong weathering signal for most analytes on all substrates. The aggregated data using all experiments conducted on granite, andesite and vermiculite (except for early experiments in the method development phase or experiments with a microcosm n<5) are presented in Figures 4.3-4.17. The individual data for the one chlorite experiment is presented in Figures 4.18/19. Granite and andesite will be the two main substrates of focus as these substrates have the highest number of experiments conducted upon them (six and three respectively).

4.2 Statistical Analysis of Experimental Data

4.2.1 Error Bars

4.2.1.1 Aggregated Data

The majority of the graphs presented in this section represent population mean values ($\bar{\mu}$), i.e. the mean of all the mean values for all the individual experiments for a given analyte. For simplicity this data will henceforth be referred to as the 'Aggregated Data'. In graphs of aggregated data, error bars represent the standard error of the standard deviations of the data for a given analyte on a given substrate, calculated thus:-

$$S.E. = \frac{\sigma_{x,y\ldots}}{\sqrt{n}}$$

Equation 4.1 – The Standard Error calculation as used to calculate error bars on graphs of aggregated data, where $\sigma_{x,y\ldots}$ are the standard deviations of a specific portion of the dataset in different experiments (e.g. the standard deviation of the Al in W_a in the 30/4/08 experiment, the 24/6/08 experiment, the 2/9/08 experiment etc.)

All error bars in this section represent the standard error (calculated as shown in Equation 4.1) unless otherwise stated.

4.2.1.2 Individual Experimental Data

Error bars on graphs for individual experiments represent the 95% confidence interval (or a probability of the results being due to chance of 5%, P<0.05). The 95% confidence interval was calculated using Microsoft Excel's 'tinv' function (which gives the Student's t value for a given n at P<0.05) as shown in Equation 4.2 (below):-

$$95\%\ conf. = tinv\ \left(\frac{\sigma}{\sqrt{n}}\right)$$

Equation 4.2 – Equation for calculating the 95% confidence interval (P<0.05).

4.2.2 Mann-Whitney U Test

SPSS Statistics v17.0 software was used to perform the Mann-Whitney U test on the experimental data in order to validate or falsify the hypotheses outlined in §1.9, p33 The Mann-Whitney U test (henceforth referred to as the 'U test') is a non-parametric technique that compares the difference between two groups of ranked data as opposed to scaled data (Pallant, 2007). The U test was chosen over the most appropriate alternative test (the independent t-test) for two reasons:-

1. Parametric tests (such as t-tests) can only be performed on data that follow a normal distribution. A large proportion of the data obtained in this procedure is non-Gaussian in distribution.
2. By substituting non-detects for <LODs an ordinal character has been introduced to the dataset. The data can no longer be regarded as scaled data in the strictest sense of the term.

The U test (unlike the t-test) compares data by comparing medians as opposed to means (*Op. cit.*). The major disadvantage of non-parametric tests over parametric tests is that they are less sensitive and therefore may not detect differences between two sets of data that actually exist. The benchmark for statistical significance will be $P<0.05$ (the probability of results being due to chance is less than 5%, the 95% confidence interval) with a $P<0.01$ (a probability of the results being due to chance of 1%) or lower considered to be a very strong, statistically significant result. The results of the U test are arranged by experimental substrate later in this section. The SPSS outputs, including Mann-Whitney U score and the Asymptotic Significance (P value) are reproduced in Appendix iv.i.

The following U tests were conducted upon the aggregated data for each substrate:-

1. W_a vs. W_b – Abiotic aqueous weathering vs. Total aqueous weathering
2. W_a vs. W_{moss} - Abiotic aqueous weathering vs. Weathered analyte uptaken by moss
3. W_b vs. W_{moss} – Total aqueous weathering vs. Weathered analyte uptaken by moss
4. W_a vs. W_{tot} - Abiotic aqueous weathering vs. Total weathering

Tests 1 and 4 are presented in this thesis; test 4 being the most important as it is essentially a test of the biotic enhancement of weathering factor (Ψ) itself. When considering the P values obtained from a statistical test it is important to note the direction of the test. For example whilst conducting the test W_{tot} vs. W_a for the analyte Al the P value obtained may be 0.05 but which has the greater median rank W_{tot} or W_a?

The U test is less reliable if the sample size being tested is less than 30 as SPSS does not correct for ties (incidences where a value appears more than once) after ranking, it is therefore inappropriate to apply the U test to data for individual experiments due to the lower sample size (n). When non-detects are substituted in for <LODs ties occur as the same value is introduced to the dataset multiple times, this can affect the reliability of the U Test by rendering statistically significant results insignificant. Incidences where a level of significance or direction of result appears incongruent with the experimental data and the error bars will be tested separately using the Independent Samples t-test using SPSS.

4.3 Granite Experiments

4.3.1 Introduction

Figure 4.1 – Side and plan views of a granite control microcosm (after a weathering period of 113 days). NB the black flecks in the granite clasts which are the mineral biotite. Condensation on the walls of the jar was removed using swabs and a hairdryer prior to photographing.

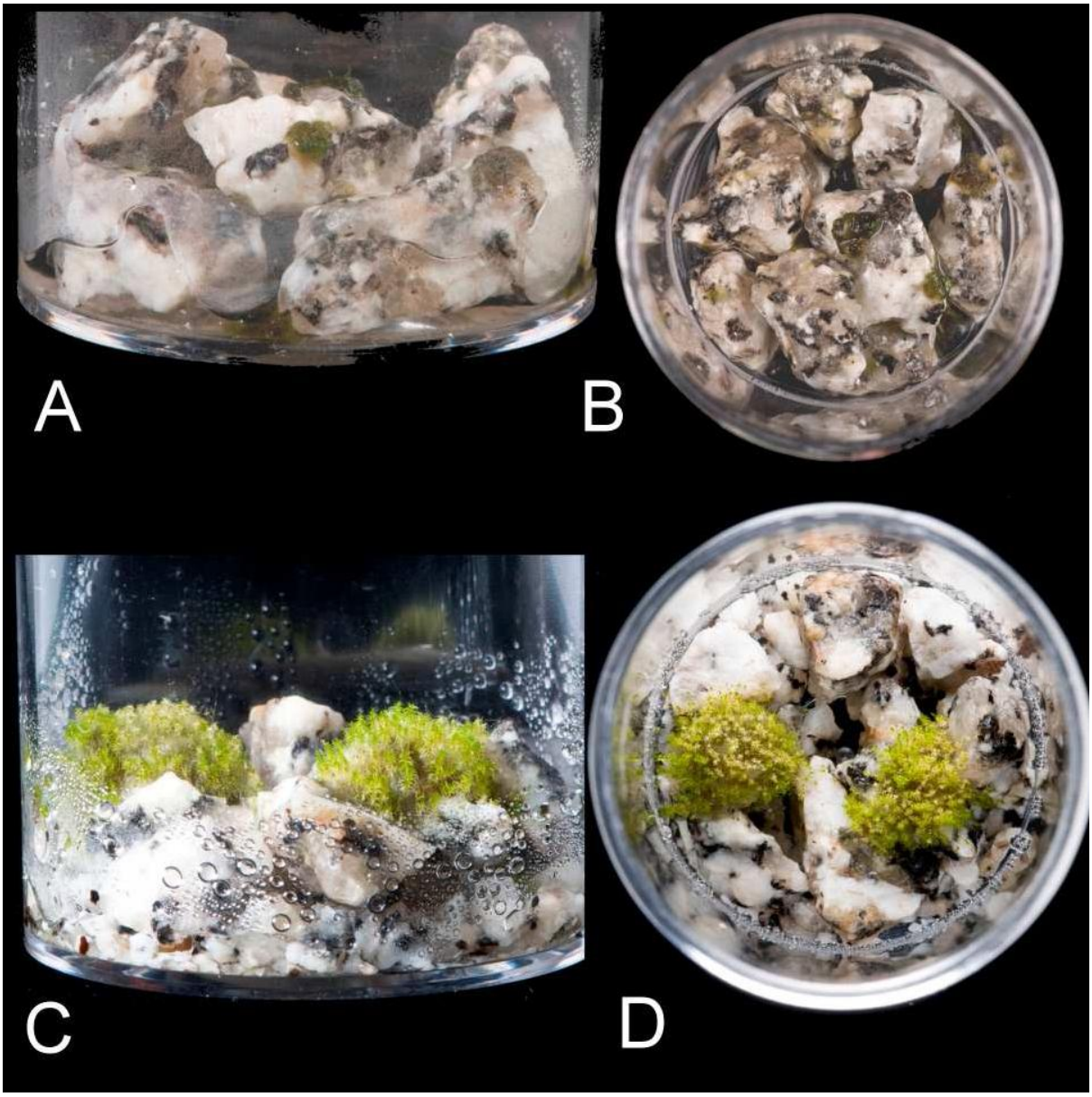

Figure 4.2 – Plan and side views of mossed granite microcosms shown at time of inoculation (A&B) and after a growth/weathering period of 113 days (C&D).

Note the increase in biomass over the weathering period. The moss has yellowed in photos C&D indicating that it has started to die. This was used as an indicator that the microcosms needed sampling.

4.3.2 Aggregated Data

In this thesis data are always presented on linear axes and the ICP data always have two graphs presented one above the other because the values for some analytes were always substantially higher than the values for others.

The following graphs show the population mean ($\bar{\mu}$) values for each analyte in all of the granite experiments except the 15/8/08 experiment that gave anomalous results due to its low sample size of 2 control microcosms and 2 mossed microcosms. The results are population means of six experiments (30/3/08, 24/6/08, 2/9/08, 19/12/08, 12/1/09, 30/7/09). Error bars represent the standard error.

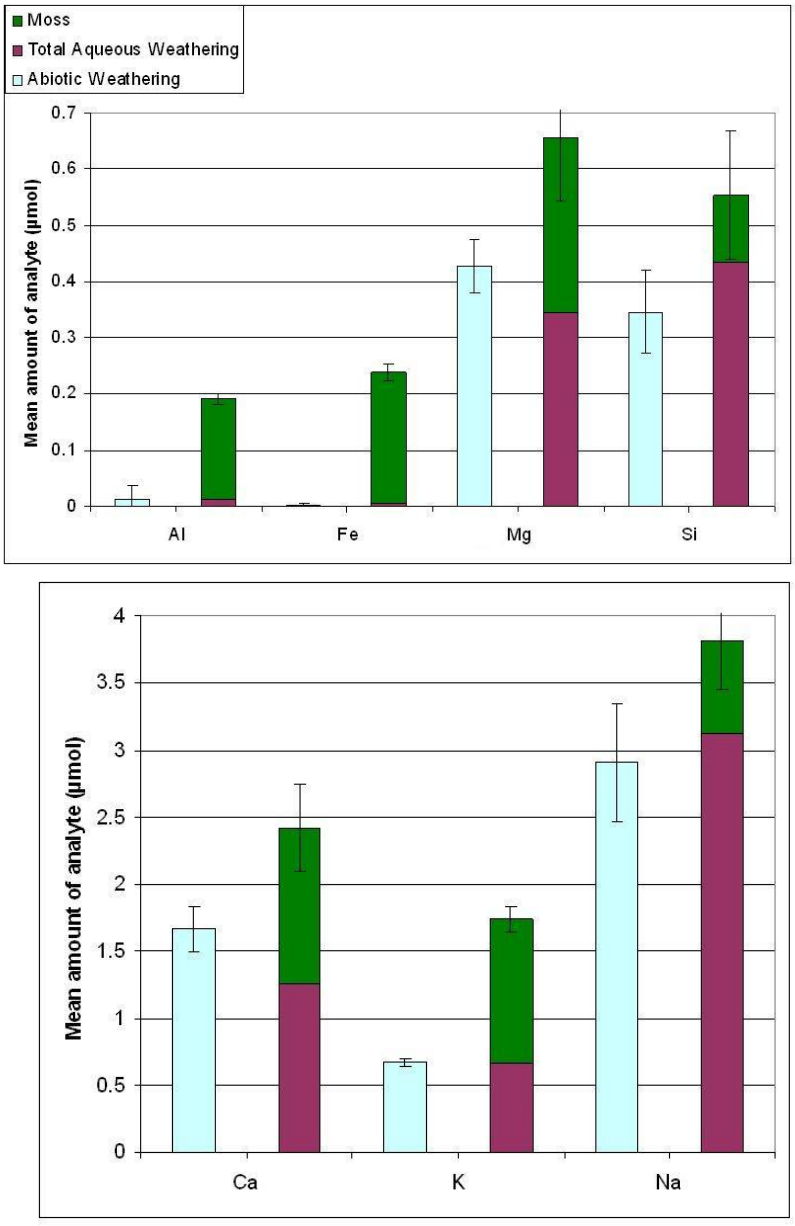

Figure 4.3 (Left) – Population mean ($\bar{\mu}$) values of the amount of analyte weathered into the different microcosm fractions in the granite microcosms.

The aqueous solution from control microcosms (W_a, abiotic weathering) is depicted in light blue bars. The other bar represents total weathering in mossed microcosms (W_{tot}); the purple portion of the bar representing analyte weathered into aqueous solution (W_b) and the green portion of the bar representing analyte taken up by the moss (W_{moss}).

Abiotic n=73, Biotic n=66. Mean weathering period = 110 days.

Figure 4.3 shows that there are higher amounts of all analytes in biotic granite microcosm fractions ($W_b + W_{moss}$) compared with the abiotic microcosm fraction (W_a). Al, Fe, K and Mg are present in higher amounts in the moss than in the biotic microcosm aqueous fraction (the inverse being true for Ca, Na and Si). On an intra-elemental basis; all error bars are non-overlapping.

The amounts of analytes contained within moss tissue increased on all substrates compared with the inoculum at initial conditions. Indeed, the values for analytes contained within the inoculum used to inoculate that particular set of microcosms are subtracted from the results obtained for the amounts of analytes within the moss biomass after the weathering period (see §3.3.3 p60). For example: the mean amount of Fe in the inoculums at initial conditions was 0.05µmol, the mean amount of Fe in moss removed from granite microcosms was 0.28µmol.

A graph of the biotic enhancements of weathering for each analyte can be plotted by presenting W_a as one bar and W_b and W_{moss} as a second stacked bar (henceforth known as W_{tot}) and normalising both of these to W_a. By normalising the sum of the biotic microcosm components to W_a the following operation is performed:-

$$\frac{W_{tot}}{W_a}$$

which is the same as the biotic enhancement of weathering (Ψ) calculation (c.f. Equation 1.8, p34. The results of this normalisation can be seen in Figure 4.4 (overleaf).

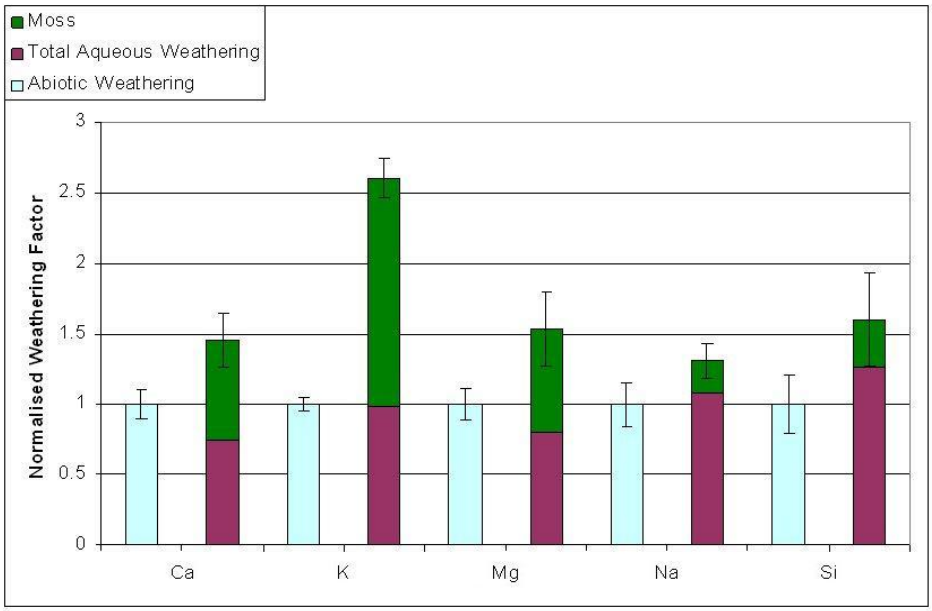

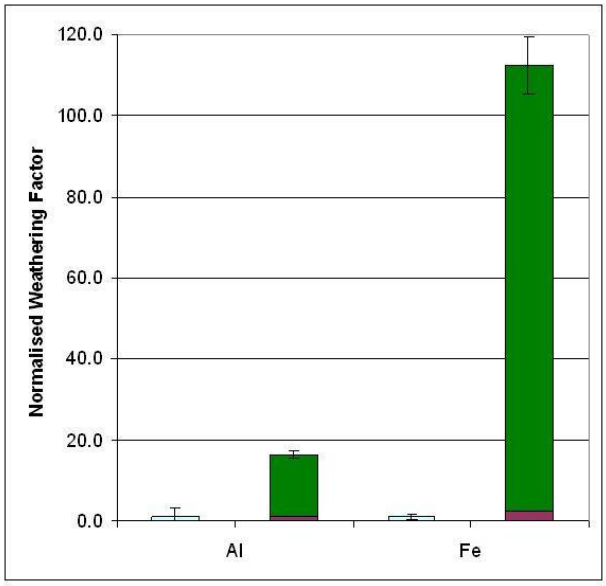

Figure 4.4 (Above and Left) – Granite dataset: population means ($\bar{\mu}$) of the total amounts of analytes weathered into the microcosm fractions normalised to abiotic aqueous weathering (light blue). Total aqueous weathering is represented in purple and analyte uptaken by the moss is represented in green.

The amount of analyte weathered into aqueous solutions in control microcosms is normalised to itself and is therefore always 1 (light blue: 'Abiotic Weathering').

Abiotic n=73, Biotic n=66. Mean weathering period = 110 days.

Figure 4.4 shows that moss biotically enhances the weathering of all analytes on granite; biotic enhancements (Ψ) are ≈ 1.5 for Ca, Mg, Na and Si, ranging from Ψ1.3 for Na through Ψ16.4 for Al, up to Ψ112.6 for Fe. The magnitude of the biotic enhancement values for Al and Fe are particularly remarkable considering that granite is widely regarded as being an unlabile substrate with low weatherability (e.g. Blatt *et al.* (2006)). Also of particular interest in Figure 4.4 is that two major plant macronutrients (Ca and Mg) are present in lower amounts in the biotic aqueous fraction than the abiotic aqueous fraction, indicating preferential uptake of Ca and Mg by the moss (See Figure 4.5, overleaf). Ca and Mg typically form 0.5% and 0.2% of dry plant tissue respectively (Taiz & Zeiger, 2002). Conversely: Si, Fe and Na are present in

higher amounts in the biotic aqueous fraction than the abiotic aqueous fraction indicating that these analytes are not preferentially uptaken (are 'purged') by the moss. Si forms 0.1% of dry plant tissue and is considered a macronutrient, Fe and Na are typically present in dry plant tissue at levels of 100ppm and 10ppm respectively and are considered plant micronutrients (*Op. cit.*).

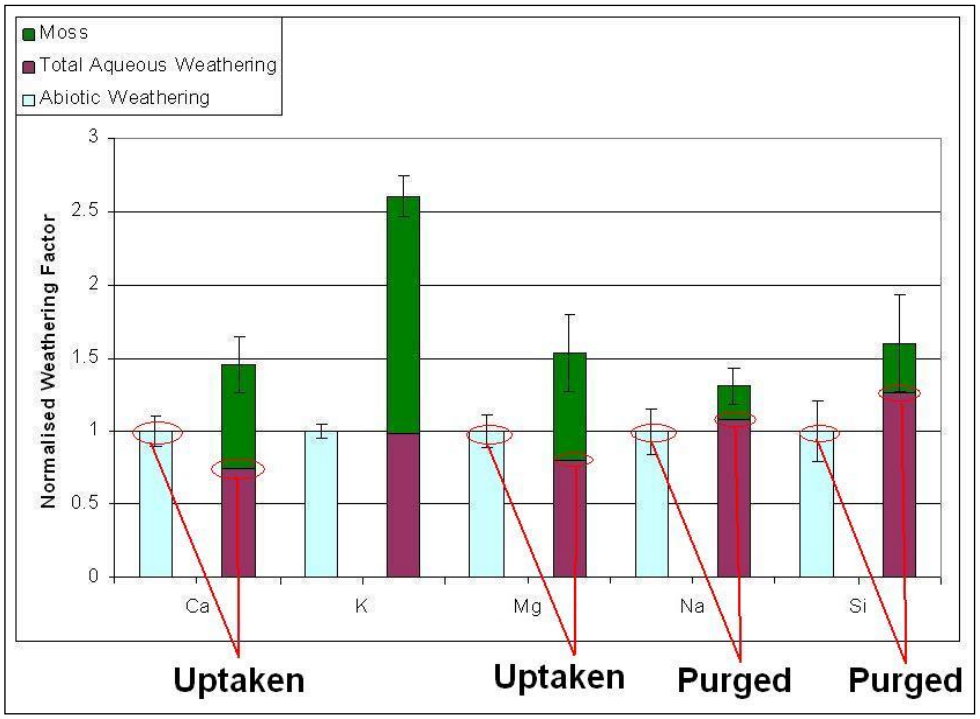

Figure 4.5 (Left) – Top half of Figure 4.4 reproduced to show which analytes are uptaken by the moss and which are purged by the moss. K is present in approximately equal proportions in the abiotic and the biotic aqueous fractions.

Table 4.1 gives the levels of significance (P values) for the data presented in Figure 4.4 as obtained by the U test:-

	Al	Ca	Fe	K	Mg	Na	Si
$W_{tot}>W_a$	<0.01	<0.01	<0.01	<0.01	<0.01		<0.01
$W_{tot}<W_a$						*0.37*	

Table 4.1 – Levels of significance (P values) for the test W_{tot} vs. W_a in the granite aggregated dataset arranged by direction. ($W_{tot}>W_a$ indicates that the median rank for W_{tot} was higher than the rank for W_a. $W_{tot}<W_a$ indicates the inverse was true). Results rounded to 2 d.p., insignificant results (P>0.05) are italicised.

Table 4.1 shows that all analytes except Na show biotic enhancements of weathering that are significant at the $P<0.01$ level. This is a highly statistically significant positive result for all analytes with the exception of Na. The insignificance of the Na result is intriguing given that the error bars are non-overlapping in Figure 4.1. This result was re-tested using the t test and a similar insignificant result was obtained (see Appendix iv.ii). A frequency distribution on the aggregated data for Na revealed that the data follow a log-normal distribution (see Appendix ii.vii), the population mean ($\bar{\mu}$) not equaling the population median (2.29µmol and 1.78µmol respectively).

Figure 4.6 (below) shows the data obtained for silicate and phosphate using the Nutrient Auto-Analyser (NAA). NB NAA datasets do not contain data for moss because of instrumental problems caused by a matrix interference (see §3.4.3 p68).

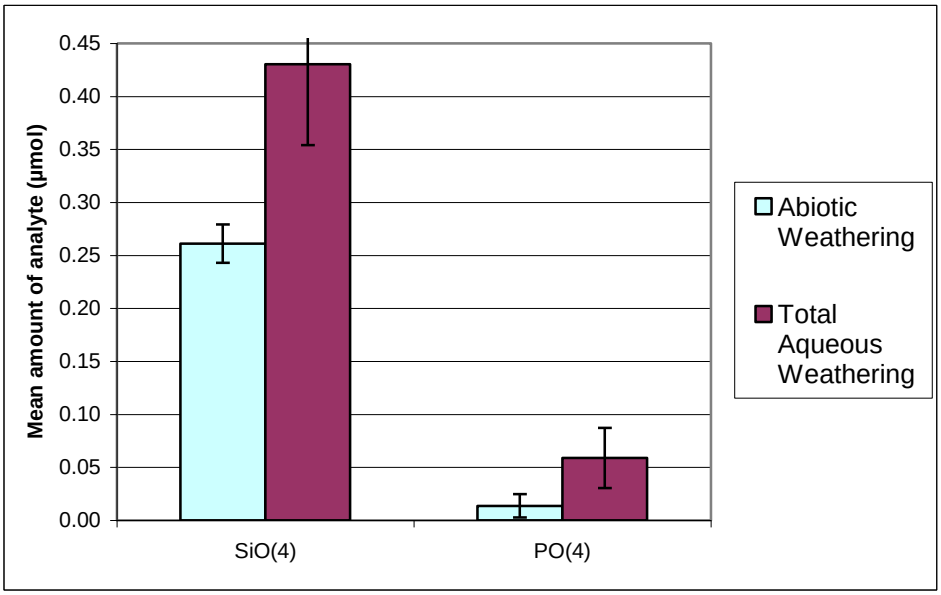

Figure 4.6 – Population mean ($\bar{\mu}$) of silicate (SiO_4^{4-}) and phosphate (PO_4^{3-}) weathered into the aqueous solutions in control microcosms (light blue: 'Abiotic Weathering') and mossed microcosms (red: Total Aqueous Weathering) in the 30/4/08, 24/6/08 and 2/9/08 granite experiments.

NB no PO_4^{3-} was detected in any of the abiotic or biotic samples in the 24/6/08 experiment (See Appendix iii.i.vi). Abiotic n = 34, Biotic n = 31.

Figure 4.6 shows aqueous-phase biotic enhancements of weathering for silicate and phosphate by moss on granite (a 1.6x aqueous phase biotic enhancement for SiO_4^{4-} and a 4.2x enhancement for PO_4^{3-}) though the statistical significance of the phosphate enhancement appears weak as the standard error bars are very close. The NAA data for silicate is in good agreement with ICP silicon data (total weathering Si = 0.435µmol, total weathering SiO_4 = 0.430µmol). It was expected that the values for NAA silicate would be less than the values obtained for Si by ICP as the ICP measures total silicon of any speciation, whereas the NAA only measures silicate (SiO_4^{4-}) speciation. Table 4.2 below gives the P values for the test W_a vs. W_b across all analytes (ICP and NAA):-

	Al	Ca	Fe	K	Mg	Na	Si	SiO_4	PO_4
$W_b>W_a$	<0.01		<0.01				*0.2*		<0.01
$W_b<W_a$		<0.01		0.02	<0.01	<0.01		*0.33*	

Table 4.2 – Levels of significance (P values) for the test W_b vs. W_a in the Granite dataset, arranged by direction. ($W_b>W_a$ indicates that the median rank for W_b was higher than the rank for W_a. $W_b<W_a$ indicates the inverse was true). Results rounded to 2 d.p., insignificant results are italicised.

Table 4.2 shows that the PO_4^{3-} weathering enhancement is in fact significant at the $P<0.01$ level, whereas the enhancement for SiO_4^{4-} is statistically insignificant. The standard error bars are widely distanced in Figure 4.5 so it was suspected that the U test had operated poorly in this instance. This result was re-tested using the t test and a result in the $W_b>W_a$ direction, significant at the $P<0.05$ level was obtained (see Appendix iv.ii). The poor result obtained using the U test is probably due to the large number of 0 values in the dataset for SiO_4^{4-}. The t test corroborated the $P<0.01$ result for PO_4^{3-}. It should be noted that if the NAA data are plotted as individual experiments, the 95% confidence error bars for both analytes always overlap (see Appendix iii.i).

4.3.3 Individual Experimental Data

The data from two individual granite experiments (24/6/08 and 12/1/09) are presented in Figures 4.7/8 below and overleaf:-

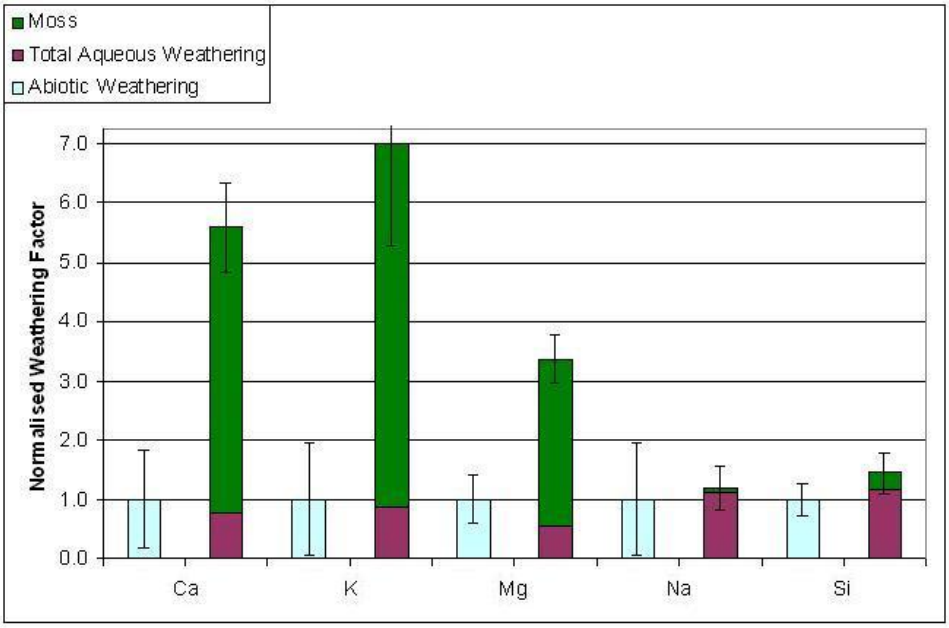

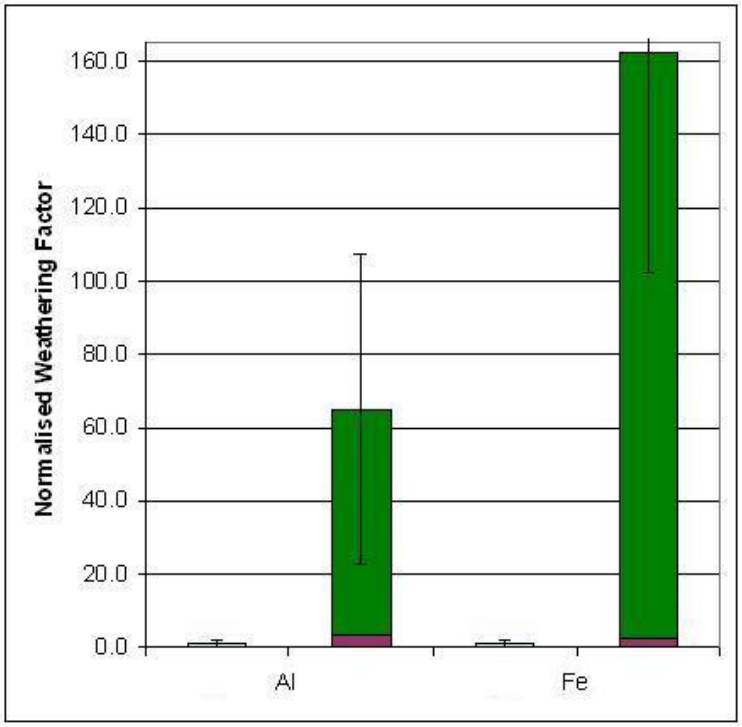

Figure 4.7 – (Above and Left) – 24/6/08 granite experiment: arithmetic means ($\bar{x}$) of the total amounts of analytes weathered into the abiotic aqueous fraction and the biotic microcosm fractions. Error bars represent the 95% confidence interval.

Abiotic n=7, Biotic n=10. Weathering period = 138 days.

Figure 4.7 generally follows the same trends as the aggregated data presented in Figure 4.4 (e.g. Fe and Al are the two most biotically enhanced analytes and Na is the least biotically enhanced analyte). The biotic enhancement values are generally greater for all analytes than the population mean values of the aggregated dataset (except for Na and Si). Higher amounts of Ca, K and Mg have been taken up by the moss in the 24/6/08 experiment than the mean for all experiments (Ca, K and Mg being the three most abundant elements in dry plant tissue (Taiz & Zeiger, 2002)). The 95% confidence error bars overlap for Na and Si indicating that the biotic enhancements for these analytes are statistically insignificant. Figure 4.8 below shows the data from the 12/1/09 granite experiment:-

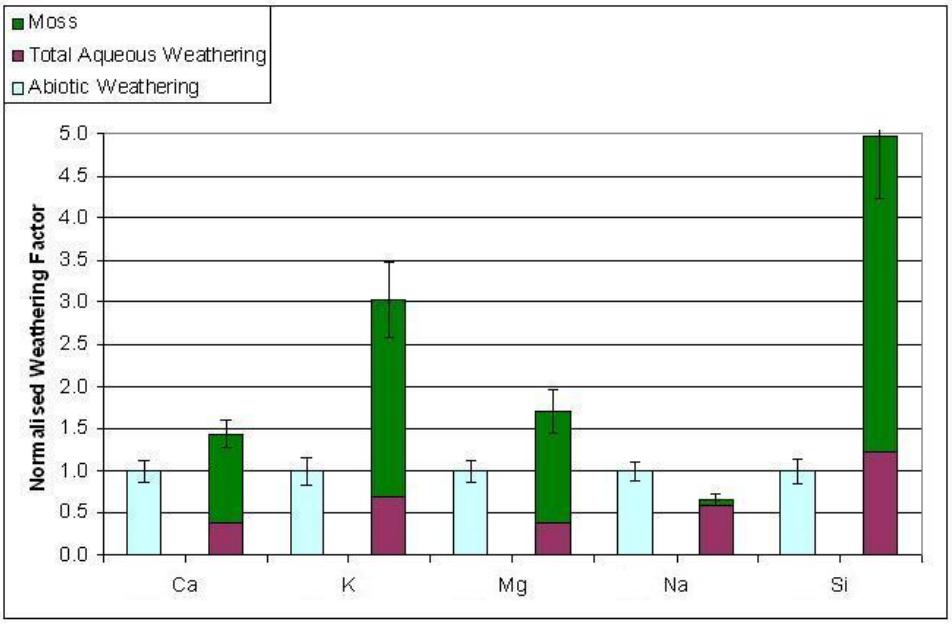

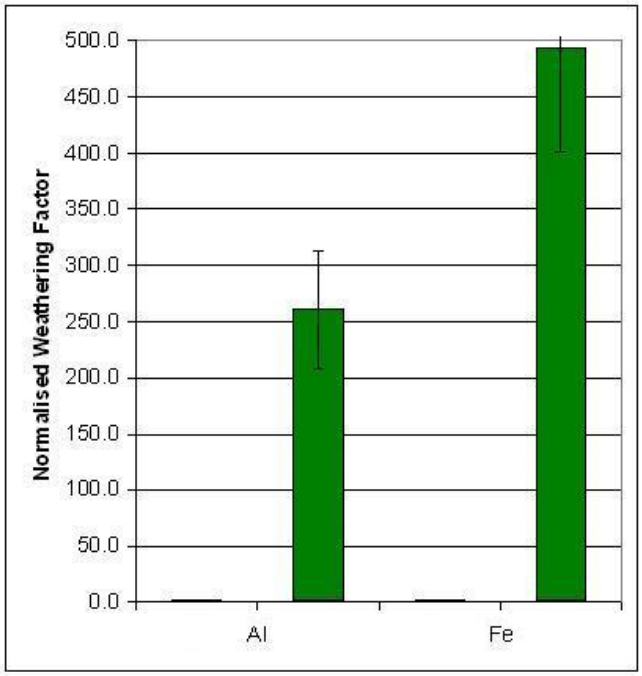

Figure 4.8 – (Above and Left) – 12/1/09 granite experiment: arithmetic means ($\bar{x}$) of the total amounts of analytes weathered into the abiotic aqueous fraction and the biotic fractions. Error bars represent the 95% confidence interval.

Abiotic n=14, Biotic n=14. Weathering period = 149 days.

The 12/1/09 experimental data also mirror some of the key trends as the aggregated dataset (e.g. Al and Fe being the most biotically enhanced analytes). There are two surprising incongruencies between the 12/1/09 data and the aggregated dataset: the biotic enhancement (Ψ) for Si in the aggregated data is 1.6 whereas in the 12/1/09 dataset it is 5.0. Furthermore: there is a $\Psi<1$ for Na which, given the fact that mosses secrete organic acids that are stronger than the carbonic acid involved in the abiotic weathering reaction, is a highly unlikely result. The 12/1/09 experimental data demonstrates the preferential uptake of key plant macronutrients and the purging of less needed micronutrients better than the 24/6/08 experiment and the aggregated dataset. Figure 4.8 demonstrates uptake of Ca, K and Mg (all plant macronutrients) and purging of Na and Si.

It should be noted that not all of the individual granite experiments exhibit relationships as strong as those exhibited by the 24/6/08 and 12/1/09 datasets; the 30/4/08 and 19/12/08 granite experiments have overlapping 95% confidence limit error bars for five analytes in each experiment (see Appendix iii.i). Fe however always exhibits a statistically significant biotic enhancement of weathering in all six granite experiments.

4.3.4 Granite Summary

The biotic enhancement of weathering values for Fe and Al as both a population mean of all granite experiments (FeΨ=112.6, AlΨ=16.4) and in the individual experiments presented (up to FeΨ=493.6 in the 12/1/09 experiment, the highest biotic enhancement in any of the granite experiments) are remarkable given that granite is usually regarded as an unlabile substrate that is highly resistant to weathering. The additional fact that all results in the W_a vs. W_{tot} U test for the aggregated dataset (with the exception of Na) are significant at the $P<0.01$ level and almost all error bars are non-overlapping lends weight to the fact that these results are statistically robust.

4.4 Andesite Experiments

4.4.1 Introduction

Figure 4.9 – Side and plan views of an andesite control microcosm shortly after preparation.

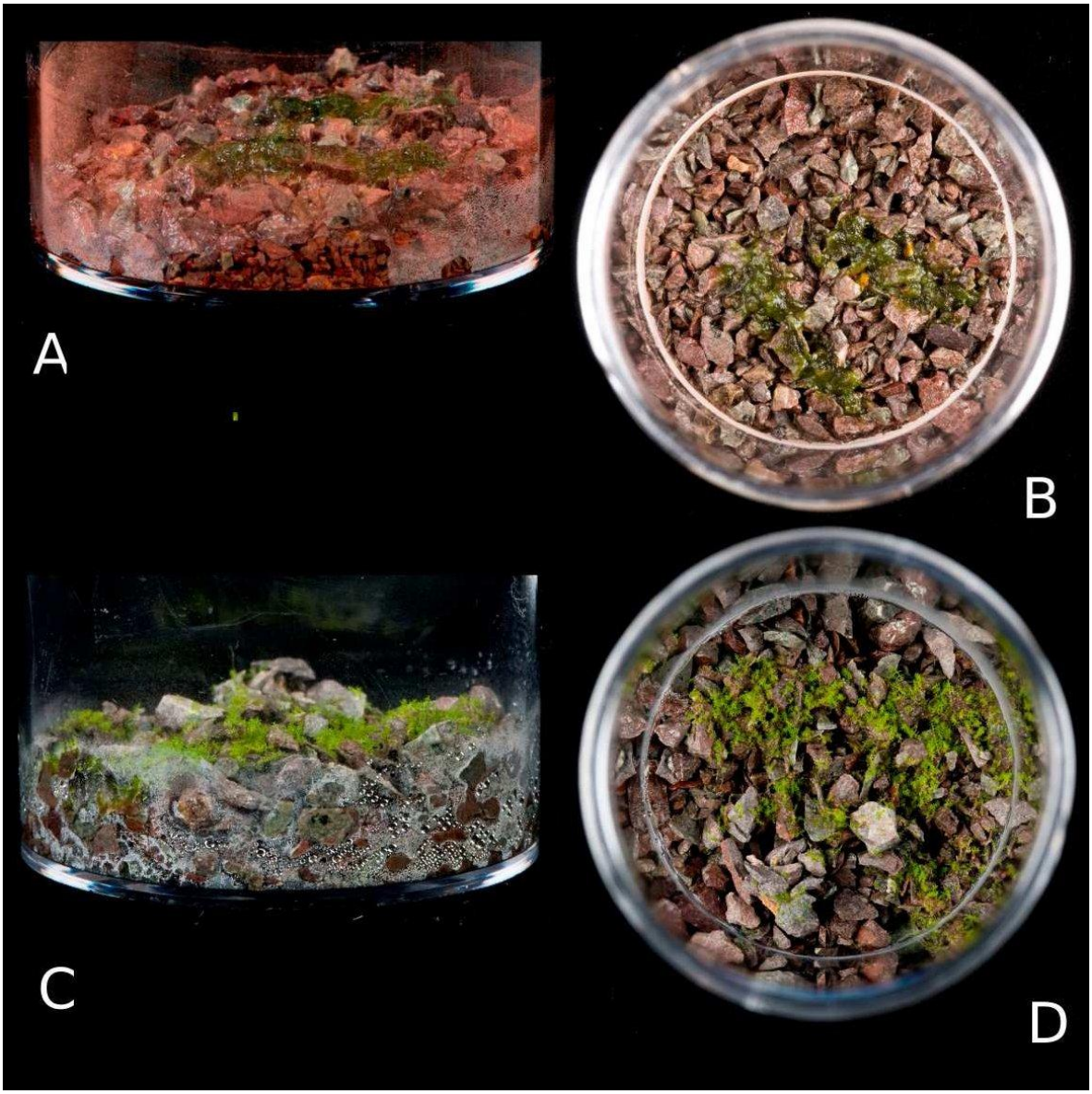

Figure 4.10 – Plan and side views of mossed andesite microcosms shown at time of inoculation (A&B) and after a growth/weathering phase of 113 days (C&D).

4.4.2 Aggregated Data

The following graphs show the population mean ($\bar{\mu}$) values for each analyte in all of the andesite experiments. The results are population means of three experiments (28/11/08, 2/12/08, 25/1/09).

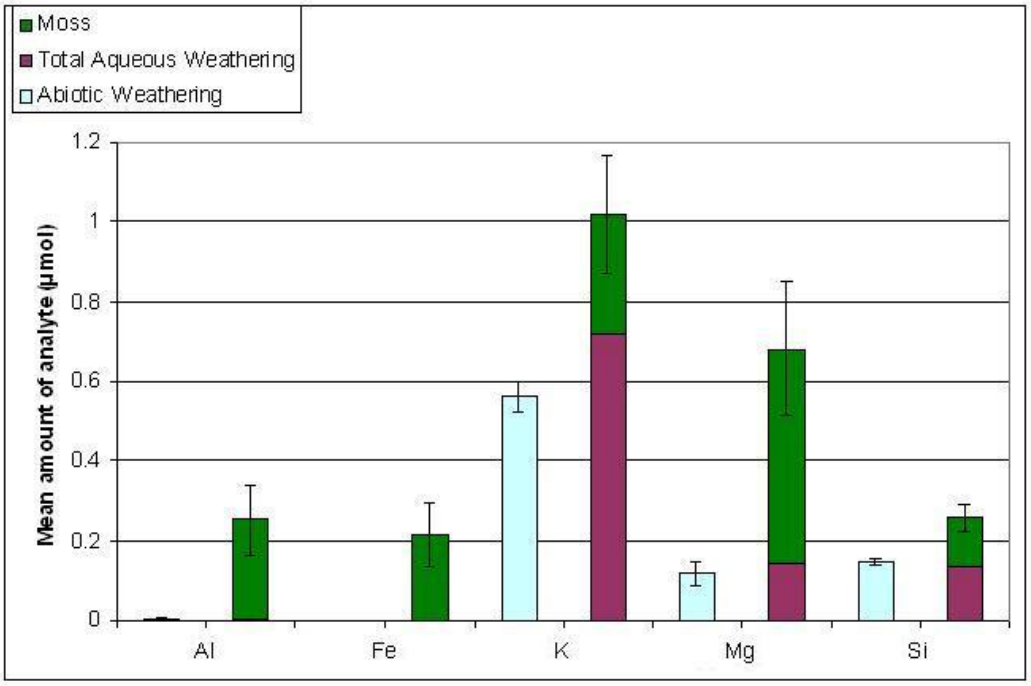

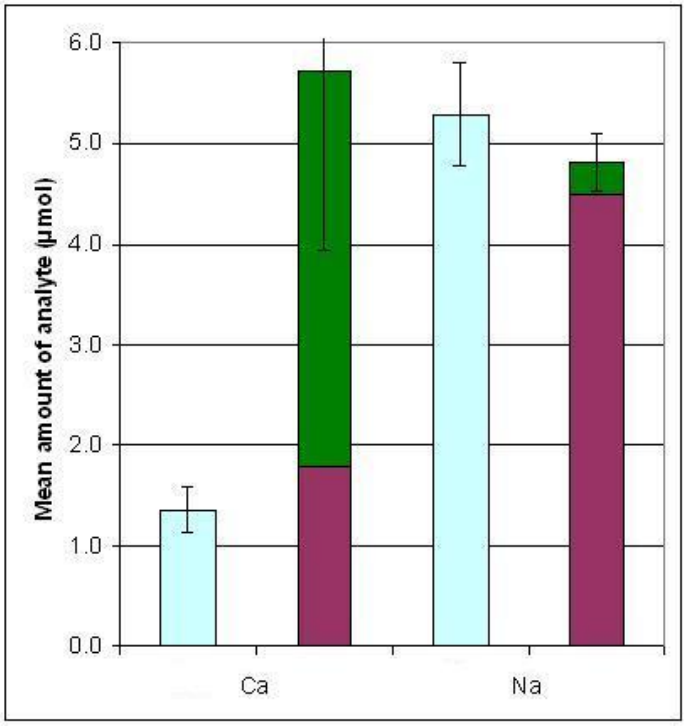

Figure 4.11 (Above and Left) – Population mean ($\bar{\mu}$) values of the amount of analyte weathered into the different microcosm fractions in the andesite microcosms.

The aqueous solution from control microcosms is depicted in light blue bars. The other bar represents total weathering in mossed microcosms; the purple bar representing analyte weathered into aqueous solution and the green portion of the bar representing analyte taken up by the moss.

Abiotic n=37, Biotic n=42. Mean weathering period = 142 days.

Figure 4.12 (below) demonstrates weathering in the three andesite experiments aggregated as population means and normalised to abiotic weathering:-

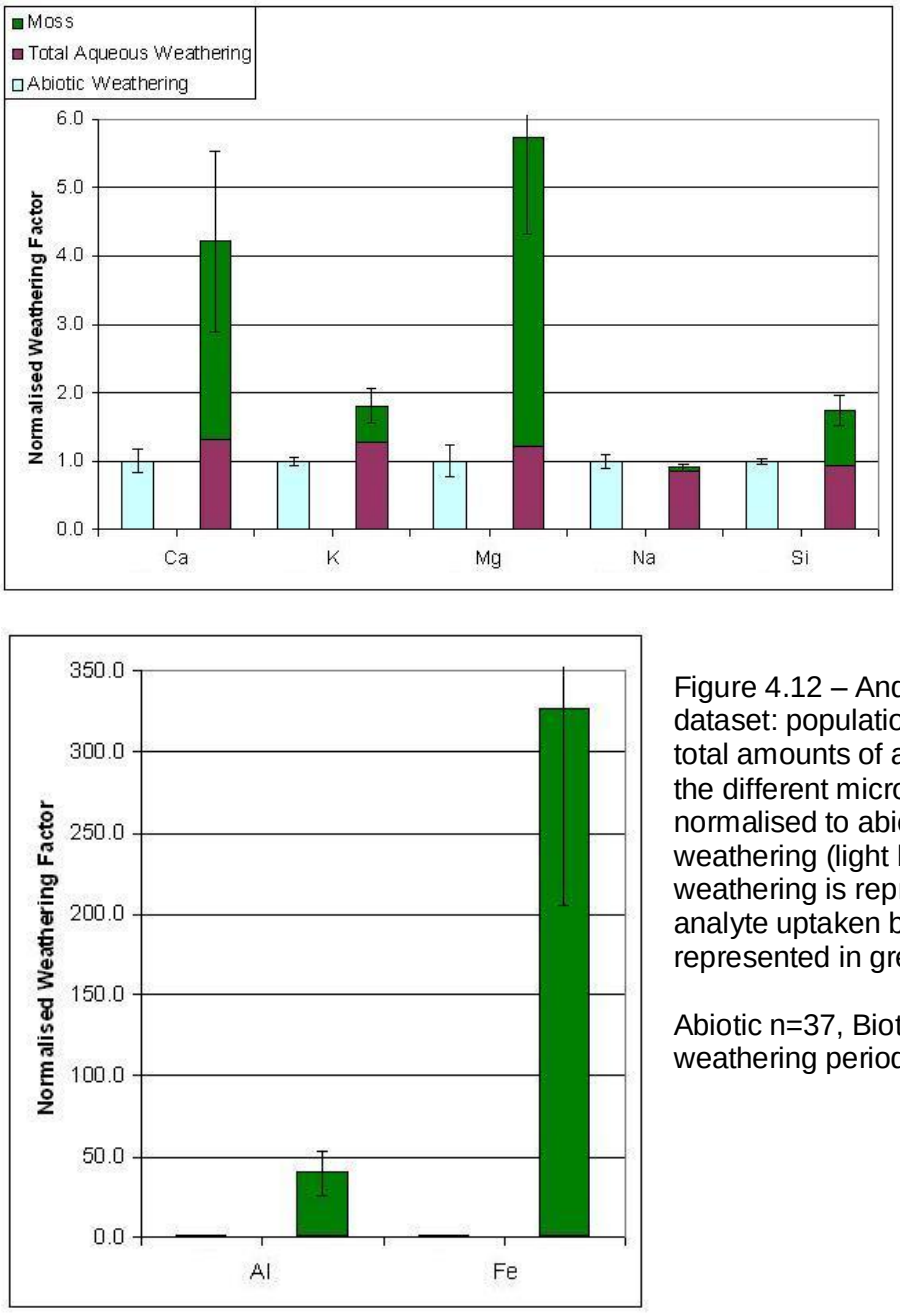

Figure 4.12 – Andesite aggregated dataset: population means ($\bar{\mu}$) of the total amounts of analytes weathered into the different microcosm fractions normalised to abiotic aqueous weathering (light blue). Total aqueous weathering is represented in purple and analyte uptaken by the moss is represented in green.

Abiotic n=37, Biotic n=42. Mean weathering period = 142 days.

Figure 4.12 shows that moss biotically enhances the weathering of all analytes on andesite except for Na (which exhibits a weak negative Ψ of -0.3 with overlapping error bars). Ψ values range from 4.1 for Ca, through 40.4 for Al up to 330.7 for Fe. The biotic enhancement values in Figure 4.12 follow a similar pattern to those in the granite aggregated dataset; Al has the highest Ψ, followed by Fe and then Ca, K and Mg (the comparison of highest-lowest Ψ

degenerates from Ca onward. Table 4.3 (below) shows the levels of significance for the data obtained using the U test. The distinctive signature of an element being preferentially taken up by the moss (the purple bar being lower than the light blue bar as in Figure 4.5) does not appear to be present for any analytes in the andesite aggregated dataset (with the exception of Na).

	Al	Ca	Fe	K	Mg	Na	Si
$W_{tot}>W_a$	<0.01	<0.01	<0.01	<0.01	<0.01		<0.01
$W_{tot}<W_a$						*0.47*	

Table 4.3 – Levels of significance (P values) for W_{tot} vs. W_a in the andesite dataset arranged by direction. ($W_{tot}>W_a$ indicates that the median rank for W_{tot} was higher than W_a. $W_{tot}<W_a$ indicates the inverse was true). Results rounded to 2 d.p., insignificant results are italicised.

Table 4.3 shows that all Ψ values are highly significant at the P<0.01 level except for the Na result which is statistically insignificant (indicating that the weakly –ve Ψ value for Na falls within the pre-determined range of uncertainty). No nutrient auto analysis was conducted upon any of the andesite experiments due to a shortage of funds, there are therefore no data for phosphate and silicate (although silicon was analysed via ICP).

4.4.3 Individual Experimental Data

The data from two individual andesite experiments (2/12/08 and 25/1/09) are presented in Figures 4.13/14 below and overleaf:-

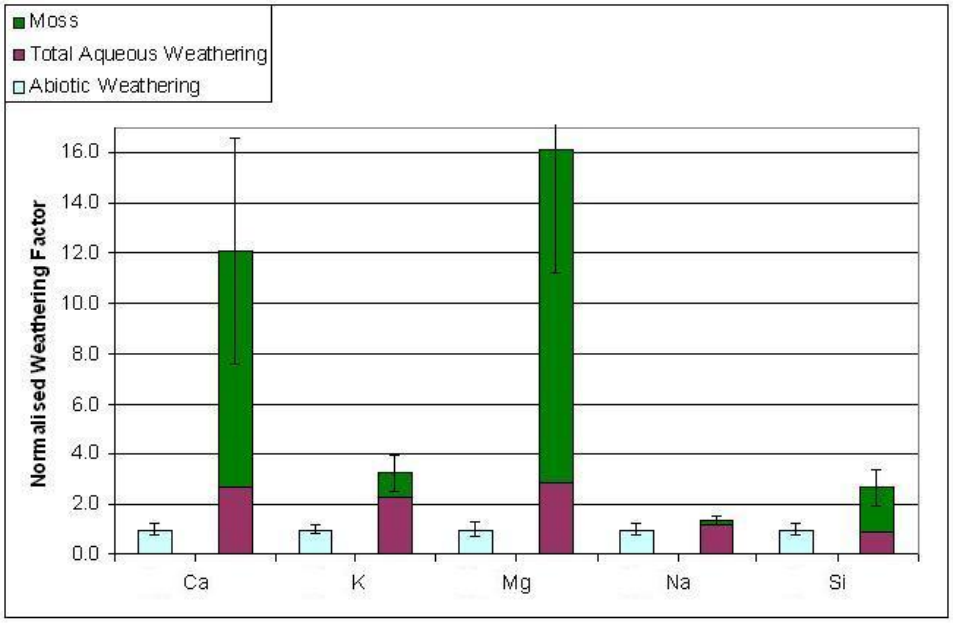

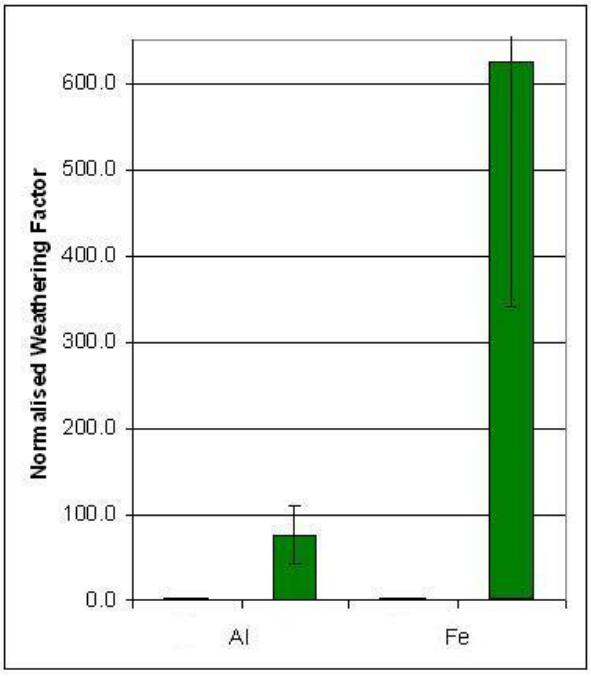

Figure 4.13 – (Above and Left) – 2/12/08 andesite experiment: arithmetic means ($\bar{x}$) of the total amounts of analytes weathered into the abiotic aqueous fraction and the biotic microcosm fractions. Error bars represent the 95% confidence interval.

Abiotic n=11, Biotic n=9. Weathering period = 202 days.

Figure 4.13 follows the exact same trend as the aggregated data for andesite presented in Figure 4.12; i.e. the order of biotic enhancement ordered highest-lowest is as follows: Fe, Al, Mg, Ca, K, Si, Na. All biotic enhancements in the 2/12/08 experiment are higher than those in

the aggregated dataset, with more Ca, Mg and Si entering the moss than the average for all three andesite experiments. The Ψ value for Fe of 625.0 is the highest biotic enhancement recorded in any experiment conducted on any substrate in this procedure.

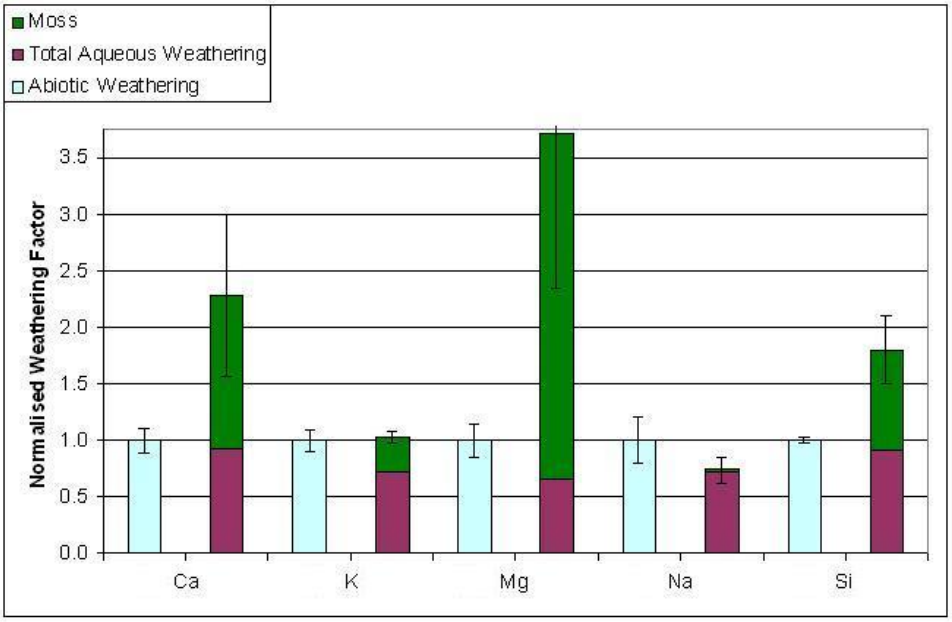

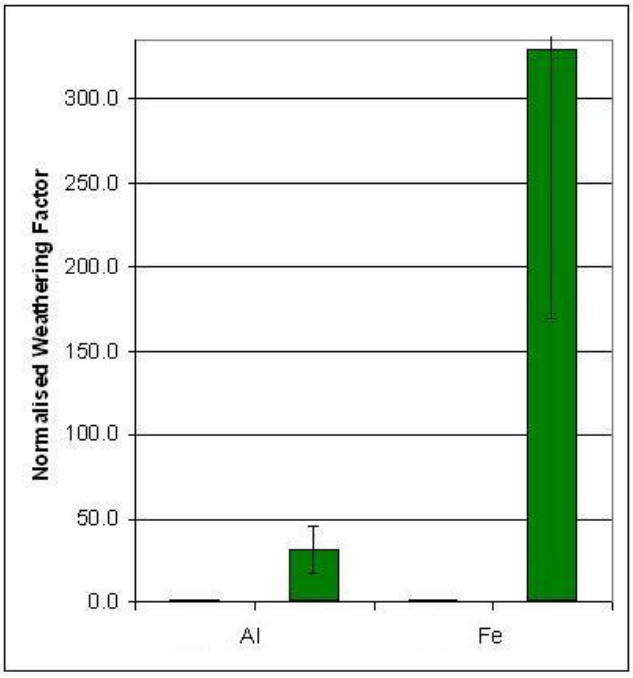

Figure 4.14 – (Above and Left) – 25/1/09 andesite experiment: arithmetic means ($\bar{x}$) of the total amounts of analytes weathered into the abiotic aqueous fraction and the biotic microcosm fractions. Error bars represent the 95% confidence interval.

Abiotic n=24, Biotic n=21. Weathering period = 158 days.

Figure 4.14 also broadly follows the same trends as the aggregated dataset; Fe, Al, Mg and Ca being the four most biotically enhanced analytes (in that order). The biotic enhancement for K is extremely marginal in the 25/1/09 experiment ($K\Psi$ = 1.03 to 2 d.p. with overlapping error

bars). All biotic enhancements are lower than the 2/12/08 experiment, the Ψ value for Fe is approximately half that of the Ψ value for Fe in the 2/12/08 experiment (339.1 c.f. 625.0). This decrease in overall Ψ may be a function of weathering period (158 days in the 25/1/09 experiment c.f. 202 days in the 2/12/08 experiment). Figure 4.14 also demonstrates the preferential uptake of micronutrients (unlike the 2/12/08 data and the aggregated dataset): K, Ca and Mg appear strongly uptaken (typically forming 1.0%, 0.5% and 0.2% of dry plant tissue respectively (Taiz & Zeiger, 2002)) with Si being weakly uptaken (0.1% of dry plant tissue (*Op. cit.*)).

4.4.4 Andesite Summary

The biotic enhancements of weathering for Fe on andesite were the highest biotic enhancements encountered across all experiments on all substrates (the highest being FeΨ = 625.0 in the 2/12/08 experiment), the population mean of all three andesite experiments being FeΨ = 330.7 (this compares with an FeΨ of 112.6 for the granite aggregated dataset). AlΨ on andesite was approximately double its value on granite. A comparison of the smaller biotic enhancements in the andesite and granite aggregated datasets is more fluid: SiΨ and NaΨ are $\approx$ 1.5 in both datasets, the CaΨ and the *Mg*Ψ are higher in the andesite dataset than the granite dataset, but KΨ is slightly lower in the andesite dataset than the granite dataset.

All results in the W_a vs. W_{tot} U test for the andesite aggregated dataset (with the exception of Na) are significant at the $P<0.01$ level and the fact that very few error bars overlap mean that these data (like those for the granite dataset) are statistically reliable. The 25/1/09 experimental data shows evidence of the preferential uptake of plant macronutrients, such trends are however not identifiable in the 2/12/08 and the aggregated experimental data.

4.5 Vermiculite Experiments

4.5.1 Introduction

Three experiments were conducted using vermiculite. The 18/12/07 experiment provided a null result due to over-dilution of the sample with upH_2O associated with Microcosm water sampling method 2 (all data points were non-detects). The 14/2/08 experiment yielded positive results for all analytes and the 17/2/09 experiment yielded positive results for all analytes except Na. The 14/2/08 and 17/2/09 datasets have been combined to form an aggregated dataset; however, unlike the aggregated data presented for granite and andesite the error bars on vermiculite experimental graphs represent the 95% confidence interval as the author felt that presenting a standard error on a population mean based on two experiments would have been statistically inappropriate (three experiments being the minimum acceptable for that method of error representation).

4.5.2 Aggregated Data

The following graphs show the population mean ($\bar{\mu}$) values for each analyte in the two successful vermiculite experiments. The results are population means of two experiments (14/2/08 and 17/2/09). Error bars represent the 95% confidence interval.

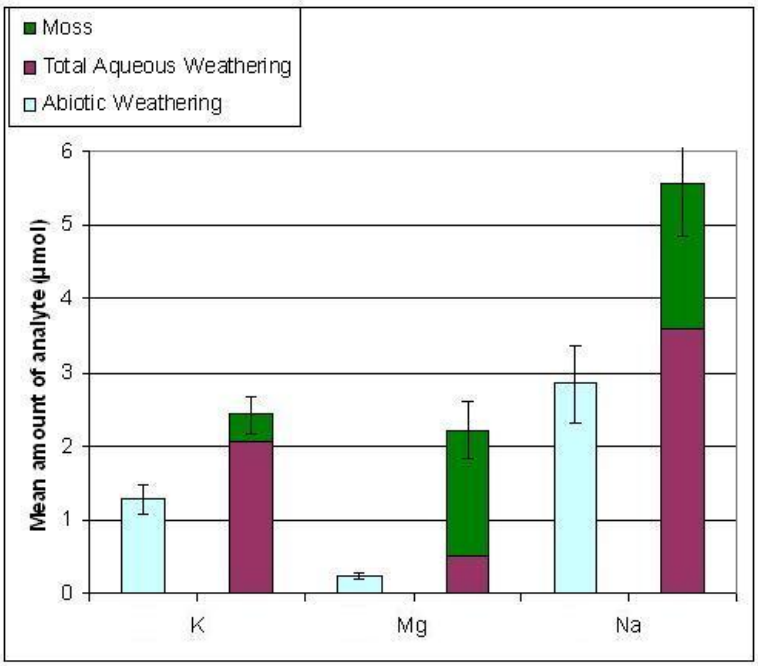

Figure 4.15 (Left and Below) – Population mean ($\bar{\mu}$) values of the amount of analyte weathered into the different microcosm fractions in the vermiculite microcosms.

The aqueous solution from control microcosms is depicted in light blue bars. The other bar represents total weathering in mossed microcosms; the purple bar representing analyte weathered into aqueous solution and the green portion of the bar representing analyte taken up by the moss.

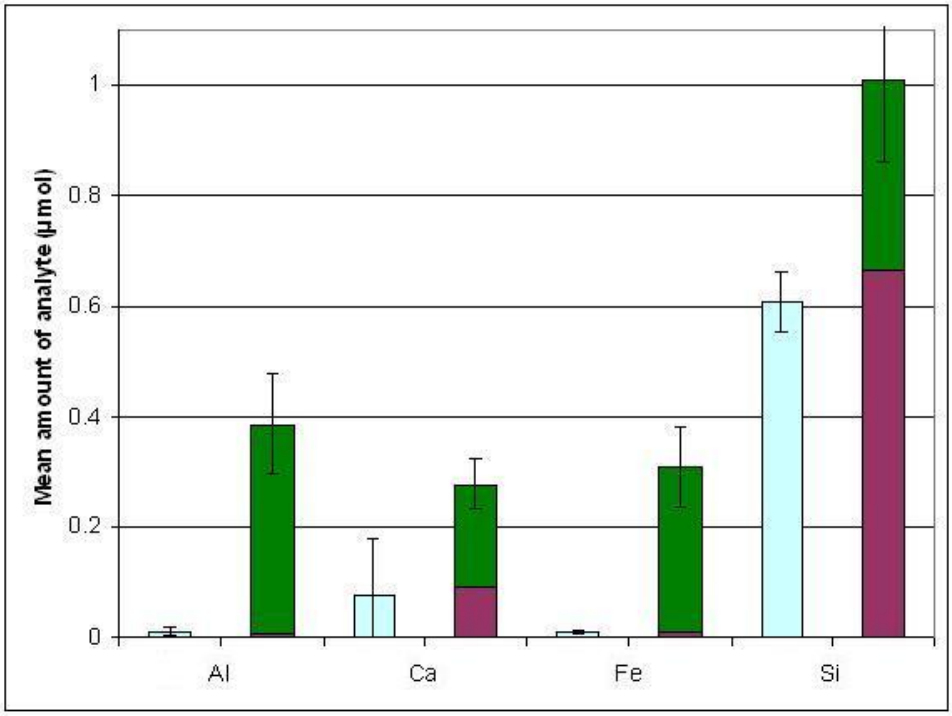

Abiotic n=37, Biotic n=37. Mean weathering period = 109 days.

Figure 4.16 (below) demonstrates weathering in the two vermiculite experiments aggregated as population means and normalised to abiotic weathering:-

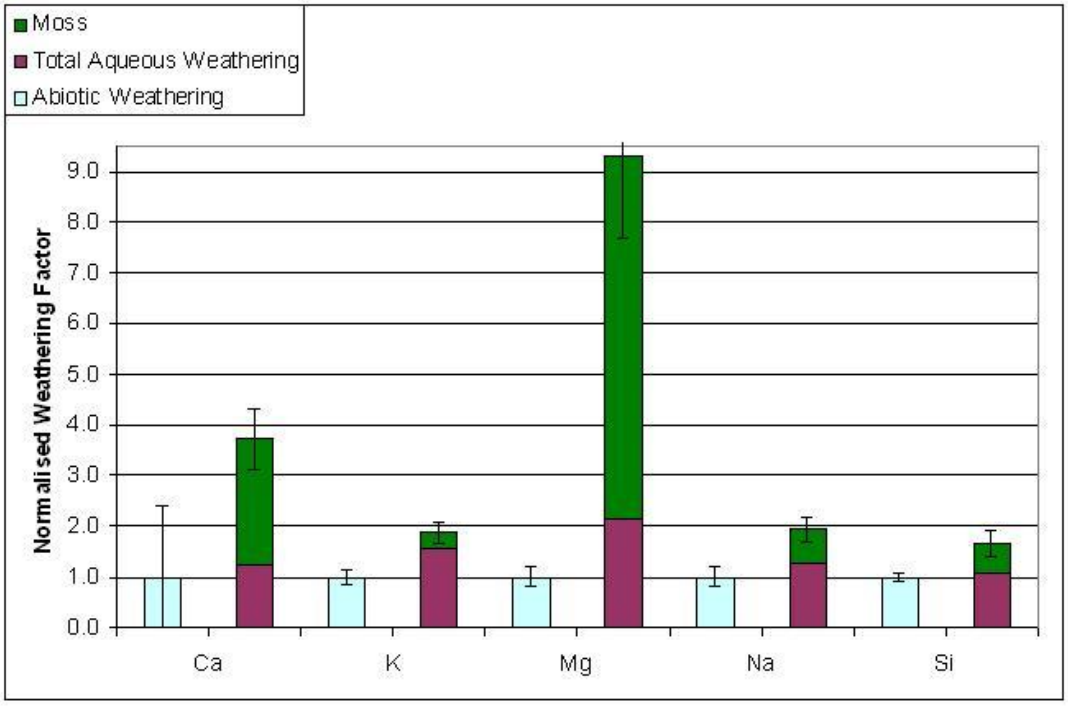

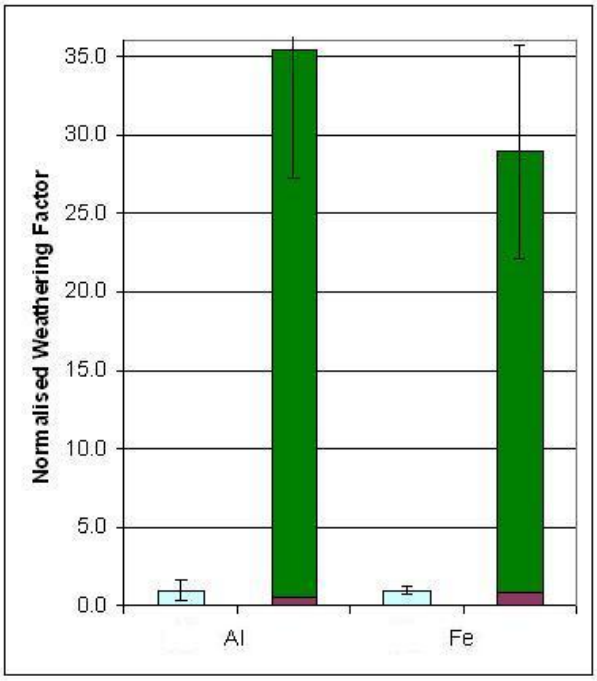

Figure 4.16 (Above and Left) – Vermiculite dataset population means ($\bar{\mu}$) of the total amount of analyte weathered into the different microcosm fractions normalised to abiotic aqueous weathering (NB error bars represent the 95% confidence interval of the aggregated dataset for each analyte).

Abiotic n=37, Biotic n=37. Mean weathering period = 109 days.

Figure 4.16 shows that all analytes are biotically enhanced on vermiculite. Ψ values range from 1.7 for Si, through 29.0 for Fe up to 35.5 for Al (NB the vermiculite aggregated dataset is the only aggregated dataset where AlΨ >FeΨ). The maximum Ψ value on vermiculite is substantially lower than that for the granite and andesite aggregated datasets (Ψ35.5 c.f. Ψ112.6 and Ψ330.7 for granite and andesite respectively). None of the 95% confidence limit error bars in Figure 4.16 are overlapping, which is an indication that the data are significant at least at the P<0.05 level. The U test was also conducted on the vermiculite aggregated dataset (see Table 4.4, below):-

	Al	Ca	Fe	K	Mg	Na	Si
$W_{tot}>W_a$	<0.01	<0.01	<0.01	<0.01	<0.01	<0.01	<0.01
$W_{tot}<W_a$							

Table 4.4 – Levels of significance (P values) for W_{tot} vs. W_a in the vermiculite aggregated dataset arranged by direction. ($W_{tot}>W_a$ indicates that the median rank for W_{tot} was higher than W_a. $W_{tot}<W_a$ indicates the inverse was true). Results rounded to 2 d.p.

Table 4.4 shows that all biotic enhancements on vermiculite are significant at the P<0.01 level, meaning that the probability that the data shown in Figure 4.16 being due to chance is less than 1% (a highly statistically significant positive result). Figure 4.17 (overleaf) shows the data obtained for silicate and phosphate using the NAA in the 14/2/08 Vermiculite experiment, the only vermiculite experiment analysed via NAA (due to a shortage of funds):-

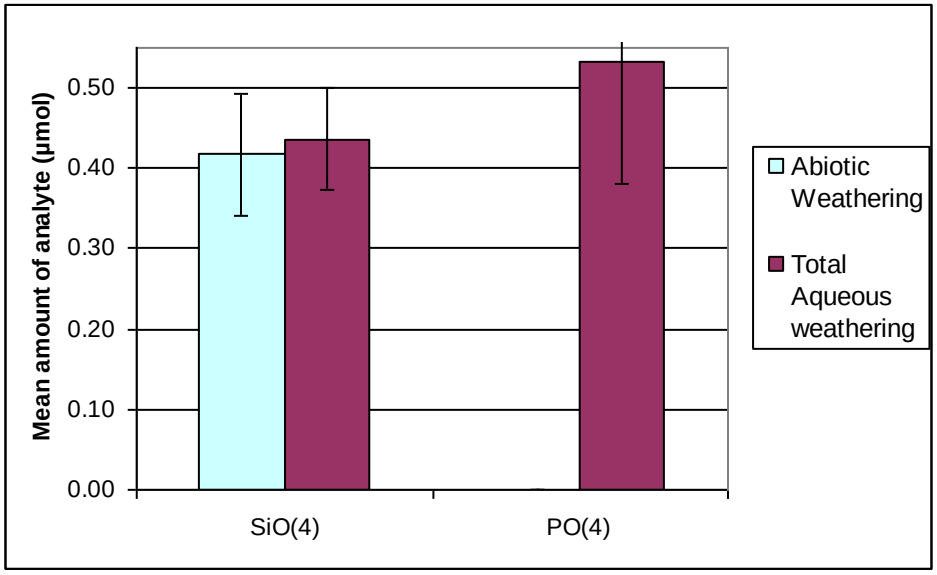

Figure 4.17 (Left) – Arithmetic mean values ($\bar{x}$) of silicate (SiO_4^{4-}) and phosphate (PO_4^{3-}) weathered into aqueous solution in control microcosms in the 14/2/08 Vermiculite experiment (NB error bars represent the 95% confidence interval).

Abiotic n = 20, Biotic n=20.

	Al	Ca	Fe	K	Mg	Na	Si	SiO_4	PO_4
$W_b > W_a$		<0.01		<0.01		<0.01			*0.146*
$W_b < W_a$	<0.01		*0.383*		<0.01		<0.01	<0.01	

Table 4.5 – P values for W_b vs. W_a in the 14/2/08 Vermiculite dataset arranged by direction.

Table 4.5 shows that the result for PO_4 is not significantly different and SiO_4^{4-} is present at a higher level in W_a than W_b ($P<0.01$). Given the fact that no PO_4 was detected in any of the abiotic aqueous fractions and a mean of 0.53µmol was detected into the biotic aqueous fraction; this appears to be another spurious U test result (probably due to the large number of 0 values in the W_a dataset and because SPSS does not correct for ties where $n<30$). This result was re-tested using the t test and a $P<0.01$ result in the $W_b>W_a$ direction was obtained (see Appendix iv.ii). The t test also showed that SiO_4^{4-} $W_b>W_a$, but this result is statistically insignificant at the $P<0.05$ level.

4.5.3 Vermiculite Summary

Even though a third experiment for vermiculite is lacking; it appears that the vermiculite aggregated dataset is robust: no error bars overlap on the ICP data (Figure 4.15/6) and all biotic enhancements yield P values of <0.01 after testing with the U test (Table 4.5). The weak aqueous phase biotic enhancement for silicate is statistically insignificant (overlapping error bars and T test gives a $P>0.05$). The 5.3x aqueous phase biotic enhancement of phosphate is highly statistically significant (t test $P<0.01$). The vermiculite data do not show evidence for the preferential uptake of plant macronutrients by moss.

4.6 Chlorite Experiment

Figure 4.18 (below) represents data from the one experiment started on 24/6/08 using a rock that contained the mineral chlorite:-

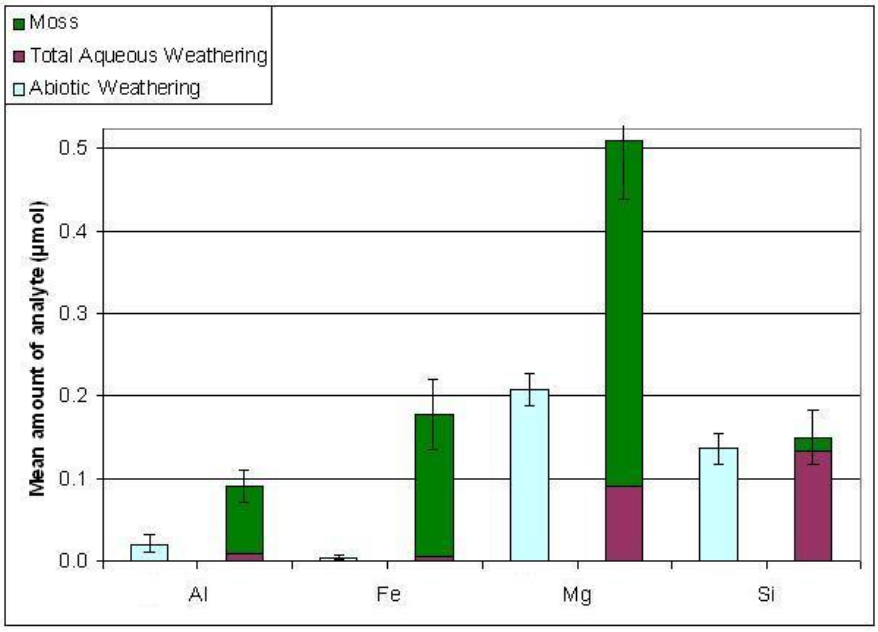

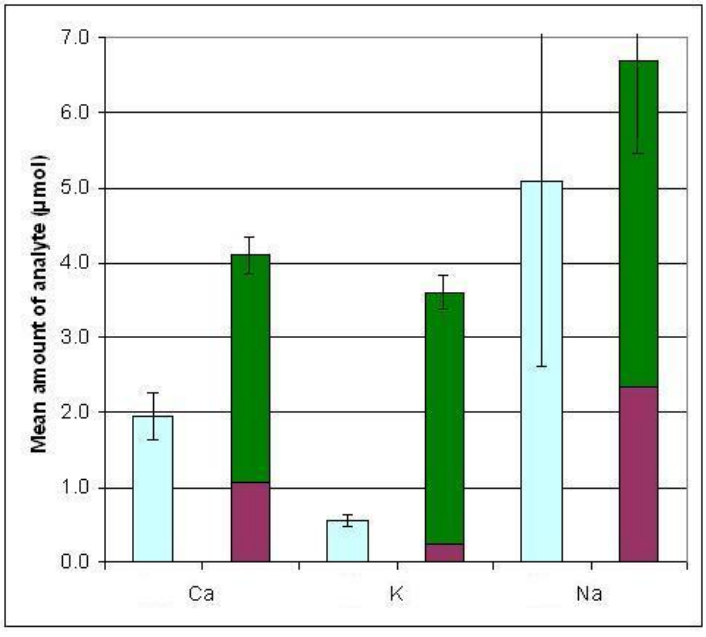

Figure 4.18 (Above and Left) - 24/6/08 Chlorite experiment: arithmetic means ($\bar{x}$) of the amount of analyte weathered into the different microcosm fractions in the chlorite microcosms. (NB error bars represent the 95% confidence interval).

The aqueous solution from control microcosms is depicted in light blue bars. The other bar represents total weathering in mossed microcosms; the purple bar representing analyte weathered into aqueous solution and the green portion of the bar representing analyte taken up by the moss. Abiotic n=7, Biotic n=7.

Weathering period = 72 days.

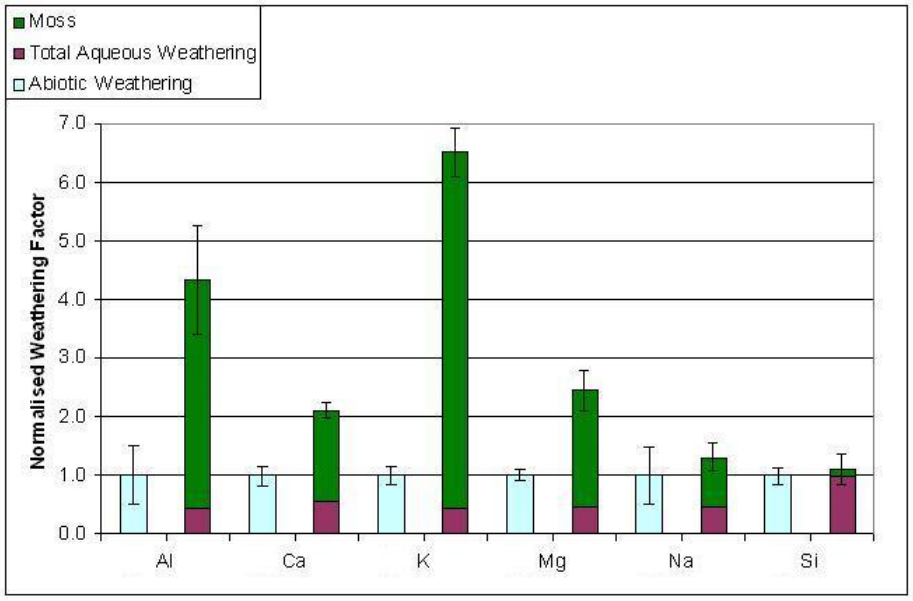

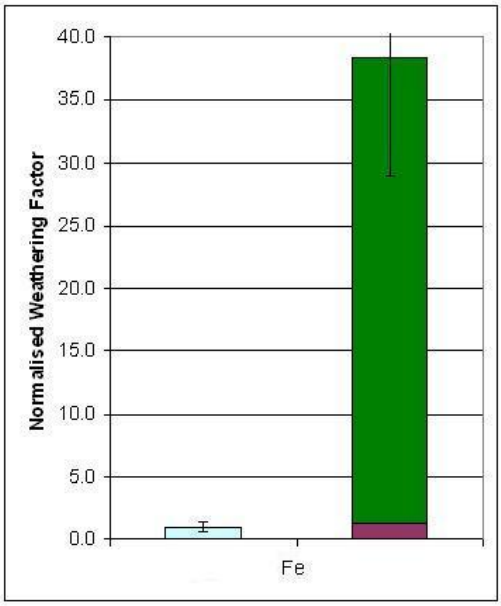

Figure 4.19 (Above and Left) – 24/6/08 Chlorite experiment: arithmetic means ($\bar{x}$) for the total amount of analyte weathered into the different microcosm fractions normalised to abiotic aqueous weathering (NB error bars represent the 95% confidence interval).

Abiotic n=7, Biotic n=7. Weathering period = 72 days.

Figure 4.19 demonstrates Ψ values ranging from 1.1 for Si up to 38.3 for Fe. All 95% confidence interval error bars are non-overlapping, with the exception of Na and Si (which had the smallest biotic enhancements). The chlorite containing rock was cut into rectangular prisms and was very glassy (vitreous) in nature indicating that it was highly felsic (contained a high proportion of SiO_2). Rocks containing a high proportion of SiO_2 are very difficult to weather, which may explain the lower maximum biotic enhancement encountered on chlorite relative to the other substrates.

Figure 4.19 shows the preferential weathering signal for all analytes except Fe and Si (including Na which is a micronutrient usually present in dry plant tissue at lower amounts

than Fe). Al shows signs of preferential uptake by the moss even though it is not generally considered a plant nutrient (Taiz & Zeiger, 2002). This almost universal demonstration of preferential weathering could be a response by the moss to the highly unlabile nature of the felsic chlorite rock; the moss could be exerting a strong weathering effect upon the substrate and in the process taking up nutrients in larger amounts than it requires.

The U test was conducted upon the chlorite dataset but it is important to note that the sample size of only seven mossed and seven control microcosms is very low and so statistical analysis of the dataset should be treated with caution.

	Al	Ca	Fe	K	Mg	Na	Si
$W_{tot}>W_a$	<0.01	<0.01	<0.01	<0.01	<0.01	*0.32*	
$W_{tot}<W_a$							*0.90*

Table 4.6 – Levels of significance (P values) for W_{tot} vs. W_a in the 24/6/08 Chlorite dataset arranged by direction. ($W_{tot}>W_a$ indicates that the median rank for W_{tot} was higher than W_a. $W_{tot}<W_a$ indicates the inverse was true). Results rounded to 2 d.p., insignificant results are italicised.

Table 4.6 demonstrates that all positive results were significant at the $P<0.01$ level except for Na and Si which are insignificant. Whilst the low sample size means that the analysis presented in Table 4.6 should be treated with caution, the data in Table 4.6 are congruent with the 95% confidence limit error bars on Figure 4.19. The NAA PO_4 and SiO_4 data were both statistically insignificant, most likely due to the low sample size. These data are not presented here but are presented in Appendix iii.iv.

Considering the highly felsic nature of the chlorite rock, the results presented here are impressive. A repeat experiment with a greater sample size would be highly informative.

4.7 Inoculum only experiment

4.7.1 Introduction

On 30/7/09 a batch of moss inoculum and filtrate was used to prepare 15 granite mossed and 15 granite control microcosms. On this day the same volume of inoculum as was added to mossed microcosms (3ml) was added to microcosm containers which did not contain any substrate. The procedures were standardised in all respects, the only exception being that a substrate was not added to the no substrate or 'bare' microcosms prior to inoculation. After 50 days the moss in the bare microcosms had died, so all microcosms initiated on 30/7/09 were sampled at this point (NB this was a much shorter weathering period than the mean 112 days when a substrate was present. The data from the 30/7/09 experiments are presented in Figure 4.20 (overleaf).

4.7.2 Experimental Data

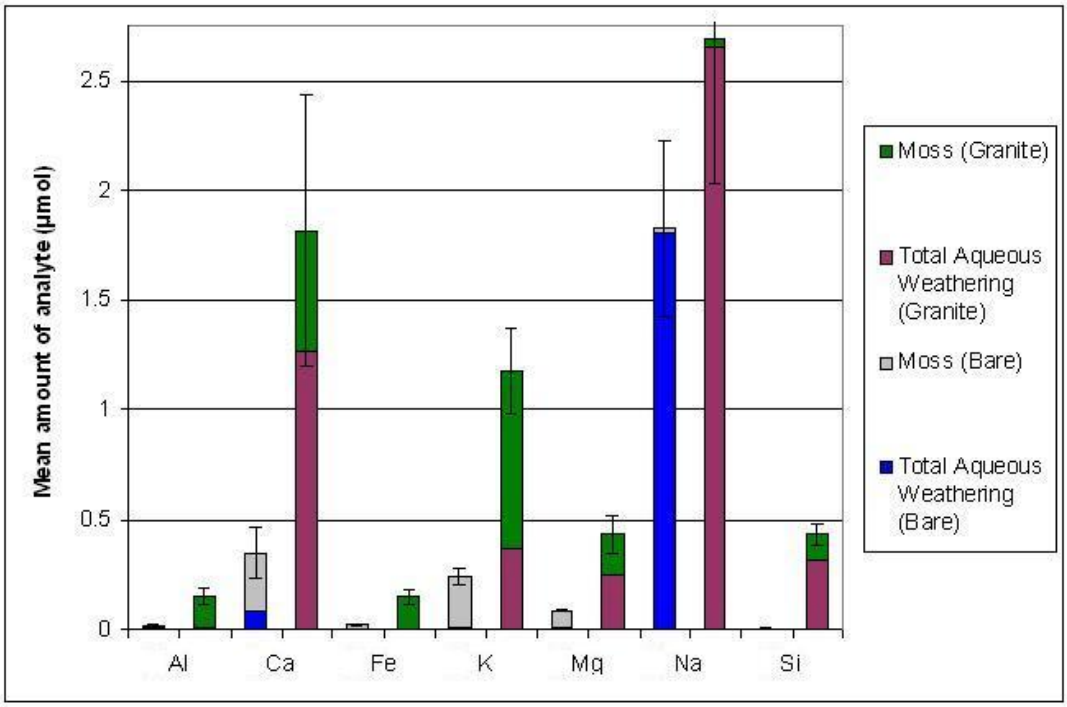

Figure 4.20 – Amount of analyte in the mossed microcosm components from bare microcosms (grey and blue) and the mossed microcosm components from granite microcosms (dark green and burgundy) in the 30/7/09 experiments. The sum of analyte within both mossed microcosm components is regarded as 'Total Weathering' or W_{tot}.

Error bars represent the W_{tot} 95% confidence limit. Bare n=14, Granite n=14. Weathering period = 50 days.

The most noticeable facet of the data presented in Figure 4.20 (above) is that all analytes are present in much higher amounts in the biotic components from granite microcosms than the biotic components from bare microcosms. The amounts of analytes (µmol) weathered in granite microcosms is statistically greater than the amounts weathered in bare microcosms at the 95% confidence interval for all analytes except for Na (error bars overlap). The concentration of analyte in the fractions from all microcosms has been corrected for blanks (See Figure 3.3 p60) and therefore the amounts of analytes in bare microcosm fractions must result from contamination from the microcosm jars themselves or additional contamination that occurred during sampling (every effort was made to minimise this using a semi-clean technique). Figure 4.20 shows that this contamination was, for the most part, very small, the

exception being Na (1.83µmol). Figure 4.21 (below) represents the granite and bare microcosm W_{tot} data, normalised to bare W_{tot}.

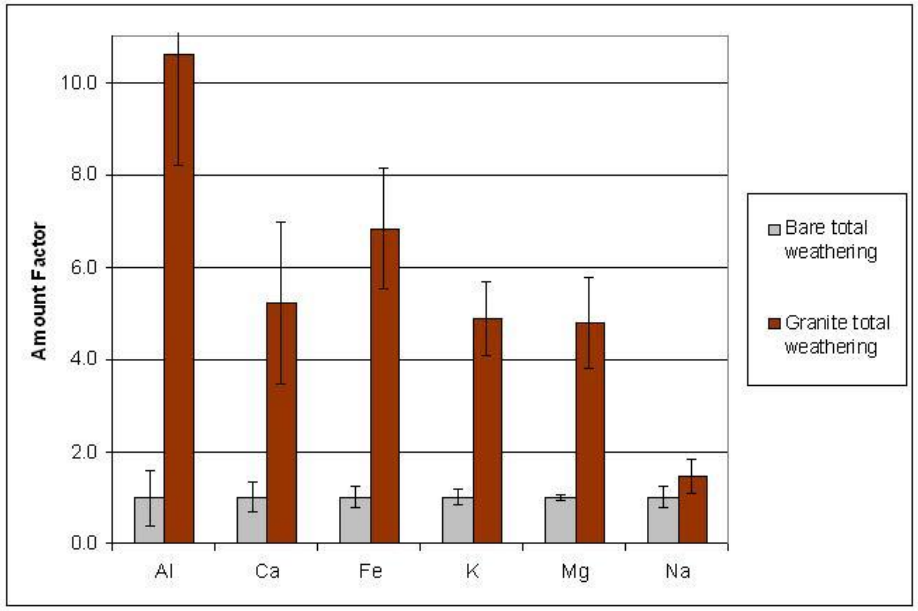

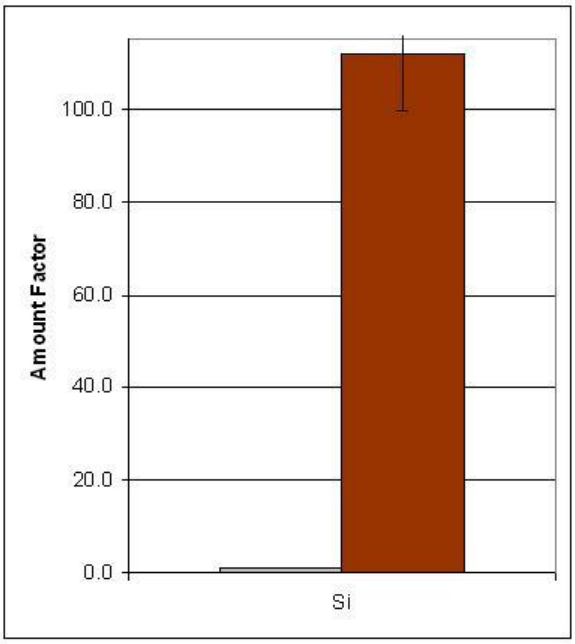

Figure 4.21 – Mean total weathering in the 30/7/09 bare microcosms normalised to itself (grey bar) versus mean total weathering in the 30/7/09 granite microcosms normalised to bare W_{tot} (russet coloured bar). NB Error bars are 95% confidence limits normalised to bare W_{tot}.

Bare n=14, Granite n=14. Weathering period = 50 days.

Figure 4.21 demonstrates the differences in ionic dissolution when a substrate is present (russet) compared with when a substrate is absent (grey). Bare:Granite weathering enhancement factors range from 1.5 for Na (overlapping 95% confidence limit bars) to 111.7 for Si. The Si enhancement is perhaps unremarkable as Si is the primary constituent of granite (and indeed any rock/mineral) after oxygen (Blatt *et al.*, 2006). The increase in amounts of

analytes entering solution and being taken up by moss when granite is present compared to when no substrate is present is striking. A U test was performed comparing the 30/7/09 Granite W_{tot} with the 30/7/09 Bare $W_{tot,}$ the results obtained are presented in Table 4.7 (below).

	Al	Ca	Fe	K	Mg	Na	Si
Granite>Bare	<0.01	<0.01	<0.01	<0.01	<0.01	0.03	<0.01
Granite<Bare							

Table 4.7 – Levels of significance (P values) for W_{tot} in the granite dataset vs. W_{tot} in the bare dataset arranged by direction. Granite>Bare indicates that the median rank for Granite W_{tot} was higher than that for Bare W_{tot}. Granite<Bare indicates the inverse was true. Results rounded to 2 d.p.

4.7.3 Summary

Table 4.7 demonstrates that W_{tot} in granite microcosms was greater than W_{tot} on bare microcosms and that this result is statistically significant for all analytes except Na at the $P<0.01$ level. The Na result is statistically significant at the $P<0.05$ level. Figure 4.20/1 and Table 4.7 taken collectively demonstrate that the effects observed in the microcosm experiments occur as a result of the weathering of the substrate and are not (for example) an effect of ions diffusing out of the moss during growth.

4.8 Masses of moss recovered

Table 4.8 (below) shows the mean mass of moss obtained from the microcosm experiments arranged by substrate with the mean mass of moss inoculum at initial conditions for comparison:-

	Mean amount of moss recovered (mg)	Sample size (n)	σ
Inoculum	**4.12**	**4**	**1.10**
Granite	17.92	70	19.21
Basalt	15.07	6	4.02
Andesite	11.17	42	10.61
Chlorite	10.94	8	2.49
Vermiculite	3.24	49	2.96

Table 4.8 – Mean amounts of moss recovered from mossed microcosms (mg) by analyte. 'Inoculum' gives mass of 3ml of moss inoculum at the time of inoculation.

NB the mean amount of moss recovered from mossed vermiculite microcosms falls below the inoculum mean due to the vastly reduced recovery efficiency associated with this fine-grained, highly exfoliated substrate (see §2.8 p47).

The difference between the 'Inoculum' and the mean amounts of moss recovered can be taken as a crude indicator of carbon fixation and growth. Caution must however be observed here as the inoculum comparison n is small (this represented two pseudo-replicated aliquots of inoculums prepared on 7/5/08 and 23/6/08 respectively). However, the means of moss recovered are under-estimates of the actual biomass grown as not all of the moss was recovered during microcosm sampling. In experiments such as this, a substantial portion of the rooting structure is always irrecoverable (c.f. other studies such as Lewis & Quirk (1967)).

4.9 Weathering per unit Moss Biomass

4.9.1 Introduction

After the weathering period the moss biomass was removed from the microcosm, the moss was weighed and the mass of moss was recorded prior to the moss being oxidised in a mixture of acids. If the chemical data are normalised to the mass of moss biomass recovered then the data presented in Tables 4.9-4.12 is obtained. Such analyses are important in modelling terms as they enable calculation of the likely amount of an analyte weathered per unit mass of moss biomass grown on Earth's surface.

4.9.2 Normalised data

	Al	Ca	Fe	K	Mg	Na	Si
$\mathbf{W_a}$	0.012 (±0.026)	1.664 (±0.172)	*0.002* (±0.002)	0.669 (±0.031)	0.427 (±0.047)	2.908 (±0.441)	0.346 (±0.072)
$\mathbf{W_b}$	0.013 (±0.005)	1.252 (±0.374)	0.005 (±0.003)	0.658 (±0.096)	0.344 (±0.124)	3.120 (±0.349)	0.435 (±0.111)
$\mathbf{W_{moss}}$ **(per mg)**	0.017 (±0.002)	0.109 (±0.008)	0.022 (±0.002)	0.101 (±0.008)	0.031 (±0.002)	0.044 (±0.025)	0.012 (±0.001)

Table 4.9 – Granite aggregated data (to 3d.p.) values in µmol except for W_{moss} (values in µmol/mg). ± value is the standard error (instances where SE≥value are italicised).

The data in Table 4.9 will be used to place weathering within a whole Earth context in §5.2 of the Conclusions.

	Al	Ca	Fe	K	Mg	Na	Si
W_a	0.006 (±0.001)	1.356 (±0.221)	0.001 (±1.76 E-21)	0.563 (±0.037)	0.119 (±0.029)	5.292 (±0.518)	0.148 (±0.007)
W_b	0.006 (±2.86 E-4)	1.798 (±0.154)	0.001 (±9.31 E-2)	0.720 (±0.029)	0.144 (±0.013)	4.490 (±0.376)	0.137 (±0.001)
W_{moss} **(per mg)**	0.042 (±0.010)	0.535 (±0.116)	0.035 (±0.010)	0.073 (±0.015)	0.089 (±0.018)	0.042 (±0.002)	0.022 (±0.004)

Table 4.10 – Andesite aggregated data (to 3d.p.) values in µmol except for W_{moss} (values in µmol/mg). ± value represents the standard error (instances where SE≥value are italicised). Where SE is 0 to 3d.p. the figure is given in scientific notation.

	Al	Ca	Fe	K	Mg	Na	Si
W_a	*0.011* (±0.012)	*0.079* (±0.204)	0.011 (±1.35 E-4)	1.323 (±0.086)	0.240 (±0.019)	2.942 (±0.480)	0.606 (±0.072)
W_b	0.005 (±0.003)	0.089 (±0.003)	0.009 (±0.003)	2.046 (±0.267)	0.499 (±0.081)	3.607 (±0.592)	0.654 (±0.073)
W_{moss} **(per mg)**	0.161 (±0.065)	0.083 (±0.016)	0.125 (±0.026)	0.172 (±0.085)	0.710 (±0.165)	*1.060* (±1.346)	0.172 (±0.145)

Table 4.11 – Vermiculite aggregated data (to 3d.p.) values in µmol except for W_{moss} (values in µmol/mg). ± value is the standard error (instances where SE≥value are italicised). Where SE is 0 to 3d.p. the figure is given in scientific notation.

The larger number of instances of the standard error exceeding the values in Table 4.11 compared with Tables 4.9 and 4.10 for vermiculite is likely due to the reduced recovery efficiency for moss from vermiculite mossed microcosms and the fact that the summary data only represents two experiments whereas the andesite dataset represents three experiments and the granite dataset six experiments.

	Al	Ca	Fe	K	Mg	Na	Si
W_a	0.021 (±0.011)	1.946 (±0.312)	0.005 (±0.002)	0.554 (±0.080)	0.209 (±0.019)	5.095 (±2.481)	0.137 (±0.019)
W_b	0.009 (±0.003)	1.082 (±0.171)	*0.006* (±0.007)	0.241 (±0.034)	0.092 (±0.011)	2.344 (±1.563)	0.133 (±0.020)
W_{moss} **(per mg)**	0.008 (±0.003)	0.291 (±0.090)	0.017 (±0.007)	0.325 (±0.108)	0.040 (±0.013)	0.420 (±0.150)	*0.001* (±0.001)

Table 4.12 – 24/6/08 Chlorite data (to 3d.p.) values in µmol except for W_{moss} (values in µmol/mg). ± value is the 95% confidence interval (instances where 95% conf.≥value are italicised).

4.9.3 Moss growth under optimal conditions

P. patens was grown from spores to gametophyte phase on plugs of peat known as jiffys. The diameter of the end of each jiffy cylinder was measured and the surface area of the circle on which the moss was grown calculated using the formula: $\pi(r^2)$. The moss tissue was then collected from the jiffy using forceps and was air-dried on filter paper for approximately 48 hours in the same fashion as moss removed from microcosms is dried. After 48 hours the moss was weighed, the resulting data is summarised in Table 4.13 below:-

Date cultured	n	Jiffy Radius (cm)	Jiffy Area (m^2)	Dry mass (mg)	Dry mass per unit area (mg/m^2)
17/10/2008	4	2.0	0.13	816.5	6268.1 (±291.5)
27/01/2009	4	2.1	0.13	812.7	6155.6 (±35.7)
	Mean	2.05	0.13	814.6	**6211.8 (±201.4)**

Table 4.13 - Mean mass of moss obtained from jiffys, scaled up to $1m^2$ of jiffy area ('±' represents 1σ).

Table 4.13 quantifies the mass of moss that grows per unit area under optimal conditions, i.e. an abundance of nutrients in the form of peat and the 16 hours light followed by 8 hours of darkness at 25°C growth regime (as per Marienfeld *et al.* (1989)).

4.9.4 Utilising normalised data

To test the appropriateness of presenting the biotic weathering data normalised to mass of moss recovered the amounts of each analyte were plotted against the mass of moss recovered from that microcosm (see Figures 4.22/23 below).

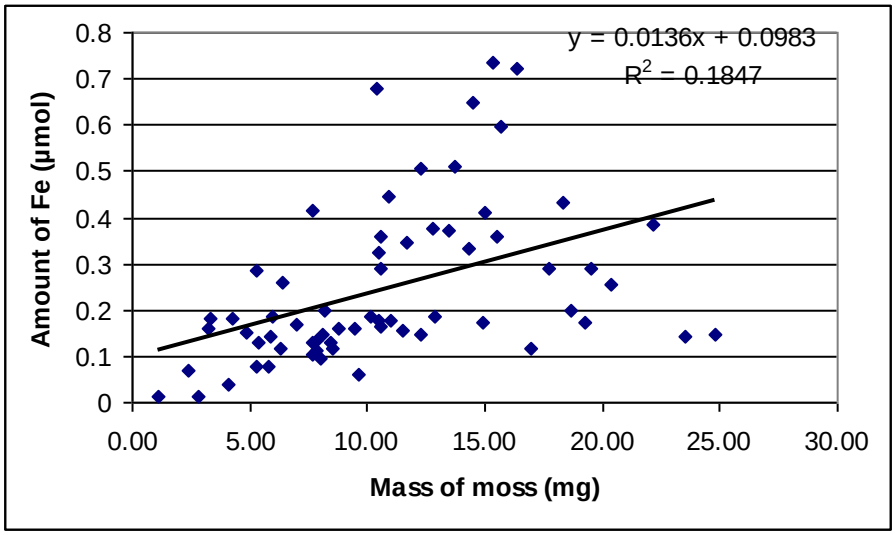

Figure 4.22 (Left) – Amounts of Fe in moss (µmol) from all granite microcosms plotted against the mass of moss (mg) recovered from the microcosm.

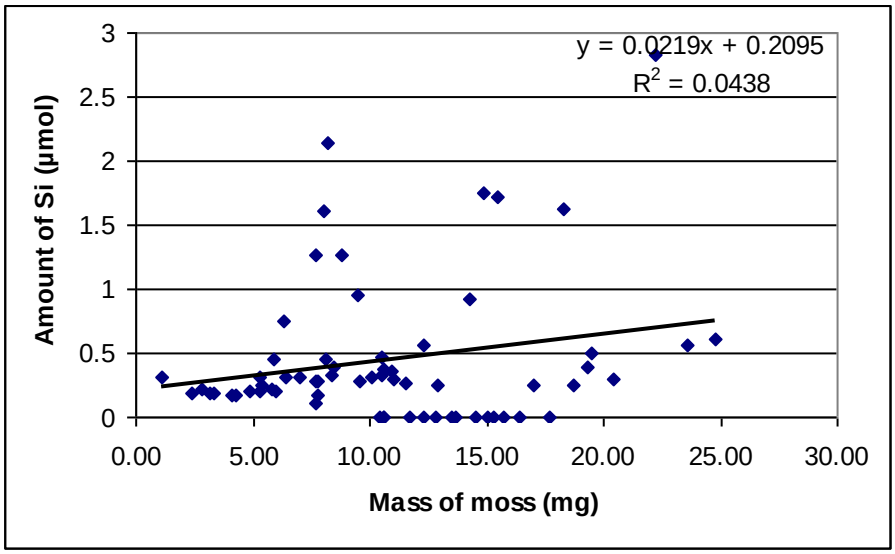

Figure 4.23 (Left) – Amounts of Si in the biotic aqueous fraction (µmol) from all granite microcosms plotted against the mass of moss (mg) recovered from the microcosm.

Figures 4.22/23 demonstrate the strongest positive correlation co-efficients obtainable for analytes in moss and the biotic aqueous fraction respectively. The figures demonstrate a positive relationship between mass of moss (mg) and the amount of analyte (µmol) (which is to be expected because the greater the mass of moss oxidised, the greater the amount of

intracellular ions contained within it will enter solution). The relationships, however, are very weak (R_2 0.18 and 0.04 respectively) and a number of data points deviate widely from the trendline in both plots. Due to the lack of a positive 1:1 relationship between mass of moss and the amounts of analytes the author chose not to normalise data to mass of moss recovered as a matter of routine.

If one normalises the data to time (calculates a rate) and then normalises the time-normalised data to mass of moss (mg) the data depicted in Figures 4.24/25 (below) are obtained.

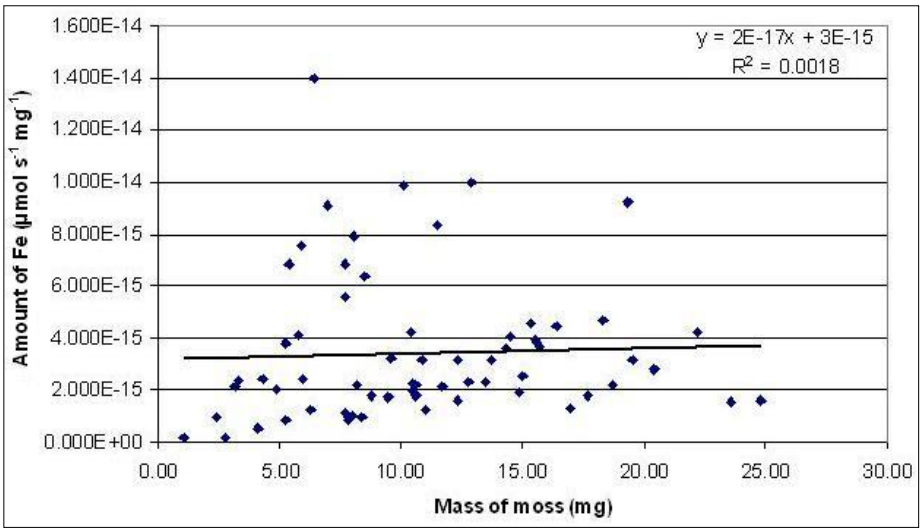

Figure 4.24 (Left) – Amounts of Fe in moss normalised to weathering period (s^{-1}) and normalised to mass of moss (mg^{-1}) giving a weathering rate per mg of moss biomass ($\mu mol\ s^{-1}\ mg^{-1}$) plotted against mass of moss (mg^{-1})

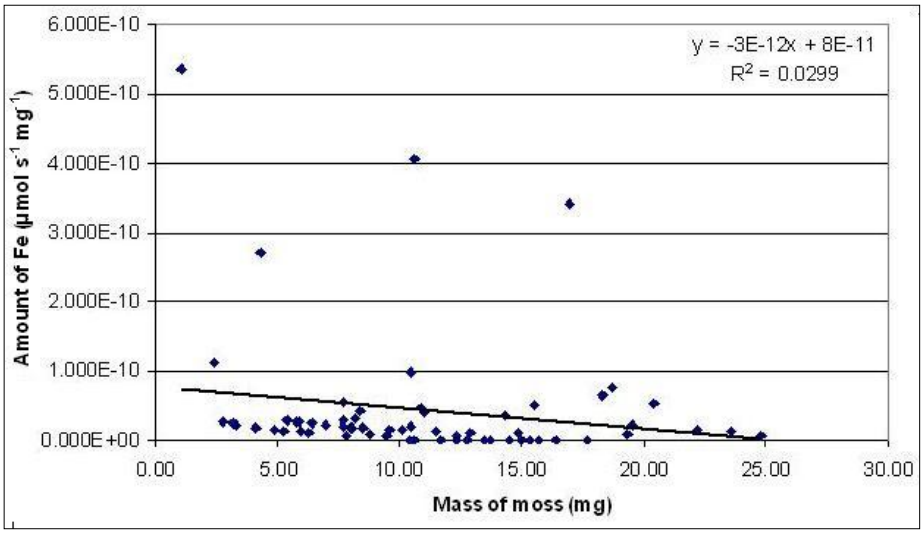

Figure 4.25 (Left) – Amounts of Fe in the biotic aqueous fraction normalised to weathering period (s^{-1}) and normalised to mass of moss (mg^{-1}) giving a weathering rate per mg of moss biomass ($\mu mol\ s^{-1}\ mg^{-1}$) plotted against mass of moss (mg^{-1})

Figures 4.24/25 indicate that time normalising the data prior to mass normalisation establishes even weaker relationships than those established by mass normalisation alone (R_2 0.002 and -0.03 respectively). Figure 4.25 demonstrates a negative relationship between mass of moss and amount of Fe per unit time and mass that is clearly erroneous.

4.10 Stoichiometries

4.10.1 Substrate Petrologies

At least two samples of washed and unwashed granite, andesite and vermiculite were analysed using X-Ray Fluorescence Spectroscopy (XRF). Two samples of unwashed chlorite were also analysed using XRF. There was no significant difference between washed and unwashed samples (all samples fell within $\pm 1\sigma$ of the mean of the washed and unwashed samples added together, see Appendix iv.iii), the data was therefore aggregated together and a mean taken in order to provide a larger n upon which error analysis could be reliably performed.

Table 4.14 (overleaf) shows the mean amounts of the ten major crustal elements (those found in greatest abundance in the Earth's crust) for three experimental substrates with corresponding reference values for those substrates:-

	Granite	Granite Ref.[28]	Andesite	Andesite Ref.[29]	Vermic.	Vermic. Ref.[30]
MgO	0.43	0.71	3.02	0.12	20.92	16-35
Al_2O_3	15.67	14.42	15.18	15.57	8.66	10-16
SiO_2	69.76	72.04	59.05	60.34	34.86	38-46
P_2O_5	0.24	0.12	0.26	0.28	0.08	?
CaO	0.81	1.82	4.50	5.20	0.38	1-5
TiO_2	0.24	0.30	0.71	0.72	1.00	1-3
MnO	0.04	0.05	0.12	0.19	0.05	?
K_2O	5.32	4.12	2.11	1.88	5.07	1-6
Fe_2O_3	1.73	1.22	5.86	6.07	7.69	6-13
Na_2O	3.19	3.69	4.07	3.62	0.63	?
Other	2.58	1.51	5.14	6.01	20.65	?

Table 4.14 – The amount of analytes (wt. %) in three experimental substrates as measured by XRF compared with reference values for those substrates.

Table 4.14 shows that the XRF analyses are, for the most part, congruent with reference values, with some outliers (often amongst the trace elements comprising the rock/mineral). Table 4.15 (overleaf) gives the XRF data for the experimental substrates in μmol g^{-1} to facilitate comparison with experimental values.

[28] Source: Blatt *et al.* (2006).
[29] Source: Wainwright (2010).
[30] Source: TVA (2010)

	Granite	Andesite	Chlorite	Vermiculite
Si	4797.0	4112.2	4638.7	2560.3
Al	1268.8	1246.2	1190.4	749.9
K	466.7	187.3	359.5	474.9
Na	424.1	548.9	482.9	85.6
Fe	89.4	307.0	184.4	424.9
Ca	59.6	335.9	93.5	30.1
Mg	43.6	313.4	32.5	2291.4
P	14.0	15.2	18.2	5.1
Ti	12.2	37.1	13.6	54.9
Mn	2.4	7.2	6.9	3.3

Table 4.15 – Mean amounts of the major crustal elements within the experimental substrates (µmol g^{-1}). Granite n = 5, Andesite and Vermiculite n = 4, Chlorite n = 2. Correct to 1 d.p.

To enable comparison between the petrologies of the experimental substrates and the blanks and microcosm fractions the data in Table 4.15 have been normalised to Fe (as Fe was frequently the least abundant element in the microcosm fractions). The resulting normalised data can be seen in Table 4.16 (below):-

	Granite	Andesite	Chlorite	Vermic.
Si	5363.98	1339.32	2515.90	602.56
Al	1418.76	405.90	645.61	176.50
K	521.87	60.99	194.99	111.77
Na	474.25	178.78	261.93	20.14
Fe	100.00	100.00	100.00	100.00
Ca	66.62	109.41	50.69	7.09
Mg	48.79	102.06	17.63	539.27
P	15.63	4.94	9.86	1.21
Ti	13.61	12.07	7.37	12.93
Mn	2.73	2.35	3.76	0.77

Table 4.16 - Mean amounts of the major crustal elements within the experimental substrates, normalised to the mean amount of Fe for that substrate (x100 to enable resolution of analytes less abundant than Fe). Correct to 2 d.p.

The data in Table 4.16 can be used to form stoichiometric formulae for each of the substrates (in a similar approach to Sterner & Elser (2002)) thus:-

Granite – $(Si_{54}\ Al_{14}\ K_5\ Na_5\ Fe_1)_{100}\ (Ca_7\ Mg_5\ P_2\ Ti_1)_{10}\ Mn_3$

Andesite – $(Si_{13}\ Al_4\ Na_2\ Ca_1\ Mg_1\ Fe_1)_{100}\ (K_6\ Ti_1)_{10}\ P_5\ Mn_2$

Vermiculite – $(Si_6\ Mg_5\ Al_2\ K_{1.1}\ Fe_{1.0})_{100}\ (Na_2\ Ti_1)_{10}\ Ca_7\ P_1\ Mn_1$

Chlorite – $(Si_{25}\ Al_6\ Na_3\ K_2\ Fe_1)_{100}\ (Ca_5\ Mg_2\ P_1)_{10}\ Ti_7\ Mn_1$

Equations 4.3 – Stoichiometric formulae for four of the experimental substrates calculated using data from XRF analyses, relative to Fe. Numbers given to 1 significant figure and are arranged in order of stoichiometric abundance.

The formulae in Equations 4.3 can be read thus: for every atom of iron (Fe) in granite there are 54 atoms of silicon (Si). For every 100 atoms of iron there are three of manganese (Mn) etc. Some facets of the stoichiometries presented in Equations 4.3 can be easily explained petrologically e.g. Si is always the most abundant XRF analyte in each substrate and aluminium (Al) is the second most abundant element in all substrates with the exception of vermiculite. This can be explained by the fact that Al readily isomorphically substitutes in-between SiO_4 tetrahedra in plate silicates (Andrews *et al.*, 2004). Also the fact that Mg is the second most abundant analyte in vermiculite is explained by the fact that it is the main inter-sheet cation in vermiculite (Deer *et al.*, 1966), hence why Mg is the second most abundant element in vermiculite rather than Al.

Broadly; the stoichiometries of granite, andesite and chlorite are similar with respect to the most abundant and least abundant elements, with no concordance for the other elements. The pattern followed can be described thus:-

Si, Al,… Ti… Mn.

4.10.2 Stoichiometries of the Microcosmal Fractions and Blanks

The stoichiometries of blanks of moss inoculum and filtrate (i.e that which was added to mossed and control microcosms respectively) and the stoichiometries of the microcosm fractions (i.e. the aqueous solutions resulting from control and mossed microcosms and the moss from mossed microcosms) were analysed in order to provide an indication of any trends that exist in the order of elemental abundance and the relative abundance of the elements themselves at an intra-elemental level, which could be indicative of weathering. NB All analysis of blanks and microcosm components was by ICP, with the exception of analysis for P which was by NAA (where such data are available). The typical stoichiometry of dry plant tissue can be given as:-

$$(K_{13}\ Ca_{7}\ Mg_{4}\ P_{3}\ Si_{2}\ Fe_{1})_{100}\ Na_{20}\ Al_{2}$$

Equation 4.4 – Stoichiometric ratio of the experimental analytes as commonly found in dry plant tissue, relative to Fe (data from Taiz & Zeiger (2002)). Note that the most abundant elements K to Si are the plant macronutrients.

The mean of inoculum initial conditions samples analysed in round 5 differs substantially from those analysed in rounds 8&9. The mean stoichiometries of inoculums analysed in rounds 5 and rounds 8&9 respectively, relative to Fe, are given in Equations 4.5 (below).

Round 5 – $(Na_{17}\ Ca_{6}\ Mg_{3}\ K_{2}\ Fe_{1})_{100}\ Al_{16}\ Si_{4}$

Rounds 8&9 – $(Ca_{13}\ K_{12}\ Mg_{5}\ Fe_{1})_{100}\ Na_{55}\ Al_{12}\ Si_{2}$

Equations 4.5 – Stoichiometric formulae for the moss inoculums at initial conditions, arranged by the ICP round the inoculums were analysed in, relative to Fe. Numbers given to 1 significant figure and are arranged in order of stoichiometric abundance.

In both sets of inoculums Al and Si are the least abundant analytes. Na was far more abundant in the round 5 inoculums, but was much less abundant in the rounds 8&9 inoculums. The reasons for this are unclear except that instrumental problems can be ruled out as other samples were unaffected. There is some congruity between the rounds 8&9 inoculums and Equation 4.4 in that the plant macronutrients are more abundant in the rounds 8&9 inoculums (a noticeable incongruity being that Si is the least abundant analyte in the inoculums yet is a plant macronutrient).

The stoichiometry of the filtrate initial conditions samples (calculated using a median of all samples taken in the procedure, is as follows):-

$(K_{10}\ Na_{10}\ Ca_{6}\ Mg_{2}\ Si_{2})_{100}\ Fe_{10}\ Al_{7}$

Equation 4.6 – Stoichiometric formula for filtrate at initial conditions, relative to Fe. Numbers given to 1 significant figure and are arranged in order of stoichiometric abundance.

The filtrate and the inoculum differ in the fact that the filtrate is what remains after the inoculum has been passed through a 0.2μm filter (the filtrate is devoid of biota). When Equation 4.6 is compared with Equations 4.5 it is clear that the presence of biota in the form of moss does affect the stoichiometry of the suspension (e.g. Si is about an order of magnitude more abundant in the filtrate than in the inoculums; there are 20 atoms of Si for every 1 of Fe in the filtrate, yet there are 2-4 atoms of Si for every 100 of Fe in the moss inoculums).

4.10.3 Microcosmal Stoichiometry Summary

If substrate petrology is compared with the stoichiometries of the microcosmal fractions connected with that substrate it is possible to see any abiotic and biotic enhancements relative to the baseline stoichiometry of the substrate itself (enhancements in a stoichiometric context will henceforth be referred to as ‘enrichments’). Figure 4.26 (overleaf) presents the stoichiometry of microcosmal components arranged by substrate.

Granite

Granite - $(Si_{54}\ Al_{14}\ K_5\ Na_5\ Fe_1)_{100}\ (Ca_7\ Mg_5\ P_2\ Ti_1)_{10}\ Mn_3$

Control aq. - $(Na_{14}\ Ca_8\ K_3\ Mg_2\ Si_{1.6})_{100}\ P_6\ Al_5\ Fe_1$

Mossed aq. - $(Na_6\ Ca_3\ K_1)_{100}\ (Si_9\ Mg_7\ P_1)_{10}\ Al_3\ Fe_1$

Moss - $(Ca_5\ K_5\ Na_3\ Mg_1\ Fe_1)_{10}\ Al_8\ Si_5$

Andesite

Andesite - $(Si_{13}\ Al_4\ Na_2\ Ca_1\ Mg_1\ Fe_1)_{100}\ (K_6\ Ti_1)_{10}\ P_5\ Mn_2$

Control aq. - $(Na_{80}\ Ca_{21}\ K_9\ Si_2\ Mg_1)_{100}\ Al_{10}\ Fe_1$

Mossed aq. - $(Na_{51}\ Ca_{20}\ K_8\ Mg_1\ Si_1)_{100}\ Al_6\ Fe_1$

Moss - $(Ca_{18}\ Mg_3\ Na_2\ K_1\ Al_1\ Fe_1)_{10}\ Si_6$

Vermiculite

Vermiculite - $(Si_6\ Mg_5\ Al_2\ K_1\ Fe_1)_{100}\ (Na_2\ Ti_1)_{10}\ Ca_7\ P_1\ Mn_1$

Control aq. - $(Na_3\ K_1)_{100}\ (Si_6\ Mg_2)_{10}\ Ca_7\ Al_1\ Fe_1$

Mossed aq. - $(Na_{41}\ K_{23}\ Si_7\ Mg_6\ P_3\ Ca_1)_{100}\ Fe_{10}\ Al_6$

Moss - $(Na_6\ Mg_6\ Al_1\ K_1\ Si_1\ Fe_1)_{100}\ Ca_{63}$

NB No P was detectable in vermiculite control aq.

Chlorite

Chlorite - $(Si_{25}\ Al_6\ Na_3\ K_2\ Fe_1)_{100}\ (Ca_5\ Mg_2\ P_1)_{10}\ Ti_7$

Control aq. - $(Na_{11}\ Ca_4\ K_1)_{100}\ (Mg_5\ Si_3)_{10}\ Al_5\ P_1\ Fe_1$

Mossed aq. - $(Na_4\ Ca_2)_{100}\ (K_4\ Si_2\ Mg_2)_{10}\ Al_2\ Fe_1\ P_1$

Moss - $(Na_3\ K_2\ Ca_2)_{100}\ (Mg_2\ Fe_1)_{10}\ Al_5\ Si_1$

Figure 4.26 – Substrate petrology and the stoichiometries of microcosmal components related to that substrate, relative to Fe. Numbers given to 1 significant figure and are arranged in order of stoichiometric abundance.

Below the stoichiometries for granite are reproduced in a table to facilitate comparison:-

	Granite Substrate	Control aq.	Mossed aq.	Moss	(Moss/Control aq.) x1000	Moss/ Substrate	Ψ
Al	14.2	5.5	2.9	0.8	138.2	0.1	16.4
Ca	0.7	789.5	254.5	5	6.4	7.1	1.5
Fe	1	1	1	1	1000	1.0	112.6
K	5.2	313.7	131.6	4.7	14.9	0.9	2.6
Mg	0.5	202.6	70.8	1.3	6.6	2.6	1.5
Na	4.7	1379.4	639	3	2.1	1.6	1.3
Si	53.6	164.2	92.7	0.5	3.1	0.0	1.6
P	0.2	6.5	13	?	?	?	?

Table 4.17 – Stoichiometry of the granite substrate and the mean stoichiometries of granite microcosmal components (all relative to Fe). The value for moss is divided by the value for control aq to reveal the stoichiometric enrichment of each analyte in the moss relative to control aq (values x1000 to resolve small enrichments). The value for moss is also divided by the value for the substrate to reveal the stoichiometric enrichment in the moss relative to the substrate. Biotic enhancement (Ψ) values are also reproduced for comparison.

Table 4.17 (above) shows that some analytes (e.g. Ca, K, Mg, Na and P) are heavily enhanced in the microcosm aqueous fractions relative to their baseline stoichiometry in the granite (e.g. Ca is present at 0.7 relative units in granite, but reaches levels of 789.5 and 254.5 rel. units in the control and mossed aqueous fractions respectively). Most of these analytes (Ca, K, Mg and P) are macronutrients that are essential for plant growth (Taiz & Zeiger, 2002). The enrichment in moss relative to substrate (Moss/Substrate) does not however appear to follow macro/micronutrient trends. Al is the second most abundant analyte in granite but is present at levels of about one third its baseline stoichiometry in the control microcosm aqueous fraction. It is interesting that the plant macronutrients appear to experience enhanced weathering into aqueous solution even when there are no biota present. Table 4.18 (overleaf) reproduces the stoichiometries for andesite in tabular format:-

	Andesite Substrate	Control aq.	Mossed aq.	Moss	(Moss/Control aq.) x1000	Moss/ Substrate	Ψ
Al	4.1	9.6	6.3	1.1	120.2	0.3	40.4
Ca	1.1	2052.9	2039.0	18.2	8.9	16.5	4.1
Fe	1.0	1.0	1.0	1.0	1000.0	1.0	330.7
K	0.6	852.2	816.5	1.4	1.6	2.3	1.8
Mg	1.0	180.6	162.8	2.5	13.8	2.5	5.7
Na	1.8	8011.2	5091.3	1.5	0.2	0.8	0.9
Si	13.4	223.6	155.6	0.6	2.5	0.0	1.7

Table 4.18 – Stoichiometry of the andesite substrate and the mean stoichiometries of andesite microcosmal components (all relative to Fe). The value for moss is divided by the value for control aq to reveal the stoichiometric enrichment of each analyte in the moss relative to control aq (values x1000 to better resolve small enrichments). The value for moss is also divided by the value for the substrate to reveal the stoichiometric enhancement in the moss relative to the substrate. Biotic enhancement (Ψ) values are also reproduced for comparison. NB there are no values for P as no andesite experiments were analysed using the NAA.

Overall from a petrological perspective: granite appears to be more heterogeneous than andesite with respect to the ICP analytes (granite has a relatively large proportion of Si, Al, K and Na whereas andesite seems more deplete in all analytes other than Si and Al, c.f. Figures 4.17/18). In granite only two analytes were enriched in the moss relative to substrate (Ca and Mg) whereas on andesite Ca, K and Mg are enriched in the moss relative to the substrate (K, Ca and Mg being the three most abundant nutrients in plant tissue (Taiz & Zeiger, 2002)). This enrichment could be indicative of preferential weathering. Fe followed by Al have the highest Moss:Control aq ratios, however the order degenerates from this point onward due to the effect of the mossed microcosm aqueous component in increasing the Ψ value.

4.11 Discussion

4.11.1 Microcosm Experiments

The most congruent facet of the biotic enhancement of weathering data across all substrates is that iron (Fe) is the most biotically enhanced analyte, followed by aluminium (Al) across all substrates except for the chlorite dataset (which was based on only one experiment with a small sample size). These results are probably largely due to the affect of oxalic acid which is capable of solubilising Fe and Al (which are normally insoluble in water) (Moulton & Berner, 1998). The accumulation of Fe and Al levels to such great levels in moss tissue (the mean value for moss recovered from andesite was 0.2μmol) is however difficult to explain. Fe is a plant micronutrient typically only found at levels of ~100ppm in dry plant tissue (Taiz & Zeiger, 2002), Al is not even considered a plant micronutrient by most plant scientists (though there is evidence that low levels of Al enhance plant growth) (*Op. cit.*).

The pertinent questions must be: why is the magnitude of the biotic enhancement of both Fe and Al so great and why do these two elements accumulate to such excess in moss biomass when they are not physiologically required in as great a quantity? A possible explanation in the case of Fe from granite is that the Fe^{2+} in biotite is being altered to Fe^{3+} and weathered. Flecks of biotite were commonly present within clasts of the granite used in this study (see Figure 4.1, p79). Isherwood & Street (1976) found that iron oxidation as a result of the weathering of the biotite within granite-like rocks increased the proportion of Fe^{3+} by ~320%, staining the soil a brown/red colour at all depths of the profile.

Another possible explanation lies in the fact that plants secrete only weak organic acids and chelating agents (Moulton & Berner, 1998) and as such are only able to weather small ions (i.e. those with a relatively low ionic radius) and therefore the smaller an ion is, the greater the ability of the moss exudates to weather it. Table 4.19 (overleaf) gives the minimum ionic radii of the key species relevant to this study.

Species	Minimum Ionic Radius
Potassium	1.37
Oxygen	1.35
Calcium	1
Sodium	0.99
Magnesium	0.57
Aluminium	0.39
Silicon	0.26
Iron	0.25
Phosphorus	0.17

Table 4.19 – The minimum Shannon ionic radii for key species (i.e. the most oxidised species possible with the closest co-ordination), arbitrary units (Imperial, 2010).

Broadly speaking: the analytes with larger minimum ionic radii are those which had lower weathering enhancements (across all substrates). The quantification of phosphorus weathering (in the form of phosphate) has been imperfect in this procedure due to the inability to measure phosphate in moss. The noticeable incongruity is that silicon (one of the least biotically enhanced analytes) has almost the same ionic radius as iron (the most biotically enhanced analyte). A probable reason for this incongruity is that silicon will mostly be present as silicate (SiO_4^{4-}) and so will have a much larger radius due to the presence of the four oxygen atoms.

The ionic radii of species may also explain some other facets of the microcosm experiment data; for example why aluminium (Al) was the most biotically enhanced analyte on vermiculite whereas on all other substrates iron (Fe) was the most biotically enhanced analyte. Vermiculite is a framework silicate with magnesium (Mg) as the main inter-sheet cation (Andrews *et al.* (2004); Deer *et al.* (1966)). Table 4.19 shows that the next smallest analyte after Mg is Al so it is probable that Al substitutes for Mg in the framework structure of vermiculite.

The occurrences of a lower mean amount of an analyte being recorded in the biotic aqueous fraction compared with the mean value for the abiotic aqueous fraction (Wb<Wa) do appear to

be a signal of preferential uptake of an analyte by moss (and vice-versa). Evidence for this is that the effect appears to occur mostly with plant macronutrients with the reverse effect (Wa>Wb) tending to occur for the more minor plant macronutrients (e.g. Si) and the plant micronutrients. The signal appears to be most pronounced in the granite datasets and in the chlorite experiment and is not perceptible in the vermiculite aggregated dataset or the andesite aggregated dataset (but is noticeable in the 25/1/09 andesite experiment). Further research is required to determine why this effect is noticeable in some experiments on a substrate and not in others (weathering period does not influence the effect).

The lower maximum Ψ on vermiculite is likely to be due to the much reduced recovery efficiency when removing moss from the highly exfoliated vermiculite clasts. The lower maximum Ψ value could also be due to the fact that vermiculite is a highly altered mineral (being a weathering product of biotite, which is itself a rock denudation product (Blatt *et al.*, 2006)) meaning that vermiculite is somewhat depleted in ions as a result of antecedent alteration. This hypothesis is corroborated by the XRF data (see Table 4.16) which indicates that of all the experimental substrates vermiculite has the lowest abundance of Si, Al, Na, Ca and P but the highest abundance of K, Fe and Mg. It is also possible that the general lack of essential plant nutrients relative to the other experimental substrates (particularly of P) compromised moss growth and thus also the biotic enhancement of weathering.

Sodium sometimes exhibited Ψ values of <1 (e.g. in the 12/1/09 granite experiment and the andesite aggregated dataset, the error bars overlapping in the andesite aggegated dataset indicating that this relationship is statistically insignificant). It is likely that these incidences of Ψ<1 are caused by the analytes accumulating in the rooting structure of the moss (the rhizines) as it is this portion of the moss that is never fully recovered from the microcosms (thus the budget for these analytes is incomplete). Sodium is used by plants to balance the water potential between cells (sometimes referred to as ‘osmotic’ or ‘turgor pressure’) (Taylor *et al.* (1997) and Taiz & Zeiger (2002)). It is possible that mosses actively transport sodium into their root hair cells (possibly using selective ion channels) in order to drive a concentration gradient between the interior of root hair cells and the aqueous solution within the microcosm, thus drawing in water by osmosis. This would explain why sodium (for example) sometimes exhibits Ψ values of <1 as the sodium may be hyper-accumulating in the rhizines that are incompletely recovered.

It is likely that the Ψ values obtained in this procedure are an underestimate of the true biotic enhancements of weathering, not just because of incomplete budget closing, but also due to the lack of 'flushing' (Berner, 1992). The microcosm system is essentially a closed system unlike a natural system which is often considered open (*Op. cit.*). In a natural system weathering rates will be increased as a result of flushing by rainwater removing the products of weathering. Le Chatelier's Principle states that "if a system at equilibrium is perturbed, the system will react in such a way as to minimize the imposed change" (Andrews *et al.*, 2004) flushing removes weathering products from the immediate system and so will increase the rate of the forward weathering reaction as flushing removes the products of weathering (Lenton, 2001).

The finding that phosphate weathering in the aqueous phase on granite is biotically enhanced four-fold (Control $\bar{\mu} = 0.014$µmol, Mossed $\bar{\mu} = 0.059$µmol) is highly important as the flux of phosphate from the land surface to the oceans is a key limiting factor in the growth of marine autotrophs and hence a key factor in the net flux of organic carbon from the surface to the deep ocean (Libes (1992); Lenton (2001)). The presence of stronger weathering signals in some experiments relative to others, could be due to the fact that rocks are highly heterogeneous in nature and that some rocks in some experiments may have had particular inclusions (e.g. in the case of phosphate, apatite inclusions) increasing bulk weathering of analytes such as phosphate in some microcosms in those experiments.

4.11.2 Statistics

The standard error has been used as a means of quantifying error in the aggregated datasets, it should however be noted that the standard error is an imperfect form of error quantification because by dividing the cumulative standard deviations by the $\sqrt{n}$ (see Equation 4.1) the error value decreases substantially with increasing n. However the n values in the cases of the granite and andesite summary data are low values (6 and 3 respectively), n representing the number of individual experiments. However: by treating each experiment as a distinct entity and then aggregating the data together and performing error analysis using the standard deviations of each individual experiment, this approach is similar to that of a meta-analysis.

Deficiencies in the standard error as a method of error representation are overcome by conducting statistical analyses upon the data.

	Al	Ca	Fe	K	Mg	Na	Si
Granite Aggregated	Non <0.01	Non <0.01	Non <0.01	Non <0.01	Non <0.01	Close *0.37*	Close <0.01
Andesite Aggregated	Non <0.01	Non <0.01	Non <0.01	Non <0.01	Non <0.01	Overlap *0.47*	Non <0.01
Vermiculite Aggregated†	Non <0.01	Non <0.01	Non <0.01	Non <0.01	Non <0.01	Non <0.01	Close <0.01

Table 4.20 – Comparison between error bars on aggregated data graphs and P values obtained via the U test. 'Non' indicates that error bars were non-overlapping, 'Close' indicates that error bars were close to overlapping and 'Overlap' indicates that error bars were overlapping. P values >0.05 are italicised. †NB granite and andesite aggregated datasets used standard error bars, the vermiculite aggregated dataset used 95% confidence error bars.

Table 4.20 (above) shows that the error bars presented on graphs are a reliable method of indicating statistical significance (though it is important to conduct statistical analyses as error bars that appeared close actually yielded P<0.01 results in some cases). The U test did not perform well when applied to less than 30 datapoints; in these circumstances the U test frequently yielded insignificant P values for data that were clearly significant (e.g. PO_4 in the vermiculite aqueous microcosm fractions see Figure 4.16). This was however overcome by checking these spurious results using the t-test for independent samples.

4.11.3 Stoichiometries

The stoichiometric analyses of the blanks and the resulting microcosmal components yielded a number of unexpected results. Contrary to one of the hypotheses: the mean stoichiometry of the aqueous component sampled from control microcosms does not follow the same pattern as the substrate stoichiometry. Also unexpectedly: the pattern of stoichiometric abundance

between the aqueous component from control microcosms and mossed microcosms was very similar across all substrates. The strong enrichments of a number of plant macronutrients (Ca, K, Mg and P) on granite in both control and mossed microcosmal aqueous fractions are very interesting.

Sodium (Na) appears to be ubiquitous as the primary constituent element of the aqueous fractions from control and mossed microcosms, as well as being the primary constituent of the moss extracted from vermiculite and chlorite microcosms. It is possible that these large amounts of Na entered the microcosm system as a result of the sodium present in 15MΩ upH_2O (see Appendix ii.i.i) though components were rinsed with 18MΩ upH_2O prior to their use in microcosm preparation. The substrate as a potential source of the Na is excluded by the fact that Na is the most abundant element in the mossed aqueous fraction from the microcosms set-up with no substrate (see Figure 4.20). Broadly speaking the plant macronutrients (e.g. K, Ca and Mg) are those found in greatest abundance in moss tissue be it the inoculum or that which is removed from microcosms (though there is widespread evidence of possible Na contamination).

5: Conclusions

5.1 Biotic Enhancements of Weathering

A summary of the key facets of the microcosm experimental data is given in Table 5.1 below:-

	Al	Ca	Fe	K	Mg	Na	Si
Granite **n=6**	16.4 (<0.01)	1.5 (<0.01)	112.6 (<0.01)	2.6 (<0.01)	1.5 (<0.01)	1.3 (Insig.)	1.6 (<0.01)
Andesite **n=3**	40.4 (<0.01)	4.1 (<0.01)	330.7 (<0.01)	1.8 (<0.01)	5.7 (<0.01)	0.9 (Insig.)	1.7 (<0.01)
Vermiculite **n=2**	35.5 (<0.01)	3.7 (<0.01)	30.0 (<0.01)	1.9 (<0.01)	9.3 (<0.01)	1.9 (<0.01)	1.7 (<0.01)
Chlorite **n=1**	4.3 (<0.01)	2.1 (<0.01)	38.3 (<0.01)	6.5 (<0.01)	2.4 (<0.01)	1.3 (<0.01)	1.1 (<0.01)

Table 5.1 – Biotic Enhancement of Weathering (Ψ) values of all analytes on all substrates with the statistical level of significance of that result (obtained via the Mann Whitney U Test) in parentheses. Shaded cells indicate a result significant at the P<0.01 level, unshaded cells are statistically insignificant (P>0.05). 'n' is the number of experiments used to form the aggregated datasets from which the Ψ values are formed.

Table 5.1 successfully demonstrates that mosses biotically enhance weathering on all substrates experimented upon. The biotic enhancement of weathering (Ψ) values obtained in this study ranging from the undetectable and insignificant for Na on andesite substrate (Ψ0.9, statistically insignificant) up to the largest biotic enhancement in an aggregated datset in this study; Ψ330.7 for Fe also on andesite (P<0.01). It is likely that Ψ values of <1 are due to incomplete recovery of the moss from the microcosms and may be due to Na accumulating in moss rhizines which bind tightly to the substrate, perhaps as a result of the active transport of Na into the rhizines in order to facilitate the uptake of water in order to maintain turgor pressure. Plants use K and Na as osmoregulators (Taiz & Zeiger, 2002). Al tended to be one of the two main analytes weathered but Al is always highly abundant in the substrates, so Al is

under-enriched in microcosmal components relative to the baseline substrate stoichiometry in the case of granite (see Table 4.17, p124).

The magnitude of some biotic enhancements derived from the experimental data may seem large, however biotic enhancements of similar magnitude have been observed in previous studies. In a mesocosm experiment in Iceland Moulton & Berner compared the flux of Ca, Mg, K and Na from watersheds colonised with mosses and lichens with the flux of the same elements from watersheds containing Birch and 'Evergreen' trees. Run-off waters were analysed by ICP spectroscopy and corrections were made for the flux of analytes present in rainwater and that which is taken up by trees (Moulton & Berner, 1998). The K flux from tree colonised watersheds was 110-150 times the K flux from the mossed/lichenised watersheds (*Op. cit.*) a very similar magnitude to the enhancements observed for Fe on granite and andesite in this study, suggesting that the biotic enhancement of weathering by trees compared with lichens/bryophytes is approximately of the same magnitude as the biotic enhancement of weathering by bryophytes relative to a total absence of biota.

A key benefit of microcosm experiments is the ability to compare biotic weathering with a system that is completely sterile and therefore devoid of biota. Such comparisons are impossible in field studies. Using the data presented in Table 5.1; a weathering series can be formed to compare the magnitude of the biotic enhancement of weathering across the different experimental substrates:-

Granite – $Fe_{113} > Al_{16} > K_3 > Si_2 > Mg_2 > Ca_2 > Na_1$

Andesite – $Fe_{331} > Al_{40} > Mg_6 > Ca_4 > K_2 > Si_2 > Na_1$

Vermiculite – $Al_{36} > Fe_{30} > Mg_9 > Ca_4 > Na_2 > K_2 > Si_2$

Chlorite – $Fe_{38} > K_7 > Al_4 > Mg_2 > Ca_2 > Na_1 > Si_1$

Figure 5.1 – Biotic weathering series comparing the relative magnitude of the Ψ values (to the nearest whole number, in subscript), across the different experimental substrates.

Figure 5.1 shows that the ordering of Ψ values in a highest-lowest sense is broadly similar for granite and andesite, following the pattern:

Fe, Al… Na

The relatively lower Ψ values for vermiculite and chlorite are probably due to the fact that one is a highly altered denudation product (vermiculite) and the other is vitreous and so less weatherable (chlorite).

5.2 Modelling Biotic Weathering of the Earth's Crust by Moss

Drawing on data from the different experiments presented in this thesis and the estimation of Crowley & Baum (1991) that the area of Earth's land surface at 440Ma was 73.6×10^6 km^2, it is possible to estimate the flux of the ICP analytes in this study under different moss/land-surface colonisation scenarios. The summary data for granite will be used for this purpose as the stoichiometry of granite is very similar to the stoichiometry of continental crust taken as a whole (Blatt *et al.*, 2006). Table 5.2 below presents the different colonisation scenarios:-

Colonisation Scenario	Actual Earth surface (m^2)
Whole Earth surface	7E+13
¼ Earth surface	2E+13
½ Earth Surface	4E+13
¾ Earth Surface	5E+13

Table 5.2 – Bryophyte colonisation scenarios and their corresponding Ordovician land surface area correct to 1 significant figure (calculated from Crowley & Baum (1991)).

All figures in these calculations will be rounded to 1 significant figure as there is a large margin of error. Table 4.13, p114 shows that moss grown under optimal conditions has a mean dry mass of 6000 mg/m^2 (to 1 sig. fig.), if the value for mean dry mass of moss grown under optimal conditions is multiplied by the data for analyte contained within the moss recovered

from granite mossed microcosms per mg of moss biomass oxidised (Table 4.9, p112) the following data are obtained:-

Al	Ca	Fe	K	Mg	Na	Si
1.E-04	7.E-04	1.E-04	6.E-04	2.E-04	3.E-04	7.E-05

Table 5.3 – Fluxes of analytes from granite colonised by moss (mol/m^2) over the 149 day mean growth period, correct to 1 sig. fig.

If the data in Table 5.3 are scaled to give a flux per second (1.287E7s in 149 days) the following data are obtained:-

Al	Ca	Fe	K	Mg	Na	Si
8.E-12	5.E-11	1.E-11	5.E-11	1.E-11	2.E-11	6.E-12

Table 5.4 – Fluxes of analytes from granite colonised by moss (mol/m^2/s), correct to 1 sig. fig.

The data in Table 5.4 can then be multiplied by the different land surface colonisation scenarios (m^2) presented in Table 5.2 to give a net flux of analyte under different moss/land surface colonisation scenarios, thus:-

	Al	Ca	Fe	K	Mg	Na	Si
¼	2.E+02	1.E+03	2.E+02	9.E+02	3.E+02	4.E+02	1.E+02
½	3.E+02	2.E+03	4.E+02	2.E+03	8.E+02	8.E+02	2.E+02
¾	4.E+02	3.E+03	5.E+02	2.E+03	1.E+03	1.E+03	3.E+02

Table 5.5 – Fluxes of the ICP analytes from a hypothesised Ordovician land surface (mol/m^2/s), correct to 1 sig. fig., under different colonisation scenarios (one quarter, one half and three quarters of earth surface respectively).

The data in Tables 5.3 to 5.5 are fluxes from the lithosphere into solution (which would be flushed into rivers and the oceans) and into the moss itself. No attempt has been made to take account of nutrient retainment and recycling by living and dead moss respectively. The formula for calculating the flux of analyte under different colonisation scenarios is as follows:-

$$\left(\frac{\frac{nm}{c}}{t}\right)e$$

Equation 5.1 – Formula for calculating the flux of analyte (mol/m^2/s) per unit of land surface where n=amount of analyte weathered per mg of moss biomass (µmol mg^{-1}), m=mean dry mass of moss that grows per m^2 under optimal conditons, c = 1x10E6 and is the µmol to mol conversion factor, t=time moss was grown for (s) and e=earth surface colonisation scenario (m^2).

The two largest fluxes obtained are for Ca and K respectively, which are the two primary plant macronutrients (Taiz & Zeiger, 2002). The effect of these elemental fluxes upon the earth system can only be ascertained by incorporating the values in Table 5.4 into an appropriate biogeochemical model. An estimation of the land surface area colonised by bryophytes in the Ordovician may be obtainable by close examination of the palynological record from a number of core holes distribued across the former Ordivician land surface (in the manner of Steemans *et al.* (2009)).

5.3 Proposed Improvements to Experimental Methodology

In future experiments 18MΩ upH_2O should be used throughout the experimental procedure, 15MΩ upH_2O should not be used due to significant contamination (particularly of sodium). It is possible that the inoculum washing procedure could be improved to create a less time-consuming procedure, possibly by autoclaving filter funnels and filter papers and filtering the inoculum under the sterile conditions. The risk of contamination, however, would be greater by this method and the filter papers may not filter well after being autoclaved due to the absorption of steam.

Nitric acid should be used as the ICP desorbing agent in future (instead of hydrochloric acid) as nitric acid is cleaner (Lajunen & Peramaki, 2004). In between preparation and analysis samples should be stored in polyethylene bottles leaving 40% volume free for expansion (as per Parsons *et al.* (1984). Unfortunately, the author was unaware of both of those references until after the experimental procedure had been completed.

5.4 Proposed Improvements to Analytical Methodology

Future experimental samples could be analysed via ICP Mass Spectrometry (ICP-MS) as opposed to ICP-AES in order to try and reduce the number of data-points which fall between 0 and the level of precision of the instrument (non-detects). However ICP-MS analyses (whilst having a lower limit of detection than ICP-AES analyses) are a lot more susceptible to problematic matrix interferences, however, the author believes that analysis via ICP-MS should still be attempted. Instrumental precision, particularly with respect to non-detects, could be improved by the employment of the standard additions method of calibration. For standard additions; the sample is split into ≥3 aliquots, one of these aliquots is left unaltered and the others have an increasing, standardised amount of the experimental analytes added to them (Lajunen & Peramaki, 2004).

The developed biomass oxidation method dissolves intracellular ions into solution in a satisfactory and safe manner and has scope to be applied to the analysis of plant materials other than moss. However; the interference caused by the reaction of hydrogen peroxide with the phosphate and silicate reagents suggests that hydrogen peroxide should be precluded in any future oxidation mix where nutrient auto analysis is planned. Mixtures of hydrogen peroxide and nitric acid are however regarded as providing a matrix that is highly resistant to interferences when analysed via ICP spectroscopy (Sucharova & Suchara, 2006). All 'wet chemical' methods used for the detection of phosphate use similar reagents to those used in the NAA procedure (Parsons *et al.*, 1984) and are therefore not suitable for use with the hydrogen peroxide matrix. A solid-phase analytical method that detects phosphate at levels >1µmol l^{-1} would be ideal.

Detection of phosphate in moss is a highly important addition that must be brought to any future experiments in order to close the budget thoroughly for phosphate in mossed microcosms. This is especially important given that this study appears to indicate that the enhancement of phosphate in moss would be substantial (following the trends indicated in Table 4.17). Given the link between increased bulk phosphate weathering and marine organic carbon burial (Lenton, 2001), complete phosphate analysis of both the aqueous microcosmal fractions and the moss biomass is especially needed.

Kurtosis analysis could be used to distinguish between the different types of normal distribution rather than using a visual examination of the graphs. Instead of censoring non-detects and substituting in a value that is half of the limit of detection: a Survival Analysis method (such as Kaplan-Meier filtering) could be used (She, 1997). Helsel (2006) strongly recommends against substituting non-detects for fractions of the limit of detection, but argues that this is better than excluding or deleting non-detects as this can cause "a strong upward bias in… means and medians." However survival analysis techniques are not routinely used in the environmental sciences at present and their application requires substantive specialist knowledge that was considered beyond the scope of this study.

5.5 Proposed Further Experimental Work

Any future study of mineral weathering by biota could be greatly informed by a number of experiments. Firstly: a large number of microcosms using each experimental substrate could be initiated, then a small portion of these microcosms could be sampled every week and the resulting samples kept in cold storage and then analysed in a single round. Such an experiment would enable the plotting of a 'weathering curve'; the peak of which would inform when maximum weathering has occurred and this could be used as the weathering period in future experiments using that particular substrate. This assumes that there is a maximum period of weathering beyond which moss tissue starts to die releasing weathered ions back into the biotic aqueous solution.

Future studies into preferential weathering effects could be greatly informed if the acids produced by mosses could be identified. Acids secreted by moss could be identified using

High Performance Liquid Chromatography (HPLC), this would enable validation or falsification of the hypothesis linking moss exudates with the ionic radii of different analytes. Whilst wild-type *P. patens* was used in this study there already exist a number of *P. patens* mutants which are deficient in rhizines (roots), making *P. patens* the candidate model bryophyte for future weathering studies (see Menand *et al.* (2007) for an in-depth discussion of *P. patens* mutants). Similarly: thin-section and ion microprobe analysis (in the manner of Isherwood & Street (1976)) could be used on unweathered and weathered granite clasts to prove whether or not biotically weathered iron is derived from biotite

In addition to the control experiment using microcosms with moss inoculum but no substrate: an experiment with microcosms containing only the filtrate could be set up in order to ensure that the analyte present in bare microcosm fractions (see Figure 4.20, p108) is there as a result of contamination and not due to an unknown biotic factor associated with the moss.

5.6 Concluding Statements

The temporal matching of the $\delta^{13}C$ excursion in the Darriwilian age of the Ordovician with the appearance of bryophyte-like spores in the stratigraphic record (Steemans *et al.*, 2009), coupled with the successful demonstration by this study that mosses biotically enhance weathering even on unlabile substrates representative of the Ordovician land surface (such as granite) up to 113 times the level of abiotic weathering: is conducive with hypotheses linking increased terrestrial weathering to the Ordovician glaciation (Kump *et al.* (1999); Sheehan (2001); Saltzman & Young (2005)). The results of this study suggest that weathering by bryophytes radiating across Earth's surface is indeed a likely cause of the Ordovician glaciation. However such an inference cannot be made without the incorporation of the biotic enhancement factors obtained in this study into an appropriate biogeochemical earth system model.

The impact of the different biotic enhancement values obtained by this study after incorporation into biogeochemical models will be highly variable. It is likely that each analyte would be modelled separately, the impacts of biotic Al and Fe weathering compared with weathering for the other analytes will be substantial (c.f. hundred-fold FeΨ values on granite

and andesite with Ψ values of ~1.5 and ~2.5 for Ca, K, Mg and Si on granite and andesite respectively). The evidence for preferential uptake of plant macronutrients by moss (see Figure 4.5, p84) is very interesting. It is possible that by utilsing ICP-MS as the method of analysis in future experiments appearences of this effect could be better resolved. If ICP-MS were used in tandem with HPLC characterisation of moss exudates (see previous section) a much greater understanding of how mosses (and plants in general) weather minerals in order to meet their nutritional requirements would be obtained.

The strong enrichments of ions into the control aqueous fractions in micrococosms where no biota was present over the baseline stoichiometry of the substrates is indicative that abiotic weathering plays a strong role in making plant macronutrients available and is likely to have been a key mechanism facilitating the evolution of plant life on Earth by making physiologically useful compounds available. The fact that Al was commonly the analyte with the second highest biotic enhancement value is interesting. Al was frequently found to accumulate in moss tissue to levels up to 0.2µmol in moss that appeared to be thriving. This contrasts with the view of aluminium as an analyte with a low toxic threshold in plants, and lends weight to the findings of Marschner (1995) cit. in Taiz & Zeiger (2002) that low levels of aluminium are beneficial to plant growth.

The fact that Fe was the most biotically enhanced analyte on all substrates except vermiculite and that the biotic enhancements of Fe were always of a very high magnitude compared to the other analytes is very interesting. An issue pertinent to the Ordovician glaciation is that its onset occurred when atmospheric pCO_2 was 10-18x PAL (Yapp & Poths (1992) and Pope & Steffen (2003)). Central to this issue is what caused atmospheric pCO_2 to decline to the levels necessary to trigger the glaciation? Kump & Arthur (1999) suggest a level of 10x PAL as sufficient.

This study hints at a possible explanation for the decrease in atmospheric pCO_2 in the form of an increase in Fe export to the oceans via rivers as a result of increased biotic terrestrial weathering. Cooper *et al.* (1996) found that adding (or 'fertilising') Fe-deplete regions of the ocean (known as 'High-Nitrate Low-Chlorophyll' or 'HNLC' regions) with Fe to concentrations in the seawater as low as 2nM led to a 60% reduction in the ocean to atmosphere $CO_{2(g)}$ flux as a result of the increasing productivity of marine phytoplankton. This

60% reduction equates to 2850 tonnes of carbon over the 30x25km test area over the 17 day experiment (*Op. cit.*). This carbon is eventually sequestered in the deep ocean as the phytoplankton die and form a part of the Particulate Organic Carbon (POC) flux from the surface to the deep ocean (also known as the 'Biological Pump') (*Op. cit.* and Watson *et al.* (2000). Watson *et al.* demonstrated that accumulation of Fe in dust in the Vostok ice core matches decreases in atmospheric pCO_2 found in the same ice core (indicating that an increase in aeolian deposition of Fe leads to a decrease in atmospheric pCO_2). Watson *et al.* proved empirically that these factors are linked to Fe-fertilisation of phytoplankton in HNLC regions of the oceans using an ocean-atmosphere carbon-cycle box model. The atmospheric pCO_2 output of the model closely matches the profile of atmospheric pCO_2 obtained from the Vostok ice core where ΔpCO_2 <40ppmv and aeolian deposition of Fe is altered to match the levels in the ice core over time (*Op. cit.*).

To conclude: the author's hope is that this study will be viewed as a good example of what can successfully be achieved when an Earth systems science approach is adopted and collaborations are formed between scientists from seemingly disparate disciplines (e.g. as in this study; geochemists and plant scientists). More importantly; the author hopes that this thesis will prompt others to study the effects biota have upon mineral weathering and that the resulting data obtained from these studies will improve understanding of the effects of mineral weathering as an input to global biogeochemical cycles and that this will lead to an improved understanding of the long-term carbon cycle and reduce the error currently associated with some parameters in biogeochemical models.

6: List of References

Aghamiri, R., & Schwartzman, D. W. (2002). Weathering rates of bedrock by lichens: a mini watershed study. *Chemical Geology, 188*(3-4), 249-259.

Andrews, J. E.,Brimblecombe, P.,Jickells, T. D., & Reid, B. (2004). *An Introduction To Environmental Chemistry* (2nd ed.). Oxford: Blackwell.

Baars, C.,Jones, T. H., & Edwards, D. (2008). Microcosm studies of the role of land plants in elevating soil carbon dioxide and chemical weathering. *Global Biogeochemical Cycles, 22*(3).

Banwell, C. N. (1983). *Fundamentals of Molecular Spectroscopy* (Vol. 3rd Ed.). Maidenhead: Mc-Graw Hill Education.

Barry, R. G., & Chorley, R. J. (2003). *Atmosphere, Weather And Climate*. London: Routledge.

Berner, R. A. (1992). Weathering, plants, and the long-term carbon cycle. *Geochimica et Cosmochimica Acta, 56*(8), 3225-3231.

Berner, R. A. (1998). The carbon cycle and CO(2) over Phanerozoic time: the role of land plants. *Philosophical Transactions of The Royal Society of London (B), 353*, 75-82.

Berner, R. A. (2004). *The Phanerozoic Carbon Cycle: CO2 and O2.* Oxford: Oxford University Press.

Blakey, R. (2009). *Late Ordovician (450Ma)*. Retrieved 16 December 2009, from http://jan.ucc.nau.edu/~rcb7/450moll.jpg

Blatt, H.,Tracy, R. J., & Owens, B. E. (2006). *Petrology: Igneous, Sedimentary and Metamorphic* (3rd Edition ed.). Basingstoke: W.H. Freeman and Company.

Brenchley, P. J.,Marshall, J. D.,Carden, G. A. F.,Robertson, D. B. R.,Long, D. G. F.,Meidla, T.,Hints, L., & Anderson, T. F. (1994). Bathymetric and isotopic evidence for a short-lived Late Ordovician glaciation in a greenhouse period. *Geology, 22*(4), 295-298.

Cooper, D. J.,Watson, A. J., & Nightingale, P. D. (1996). Large decrease in ocean-surface CO2 fugacity in response to in situ iron fertilization. *Nature, 383*(6600), 511-513.

Crouch, M. J. C. (2007). *On the Biotic Enhancement of Weathering by Lichens.* University of East Anglia, Norwich.

Crowley, T. J., & Baum, S. K. (1991). Toward reconciliation of late Ordovician (~440 Ma) glaciation with very high CO2 levels. *Journal of Geophysical Research, 96*(D12).

Deer, W. A.,Howie, R. A., & Zussman, J. (1966). *An Introduction to the Rock Forming Minerals*. London: Longman.

Fairchild, I. J., & Kennedy, M. J. (2007). Neoproterozoic glaciation in the Earth System. *Journal of the Geological Society, London, 164*, 895-921.

Ford Cochran, M., & Berner, R. A. (1996). Promotion of chemical weathering by higher plants: field observations on Hawaiian basalts. *Chemical Geology, 132*(1-4), 71-77.

Gibbs, M. T.,Barron, E. J., & Kump, L. R. (1997). An atmospheric pCO(2) threshold for glaciation in the Late Ordovician. *Geology, 25*(5), 447-450.

Gradstein, F. M.,Ogg, J. G., & Smith, A. G. (2004). *A Geologic Timescale 2004*. Cambridge: Cambridge University Press.

Graham, R. C.,Rossi, A. M., & Hubbert, K. R. (2010). Rock to regolith conversion: Producing hospitable substrates for terrestrial ecosystems. *GSA Today, 20*(2), 4-9.

Hasebe, M. (2009). *The Life-Cycle of Physcomitrella patens*, from http://moss.nibb.ac.jp/images/life2.gif

Hatcher, W. H., & MacLauchlan, D. W. (1938). The Conductivity and Reactivity of Nitric Acid and Hydrogen Peroxide Mixtures. *Canadian Journal of Research, 16B*.

Hazen, R. M. (2009). Animal, vegetable: both made mineral. *New Scientist*, 14.

Helsel, D. R. (2006). Fabricating data: How substituting values for nondetects can ruin results, and what can be done about it. *Chemosphere, 65*(11), 2434-2439.

Hoffland, E.,Kuyper, T. W.,Wallander, H.,Plassard, C.,Gorbushina, A. A.,Haselwandter, K.,Holmstrom, S.,Landeweert, R.,Lundstrom, U. S.,Rosling, A.,Sen, R.,Smits, M. M.,van Hees, P. A., & van Breemen, N. (2004). The role of fungi in weathering. *Frontiers in Ecology and the Environment, 2*(5), 258-264.

Imperial. (2010). *Imperial College, London: Database of Ionic Radii*. Retrieved 24th March 2010, 2010, from http://abulafia.mt.ic.ac.uk/shannon/ptable.php

Isherwood, D., & Street, A. (1976). Biotite-induced grussification of the Boulder Creek Granodiorite, Boulder County, Colrado. *Geological Society of America Bulletin, 87*, 366-370.

Jackson, T. A., & Keller, W. D. (1970). A comparative study of the role of lichens and "inorganic" processes in the chemical weathering of Recent Hawaiian lava flows. *American Journal of Science, 269*(5), 446-466.

Kump, L. R., & Arthur, M. A. (1999). Interpreting carbon-isotope excursions: carbonates and organic matter. *Chemical Geology, 161*(1-3), 181-198.

Kump, L. R.,Arthur, M. A.,Patzkowsky, M. E.,Gibbs, M. T.,Pinkus, D. S., & Sheehan, P. M. (1999). A weathering hypothesis for glaciation at high atmospheric pCO(2) during the Late Ordovician. *Palaeogeography Palaeoclimatology Palaeoecology, 152*(1-2), 173-187.

Lajunen, & Peramaki. (2004). *Spectrochemical Analysis by Atomic Absorption and Emission* (2nd ed.). London: Royal Society of Chemistry.

Lenton, T. M. (2001). The role of land plants, phosphorus weathering and fire in the rise and regulation of atmospheric oxygen. *Global Change Biology, 7*(6), 613-629.

Lenton, T. M., & Watson, A. J. (2004). Biotic enhancement of weathering, atmospheric oxygen and carbon dioxide in the Neoproterozoic. *Geophysical Research Letters, 31*(5), 5.

Lewis, D. G., & Quirk, J. P. (1967). Phosphate diffusion in soil and uptake by plants P-31 movement and uptake by plants as indicated by P-32 autoradiography. *Plant and Soil, 26*(3), 445-&.

Libes, S. M. (1992). *An Introduction To Marine Biogeochemistry*. New York, NY, USA.: John Wiley & Sons, Inc.

Liss, P. S., & Spencer, C. P. (1969). An investigation of some methods used for determination of silicate in sea water. *Journal of the Marine Biological Association of the United Kingdom, 49*(3), 589.

Lovelock, J. E. (1979). *Gaia: A New Look At Life On Earth*. Oxford: Oxford University Press.

Mackenzie, W. S., & Adams, A. E. (1994). *A Colour Atlas of Rocks and Minerals in Thin Section*. London: Manson Publishing Ltd.

Marienfeld, J. R.,Reski, R.,Friese, C., & Abel, W. O. (1989). Isolation of Nuclear, Chloroplast and Mitochondrial DNA from the Moss Physcomitrella patens. *Plant Science, 61*, 235-244.

Menand, B.,Yi, K. K.,Jouannic, S.,Hoffmann, L.,Ryan, E.,Linstead, P.,Schaefer, D. G., & Dolan, L. (2007). An ancient mechanism controls the development of cells with a rooting function in land plants. *Science, 316*(5830), 1477-1480.

Moulton, K. L., & Berner, R. A. (1998). Quantification of the effect of plants on weathering: Studies in Iceland. *Geology, 26*(10), 895-898.

Pallant, J. (2007). *SPSS Survival Manual (3rd Ed.)*. Maidenhead.: McGraw-Hill/Open University Press.

Parsons, T.,Maita, V., & Lalli, C. (1984). *A manual of chemical and biological methods for seawater analysis*. Oxford: Pergamon.

Pope, M. C., & Steffen, J. B. (2003). Widespread, prolonged late Middle to Late Ordovician upwelling in North America: A proxy record of glaciation?: Correction. *Geology, 31*(7), 656-656.

Reski, R., & Cove, D. J. (2004). Physcomitrella patens. *Current biology : CB, 14*(7), R261-262.

Saltzman, M. R., & Young, S. A. (2005). Long-lived glaciation in the Late Ordovician? Isotopic and sequence-stratigraphic evidence from western Laurentia. *Geology, 33*(2), 109-112.

Schaefer, D. G. (2002). A new moss genetics: Targeted mutagenesis in Physcomitrella patens, *Annual Review of Plant Biology* (Vol. 53, pp. 477-501).

Schwartzman, D. W. (2000). *Life, Temperature and the Earth: The Self-Organizing Biosphere*. New York, NY, USA.: Columbia University Press.

She, N. (1997). Analyzing censored water quality data using a non-parametric approach. *Journal of the American Water Resources Association, 33*(3), 615-624.

Sheehan, P. M. (2001). The Late Ordovician Mass Extinction. *Annual Review of Earth and Planetary Sciences, 29*, 331-364.

Spokes, L. J.,Yeatman, S. G.,Cornell, S. E., & Jickells, T. D. (2000). Nitrogen deposition to the eastern Atlantic Ocean. The importance of south-easterly flow. *Tellus B, 52*(1), 37-49.

Steemans, P.,Herisse, A. L.,Melvin, J.,Miller, M. A.,Paris, F.,Verniers, J., & Wellman, C. H. (2009). Origin and Radiation of the Earliest Vascular Land Plants. *Science, 324*(5925), 353-.

Sterner, R. W., & Elser, J. J. (2002). *Ecological stoichiometry: the biology of elements from molecules to the biosphere*. Woodstock: Princeton University Press.

Street-Perrott, F. A., & Barker, P. A. (2008). Biogenic silica: a neglected component of the coupled global continental biogeochemical cycles of carbon and silicon. *Earth Surface Processes and Landforms, 33*, 1436-1457.

Sucharova, J., & Suchara, I. (2006). Determination of 36 elements in plant reference materials with different Si contents by inductively coupled plasma mass spectrometry: Comparison of microwave digestions assisted by three types of digestion mixtures. *Analytica Chimica Acta, 576*(2), 163-176.

Taiz, L., & Zeiger, E. (2002). *Plant Physiology (3rd Ed.)* (Vol. Sunderland, MA, USA.): Sinauer Associates Inc.

Taylor, D. J.,Green, N. P. O., & Stout, G. W. (Eds.). (1997). *Biological Science 1* (3rd ed.). Cambridge: Cambridge University Press.

TVA. (2010). *The Vermiculite Association: Properties*. Retrieved 15/01/2010, from http://www.vermiculite.org/Properties6.html

UBC. (2010). *Bryophytes of Stanley Park: Bryophyte Evolution*. Retrieved 7/1/2010, 2010, from http://www.botany.ubc.ca/bryophyte/stanleypark/evolution.htm

UNU. (1992). *The Evolving Gaia Theory: Paper presented at The United Nations University Lectures*, from http://www.unu.edu/unupress/lecture1.html

USGS. (2003). *The Highlands Province: The Taconic Orogeny*. Retrieved 6/1/2010, 2010, from http://3dparks.wr.usgs.gov/nyc/highlands/highlands.html

Wainwright. (2010). *geology*. Retrieved 15/01/2010, from http://www.wainwright.co.uk/geology.php

Watson, A. J.,Bakker, D. C. E.,Ridgwell, A. J.,Boyd, P. W., & Law, C. S. (2000). Effect of iron supply on Southern Ocean CO2 uptake and implications for glacial atmospheric CO2. *Nature, 407*(6805), 730-733.

Wellman, C. H.,Osterloff, P. L., & Mohiuddin, U. (2003). Fragments of the earliest land plants. *Nature, 425*, 282-285.

White, A. F., & Brantley, S. L. (2003). The effect of time on the weathering of silicate minerals: why do weathering rates differ in the laboratory and field? *Chemical Geology, 202*(3-4), 479-506.

Yapp, C. J., & Poths, H. (1992). Ancient atmospheric CO(2) pressures inferred from natural goethites. *Nature, 355*, 342-344.

Zhang, J. Z.,Fischer, C. J., & Ortner, P. B. (1999). Laboratory glassware as a contaminant in silicate analysis of natural water samples. *Water Research, 33*(12), 2879-2883.

Index to Appendices

Appendix i – Further Methodology

i.i Method Development

i.i.i Pilot Oxidation Experiments using *Arabidopsis* Tissue

A small amount of tissue from the flowering plant *Arabidopsis thaliana* was added to five centrifuge tubes. 10ml of 10% Nitric Acid was then added to these tubes and the tubes were vortexed for 10 seconds before 10ml of 10% Hydrogen Peroxide was added and the tubes vortexed again for 10 seconds. The tubes were then incubated in a heat block at 40°C for one hour; the tubes were shaken by hand periodically. The entire procedure was conducted in a fume cabinet with the sash ¾ lowered, and personal protective equipment was worn at all times.

After one hour the plant tissue did not visibly appear to have degraded beyond the fact that the chlorophyll had been released, turning the solution a pale green. I therefore increased the concentrations of the Nitric Acid and the Hydrogen Peroxide to 20% and repeated the procedure: this caused the plant tissue to turn more translucent and more chlorophyll to be released, but did not result in the complete oxidation of tissue required. I then increased the concentrations of Nitric Acid and the Hydrogen Peroxide to 30%, at these concentrations the tissue began to degrade.

Increasing the concentrations of the oxidation mix still further would have been ill-advised because Hydrogen Peroxide becomes unstable at concentrations >32% (Hatcher & MacLauchlan, 1938), it was therefore decided to increase the incubation temperature in a series of experiments to 50°C, 60°C and finally 70°C. At 70°C the reaction was found to proceed so well that the reaction time could be halved to 30 minutes for new moss biomass samples. The experiment was then repeated with moss inoculum and found to work satisfactorily.

i.i.ii Initial Microcosm Water Sampling Methods

i.i.ii.i Method 1

150µl of the aqueous solution within the microcosm was pipetted off into a new centrifuge tube using a 1000µl pipette and tip, a new tip being used for each microcosm to prevent contamination. In order to make up the resulting solution to the minimum volume for ICP analysis; 3.45ml of upH_2O was added to each centrifuge tube using a 5ml pipette and tip, and the tubes were lightly shaken to homogenise the contents. On addition of 400µl of desorbing agent a resulting solution of 4000µl was produced for ICP analysis.

i.i.ii.ii Method 2

Sampling Method 2 is identical to Method 1 with the following exceptions:-

1. 200µl of aqueous solution was pipetted off each microcosm.
2. 3720µl of upH_2O was added to each centrifuge tube.
3. 80µl of desorbing agent was added to each centrifuge tube.

i.ii Laboratory Protocols

i.ii.i Substrate Washing Protocol

1. In a 1L glass beaker add substrate to 400ml line.
2. Add 15MΩ upH_2O to 1L line.
3. Mix with a clean spoon and stand for 10mins.
4. After 10mins pour suspension through a sieve (retaining 50ml for analysis).
5. Rinse spoon, beaker and sieve clean of material with dH_2O.
6. Add substrate from sieve back to beaker and repeat stages 2-6 **without** standing for 10mins.
7. Repeat 6.
8. Add substrate from sieve, add **18**MΩ upH_2O to 1L line and repeat stage 6.
9. Place substrate into a clean 500ml glass beaker. Place two sheets of aluminium foil over the top of the beaker and seal around the rim.
10. Heat sterilise.

i.ii.ii Knop's Plates Preparation Protocol

The media was prepared and stored in an oven at 55°C for no more than three days prior to use. Plates were made by adding 10ml of molten Knop's media to sterile plastic petri dishes and allowing the media to solidify and cool. Circular cellulose discs[31] 80mm in diameter were then placed on top of the media using forceps, without these discs the moss grows into the media and is very difficult to remove. The lids were then placed on top of the plates and the plates were placed in a growth room for five days. After five days the moss was collected from each plate using a sterilised metal spatula, the moss from each plate being placed into a 5ml bijou jar of sterile water.

[31] Custom manufactured by: A.A. Packaging Ltd., Preston, Lancashire, UK.

i.ii.iii Nutrient Auto Analyser (NAA) Protocols

Reagent	Feedstock Chemicals
Phosphate 1	125ml of 280ml/l concentrated Sulphuric Acid
	3.0g Ammonium Molybdate Tetrahydrate
	0.115g Potassium Antimonyl Tartrate†
	0.1g Sodium Dodecyl Sulfate‡
Phosphate 2	5.5g Ascorbic Acid
	30ml Propanone
	0.1g Sodium Dodecyl Sulfate
Silicate 1	10.0g Ammonium Molybdate Tetrahydrate
	0.25g Sodium Dodecyl Sulfate
Silicate 2	22.0g Oxalic acid‡
Silicate 3	20.0g Ascorbic acid‡

Feedstock chemicals used to produce the Nutrient Auto Analyser reagents. All chemicals were added to a 500ml volumetric flask and made up to volume with upH_2O. Chemicals were supplied by Fisher Chemical[32] unless otherwise stated:-

†Supplied by: BDH/Merck.[33]
‡Supplied by: Sigma–Aldrich.[34]

[32] Fisher Scientific UK Ltd, Loughborough, Leicestershire, LE11 5RG, UK.
[33] Merck Chemicals Ltd., Hull, HU1 1UY, UK.
[34] Sigma-Aldrich Company Ltd., Dorset, UK.

i.ii.iv XRF Protocol

1: Wipe disc mill pans and fusion bead crucibles with propan-2-ol. Rinse with distilled water.

2: Place crucibles onto Mettler Toledo XS205 (Dual Range) 5.d.p. balance (d=0.01mg). Ensure sides and top are fully closed. When figures stop cycling tare balance.

3: Weigh out 7.60000g of Lithium Borate flux (as accurately as possible).

4: Add 0.40000g of milled rock sample to the flux, giving a flux + sample as close to 8.00000g as possible.

5: Stir mixture using a propan-2-ol cleaned spatula. Place platinum crucibles in fusion bead machine (see next section).

6: Allow resulting beads to cool. Label them on the larger side.

7: Analyse on Bruker XRF machine.

i.ii.v Phoenix Fusion Bead Machine Protocol

1: Turn on butane cylinder at regulator. Turn on oxygen cylinder.

2: Ensure you have pressure of >4 bar.

3: Switch on 'Phoenix' machine set to the following programme:-

Pre-Melt	240s
Melt	180s
Swirl	200s
Pour	20s
Cool delay	10s
Pre-cool	40s
Total cool	240s

4: Switch on burners beneath the crucibles. Press down start button for >5s.

i.iii Mathematical Operations

i.iii.i Standard Deviation

The standard deviation was calculated using Microsoft Excel internal 'stdev' operation. Excel calculates the standard deviation using the following formula:-

$$\sqrt{\frac{\sum(x-\bar{x})^2}{(n-1)}}$$

Where: χ = sample mean and n = sample size.

i.iii.ii Standard Error

The standard error of the mean was calculated using the standard deviation from Excel above and the following formula:-

$$\frac{\sigma}{\sqrt{n}}$$

Where: σ = standard deviation and n = sample size.

Appendix ii – Blank Analysis Data

ii.i Contamination in experimental waters

ii.i.i Ultra pure waters

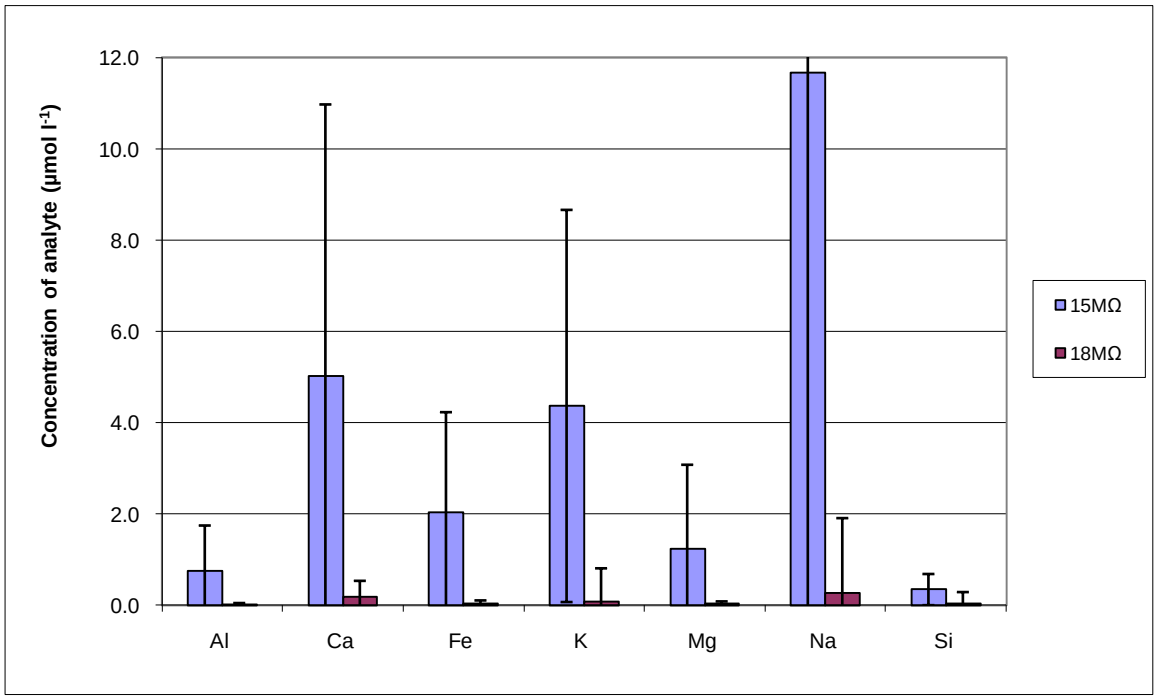

Graph showing contamination in 15MΩ and 18MΩ Ultra Pure Waters, note the substantially higher levels of contamination (8.9-62.3 times, depending on analyte) in 15MΩ upH_2O relative to 18MΩ upH_2O. Error bars represent 1σ 15MΩ n=10, 18MΩ n=98. NB the analysis shown above was conducted after all experiments had been completed and could not therefore be used to inform experimental methods.

ii.i.ii Contamination in sterile water

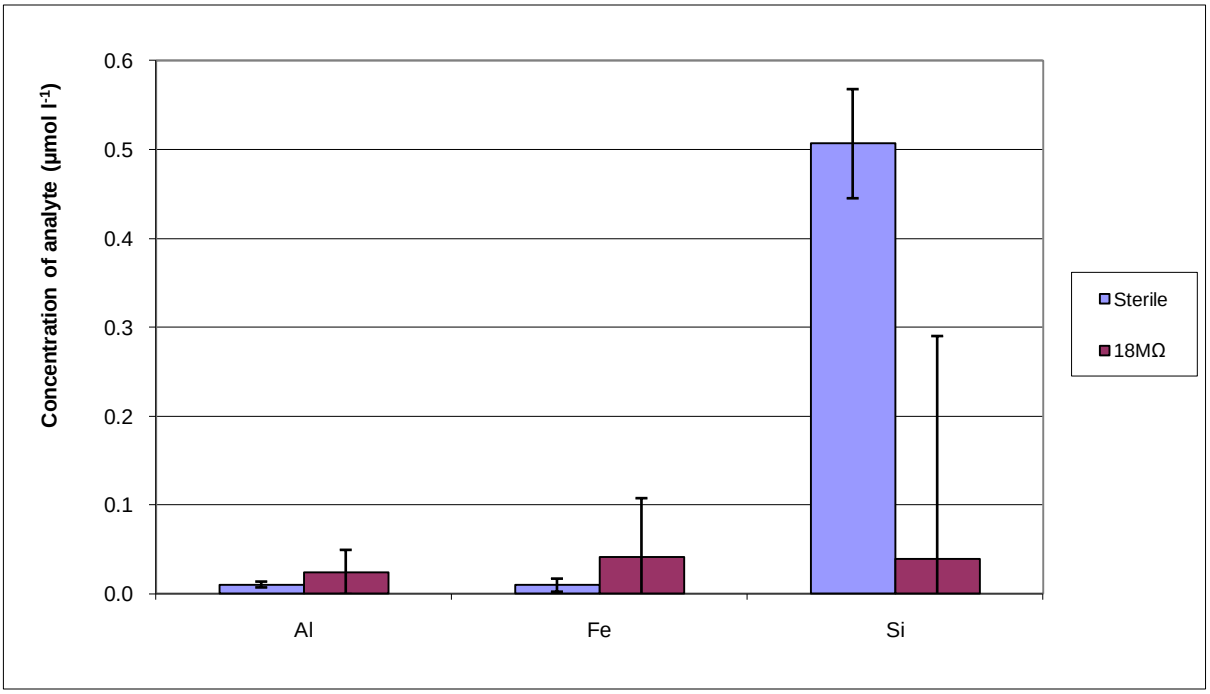

Graph showing contamination in sterile (autoclaved 18MΩ upH_2O) relative to non-autoclaved 18MΩ upH_2O (Sterile n=5, 18MΩ n=98). NB Initial pilot studies used only three analytes (Al, Fe and Si) for simplicity.

The data shown above were unexpected: the steam generator used to autoclave items generates steam using dH_2O rather than upH_2O. As the lids of the bijou jars have to be kept loosened by ¼ turn in order to stop the jars from imploding at high pressure, it was expected that dH_2O would enter the upH_2O in the vapour phase thus contaminating the upH_2O. The graph appears to be weakly demonstrating the opposite for Al and Fe. It is important to note that there are only data for three analytes and that the data for the sterile water consists of five pseudo-replicates (five sub-samples of one sample) taken on one day, whereas the upH_2O dataset represents 98 pseudo-replicates taken over 23 days. The upH_2O dataset is therefore much more robust than the sterile water dataset. The effects of contamination are mitigated by a rigorous blank correction procedure.

ii.ii Contamination during inoculum preparation stages

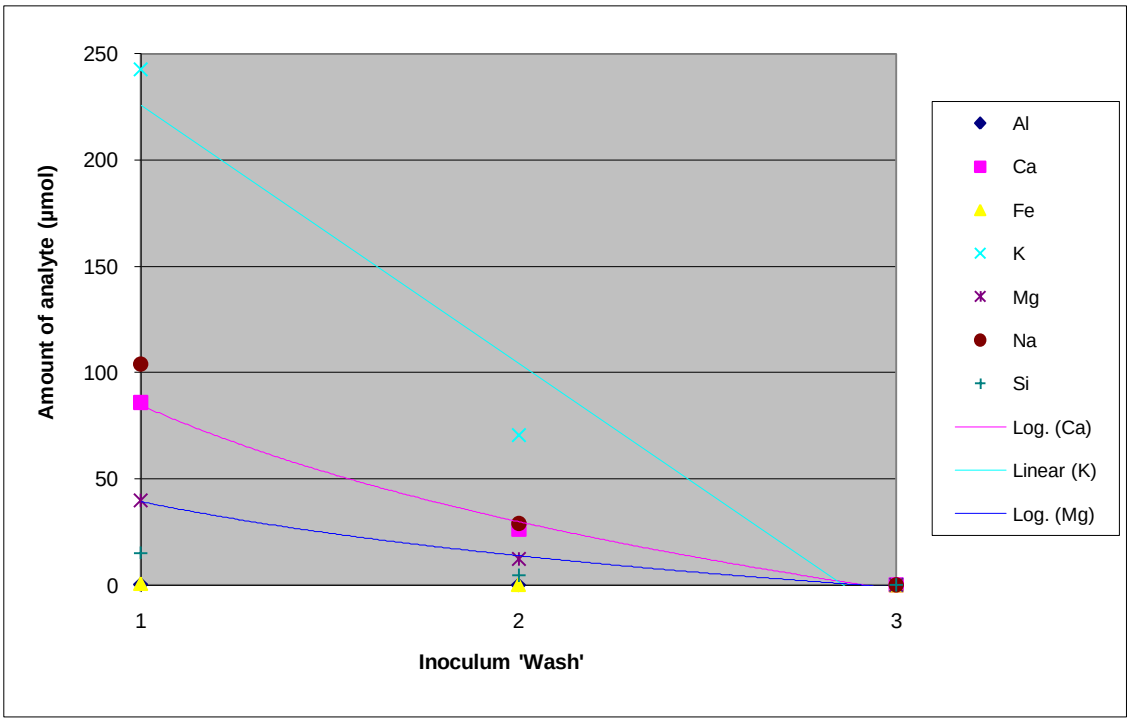

Contamination in the 1st and 2nd sterile water washes ('1' and '2') during the preparation of the 29/7/09 inoculum). '3' is the final wash in upH_2O that forms the filtrate that is added to control microcosms.

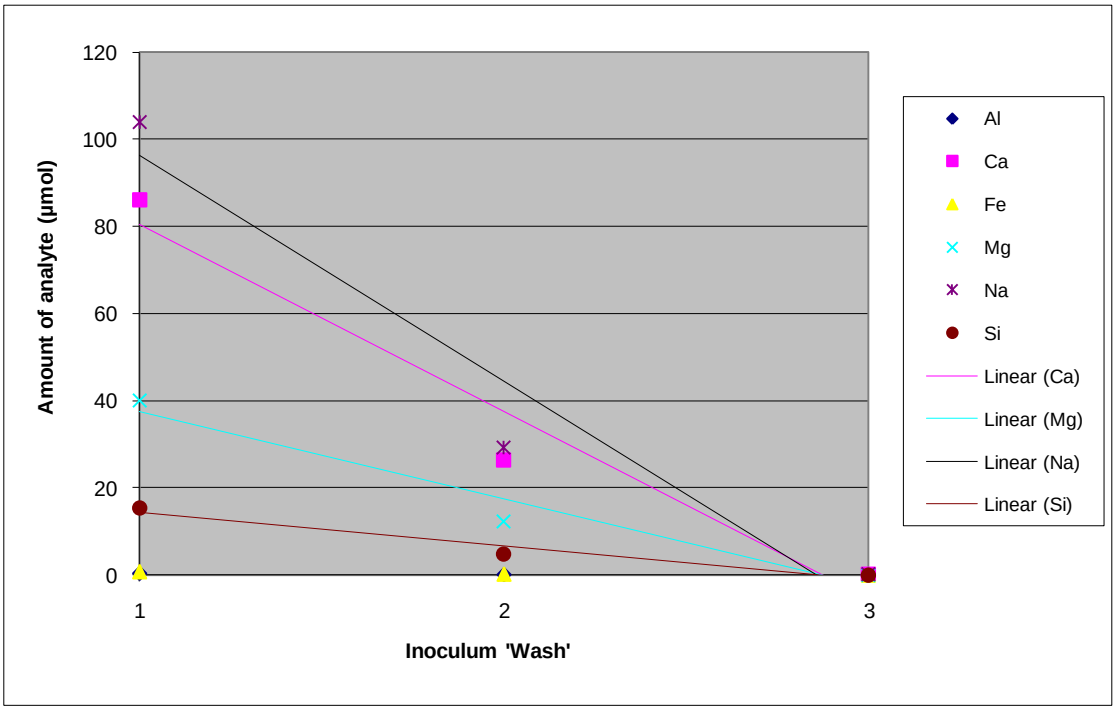

As previous figure: except the major analyte (K) is removed to more highly resolve the other analytes. All analytes show a decrease over the washes to a level slightly above or below the limit of detection of the ICP-AES.

ii.iii Substrate wash analysis

The trends for the substrate washes were mainly negative with linear or logarithmic ('curved') trend-lines. 3 out of 14 datasets formed asymmetric distributions (i.e. the final wash contained a higher amount of an analyte than the first wash). The figures below demonstrate the types of distribution observed in the substrate wash datasets:-

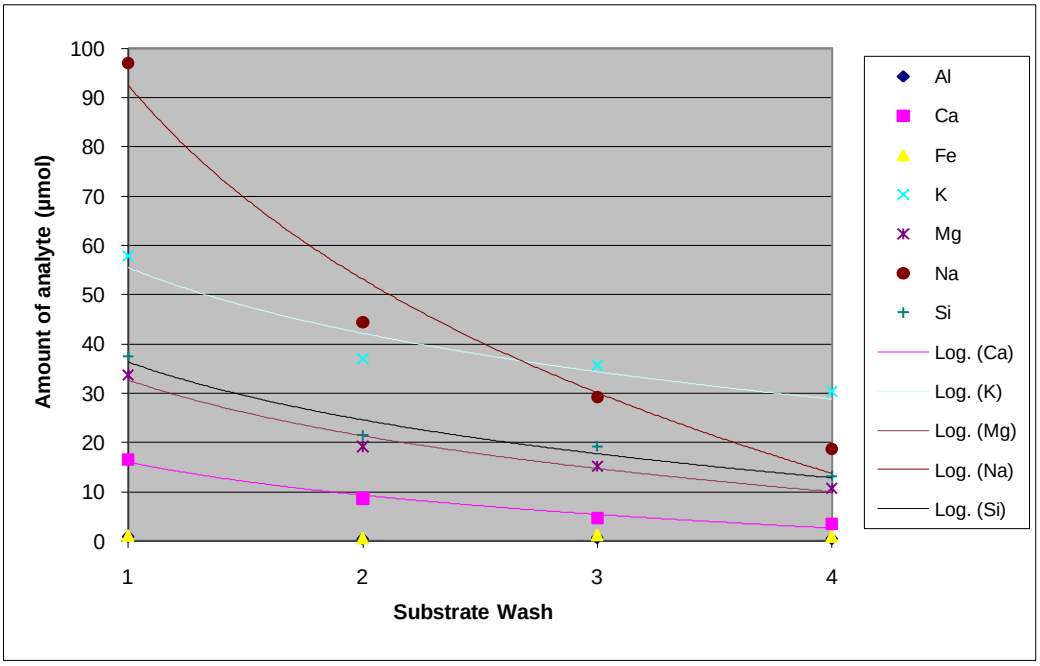

4/2/09 Vermiculite wash data, all analytes exhibiting logarithmic negative correlations. Analysis by ICP-AES.

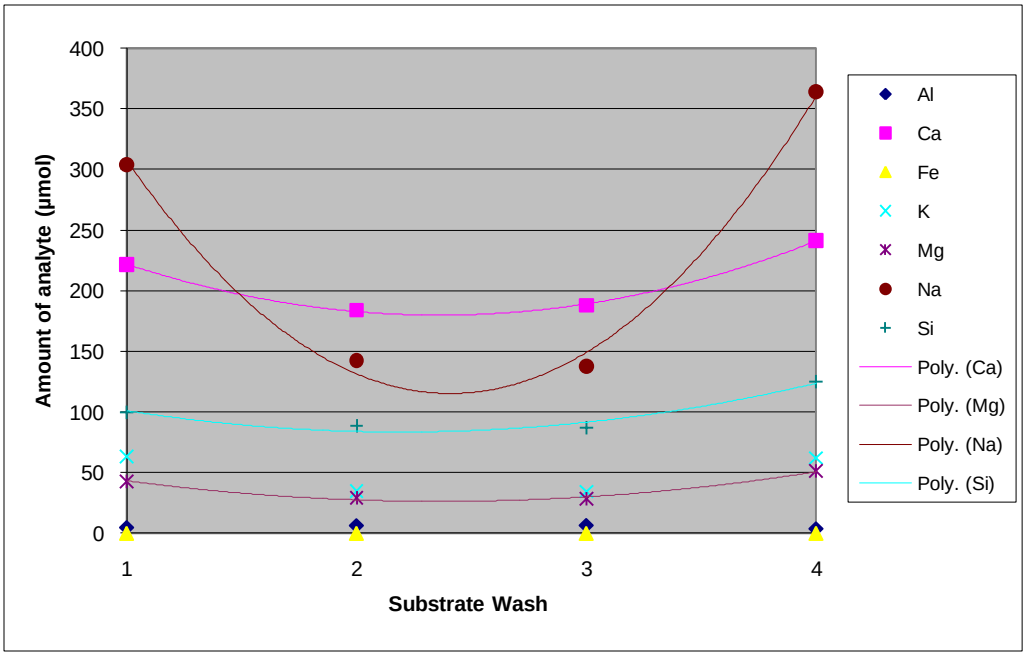

4/2/09 Andesite wash data, all analytes exhibiting two order asymmetrical distributions with many analytes exhibiting a higher amount in the final wash than the first wash.

The negative, curved trend-lines exhibited by all analytes in the 4/2/09 vermiculite wash data are to be expected; the more a substrate was washed with upH_2O the more adsorbed ions and deposited contaminants were removed from the mineral surface. This affect was observed whilst washing the mineral/rock; the solution resulting from the first wash was frequently extremely turbid (and several filters were clogged preparing the sample for analysis. The turbidity of each wash decreased until the final wash, which was normally relatively transparent to light.

The asymmetrical distributions may be explained by the fact that the 15MΩ upH_2O contained more ions such as bicarbonate (HCO_3^-) and carbonate (CO_3^{2-}) than the 'cleaner' 18MΩ upH_2O. HCO_3^- and CO_3^{2-} are the main ions responsible for alkalinity, buffering acidity in natural waters (Andrews *et al.*, 2004), therefore 18MΩ upH_2O will be more acidic than 15MΩ upH_2O and as such would have been more able to release ions adsorbed onto the rock surface. Furthermore; the increasing use of glassware across the rock wash procedure could explain any increase in Si contamination in the final washes as Si is leached from the silica glassware (Zhang *et al.*, 1999). The high amounts of analytes in the final wash results could also, simply, be experimental artefacts.

ii.iv – Contamination from heated plasticware

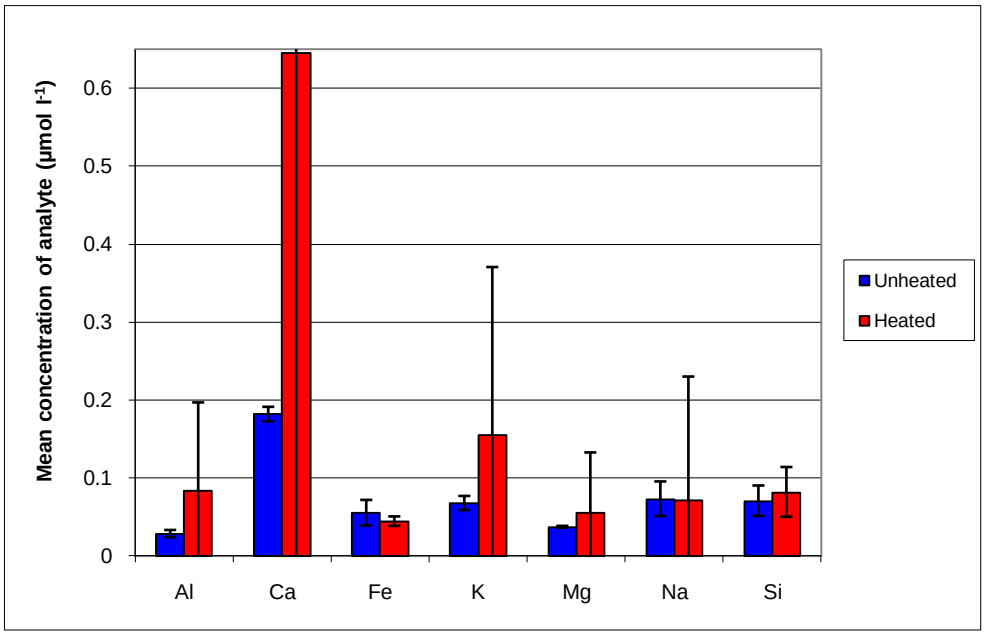

Contamination in upH_2O heated in plastic centrifuge tubes (n=5) relative to unheated upH_2O (n=4). 1σ error bars overlap for all analytes indicating that any leaching effect from plastic is statistically insignificant.

ii.v upH_2O Blanks – Frequency Distribution Analyses

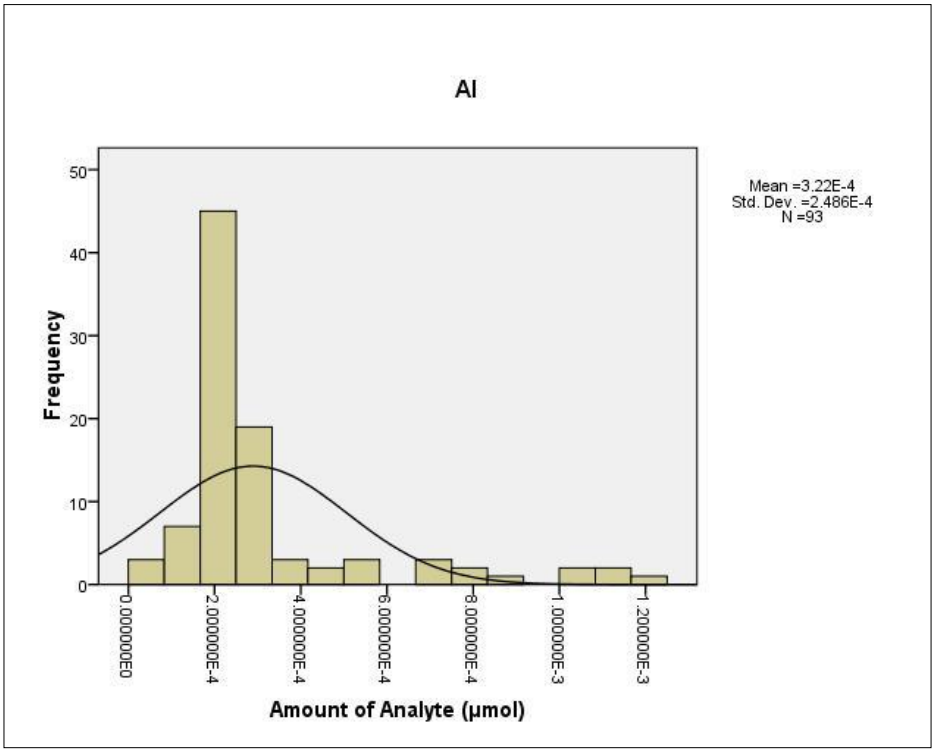

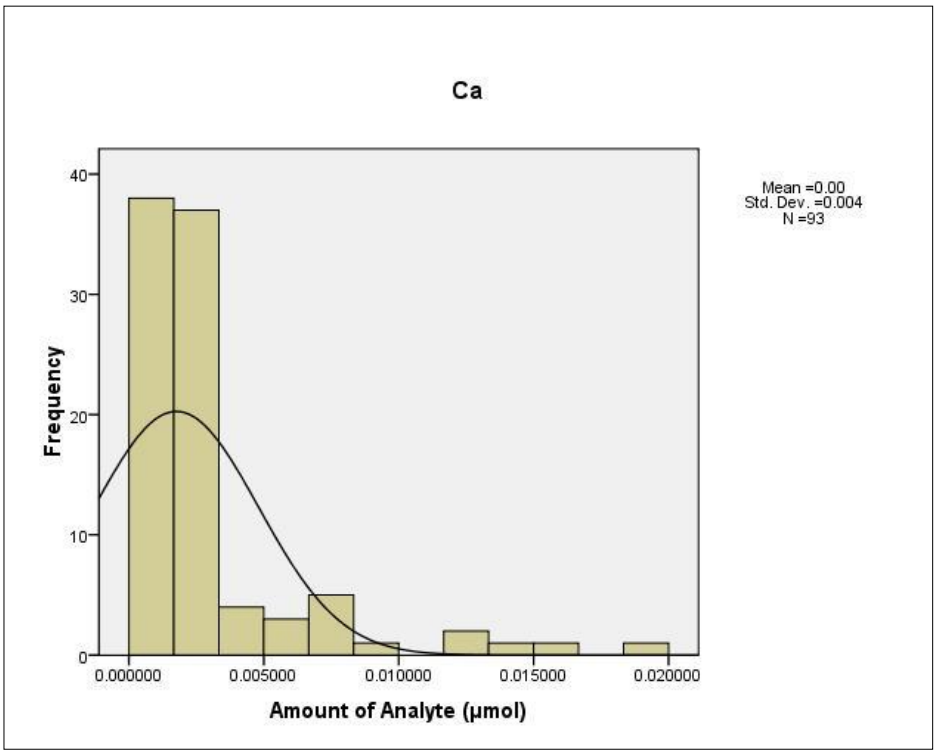

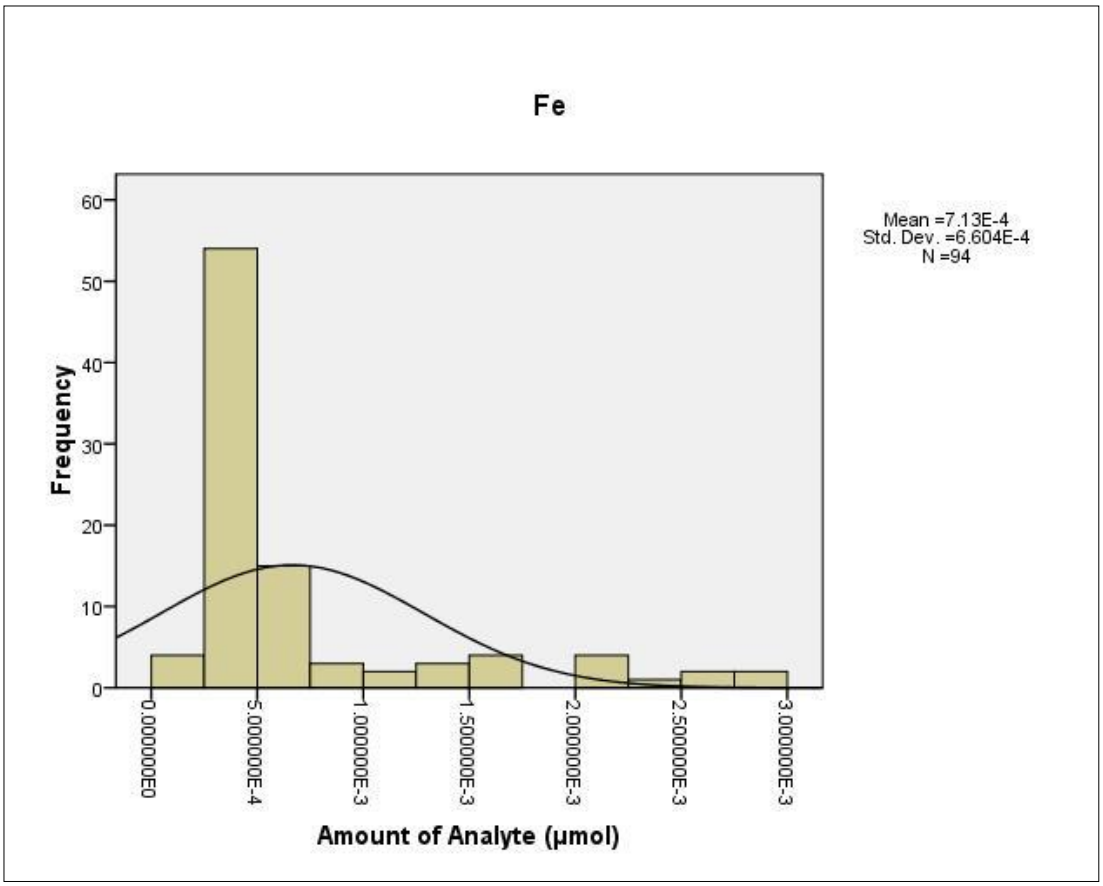
Fe
Mean =7.13E-4
Std. Dev. =6.604E-4
N =94
Frequency
60
50
40
30
20
10
0
0.000000E0
5.000000E-4
1.000000E-3
1.500000E-3
2.000000E-3
2.500000E-3
3.000000E-3
Amount of Analyte (µmol)

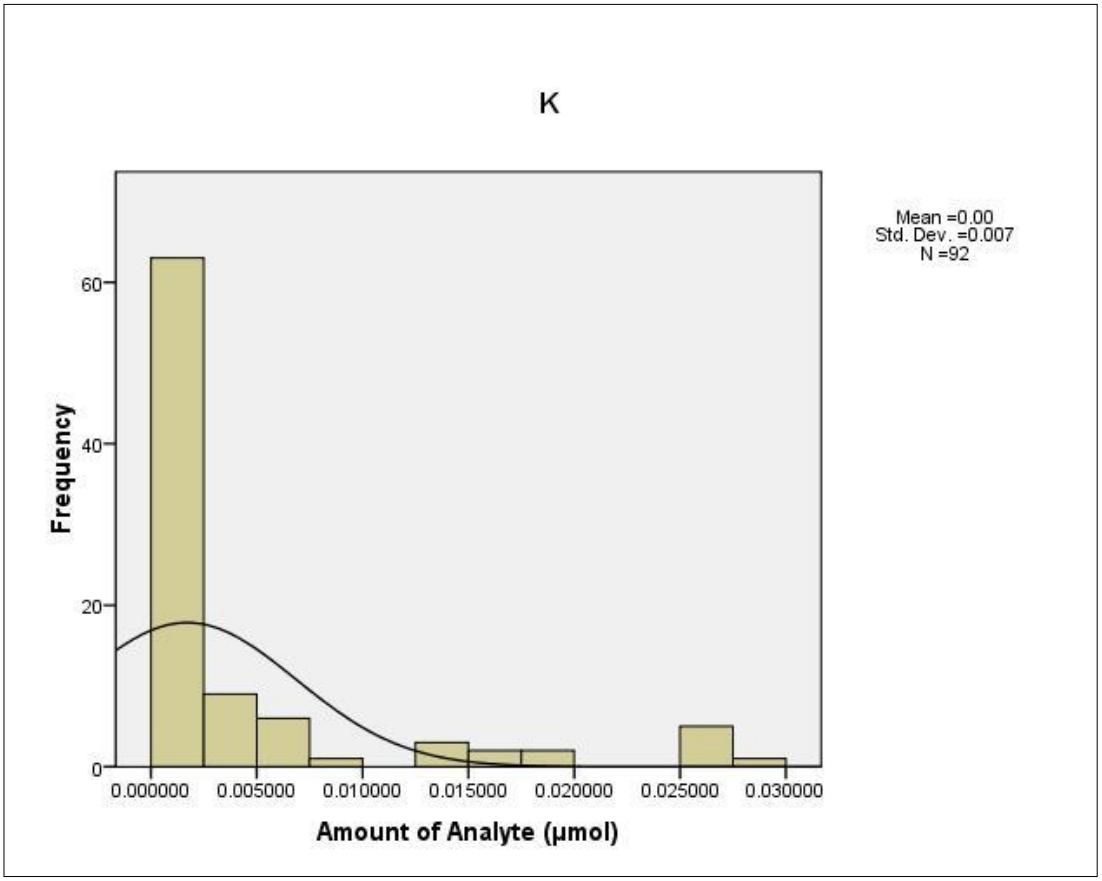
K
Mean =0.00
Std. Dev. =0.007
N =92
Frequency
60
40
20
0
0.000000
0.005000
0.010000
0.015000
0.020000
0.025000
0.030000
Amount of Analyte (µmol)

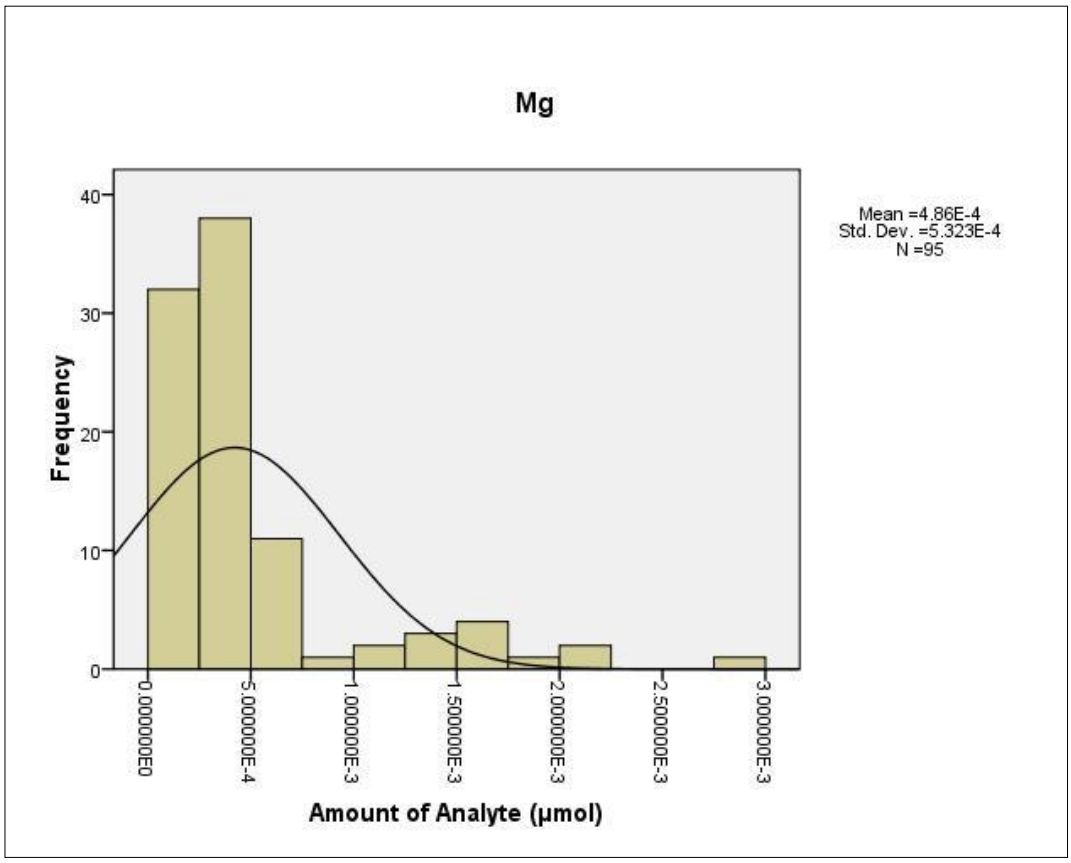
Mg
Mean =4.86E-4
Std. Dev. =5.323E-4
N =95
Frequency
40
30
20
10
0
0.000000E0
5.000000E-4
1.000000E-3
1.500000E-3
2.000000E-3
2.500000E-3
3.000000E-3
Amount of Analyte (µmol)

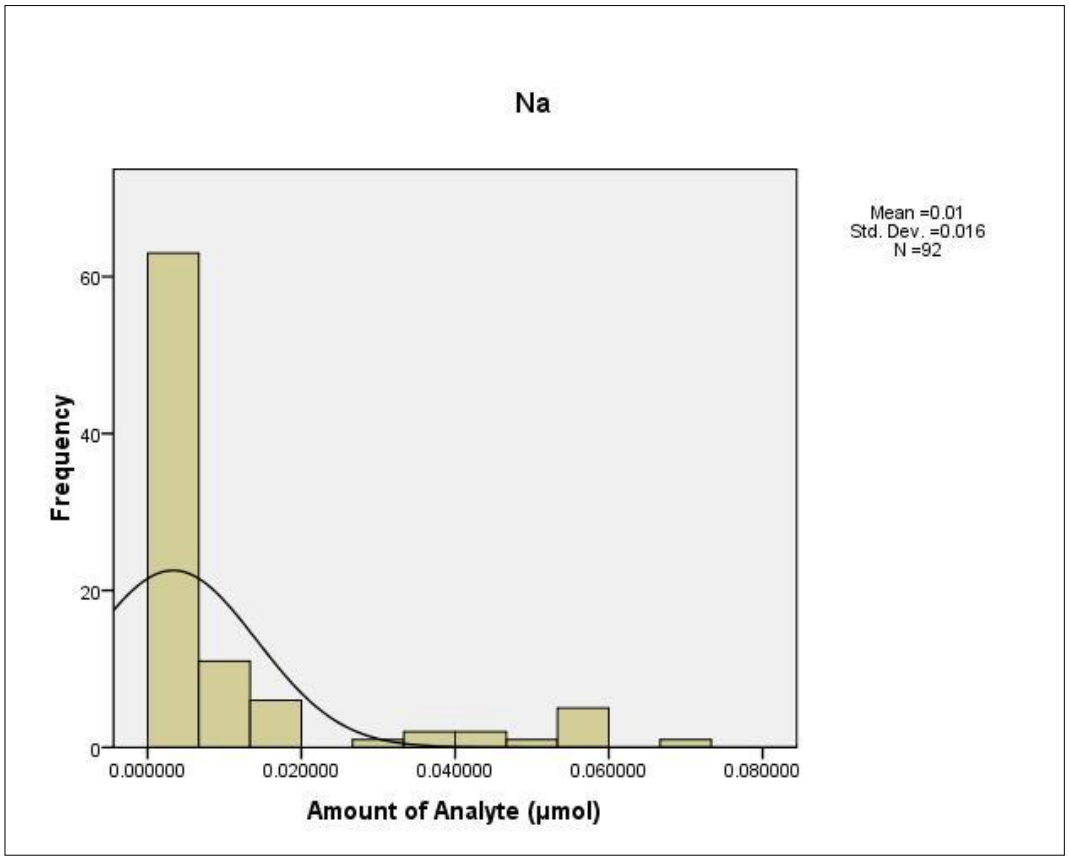
Na
Mean =0.01
Std. Dev. =0.016
N =92
Frequency
60
40
20
0
0.000000
0.020000
0.040000
0.060000
0.080000
Amount of Analyte (µmol)

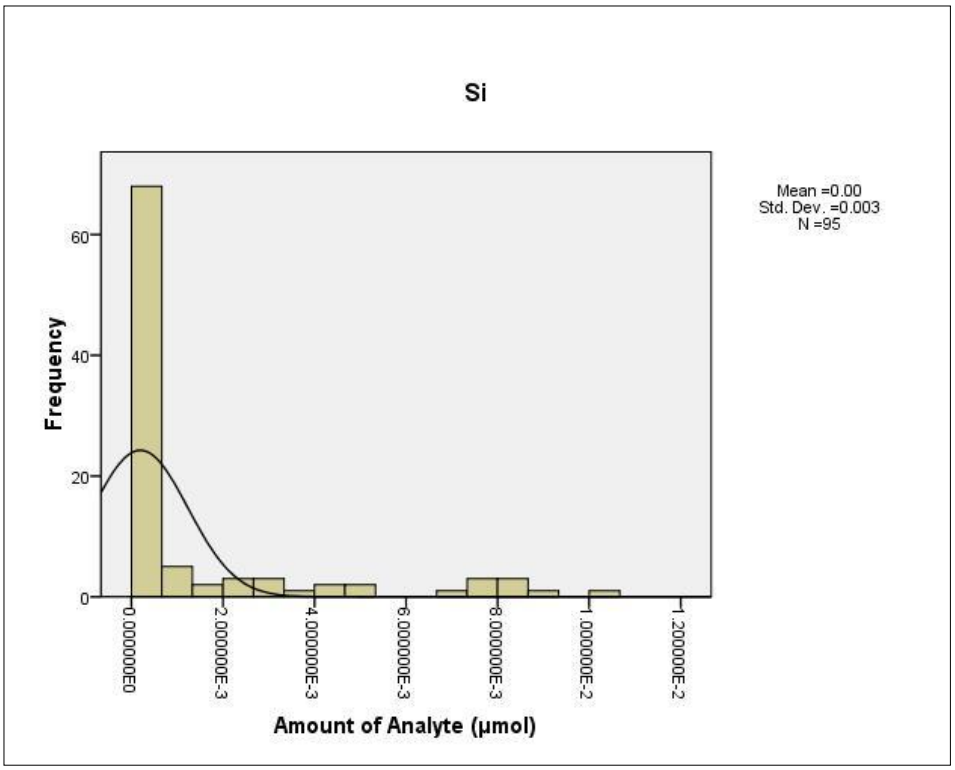

ii.vi Inoculum at initial conditions – Frequency Distribution Analyses

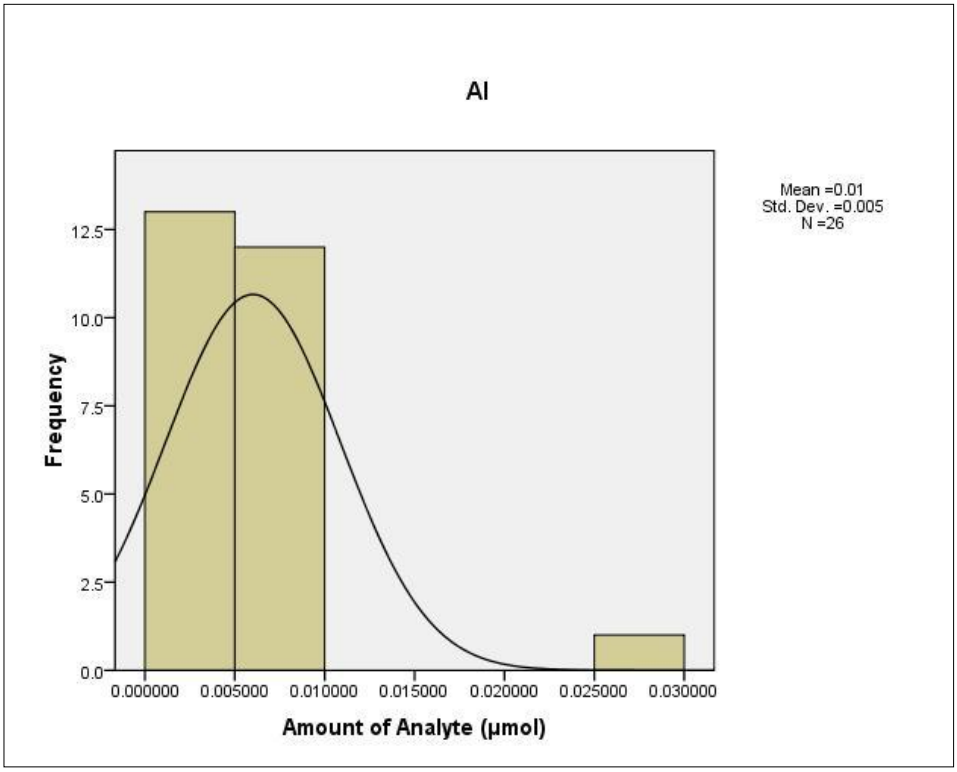

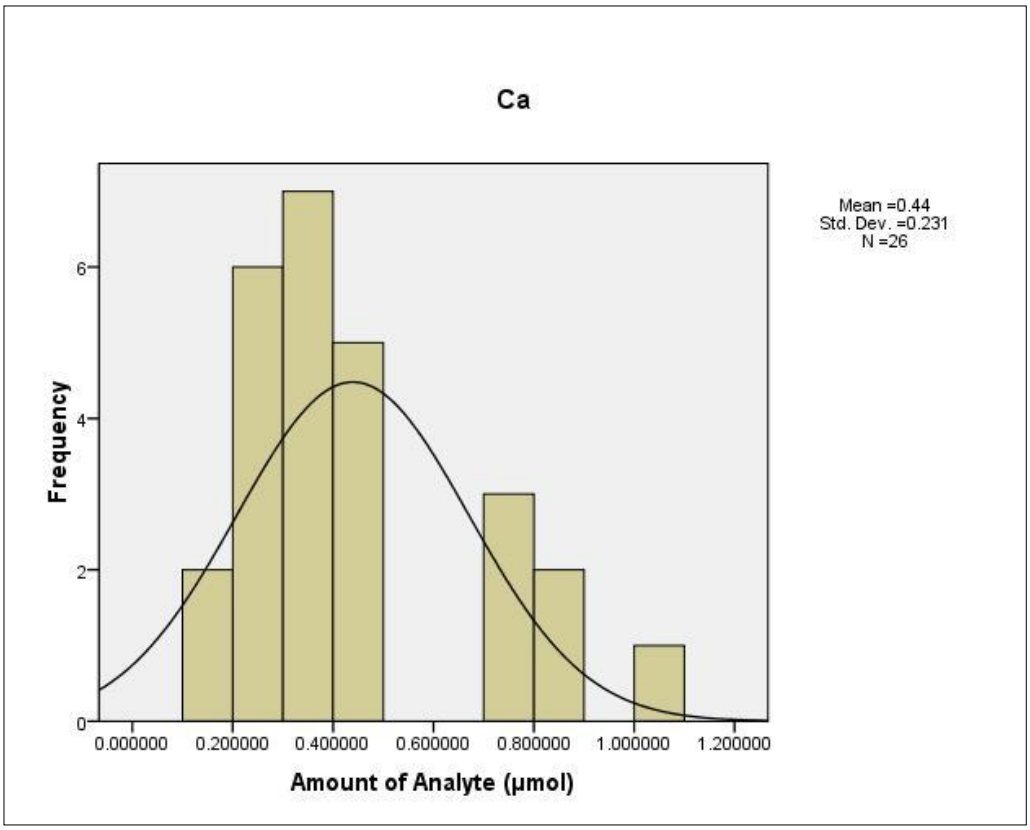
Ca
Mean =0.44
Std. Dev. =0.231
N =26
Frequency
0
2
4
6
0.000000
0.200000
0.400000
0.600000
0.800000
1.000000
1.200000
Amount of Analyte (µmol)

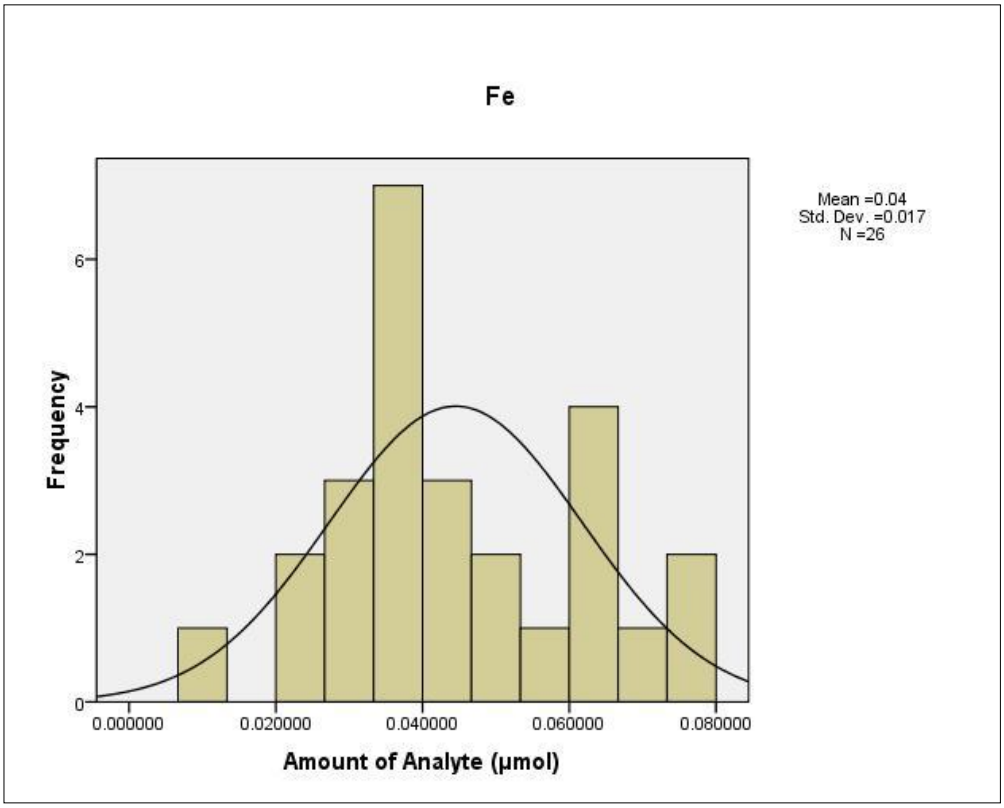
Fe
Mean =0.04
Std. Dev. =0.017
N =26
Frequency
0
2
4
6
0.000000
0.020000
0.040000
0.060000
0.080000
Amount of Analyte (µmol)

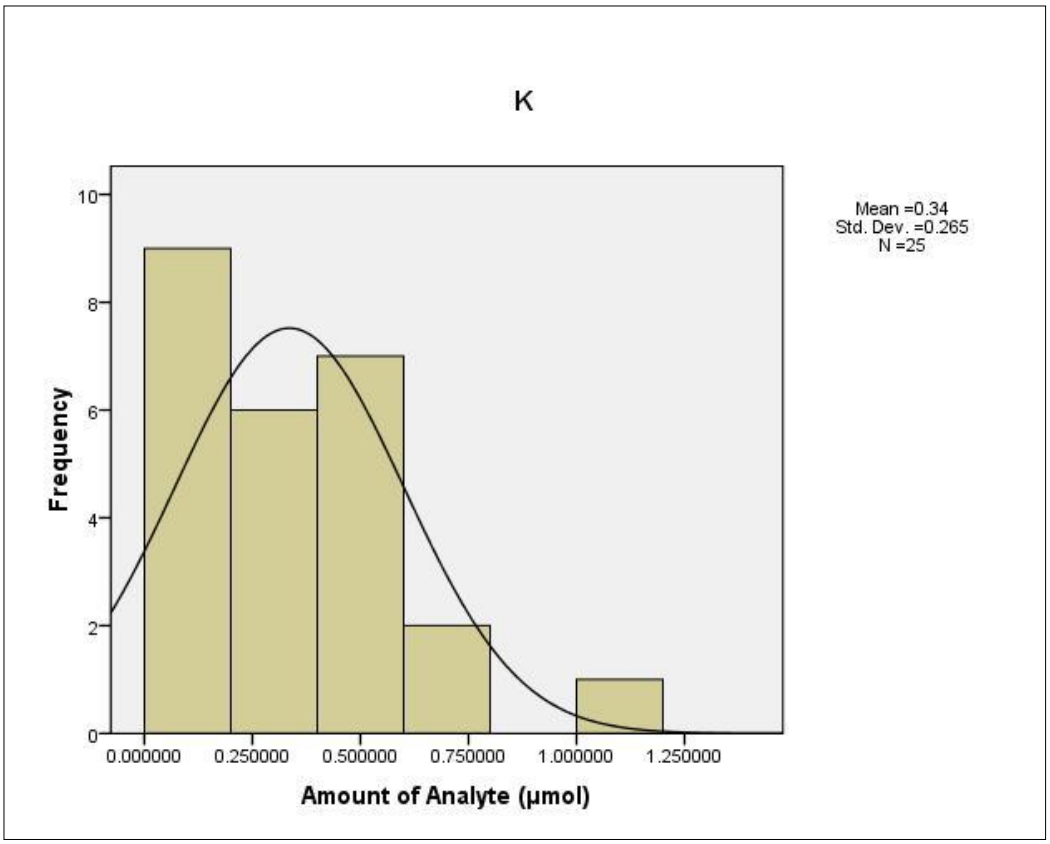
K
Mean =0.34
Std. Dev. =0.265
N =25
Frequency
0
2
4
6
8
10
0.000000
0.250000
0.500000
0.750000
1.000000
1.250000
Amount of Analyte (µmol)

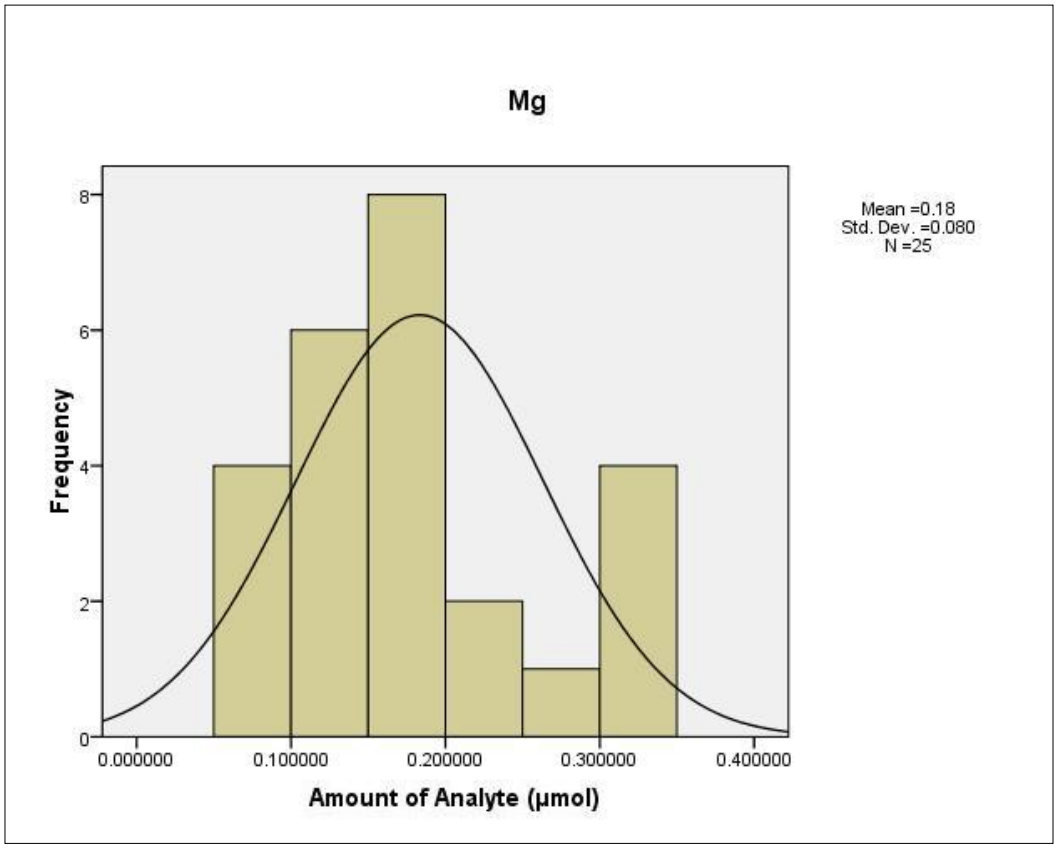
Mg
Mean =0.18
Std. Dev. =0.080
N =25
Frequency
0
2
4
6
8
0.000000
0.100000
0.200000
0.300000
0.400000
Amount of Analyte (µmol)

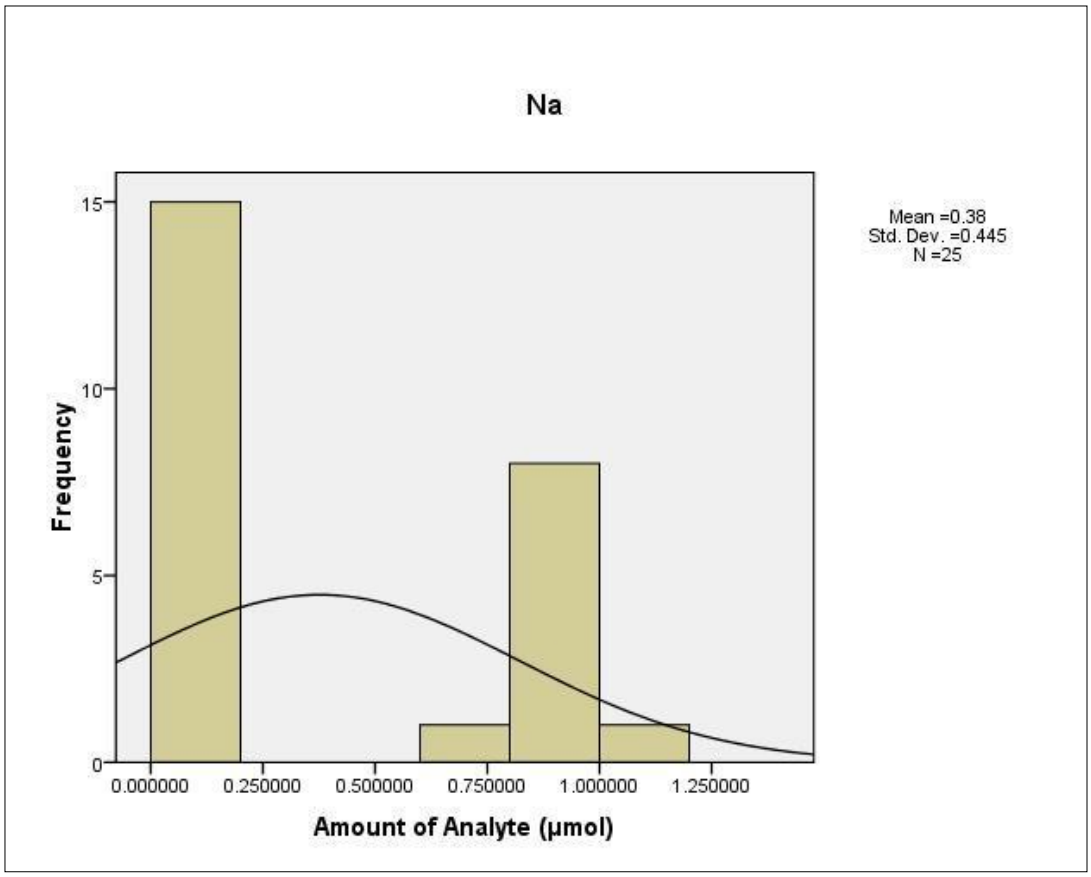
Na
Mean =0.38
Std. Dev. =0.445
N =25
Frequency
15
10
5
0
0.000000
0.250000
0.500000
0.750000
1.000000
1.250000
Amount of Analyte (µmol)

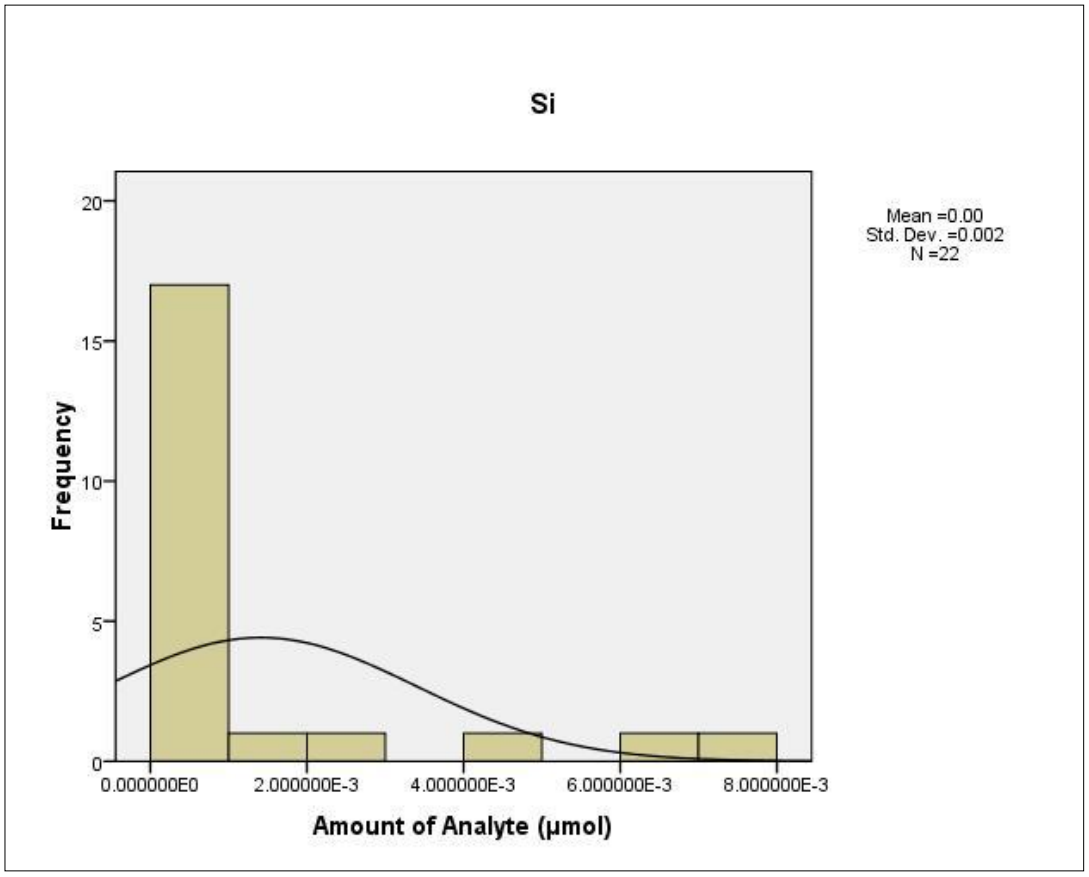
Si
Mean =0.00
Std. Dev. =0.002
N =22
Frequency
20
15
10
5
0
0.000000E0
2.000000E-3
4.000000E-3
6.000000E-3
8.000000E-3
Amount of Analyte (µmol)

ii.vii – Na in Granite Aggregated Dataset – Frequency Distribution Analysis

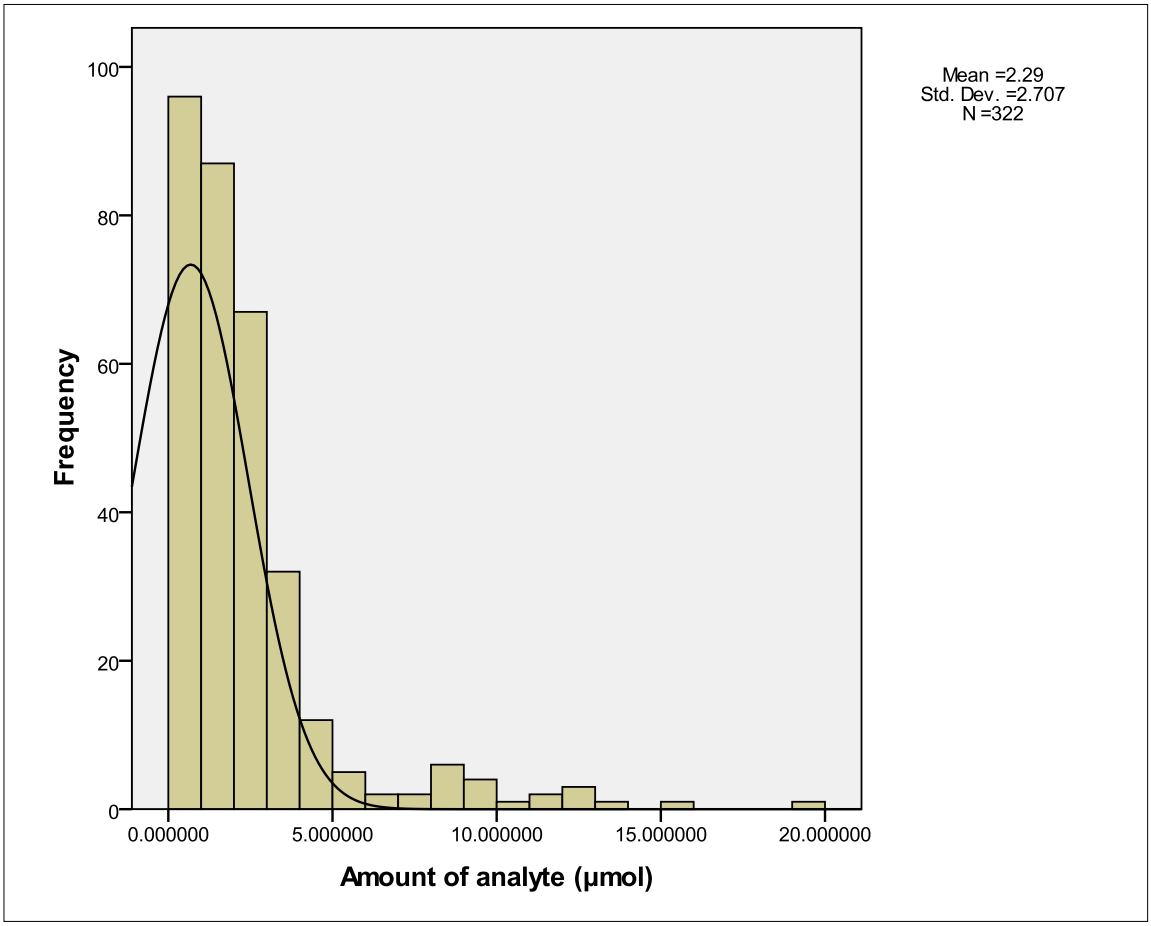

Appendix iii – Graphs of Data from Individual Experiments

iii.i Granite Experiments

Below are weathering data (normalised to abiotic weathering) for the individual granite experiments that are not presented in the main body of the text.

iii.i.i 30/4/08 Granite Experiment

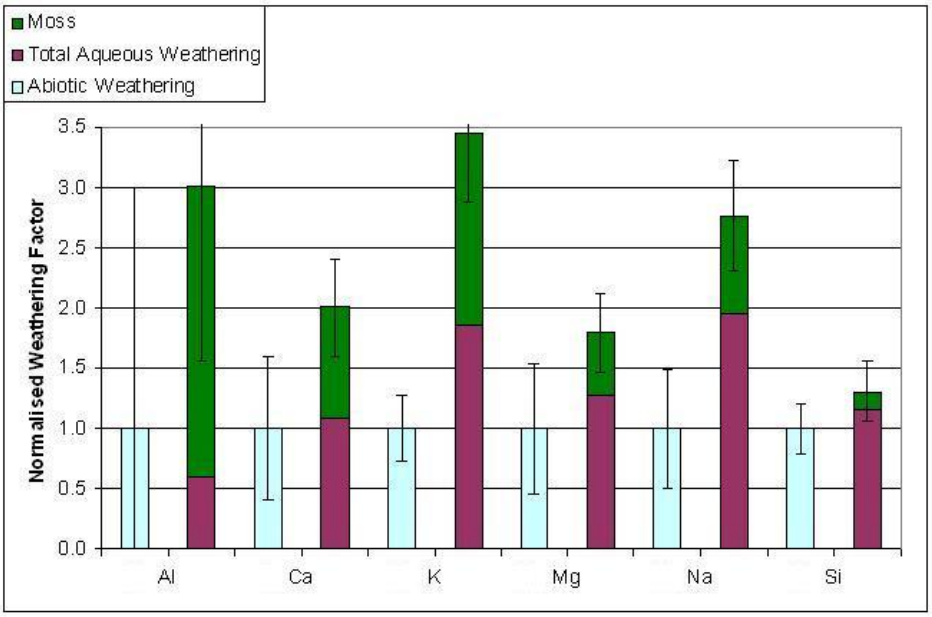

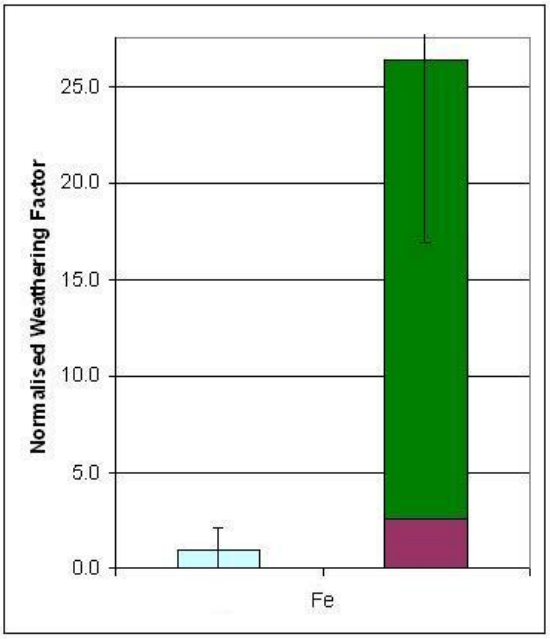

iii.i.ii 2/9/08 Granite Experiment

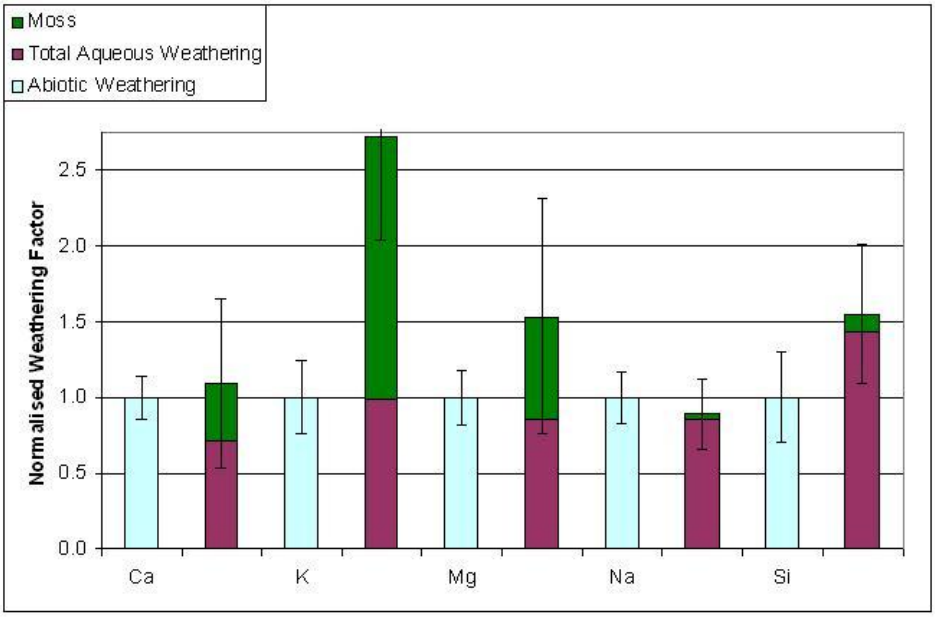

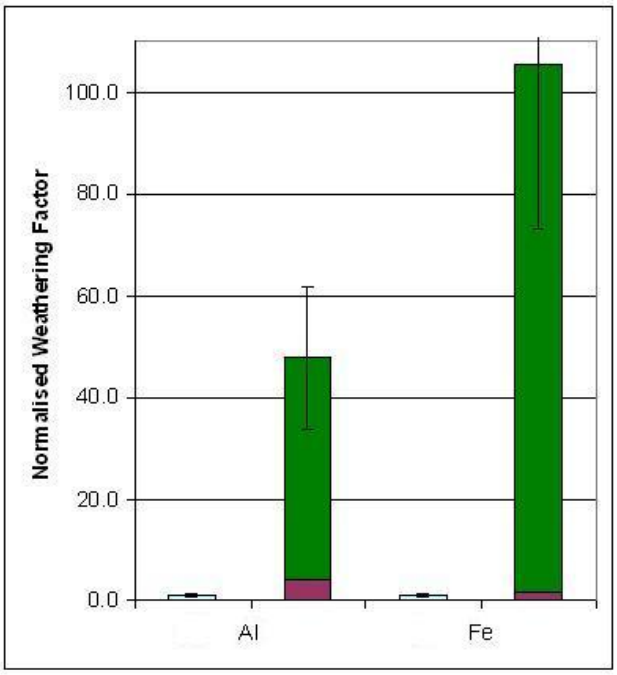

iii.i.iii 19/12/08 Granite Experiment

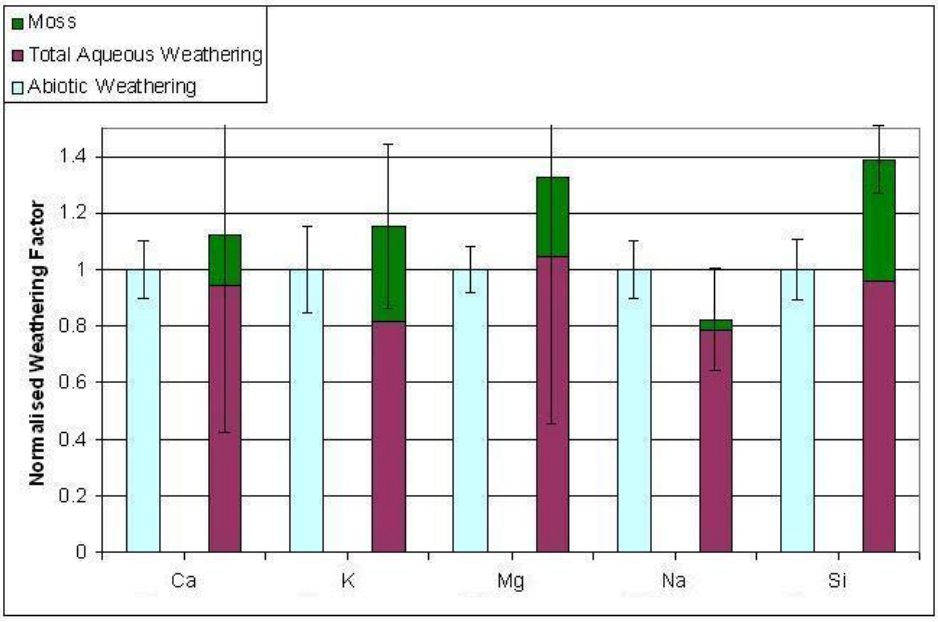

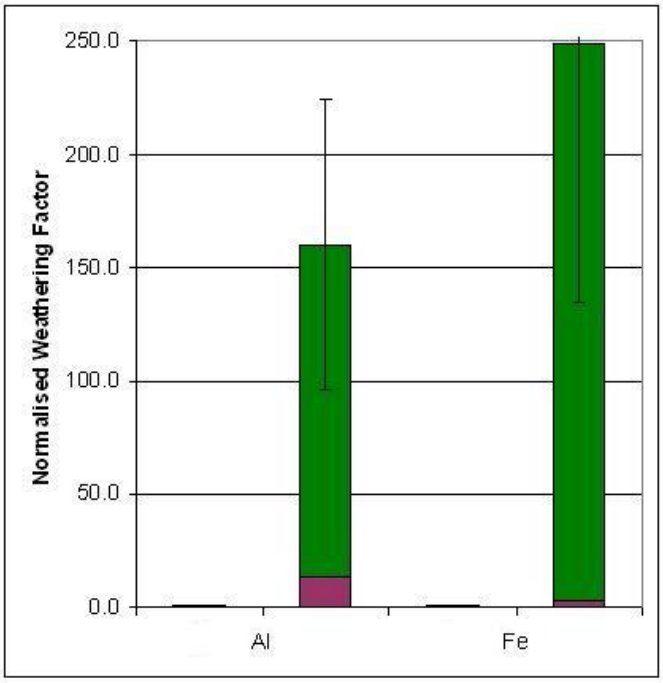

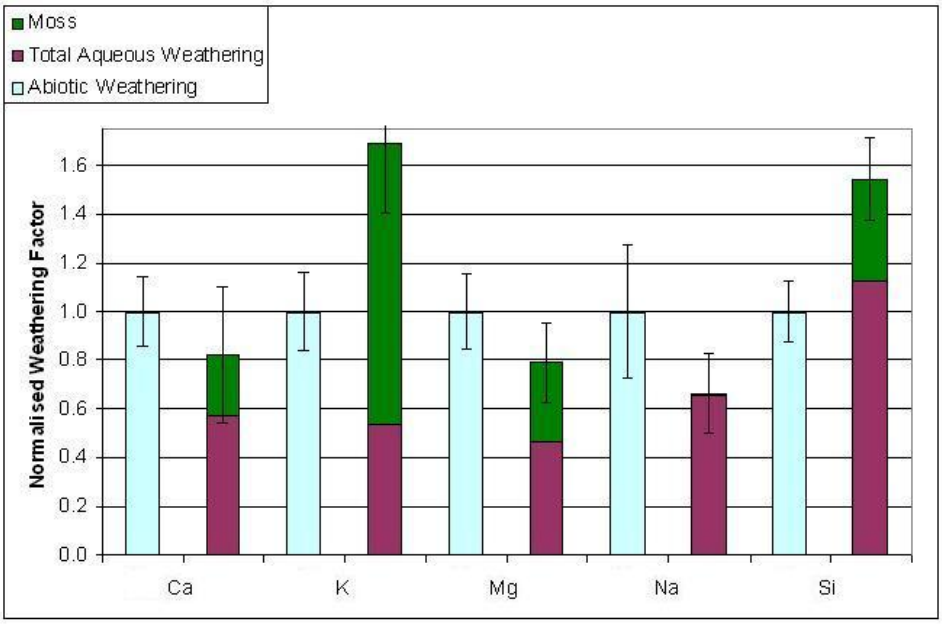
Moss
Total Aqueous Weathering
Abiotic Weathering
Normalised Weathering Factor
0.0
0.2
0.4
0.6
0.8
1.0
1.2
1.4
1.6
Ca
K
Mg
Na
Si

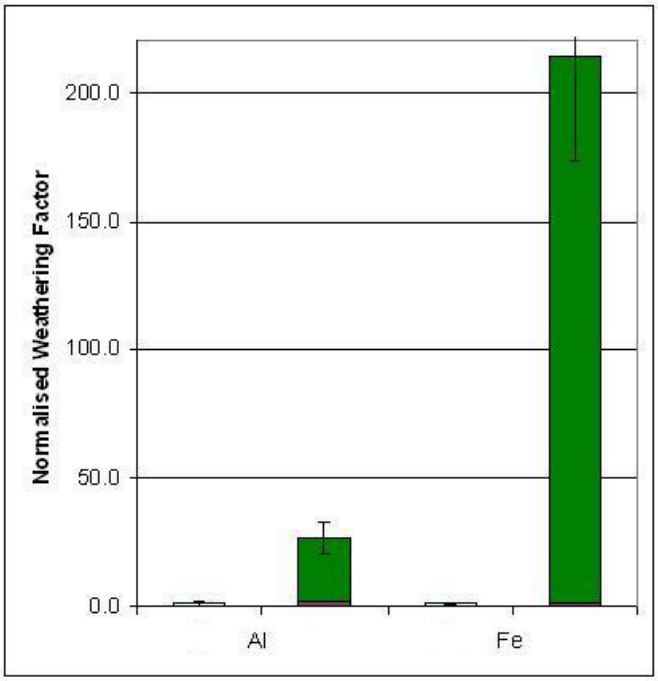
Normalised Weathering Factor
0.0
50.0
100.0
150.0
200.0
Al
Fe

iii.i.v 30/4/08 Granite Experiment – NAA Data

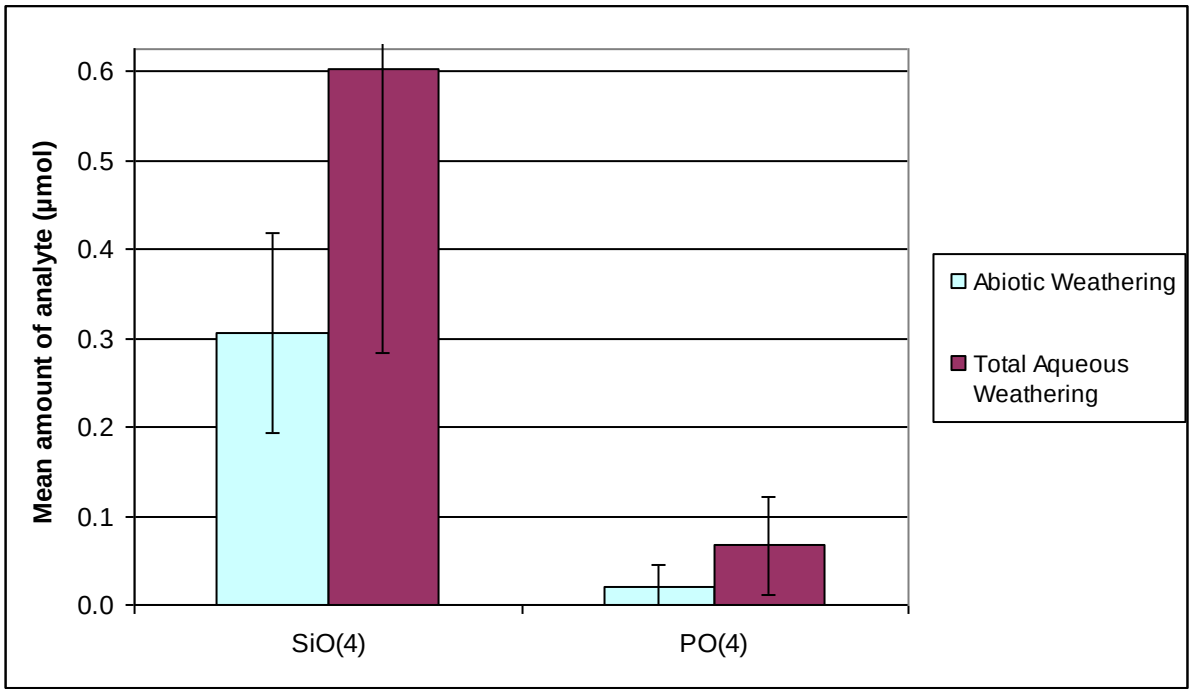

iii.i.vi 24/6/08 Granite Experiment – NAA Data

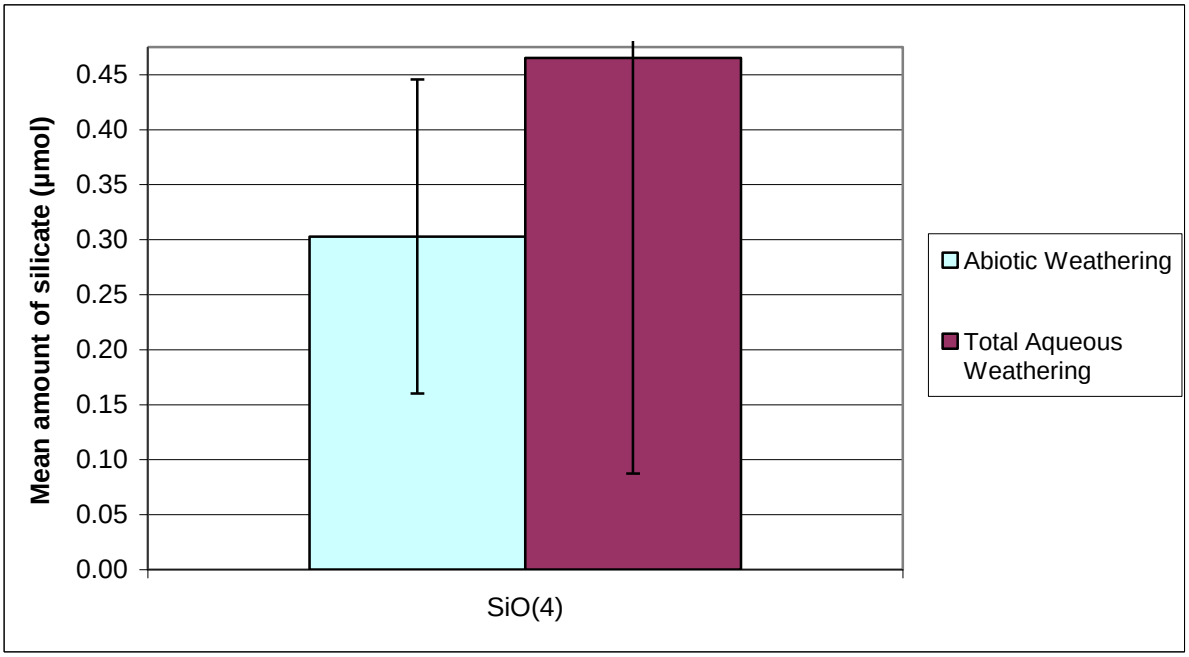

NB No phosphate was detectable in either the control microcosm aqueous fractions or the mossed microcosm aqueous fractions.

iii.i.vii 2/9/08 Granite Experiment – NAA Data

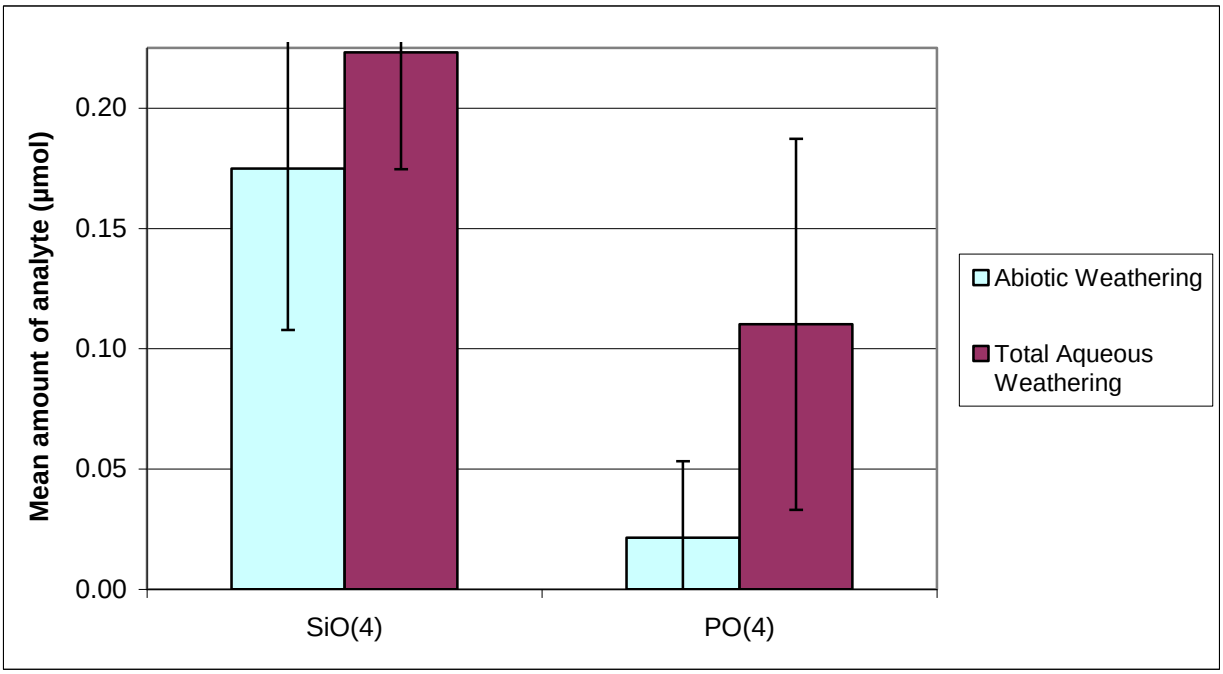

iii.ii 28/11/08 Andesite Experiment

The only andesite experiment that is not presented in the main body of the text is the 28/11/08 experiment. The weathering data (normalised to abiotic weathering) are presented below:-

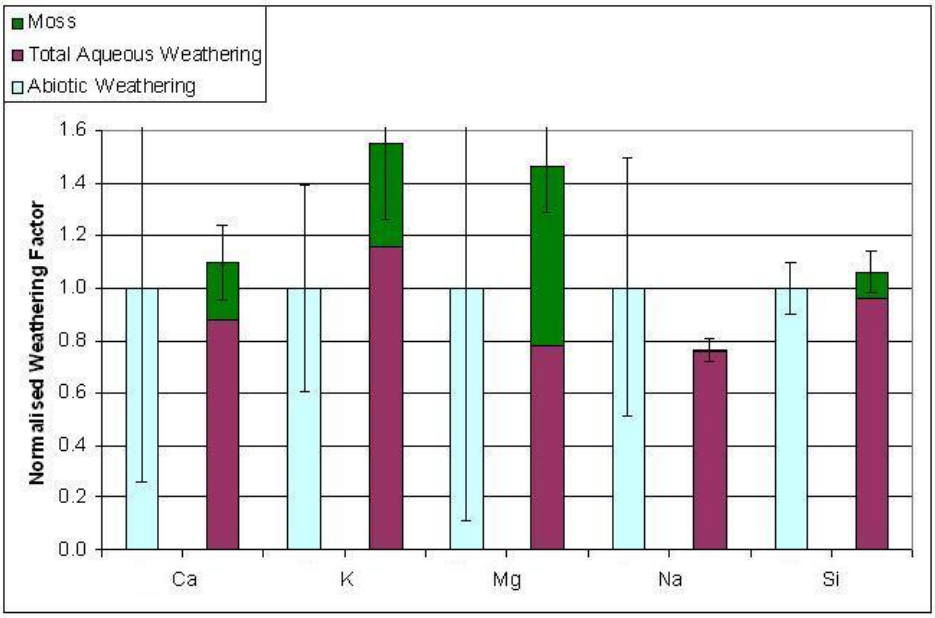

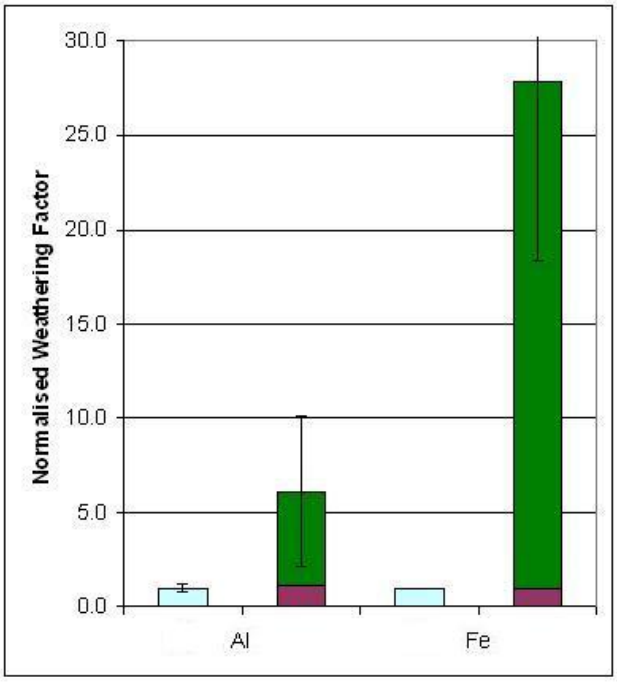

iii.iii Vermiculite experiments

Only the aggregated weathering data for vermiculite is presented in the main body of this thesis. Both the 14/2/08 and 17/2/09 individual experimental datasets are presented in graphical format below (normalised to abiotic weathering):-

iii.iii.i 14/2/08 Vermiculite Data

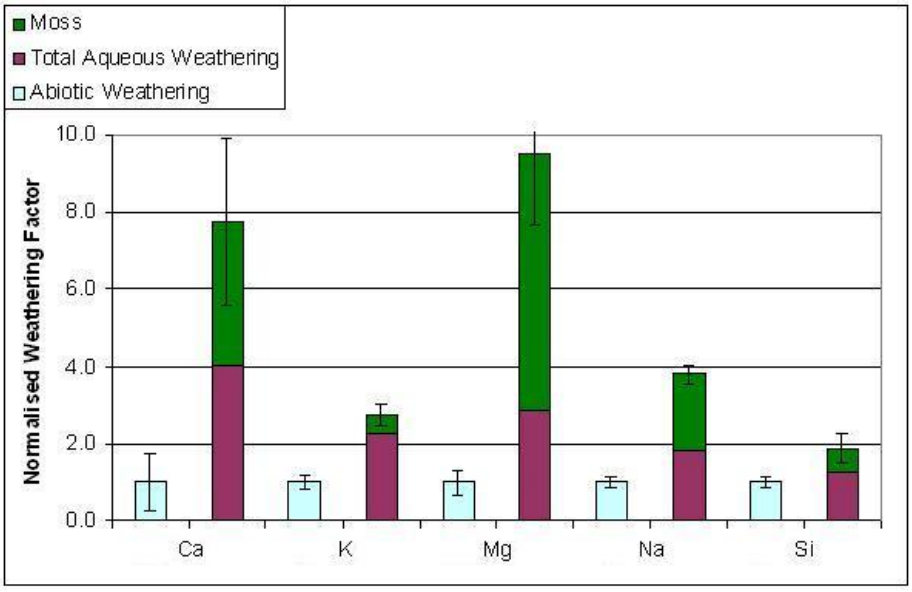

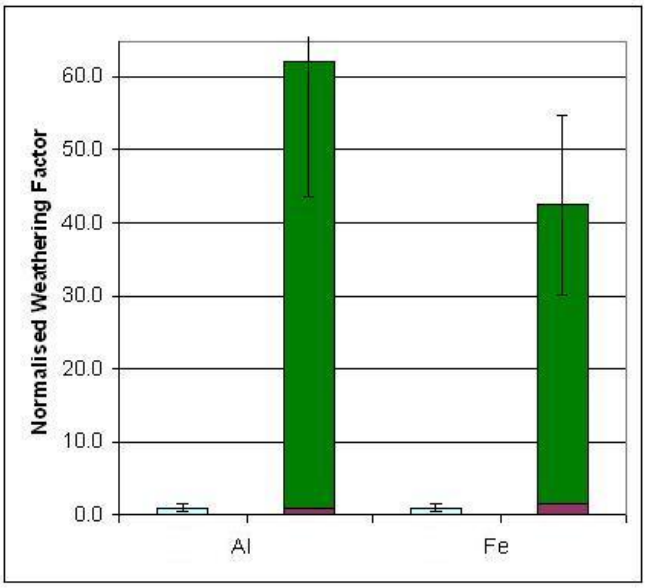

iii.iii.ii 17/2/09 Vermiculite Data

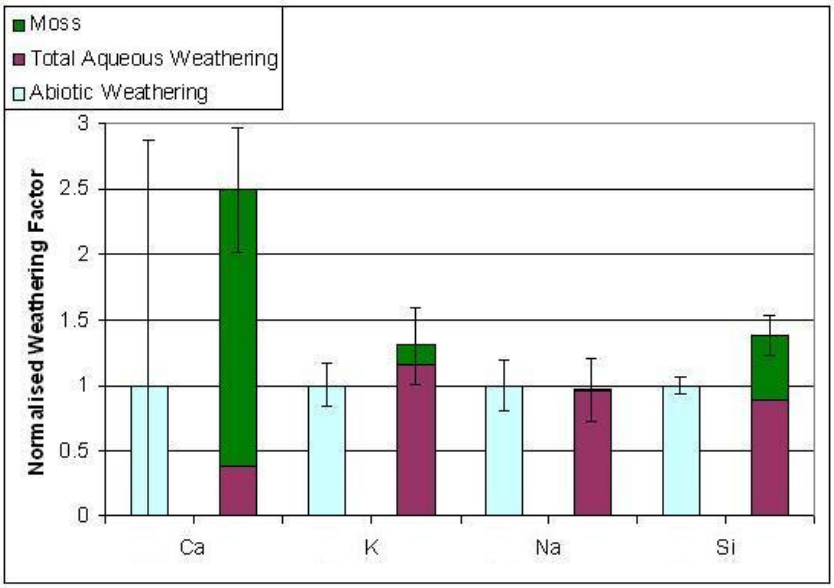

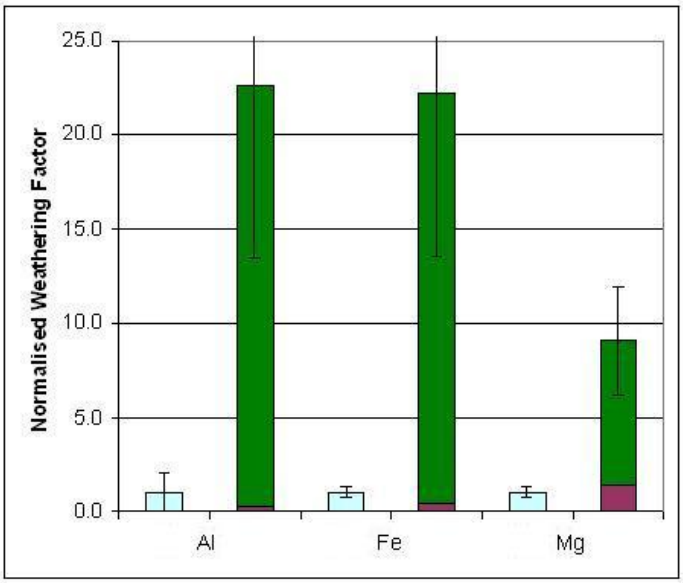

iii.iv 24/6/08 Chlorite experiment

The ICP data for the 24/6/08 chlorite is presented in the main body of the text. The statistically insignificant NAA data are presented below:-

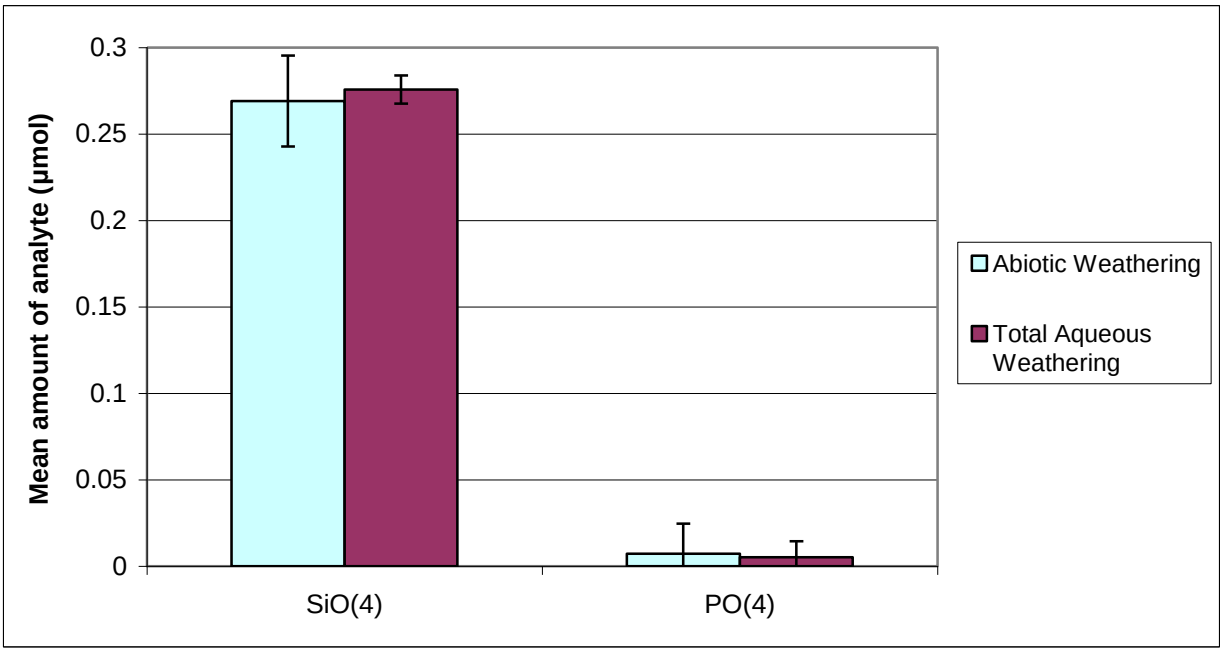

Appendix iv – Data

iv.i Mann-Whitney U Test

Below are presented the SPSS outputs for the Mann-Whitney U test. 'Asymp. Sig. (2-tailed)' is the P value for the test to three decimal places.

iv.i.i Granite Aggregated Data

Granite – Wa vs. Wtot

	Al	Ca	Fe	K	Mg	Na	Si
Mann-Whitney U	63.000	1497.000	3.000	403.000	1295.000	1764.000	1279.000
Wilcoxon W	3066.000	4500.000	3006.000	3406.000	4298.000	3475.000	4282.000
Z	-9.646	-3.272	-10.308	-8.135	-4.169	-2.085	-4.240
Asymp. Sig. (2-tailed)	.000	.001	.000	.000	.000	.037	.000

Granite – Wa vs. Wb

	Al	Ca	Fe	K	Mg	Na	Si	SiO4	PO4
Mann-Whitney U	1609.000	1409.000	2161.000	2129.000	1495.500	2032.000	2436.500	439.000	319.000
Wilcoxon W	4612.000	4037.000	5164.000	4757.000	4123.500	4660.000	5439.500	1000.000	880.000
Z	-4.418	-5.178	-2.728	-2.443	-4.849	-2.811	-1.274	-.976	-3.098
Asymp. Sig. (2-tailed)	.000	.000	.006	.015	.000	.005	.203	.329	.002

iv.i.ii Andesite Aggregated Data

Andesite – Wa vs. Wtot

	Al	Ca	Fe	K	Mg	Na	Si
Mann-Whitney U	19.000	205.000	.000	296.000	102.000	704.000	130.000
Wilcoxon W	722.000	908.000	703.000	999.000	805.000	1607.000	833.000
Z	-7.447	-5.620	-7.863	-4.726	-6.632	-.717	-6.357
Asymp. Sig. (2-tailed)	.000	.000	.000	.000	.000	.473	.000

Andesite – Wa vs. Wb

	Al	Ca	Fe	K	Mg	Na	Si
Mann-Whitney U	654.500	557.000	640.500	734.000	755.000	628.000	482.000
Wilcoxon W	1515.500	1260.000	1343.500	1595.000	1458.000	1489.000	1343.000
Z	-1.041	-2.016	-1.546	-.245	-.035	-1.306	-2.767
Asymp. Sig. (2-tailed)	.298	.044	.122	.806	.972	.192	.006

iv.i.iii Vermiculite Aggregated Data

Vermiculite – Wa vs. Wtot

	Al	Ca	Fe	K	Mg	Na	Si
Mann-Whitney U	5.000	47.000	6.000	139.000	2.000	185.000	269.000
Wilcoxon W	671.000	713.000	672.000	805.000	668.000	851.000	935.000
Z	-7.294	-6.906	-7.287	-5.815	-7.326	-5.307	-4.380
Asymp. Sig. (2-tailed)	.000	.000	.000	.000	.000	.000	.000

Vermiculite – Wa vs. Wb

	Al	Ca	Fe	K	Mg	Na	Si	SiO4	PO4
Mann-Whitney U	456.000	441.000	614.000	256.000	344.000	402.000	652.000	163.500	.000
Wilcoxon W	1197.000	1107.000	1355.000	922.000	1010.000	1068.000	1318.000	316.500	190.000
Z	-2.469	-2.730	-.758	-4.629	-3.677	-3.050	-.346	-.198	-5.633
Asymp. Sig. (2-tailed)	.014	.006	.448	.000	.000	.002	.729	.843	.000
Exact Sig. [2*(1-tailed Sig.)]								.845[a]	.000[a]

a. Not corrected for ties.

iv.ii T-test for Independent Samples

Where the Mann Whitney U test gave a result that appeared anomalous, that result was checked using the t-test for Independent Samples. The SPSS outputs for the two instances when this test was used are given below (NB outputs are edited to give key detail only):-

Granite Wa vs. Wtot

		t-test for Equality of Means				
		t	df	Sig. (2-tailed)	Mean Difference	Std. Error Difference
Na	Equal variances assumed	-1.422	133	.157	-.758507812	.533404800
	Equal variances not assumed	-1.295	74.933	.199	-.758507812	.585498230

Granite Wa vs. Wb

		t-test for Equality of Means				
		t	df	Sig. (2-tailed)	Mean Difference	Std. Error Difference
SiO4	Equal variances assumed	-2.077	62	.042	-.135357	.065174
	Equal variances not assumed	-2.037	43.008	.048	-.135357	.066455
PO4	Equal variances assumed	-2.807	62	.007	-.058035	.020675
	Equal variances not assumed	-2.738	36.885	.009	-.058035	.021194

Vermiculite Wa vs. Wb

		t-test for Equality of Means				
		t	df	Sig. (2-tailed)	Mean Difference	Std. Error Difference
SiO4	Equal variances assumed	-.360	35	.721	-.016765	.046618
	Equal variances not assumed	-.357	32.639	.724	-.016765	.047018
PO4	Equal variances assumed	-7.405	36	.000	-.531579	.071783
	Equal variances not assumed	-7.405	18.000	.000	-.531579	.071783

iv.iii XRF Data: Petrologies of Substrates

	Amount of analyte (µmol g-1)									
	Mg	**Al**	**Si**	**P**	**Ca**	**Ti**	**Mn**	**K**	**Fe**	**Na**
unwashed granite-1	43.1	1241.7	4916.8	14.4	56.4	11.2	2.5	454.3	88.2	404.2
unwashed granite-2	43.6	1295.1	4808.7	13.8	59.1	11.8	2.3	487.0	85.5	419.5
unwashed granite-3	42.5	1278.6	4750.5	13.8	59.0	11.7	2.3	479.2	86.9	414.9
washed granite-1	42.0	1271.3	4747.6	13.6	58.3	11.6	2.3	479.5	84.9	415.2
washed granite-2	46.9	1257.3	4761.6	14.2	65.2	14.6	2.8	433.5	101.7	466.9
unwashed andesite-1	324.0	1244.5	4073.0	14.8	357.6	36.9	7.7	189.6	312.9	554.6
unwashed andesite-2	323.2	1243.9	4078.3	14.8	355.9	36.8	7.7	188.3	316.3	532.9
washed andesite-1	300.1	1233.5	4108.1	15.2	311.3	36.9	6.4	182.7	295.1	548.5
washed andesite-2	306.1	1263.1	4189.2	15.9	318.8	37.6	7.1	188.5	303.8	559.5
chlorite-1	31.6	1179.4	4596.3	18.0	92.4	13.4	7.0	356.3	184.9	472.5
chlorite-2	33.4	1201.3	4681.1	18.4	94.5	13.8	6.9	362.7	183.8	493.4
unwashed vermic.-1	2627.0	858.2	2943.1	6.9	39.6	62.8	3.8	544.6	484.6	35.8
unwashed vermic.-2	2629.6	861.5	2946.2	6.9	39.6	63.4	3.8	544.6	487.7	14.3
washed vermic.-1	1248.2	412.5	1413.1	2.3	14.7	31.5	1.7	269.7	247.4	267.5
washed vermic.-2	2661.0	867.5	2939.0	4.4	26.5	62.1	3.8	540.8	479.9	24.7

iv.iv Data Summaries

Summaries are presented of the key experimental data below. See §1.9 p33 for a description of the data labels.

iv.iv.i Granite Aggregated Data

Below are summaries of the granite aggregated dataset formed using population means ($\bar{\mu}$) formed from the 30/4/08, 24/6/08, 2/9/08, 19/12/08, 12/1/09 and 30/7/09 experiments:-

	Al	Ca	Fe	K	Mg	Na	Si	SiO(4)	PO(4)
Wa	0.01159	1.66429	0.00211	0.66892	0.42707	2.90788	0.34608	0.26100	0.01365
Wa st error	0.02558	0.17155	0.00166	0.03051	0.04653	0.44054	0.07232	0.01810	0.01104
Wb	0.01324	1.25229	0.00489	0.65776	0.34416	3.12012	0.43524	0.43042	0.05893
Wb st error	0.00548	0.37423	0.00258	0.09635	0.12435	0.34917	0.11106	0.07646	0.02841
Wmoss	0.17733	1.16711	0.23239	1.08393	0.31168	0.68583	0.11883		
Wmoss st error	0.01182	0.07823	0.01516	0.07211	0.01123	0.06719	0.00814		
Wtot	0.19063	2.42063	0.23728	1.73905	0.65674	3.78800	0.55057		
Wtot st error	0.00964	0.32049	0.01510	0.09119	0.11185	0.35467	0.11454		
Wnetbio	0.17904	0.75634	0.23517	1.07013	0.22967	0.88012	0.20449		

Data normalised to Wa

	Al	Ca	Fe	K	Mg	Na	Si	SiO(4)	PO(4)
Wa	1	1	1	1	1	1	1	1	1
Wa st error	2.20745	0.10308	0.78953	0.04562	0.10895	0.15150	0.20896	0.06934	0.80846
Wb	1.14220	0.75244	2.31761	0.98331	0.80587	1.07299	1.25762	1.64912	4.31648
Wb st error	0.47269	0.22486	1.22557	0.14404	0.29118	0.12008	0.32092	0.29296	2.08114
Wmoss	15.30153	0.70126	110.23765	1.62040	0.72982	0.23585	0.34335		
Wmoss st error	1.02007	0.04701	7.19317	0.10779	0.02629	0.02311	0.02352		
Wtot (Ψ)	16.44904	1.45445	112.55797	2.59978	1.53779	1.30267	1.59085		
Wtot st error	0.83150	0.19257	7.16401	0.13632	0.26191	0.12197	0.33095		
Wnetbio	15.44904	0.45445	111.55797	1.59978	0.53779	0.30267	0.59085		

iv.iv.ii Andesite Aggregated Data

Below are summaries of the andesite aggregated dataset formed using population means ($\bar{\mu}$) of the data from the 28/11/08, 2/12/08 and 25/1/09 experiments:-

	Al	Ca	Fe	K	Mg	Na	Si
Wa	0.00631	1.35620	0.00066	0.56301	0.11933	5.29233	0.14772
Wa st error	0.00092	0.22096	0.00000	0.03722	0.02860	0.51847	0.00656
Wb	0.00554	1.79834	0.00088	0.72011	0.14360	4.49034	0.13725
Wb st error	0.00029	0.15417	0.00021	0.02856	0.01251	0.37599	0.00100
Wmoss	0.24763	3.92502	0.21555	0.29864	0.53853	0.32773	0.11994
Wmoss st error	0.10443	1.96780	0.09314	0.13172	0.18872	0.41129	0.03691
Wtot	0.25509	5.59055	0.21843	1.01875	0.68404	4.81260	0.25674
Wtot st error	0.08678	1.78801	0.08081	0.14836	0.16549	0.28316	0.03317
Wnetbio	0.24353	4.23711	0.21306	0.45800	0.55234	-0.52964	0.10537

Data normalised to Wa

	Al	Ca	Fe	K	Mg	Na	Si
Wa	1	1	1	1	1	1	1
Wa st error	0.14631	0.16292	0.00000	0.06611	0.23971	0.09797	0.04441
Wb	0.87753	1.32601	1.33505	1.27904	1.20341	0.84846	0.92915
Wb st error	0.04524	0.11368	0.32082	0.05073	0.10482	0.07104	0.00676
Wmoss	39.22408	2.89413	326.28832	0.53043	4.51298	0.06192	0.81198
Wmoss st error	16.54217	1.45097	140.98552	0.23396	1.58149	0.07771	0.24984
Wtot (Ψ)	40.40679	4.12221	330.65068	1.80947	5.73244	0.90936	1.73802
Wtot st error	13.74579	1.31839	122.32354	0.26351	1.38685	0.05350	0.22454
Wnetbio	38.57553	3.12425	322.51473	0.81349	4.62875	-0.10008	0.71333

iv.iv.iii Vermiculite Aggregated Data

Below are summaries of the vermiculite aggregated dataset formed using population means ($\bar{\mu}$) formed from the 14/2/08 and 17/2/09 experiments:-

	Al	**Ca**	**Fe**	**K**	**Mg**	**Na**	**Si**
Wa	0.01091	0.07510	0.01068	1.29317	0.23883	2.85130	0.60873
Wa 95% conf.	0.00778	0.10409	0.00295	0.19934	0.04594	0.52320	0.05529
Wb	0.00524	0.09247	0.00902	2.05233	0.51200	3.58357	0.66645
Wb 95% conf.	0.00265	0.04140	0.00274	0.24759	0.12552	0.48026	0.08609
Wmoss	0.38175	0.18637	0.30044	0.37382	1.70899	1.96408	0.34345
Wmoss 95% conf.	0.09013	0.02765	0.07255	0.06899	0.39645	0.61704	0.09419
Wtot	0.38699	0.27883	0.30946	2.42616	2.22100	5.54766	1.00989
Wtot 95% conf.	0.09006	0.04534	0.07254	0.26067	0.38120	0.69968	0.15063
Wnetbio	0.37608	0.20374	0.29878	1.13299	1.98217	2.69636	0.40116

Data normalised to Wa

	Al	**Ca**	**Fe**	**K**	**Mg**	**Na**	**Si**
Wa	1	1	1	1	1	1	1
Wa 95% conf.	0.71304	1.38611	0.27624	0.15415	0.19237	0.18350	0.09083
Wb	0.48076	1.23129	0.84473	1.58706	2.14381	1.25682	1.09481
Wb 95% conf.	0.24288	0.55133	0.25652	0.19146	0.52555	0.16844	0.14142
Wmoss	35.00437	2.48168	28.13145	0.28908	7.15572	0.68884	0.56420
Wmoss 95% conf.	8.26490	0.36820	6.79295	0.05335	1.65999	0.21641	0.15472
Wtot (Ψ)	35.48513	3.71297	28.97618	1.87614	9.29953	1.94566	1.65900
Wtot 95% conf.	8.25810	0.60372	6.79250	0.20158	1.59610	0.24539	0.24745
Wnet_bio	34.48513	2.71297	27.97618	0.87614	8.29953	0.94566	0.65900

iv.iv.iv 24/6/08 Chlorite Data

Below are summaries of the data from the 24/6/08 chlorite experiment (data are simple arithmetic means ($\bar{x}$)):-

	Al	Ca	Fe	K	Mg	Na	Si	SiO(4)	PO(4)
Wa	0.02099	1.94595	0.00465	0.55352	0.20858	5.09488	0.13684	0.26905	0.00714
Wa 95% conf.	0.01065	0.31210	0.00214	0.07974	0.01936	2.48086	0.01867	0.02636	0.01748
Wb	0.00890	1.08211	0.00603	0.24067	0.09248	2.34413	0.13333	0.27569	0.00525
Wb 95% conf.	0.00281	0.17138	0.00670	0.03401	0.01128	1.56304	0.01983	0.00812	0.00918
Wmoss	0.08225	3.02756	0.17227	3.36380	0.41794	4.34899	0.01728		
Wmoss (95% conf.)	0.01975	0.24788	0.04281	0.21208	0.07607	0.76200	0.01500		
Wtot	0.09115	4.10967	0.17830	3.60447	0.51042	6.69312	0.15061		
Wtot 95% conf.	0.01957	0.24746	0.04335	0.22430	0.07257	1.23076	0.03325		
Wnetbio	0.07016	2.16372	0.17365	3.05095	0.30184	1.59824	0.01377		

Data normalised to Wa

	Al	Ca	Fe	K	Mg	Na	Si	SiO(4)	PO(4)
Wa	1	1	1	1	1	1	1	1	1
Wa 95% conf.	0.50773	0.16038	0.45991	0.14406	0.09281	0.48693	0.13643	0.09798	2.44691
Wb	0.42403	0.55608	1.29736	0.43480	0.44340	0.46010	0.97432	1.02467	0.73502
Wb 95% conf.	0.13368	0.08807	1.43948	0.06145	0.05408	0.30679	0.14491	0.03019	1.28468
Wmoss	3.91925	1.55583	37.03268	6.07715	2.00371	0.85360	0.12627		
Wmoss 95% conf.	0.94135	0.12738	9.20324	0.38316	0.36470	0.14956	0.10964		
Wtot (Ψ)	4.34329	2.11191	38.33004	6.51195	2.44711	1.31369	1.10059		
Wtot 95% conf.	4.34329	2.11191	38.33004	6.51195	2.44711	1.31369	1.10059		
Wnetbio	0.93275	0.12716	9.31879	0.40523	0.34793	0.24157	0.24301		

iv.iv.v 30/7/09 Inoculum Only Experiments

Below are summaries of the data from the 30/7/09 inoculum only experiments (data are simple arithmetic means ($\bar{x}$)):-

Bare (No Substrate)

	Al	**Ca**	**Fe**	**K**	**Mg**	**Na**	**Si**
Wb	0.00957	0.08514	0.00072	0.00741	0.00484	1.80958	0.00251
Wb 95% conf.	0.00815	0.11371	0.00012	0.00000	0.00572	0.40379	0.00000
Wmoss	0.00482	0.26452	0.02141	0.23377	0.08575	0.01798	0.00137
Wmoss 95% conf.	0.00379	0.00000	0.00521	0.03852	0.00000	0.00370	0.00034
Wtot	0.01440	0.34966	0.02213	0.24118	0.09059	1.82757	0.00389
Wtot 95% conf.	0.00860	0.11371	0.00519	0.03852	0.00572	0.40441	0.00034

With Substrate (Granite)

	Al	**Ca**	**Fe**	**K**	**Mg**	**Na**	**Si**
Wa	0.00568	2.20679	0.00071	0.69585	0.54881	4.03563	0.28184
Wa 95% conf.	0.00651	0.31431	0.00010	0.11024	0.08548	1.10540	0.03522
Wb	0.01119	1.26556	0.00081	0.37520	0.25393	2.65129	0.31591
Wb 95% conf.	0.01862	0.53473	0.00033	0.14191	0.05867	0.64059	0.04336
Wmoss	0.14157	0.55193	0.15029	0.80065	0.18005	0.03553	0.11877
Wtot	0.15276	1.81749	0.15110	1.17585	0.43398	2.68682	0.43467
Wtot 95% conf.	0.03467	0.61370	0.02870	0.19633	0.08888	0.65455	0.04757
Wnetbio	-0.14708	-0.38930	0.15039	0.48000	-0.11482	-1.34881	0.15284

Summary

	Al	Ca	Fe	K	Mg	Na	Si
Bare total	0.01440	0.34966	0.02213	0.24118	0.09059	1.82757	0.00389
Granite total	0.15276	1.81749	0.15110	1.17585	0.43398	2.68682	0.43467
Bare 95% conf.	0.00860	0.11371	0.00519	0.03852	0.00572	0.40441	0.00034
Granite 95% conf.	0.03467	0.61370	0.02870	0.19633	0.08888	0.65455	0.04757

Summary normalised to Wa

	Al	Ca	Fe	K	Mg	Na	Si
Bare total	1	1	1	1	1	1	1
Granite total	10.61182	5.19790	6.82848	4.87541	4.79068	1.47016	111.84931
Bare 95% conf.	0.59711	0.32519	0.23451	0.15972	0.06319	0.22128	0.08795
Granite 95% conf.	2.40863	1.75513	1.29691	0.81405	0.98118	0.35815	12.24084

iv.v Amounts of NAA analytes in Aqueous Microcosm Components

Below is a table showing the amounts of silicate (SiO_4^{4-}) and phosphate (PO_4^{3-}) in the aqueous microcosm components (corrected for filtrate blanks) analysed using the NAA. No correction was needed for upH_2O as there was no measurable SiO_4^{4-} or PO_4^{3-} contamination in upH_2O. NB a blank cell means that there is no successful analysis for that analyte due to an instrumental problem.

						Amount of	
						analyte	
	Tube		**Cosm.**			(µmol)	
Round	**No**	**Date**	**No**	**Subs.**	**Treat.**	**SiO(4)**	**PO(4)**
3	77	14/02/2008	11	Vermic.	Control	0.09	0.00
3	78	14/02/2008	12	Vermic.	Control	0.16	0.00
3	79	14/02/2008	13	Vermic.	Control	0.25	0.00
3	80	14/02/2008	14	Vermic.	Control	0.37	0.00
3	81	14/02/2008	15	Vermic.	Control	0.43	0.00
3	82	14/02/2008	16	Vermic.	Control	0.24	0.00
3	83	14/02/2008	17	Vermic.	Control		0.00
3	84	14/02/2008	18	Vermic.	Control	0.38	0.00
3	85	14/02/2008	19	Vermic.	Control		0.00
3	86	14/02/2008	20	Vermic.	Control		0.00
3	97	14/02/2008	31	Vermic.	Control	0.48	0.00
3	98	14/02/2008	32	Vermic.	Control	0.49	0.00
3	99	14/02/2008	33	Vermic.	Control	0.49	0.00
3	100	14/02/2008	34	Vermic.	Control	0.53	0.00
3	101	14/02/2008	35	Vermic.	Control	0.52	0.00
3	102	14/02/2008	36	Vermic.	Control	0.59	0.00
3	103	14/02/2008	37	Vermic.	Control	0.55	0.00
3	104	14/02/2008	38	Vermic.	Control	0.57	0.00
3	105	14/02/2008	39	Vermic.	Control	0.46	0.00
3	106	14/02/2008	40	Vermic.	Control	0.51	
3	67	14/02/2008	1	Vermic.	Mossed	0.65	0.97
3	68	14/02/2008	2	Vermic.	Mossed	0.22	
3	69	14/02/2008	3	Vermic.	Mossed	0.50	0.71
3	70	14/02/2008	4	Vermic.	Mossed	0.37	0.07
3	71	14/02/2008	5	Vermic.	Mossed	0.16	0.58
3	72	14/02/2008	6	Vermic.	Mossed	0.60	0.33
3	73	14/02/2008	7	Vermic.	Mossed	0.32	0.08
3	74	14/02/2008	8	Vermic.	Mossed	0.51	0.89
3	75	14/02/2008	9	Vermic.	Mossed	0.42	0.89
3	76	14/02/2008	10	Vermic.	Mossed	0.28	0.07
3	87	14/02/2008	21	Vermic.	Mossed	0.56	0.53
3	88	14/02/2008	22	Vermic.	Mossed	0.57	0.54
3	89	14/02/2008	23	Vermic.	Mossed	0.59	0.22
3	90	14/02/2008	24	Vermic.	Mossed	0.56	0.37
3	91	14/02/2008	25	Vermic.	Mossed	0.43	0.87
3	92	14/02/2008	26	Vermic.	Mossed	0.39	0.60
3	93	14/02/2008	27	Vermic.	Mossed	0.39	0.73
3	94	14/02/2008	28	Vermic.	Mossed	0.30	0.61
3	95	14/02/2008	29	Vermic.	Mossed	0.42	0.92

						Amount of	
						analyte	
	Tube		**Cosm.**			(µmol)	
Round	**No**	**Date**	**No**	**Subs.**	**Treat.**	**SiO(4)**	**PO(4)**
3	96	14/02/2008	30	Vermic.	Mossed	0.46	0.12
4	23	30/04/2008	1	Granite	Control	0.28	0.00
4	24	30/04/2008	4	Granite	Control	0.28	0.05
4	25	30/04/2008	7	Granite	Control	0.08	0.04
4	26	30/04/2008	8	Granite	Control	0.71	0.11
4	27	30/04/2008	10	Granite	Control	0.29	0.00
4	28	30/04/2008	11	Granite	Control	0.29	0.00
4	29	30/04/2008	13	Granite	Control	0.28	0.00
4	30	30/04/2008	14	Granite	Control	0.28	0.00
4	31	30/04/2008	17	Granite	Control	0.28	0.00
4	32	30/04/2008	19	Granite	Control	0.28	0.00
4	43	30/04/2008	2	Granite	Mossed	0.28	0.05
4	44	30/04/2008	3	Granite	Mossed	0.00	0.00
4	45	30/04/2008	5	Granite	Mossed	0.00	0.00
4	46	30/04/2008	6	Granite	Mossed	0.94	0.17
4	47	30/04/2008	9	Granite	Mossed	0.89	0.12
4	48	30/04/2008	12	Granite	Mossed	1.16	0.10
4	49	30/04/2008	15	Granite	Mossed	0.79	0.01
4	50	30/04/2008	16	Granite	Mossed	0.68	0.16
4	51	30/04/2008	18	Granite	Mossed	0.72	0.00
4	52	30/04/2008	20	Granite	Mossed	0.77	0.00
4	57	24/06/2008	13	Chlorite	Control	0.20	0.00
4	58	24/06/2008	14	Chlorite	Control	0.28	0.00
4	59	24/06/2008	15	Chlorite	Control	0.28	0.05
4	65	24/06/2008	21	Chlorite	Control	0.28	0.00
4	67	24/06/2008	23	Chlorite	Control	0.28	0.00
4	68	24/06/2008	24	Chlorite	Control	0.28	0.00
4	69	24/06/2008	25	Chlorite	Control	0.28	0.00
4	60	24/06/2008	16	Chlorite	Mossed	0.28	0.00
4	61	24/06/2008	17	Chlorite	Mossed	0.28	0.00
4	62	24/06/2008	18	Chlorite	Mossed	0.28	0.00
4	63	24/06/2008	19	Chlorite	Mossed	0.26	0.00
4	64	24/06/2008	20	Chlorite	Mossed	0.28	0.00
4	66	24/06/2008	22	Chlorite	Mossed	0.28	0.01
4	70	24/06/2008	26	Chlorite	Mossed	0.28	0.03
4	72	24/06/2008	28	Granite	Control	0.28	0.00
4	75	24/06/2008	31	Granite	Control	0.12	0.00
4	76	24/06/2008	32	Granite	Control	0.17	0.00
4	77	24/06/2008	33	Granite	Control	0.00	0.00
5	21	24/06/2008	35	Granite	Control	0.31	0.00
5	23	24/06/2008	37	Granite	Control	0.34	0.00
5	29	24/06/2008	44	Granite	Control	0.67	0.00
5	30	24/06/2008	47	Granite	Control	0.58	0.00
5	32	24/06/2008	49	Granite	Control	0.24	0.00
5	33	24/06/2008	50	Granite	Control	0.32	0.00
4	71	24/06/2008	27	Granite	Mossed	0.28	0.00
4	73	24/06/2008	29	Granite	Mossed	0.00	0.00

						Amount of	
						analyte	
	Tube		**Cosm.**			(µmol)	
Round	**No**	**Date**	**No**	**Subs.**	**Treat.**	**SiO(4)**	**PO(4)**
4	74	24/06/2008	30	Granite	Mossed	0.20	0.00
4	78	24/06/2008	34	Granite	Mossed	0.14	0.00
5	22	24/06/2008	36	Granite	Mossed	0.34	0.00
5	24	24/06/2008	38	Granite	Mossed	0.35	0.00
5	25	24/06/2008	39	Granite	Mossed	1.08	0.00
5	26	24/06/2008	40	Granite	Mossed	0.57	0.00
5	27	24/06/2008	42	Granite	Mossed	0.81	0.00
5	28	24/06/2008	43	Granite	Mossed	0.87	0.00
5	31	24/06/2008	48	Granite	Mossed	0.91	0.00
6	18	15/08/2008	2	Chlorite	Control	0.05	0.00
6	20	15/08/2008	4	Chlorite	Control	0.04	0.00
6	22	15/08/2008	6	Chlorite	Control	0.05	0.00
6	24	15/08/2008	8	Chlorite	Control	0.05	0.00
6	17	15/08/2008	1	Chlorite	Mossed	0.04	0.00
6	19	15/08/2008	3	Chlorite	Mossed	0.04	0.01
6	21	15/08/2008	5	Chlorite	Mossed	0.06	0.00
6	23	15/08/2008	7	Chlorite	Mossed	0.05	0.01
6	26	15/08/2008	10	Granite	Control	0.08	0.00
6	28	15/08/2008	12	Granite	Control	0.04	0.00
6	25	15/08/2008	9	Granite	Mossed	0.12	0.07
6	27	15/08/2008	11	Granite	Mossed	0.12	0.07
6	30	02/09/2008	2	Granite	Control	0.08	0.00
6	32	02/09/2008	4	Granite	Control	0.22	0.00
6	33	02/09/2008	5	Granite	Control	0.22	0.00
6	34	02/09/2008	6	Granite	Control	0.24	0.00
6	35	02/09/2008	7	Granite	Control	0.09	0.00
6	38	02/09/2008	10	Granite	Control	0.20	
6	71	02/09/2008	13	Granite	Control	0.05	0.00
6	72	02/09/2008	14	Granite	Control	0.19	0.00
6	77	02/09/2008	19	Granite	Control	0.02	0.00
6	78	02/09/2008	20	Granite	Control	0.11	0.00
6	80	02/09/2008	22	Granite	Control	0.45	0.16
6	85	02/09/2008	27	Granite	Control	0.18	0.12
6	88	02/09/2008	30	Granite	Control	0.22	0.00
6	29	02/09/2008	1	Granite	Mossed	0.27	0.00
6	31	02/09/2008	3	Granite	Mossed	0.28	0.03
6	36	02/09/2008	8	Granite	Mossed	0.21	0.19
6	37	02/09/2008	9	Granite	Mossed	0.16	0.10
6	73	02/09/2008	15	Granite	Mossed	0.24	0.52
6	74	02/09/2008	16	Granite	Mossed	0.35	0.21
6	75	02/09/2008	17	Granite	Mossed	0.27	0.25
6	76	02/09/2008	18	Granite	Mossed	0.13	0.01
6	79	02/09/2008	21	Granite	Mossed	0.17	0.00
6	81	02/09/2008	23	Granite	Mossed	0.09	0.00
6	82	02/09/2008	24	Granite	Mossed	0.39	0.04
6	83	02/09/2008	25	Granite	Mossed	0.10	0.08
6	84	02/09/2008	26	Granite	Mossed	0.28	0.00

						Amount of	
						analyte	
	Tube		**Cosm.**			(µmol)	
Round	**No**	**Date**	**No**	**Subs.**	**Treat.**	**SiO(4)**	**PO(4)**
6	86	02/09/2008	28	Granite	Mossed	0.20	0.11
6	87	02/09/2008	29	Granite	Mossed	0.21	0.11